

KATARZYNA MACIESZCZAK

METROLOGY, METASTABILITY
AND DYNAMICAL PHASE TRANSITIONS
IN OPEN QUANTUM SYSTEMS

METROLOGY, METASTABILITY
AND DYNAMICAL PHASE TRANSITIONS
IN OPEN QUANTUM SYSTEMS

KATARZYNA MACIESZCZAK



The University of
Nottingham

UNITED KINGDOM · CHINA · MALAYSIA

A THESIS SUBMITTED TO THE UNIVERSITY OF NOTTINGHAM FOR
THE DEGREE OF DOCTOR OF PHILOSOPHY

January 2017

Katarzyna Macieszczak: *Metrology, Metastability and Dynamical Phase Transitions in Open Quantum Systems*, A thesis submitted to the University of Nottingham for the degree of Doctor of Philosophy, © January 2017

*There is a saying:
Yesterday is history, tomorrow is a mystery, but today is a gift.
That is why it is called the present.*

— from Kung Fu Panda

Moim Rodzicom

ABSTRACT

In this thesis we explore aspects of dynamics of open quantum systems related to coherence and quantum correlations — necessary resources for enhanced quantum metrology and quantum computation. We first discuss limits to the precision of parameter estimation when using a quantum system in the presence of noise. To this end we introduce a variational principle for the quantum Fisher information (QFI) bounding the estimation errors of any measurement, which motivates an efficient iterative algorithm for finding optimal system preparations for noisy estimation experiments. Furthermore, we investigate influence of noise correlations on the precision in phase and frequency estimation, by delivering bounds for both spatially and temporarily correlated (non-Markovian) dephasing noise. This allows us to prove the Zeno limit in frequency estimation, conjectured in *Phys. Rev. A* **84**, 012103 (2011) and *Phys. Rev. Lett.* **109**, 233601 (2012). The enhanced estimation precision in quantum metrology can be, however, achieved only using highly entangled states. We propose a scheme of generating such highly correlated states as outputs of Markovian open quantum systems near first-order dynamical phase transitions. We show that the quadratic scaling of the QFI with time is present for experiments within the correlation time of the dynamics and describe a theoretical scheme for quantum enhanced estimation of an optical phase-shift using the photons being emitted from an intermittent quantum system. Finally, we establish the basis for a theory of metastability in Markovian open quantum systems, by extending methods from classical stochastic dynamics. We argue that the partial relaxation into long-lived metastable states — distinct from the asymptotic stationary state — may preserve initial coherences within decoherence-free subspaces

or noiseless subsystems, thus allowing for quantum computation during the metastable regime.

PUBLICATIONS

- ¹K. Macieszczak, “Quantum Fisher Information: Variational principle and simple iterative algorithm for its efficient computation,” arXiv:1312.1356 (2013).
- ²K. Macieszczak, “Upper bounds on the quantum Fisher Information in the presence of general dephasing,” arXiv:1403.0955 (2014).
- ³K. Macieszczak, “Zeno limit in frequency estimation with non-Markovian environments,” *Phys. Rev. A* **92**, 010102 (2015).
- ⁴K. Macieszczak, M. Guță, I. Lesanovsky, and J. P. Garrahan, “Dynamical phase transitions as a resource for quantum enhanced metrology,” *Phys. Rev. A* **93**, 022103 (2016).
- ⁵K. Macieszczak, M. Guță, I. Lesanovsky, and J. P. Garrahan, “Towards a Theory of Metastability in Open Quantum Dynamics,” *Phys. Rev. Lett.* **116**, 240404 (2016).
- ⁶D. C. Rose, K. Macieszczak, I. Lesanovsky, and J. P. Garrahan, “Metastability in an open quantum Ising model,” *Phys. Rev. E* **94**, 052132 (2016).

ACKNOWLEDGMENTS

I would like to thank

My supervisors: Dr Madalin Guta, Prof. Juan P. Garrahan and Prof. Igor Lesanovsky, present and former members of Quantum Information Group and Condensed Matter Theory Group at the University of Nottingham, especially Ioannis Kogias and Luis A. Correa, my Warsaw friends: Ania Maroszek, Kasia Mazowiecka, Michał Łasica, Tadeusz Rudzki and Kasia Pótrolniczak, Maryjka Menanteau, Charlotte and Rob Jacksons, my great brothers Piotr and Tom, my loving parents, and my dear husband Ben Everest.

CONTENTS

I	INTRODUCTION	1
0	INTRODUCTION	2
II	RESULTS	5
1	QUANTUM METROLOGY	6
1.1	Background	6
1.1.1	Quantum metrology setup	7
1.1.2	Errors and estimation strategies	8
1.1.3	Ultimate precision limits and quantum correlations	14
1.1.4	Metrology in the presence of noise	17
1.1.5	Resources in metrology	20
1.1.6	Multi-parameter estimation	22
1.1.7	QFI as a metric	24
1.2	Variational principle for QFI	25
1.2.1	Variational principle	25
1.2.2	Numerical algorithm to find optimal system preparation	29
1.2.3	Multi-parameter case	32
1.2.4	Summary	35
1.3	Precision in estimation with correlated noise	35
1.3.1	Semi-classical correlated Gaussian dephasing	36
1.3.2	Bound on phase estimation precision	36
1.3.3	Examples	41
1.3.4	Comments and summary	42
1.4	Frequency estimation with non-Markovian noise	43
1.4.1	Frequency estimation	45
1.4.2	Universal bounds on frequency estimation precision	46
1.4.3	Zeno limit	48

1.4.4	Non-Markovianity is (not) a resource	53
1.4.5	Summary and outlook	53
2	DYNAMICAL PHASE TRANSITIONS AS A RESOURCE FOR QUANTUM ENHANCED METROLOGY	57
2.1	Background	58
2.1.1	Markovian dynamics of open quantum system and input-output formalism	58
2.1.2	Dynamical phase transitions	61
2.1.3	Parameter estimation using both system and output	64
2.1.4	Fidelity of pure states and QFI	64
2.2	Intermittency and enhanced estimation of optical shift	67
2.2.1	Away from a DPT	68
2.2.2	At a first-order DPT in photon emissions	69
2.2.3	Near a first-order DPT in photon emissions	71
2.2.4	Optical-shift encoding and deformation of master dynamics	75
2.3	General parameter estimation and DPTs	76
2.3.1	Parameter estimation and deformation of master dynamics	77
2.3.2	Linear scaling of QFI away from a DPT	78
2.3.3	Quadratic scaling of QFI, bimodality and first-order DPTs	79
2.4	Estimation schemes	85
2.4.1	Parameters	86
2.4.2	Sensitivity over broad parameter range	89
2.4.3	Optimal measurement	92
2.5	Generalised DPTs	95
2.5.1	Observable distinguishing dynamical phases	96
2.5.2	Direct measurement of fidelity	103
2.6	Conclusions	105
3	METASTABILITY IN MARKOVIAN OPEN QUANTUM SYSTEMS	107
3.1	Background	108

3.1.1	Phenomenology of metastability in classical equilibrium systems	109
3.1.2	Metastability in classical stochastic systems	110
3.1.3	Stationary manifolds of quantum semi-group dynamics	113
3.2	Metastability in open quantum system	115
3.2.1	Review of spectral properties	117
3.2.2	Metastability and separation in generator spectrum	118
3.2.3	Geometrical description of quantum metastable manifold	121
3.2.4	Effective long-time dynamics	122
3.2.5	Experimental observation of metastability	123
3.3	Bimodal case of two low-lying modes	124
3.3.1	Classical structure of the metastable manifold	124
3.3.2	Effective classical long-time dynamics	126
3.3.3	Biased QJMC	132
3.4	Higher dimensional metastable manifolds	135
3.4.1	Metastability in class A systems	136
3.4.2	Metastability in class B systems	147
3.5	Summary and Outlook	151
III APPENDIX 155		
A	APPENDIX TO CHAPTER 1	156
A.1	Iterative Algorithm Convergence	156
A.2	Derivations for estimation with correlated dephasing	160
A.2.1	Reduction from multi-parameter to single-parameter Bayesian estimation	160
A.2.2	Bayesian estimator as optimal local estimator	161
A.2.3	Phase encoding	162
B	APPENDIX TO CHAPTER 2	166
B.1	Fidelity and QFI	166
B.2	Time dependence of QFI	166
B.2.1	General time dependence of QFI	167

B.2.2	Asymptotic QFI for a unique stationary state	171
B.2.3	Quadratic time-regime of QFI	172
B.3	Stochastic generator of parameter encoding	177
B.3.1	Average and variance of the stochastic generator	177
B.3.2	Asymptotic average and variance	182
B.3.3	Reverse engineering of dynamics for a given stochastic generator	188
C	APPENDIX TO CHAPTER 3	191
C.1	Metastability in bimodal case	191
C.2	Metastability in class A systems	192
C.2.1	Complete positivity of dynamics projected on SSM	192
C.2.2	Initial relaxation timescale	193
C.2.3	Effective long-time dynamics timescale	195
C.2.4	Coefficients of the metastable manifold	196
C.2.5	Effective long-time dynamics	198
C.2.6	Higher-order corrections	199
D	APPENDIX	201
D.1	Metastability as a resource in enhanced parameter estimation	201
D.2	Metastable phases in biased QJMC	205
D.3	Enhanced estimation in perturbed degenerate SSM	206
D.3.1	Estimation using system only	208
D.3.2	Estimation using both system and output	210
D.3.3	Estimation using output only	211
D.3.4	Enhanced estimation and metastability in general open quantum system	213
	BIBLIOGRAPHY	214

LIST OF FIGURES

Figure 1.1	Quantum metrology setup	7
Figure 1.2	Optimal frequency estimation with collective dephasing	31
Figure 1.3	Error scaling in phase estimation with correlated dephasing	42
Figure 1.4	Ramsey spectroscopy	45
Figure 1.5	Frequency estimation with non-Markovian dephasing	49
Figure 1.6	Asymptotic irrelevance of non-Markovian revivals in frequency estimation	54
Figure 2.1	Scheme of enhanced quantum metrology using output of system near a dynamical phase transition	69
Figure 2.2	Enhanced estimation of optical phase-shift using intermittent 3-level system	73
Figure 2.3	Estimation of intrinsic dynamical parameters in 3-level system	88
Figure 3.1	Example of metastability in 3-level system	126
Figure 3.2	Example of coherent metastable manifold	137

LIST OF TABLES

Table 1.1	Channel Extension bounds on frequency estimation precision	48
Table 1.2	Survival probability for spontaneous emission and depolarisation	53

ACRONYMS

MSE	mean square error
POVM	positive-operator-valued measure
SNR	signal-to-noise ratio
QFI	quantum Fisher information
SLD	symmetric logarithmic derivative
CLT	Central Limit Theorem
DPT	dynamical phase transition
MPS	matrix product state
CMPS	continuous matrix product state
CGF	cumulant generating function
DFS	decoherence free subspace
NSS	noiseless subsystem
SSM	stationary state manifold
MM	metastable manifold
eMS	extreme metastable state
QJMC	quantum jump Monte Carlo
CPTP	completely positive trace-preserving

Part I

INTRODUCTION



INTRODUCTION

In this thesis we explore aspects of quantum open systems dynamics in relation to coherence and quantum correlations, which are necessary resources for quantum technologies applications, such as enhanced quantum metrology [1–6] or quantum computation and communication protocols [7].

Experimental realisations of quantum systems can rarely be considered isolated or closed, due to interactions with external environments which introduce *decoherence* to unitary system dynamics and lead to generally mixed rather than pure system states. When the interactions are weak and environment correlations decay fast in comparison to timescales of the system dynamics, the noisy system evolution can be approximated as *Markovian* [8, 9]. This type of noise is known to be destructive for multipartite quantum entanglement — a necessary ingredient for the enhanced precision scaling with the size of a quantum system used in phase or frequency estimation [10, 11] — and the improvement of optimal quantum metrology over classical strategies is consequently reduced, for typical local noise models even just to a constant enhancement [12–16]. Such Markovian noise models are, however, just an approximation to the true system dynamics, which neglects in particular the initial regime of necessary slower decoherence [17–20]. Consequently, for the maximally entangled states undergoing local *non-Markovian* dephasing noise, it was demonstrated that the enhancement in the scaling of the spectroscopy precision, although reduced, can be still present [21–23]. In Chapter 1 we derive a general limit to the spectroscopy precision in the pres-

ence of non-Markovian dephasing noise [24]. We further show that the enhanced precision scaling can be achieved only for the initial regime of slower decoherence and any revivals of coherence or quantum correlations, usually considered as a signature of non-Markovian dynamics [25, 26], do *not* contribute to the enhancement for large system sizes. In Chapter 1 we also investigate other aspects of quantum metrology in the presence of noise. In Sec. 1.3 we derive precision bounds for spatially correlated noise models, where the noise cannot be described as local, which bounds show a transition in precision scaling depending on the decay of noise correlations [27]. In Sec. 1.2 we introduce an efficient numerical algorithm to find optimal system preparations and measurements for general quantum parameter estimation [24].

Even when the system dynamics is unitary, preparation of highly entangled states leading to enhanced parameter estimation is challenging [28]. In Chapter 2 we propose exploiting open quantum systems characterised by complex and slowly relaxing dynamics in order to prepare highly correlated states for quantum metrology [29]. We consider *Markovian* open quantum systems generating, as a result of interaction with the external environment, output fields [30], e.g. atomic ensembles emitting photons [31–33]. For the system dynamics in proximity to first-order dynamical phase transitions [34–36], we show that the precision of estimating parameters encoded on the output, e.g. optical phase-shift on emitted photons, can be quadratically enhanced for experiment times within the correlation time of the system dynamics. Furthermore, also the precision of estimating system parameters can be enhanced, which generalises the recent work on estimation limits for dynamics featuring a single stationary state [37–39].

For quantum information processing [7] decoherence free subspaces [40–43] and noiseless subsystems [44–46], where parts of the Hilbert space are protected against external noise, are ideal scenarios for experimental implementation. Since experiments are performed in finite time, however, it is sufficient to consider a larger class of systems whose coherence is only stable over

experimental timescales, i.e., *metastable*. In Chapter 3 we lay grounds for the metastability theory in Markovian open quantum systems by generalising concepts from classical stochastic systems [47–53]. Metastability, a common phenomenon in classical soft matter [54], with glasses being the paradigmatic example [55, 56], manifests itself as initial partial relaxation is into long-lived states with subsequent decay to true stationarity occurring at much longer times. We show that for Markovian open quantum systems, metastability corresponds to a separation in the spectrum of the generator governing the dynamics. This structure leads to a low-dimensional approximation of a manifold of metastable states in terms of degrees of freedom preserved in the metastable regime. Furthermore, those degrees of freedom can be quantum and correspond to the coherences inside metastable decoherence free subspaces or noiseless subsystems, where quantum computation operations can be implemented [57, 58].

Part II

RESULTS

QUANTUM METROLOGY

In this chapter we discuss aspects of *quantum metrology*. This area explores possibilities of enhancing the precision in estimation of unknown values of parameters, such as magnetic fields or optical-shifts, by using quantum systems whose dynamics depends on the estimated parameters. It is inevitably tied to experiments with the most prominent applications including spectroscopy in atomic frequency standards [4–6] and phase estimation in gravitational interferometers [59–61].

This chapter proceeds as follows. First, main questions and ongoing research efforts in the field of quantum metrology are reviewed. This is followed by three sections presenting results on quantum metrology in the presence of noise: finding optimal quantum system preparation for a given dynamics, parameter estimation in the presence of correlated noise, and precision limits to frequency estimation in the presence of non-Markovian noise. In Appendix A complementary derivations can be found. In the next chapter 2, we will discuss how dynamical phase transitions in Markovian quantum systems can be utilised for preparation of quantum states leading to the enhanced precision in quantum metrology.

1.1 BACKGROUND

Let us first review some essential aspects of quantum metrology, where a quantum system is employed in order to estimate the unknown value of a parameter determining the system dynamics.

1.1.1 Quantum metrology setup

We consider a quantum metrology setup [1, 62] in which a quantum system is first prepared in an initial state represented by a density matrix ρ ($\rho \in \mathcal{B}(\mathcal{H})$, $\rho \geq 0$ and $\text{Tr}(\rho) = 1$, where \mathcal{H} is the system Hilbert space). The system undergoes dynamics described by a completely positive and trace-preserving channel Λ_ϕ which is assumed to depend on a parameter ϕ being estimated. Information about the parameter ϕ can be retrieved via a measurement of an observable X ($X \in \mathcal{B}(\mathcal{H})$ and $X = X^\dagger$) on the system state $\rho_\phi = \Lambda_\phi(\rho)$, see Fig. 1.1. As neither the pa-

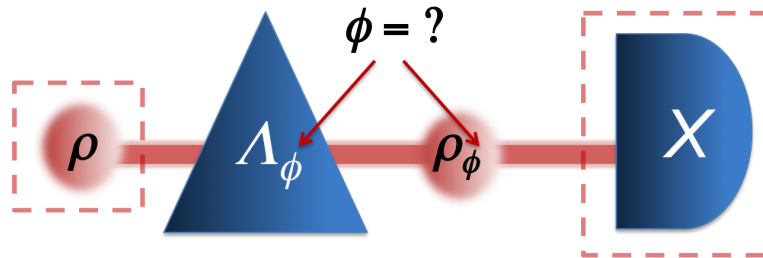


Figure 1.1: **Quantum metrology setup.** An initial state ρ undergoes the dynamics represented by a quantum channel Λ_ϕ , which imprints a parameter value ϕ on the state. An observable X is measured to obtain the information about the parameter. The choice of ρ and X is optimised to obtain the maximum estimation precision.

parameter value ϕ nor the state ρ_ϕ cannot be accessed directly, but only via measurements with an associated probability distribution, there are necessarily errors in estimation of the value ϕ . This so called *quantum noise* is present even if no interaction with an environment takes place and the channel Λ_ϕ is unitary. The *aim* of quantum metrology is to find the optimal system preparation ρ and observable X , so that the estimation errors are minimal.

1.1.2 Errors and estimation strategies

1.1.2.1 Estimation errors

There are many ways of quantifying errors given by the so called *cost function* C , so that the mean error is

$$\text{ME}_\phi = \sum_x p_\phi(x) C(\hat{\phi}(x), \phi), \quad (1.1)$$

where $\hat{\phi}$ is an *estimator* representing a guess of the parameter ϕ value, $\hat{\phi}(x)$, when a measurement result x is obtained, and $p_\phi(x)$ is the probability of obtaining x . Note that the optimal choice of ρ and X will depend on the cost function C . A common choice in statistics is the quadratic function, $C(\hat{\phi}(x), \phi) = (\hat{\phi}(x) - \phi)^2$, due to a scalar-product structure on the parameter space it originates from [63]. This leads to the mean square error (MSE),

$$\text{MSE}_\phi(\hat{\phi}) = \sum_x p_\phi(x) (\hat{\phi}(x) - \phi)^2 \quad (1.2)$$

$$= \Delta_\phi^2 \hat{\phi} + (\mathbb{E}_\phi \hat{\phi} - \phi)^2, \quad (1.3)$$

where $\mathbb{E}_\phi \hat{\phi}$ is the mean value of the estimator $\hat{\phi}$, $\mathbb{E}_\phi \hat{\phi} - \phi$ is its bias, and $\Delta_\phi^2 \hat{\phi} := \sum_x p_\phi(x) (\hat{\phi}(x) - \mathbb{E}_\phi \hat{\phi})^2$ its variance. Note that the mean error is a *local* notion, as it is calculated with respect to a given value ϕ of the estimated parameter. This may seem contradictory, as this value is exactly the quantity to be estimated, but this choice is well motivated in two following scenarios. First, consider estimation of a small parameter fluctuation $\delta\phi \approx 0$ around a known value ϕ_0 , i.e., $\phi = \phi_0 + \delta\phi$, which is the case e.g. for an optical-shift in gravitational interferometers [59]. For well behaved distribution $p_\phi(x)$ (e.g. double differentiable w.r.t. ϕ), the error does not vary for small enough perturbations $\delta\phi$. In the second scenario, we consider *asymptotic* strategies, where we assume that for large number n of independent experiments the estimator $\hat{\phi}^{(n)}(x_1, \dots, x_n)$ converges to the true parameter value ϕ (in probability or almost every-

where), i.e., is *asymptotically consistent*, cf. (1.3). This usually coincides with the bias disappearing asymptotically $\mathbb{E}_\phi \hat{\phi}^{(n)} - \phi \rightarrow 0$. This is the case for example when $\hat{\phi}$ is a maximal likelihood estimator (see also paragraph below Eq. (1.11)). The results presented in the three next sections are relevant exactly for these two scenarios. Another so called *mini-max* scenario involves considering $\min_{\hat{\phi}} \max_{\phi} \text{MSE}_\phi(\hat{\phi})$ [63].

For the metrology setup in Fig. 1.1, the result x corresponds to eigenvalue of an observable $X = \sum_x x |x\rangle\langle x|$ and the associated probability is given by $p_\phi(x) = \text{Tr}(|x\rangle\langle x| \rho_\phi)$. The estimator $\hat{\phi}$ corresponds to relabelling of the X spectrum, and for simply $\hat{\phi}(x) = x$ we obtain

$$\text{MSE}_\phi(X) = \Delta_\phi^2 X + (\langle X \rangle_\phi - \phi)^2. \quad (1.4)$$

The setup in Fig. 1.1, can be further generalised to a measurement described by a positive-operator-valued measure (POVM) — a set of positive operators $\{\Pi_x\}_x$, $\Pi_x \geq 0$, with $\sum_x \Pi_x = \mathbb{1}_{\mathcal{H}}$ — with $p_\phi(x) := \text{Tr}(\Pi_x \rho_\phi)$ yielding a probability distribution. In the case of dynamics generating an output, see Sec. 2.1.1, also *continuous measurements* of the output can be considered. This will be considered in Chapter 2.

1.1.2.2 Optimal local strategies and quantum Fisher information

Consider estimation of a small perturbation $\delta\phi$ around a known value ϕ_0 , i.e., $\phi = \phi_0 + \delta\phi$. We can shift $\hat{\phi}$ by a constant so that $\mathbb{E}_{\phi_0} \hat{\phi} = \phi_0$, but we would like its prediction to be true on average also for small perturbations, i.e., *locally unbiased*, and hence only its variance to contribute to the MSE, cf. (1.3). Therefore, we shall consider the *rescaled* estimator $\alpha^{-1} \hat{\phi} + \beta$, where $\alpha = \partial_\phi|_{\phi=\phi_0} \mathbb{E}_\phi \hat{\phi}$ and $\beta = -\alpha^{-1} \mathbb{E}_{\phi_0} \hat{\phi} + \phi_0$. In particular, for the setup in Fig. 1.1 and $\hat{\phi}(x) = x$, in such case we have that the mean square error of estimating ϕ is given by the inverse of the signal-to-noise ratio (SNR),

$$\text{SNR}_{\phi_0}(X) = \frac{(\partial_\phi|_{\phi=\phi_0} \langle X \rangle_\phi)^2}{\Delta_{\phi_0}^2 X}, \quad (1.5)$$

where the signal $\partial_\phi|_{\phi=\phi_0}\langle X \rangle_\phi$ is rescaled by measurement noise $\Delta_{\phi_0}^2 X$, which corresponds to the error propagation formula.

Optimal estimator. The variance of any locally unbiased estimator of ϕ , and thus the MSE, is bounded from below in the Cramér-Rao inequality [63]

$$\Delta_{\phi_0}^2 \hat{\phi} \geq I_{\phi_0}^{-1}, \quad \text{where} \quad I_{\phi_0} = \sum_x p_\phi(x) (\partial_\phi \log(p_\phi(x)))^2 |_{\phi=\phi_0}, \quad (1.6)$$

where I_ϕ is the *Fisher information* and we assumed that support of p_ϕ does not change with ϕ , so that $\mathbb{E}_{\phi_0} \partial_\phi|_{\phi=\phi_0} \log(p_\phi(x)) = 0$. The estimator whose variance saturates the inequality is called *efficient*. Note that the Fisher information quantifies the quality of the quantum metrology setup, as it bounds from below the precision of estimating parameter ϕ when the probability distribution of results is given by $\{p_\phi(x)\}_x$, and we no longer need to refer to an estimator. The Fisher information depends on the state ρ_ϕ and the projective measurement on the eigenbasis of X (or POVM $\{\Pi_x\}_x$), but not the spectrum of X .

Optimal measurement. The optimal measurement $\{\Pi_x\}_x$ for the state ρ_ϕ is the one that leads to the maximum Fisher information, the so called quantum Fisher information (QFI) [64–67], $F_\phi(\rho_\phi)$, which depends only on the quantum state ρ_ϕ ,

$$F_\phi(\rho_\phi) = \text{Tr}(D_{\rho_\phi}^2 \rho_\phi), \quad \text{where} \quad (1.7)$$

$$\frac{1}{2}(D_{\rho_{\phi_0}} \rho_{\phi_0} + \rho_{\phi_0} D_{\rho_{\phi_0}}) = \partial_\phi \rho_\phi |_{\phi=\phi_0}, \quad (1.8)$$

and D_{ρ_ϕ} is so called symmetric logarithmic derivative (SLD). Note that the QFI and SLD depend on both ρ_ϕ and $\partial_\phi \rho_\phi$, but we choose the notation $F_\phi(\rho_\phi)$ and D_{ρ_ϕ} for simplicity. Furthermore, it follows that the SNR of any observable X is bounded by the QFI, see e.g. [68],

$$\frac{(\partial_\phi|_{\phi=\phi_0}\langle X \rangle_\phi)^2}{\Delta_{\phi_0}^2 X} \leq F_{\phi_0}(\rho_\phi). \quad (1.9)$$

Note that we have $\text{SNR}_\phi(D_{\rho_\phi}) = F_\phi(\rho_\phi)$ since $\langle D_{\rho_\phi} \rangle_\phi = 0$ and $\partial_\phi|_{\phi=\phi_0} \langle D_{\rho_{\phi_0}} \rangle_\phi = \text{Tr}(D_{\rho_\phi}^2 \rho_\phi)$. This shows that the projections on the eigenvectors of the SLD, $D_{\rho_{\phi_0}}$, provide the optimal measurement, and the spectrum of $F_{\phi_0}(\rho_{\phi_0})^{-1}(D_{\rho_{\phi_0}} + \phi_0)$ yields the efficient locally unbiased estimator around $\phi = \phi_0$.

Optimal initial state. The optimal initial state leads to the maximum QFI, $\max_\rho F_\phi(\Lambda_\phi(\rho))$ and thus to the minimal mean square error in estimation. Since both the Fisher information, (1.6), and the QFI are convex with respect to mixing probability distributions or quantum states,

$$F_\phi(\lambda\rho_\phi^{(1)} + (1-\lambda)\rho_\phi^{(2)}) \leq \lambda F_\phi(\rho_\phi^{(1)}) + (1-\lambda) F_\phi(\rho_\phi^{(2)}), \quad (1.10)$$

it follows that the optimal initial state can be chosen *pure*.

The maximum QFI yields an *ultimate limit* to the estimation setup in Fig. 1.1 with dynamics Λ_ϕ , whatever the initial state, the measurement and the (locally unbiased) estimator are employed. When dynamics is not unitary, the state ρ_ϕ is in general mixed, and there is usually no closed formula for the QFI w.r.t. all input states, which makes $\max_\rho F_\phi(\Lambda_\phi(\rho))$ difficult to compute [69]. In Sec. 1.2 we provide a numerical algorithm which circumvents this problem by providing a variational principle for calculating the QFI.

1.1.2.3 Asymptotic strategies and quantum Fisher information

Consider performing n independent experiments in order to estimate unknown value of ϕ . We have that the joint probability $p_\phi(x_1, \dots, x_n) = p_\phi(x_1) \dots p_\phi(x_n)$, which corresponds to the system state $\rho_\phi^{\otimes n}$ measured by $\{\Pi_{x_1} \otimes \dots \otimes \Pi_{x_n}\}_{x_1, \dots, x_n}$. This leads to the following form of Cramér-Rao inequality, cf. (1.6),

$$\Delta_\phi^2 \hat{\phi}^{(n)} \geq (n I_\phi)^{-1} \quad (1.11)$$

for a locally unbiased $\hat{\phi}^{(n)}$ estimator representing a guess about ϕ from results (x_1, \dots, x_n) . In general, however, it is difficult to find estimators that are unbiased for all $\phi \in \Phi$. Even when that is the case, they are usually not efficient except special

cases, e.g. $p_\phi(x)$ being Gaussian distribution with mean ϕ and $\hat{\phi}^{(n)}(x_1, \dots, x_n) = n^{-1} \sum_{j=1}^n x_j$. Therefore, a concept of *asymptotic efficiency* has been introduced by F. Y. Edgeworth [70] and R. A. Fisher [71]. First, let us recall that a sequence of estimators $\{\hat{\phi}^{(n)}\}_{n=1}^\infty$ is *asymptotically normal* if it \sqrt{n} -converges in law to a normal distribution. When it is consistent, we furthermore have the following convergence in law, $\sqrt{n}(\hat{\phi}^{(n)} - \phi) \xrightarrow{d} \mathcal{N}(0, v_\phi)$. Finally, when the asymptotic variance $v_\phi = I_\phi^{-1}$, the estimator is considered asymptotically efficient, as it was shown by L. M. LeCam [72] that for any asymptotically normal and consistent estimator, the set $\{\phi \in \Phi : v_\phi < I_\phi^{-1}\}$ is of measure zero. An important example of an asymptotically efficient estimator is the maximal likelihood estimator under some regularity conditions on $p_\phi(x)$ [63].

We therefore see that the concept of the Fisher information is meaningful, as in general estimation it can be achieved in the asymptotic sense. In the quantum setup, however, the probability distribution of results depends on the choice of measurement and the optimal measurement given by the eigenbasis of D_{ρ_ϕ} depends in general on an unknown value ϕ . Adaptive strategies need to be employed in which the measurement is given by the SLD for the current estimate of ϕ , in order to achieve the optimal precision given by the QFI in the asymptotic sense, see [67, 73, 74].

1.1.2.4 Bayesian estimation

In an opposite scenario to the local and the asymptotic ones discussed above, when one wants to minimise errors of just a few experiments — so called *one-shot scenario* — but information about the value of ϕ is partially known, one can use a *Bayesian* approach. Prior information about the estimated parameter ϕ is represented by a probability distribution $g(\phi)$ on the parameter space Φ . After a result x is obtained, the prior information about ϕ is updated to the posterior distribution,

$$p(\phi|x) = \frac{g(\phi) p_\phi(x)}{\bar{p}(x)}, \quad (1.12)$$

where $\bar{p}(x) = \int_{\Phi} d\phi g(\phi) p_{\phi}(x)$ is the average probability of obtaining the result x . When an estimator $\hat{\phi}$ is used, the corresponding average mean error is given by

$$\text{AME}(\hat{\phi}) = \int_{\Phi} d\phi g(\phi) \text{ME}_{\phi} = \int_{\Phi} d\phi g(\phi) \sum_x p_{\phi}(x) C(\hat{\phi}(x), \phi). \quad (1.13)$$

For application of this approach to phase estimation see e.g. [14, 75, 76], for frequency estimation e.g. [77, 78]. Furthermore, for the quadratic cost function C , the van Trees inequality [79, 80] bounds the error of any (not necessarily unbiased) estimator $\hat{\phi}$ from below, by the information contained in the prior distribution and the average Fisher information,

$$\int_{\Phi} d\phi g(\phi) \sum_x p_{\phi}(x) (\hat{\phi}(x) - \phi)^2 \geq \left(I_{\text{prior}} + \int_{\Phi} d\phi g(\phi) I_{\phi} \right)^{-1},$$

where $I_{\text{prior}} = \int_{\Phi} d\phi g(\phi) (\partial_{\phi} \log(g(\phi)))^2$, (1.14)

as long as $g(\phi) = 0$ at the boundary of Φ and I_{ϕ} is well defined for all $\phi \in \Phi$. In Sec. 1.3 we will use this inequality to derive bounds on the MSE in local estimation with a quantum system in the presence of correlated noise. Let us note here that in quantum parameter estimation using highly non-Gaussian states, the so called Ziv-Zakai bound may be tighter than the van Trees inequality, see [81].

Furthermore, for the quadratic cost function, the optimal estimator minimising the average error is known to be simply the mean of the posterior distribution,

$$\hat{\phi}(x) = \frac{\int_{\Phi} d\phi g(\phi) p_{\phi}(x) \phi}{\int_{\Phi} d\phi g(\phi) p_{\phi}(x)} \quad \text{and thus} \quad (1.15)$$

$$\mathbb{E}\hat{\phi}(x) = \phi_0, \quad \text{and} \quad (1.16)$$

$$\text{AME}(\hat{\phi}) = \int_{\Phi} d\phi g(\phi) (\phi - \phi_0)^2 - \sum_x \bar{p}(x) (\hat{\phi}(x) - \phi_0)^2, \quad (1.17)$$

where ϕ_0 is the mean of the prior distribution, so that the average error is the difference between the prior distribution variance and the estimator variance.

Moreover, for the quadratic cost function in quantum parameter estimation, the optimal measurement can be found and corresponds to projections on the eigenvectors of the observable \bar{D}_ρ , which is the solution of the following equation [66, 77], cf. the SLD in Eq. (1.8),

$$\frac{1}{2} (\bar{D}_\rho \bar{\rho} + \bar{\rho} \bar{D}_\rho) = \bar{\rho}', \quad (1.18)$$

where $\bar{\rho} = \int_\Phi d\phi g(\phi) \rho_\phi$ and $\bar{\rho}' = \int_\Phi d\phi g(\phi) (\phi - \phi_0) \rho_\phi$. Moreover, the shifted observable $\bar{D}_\rho + \phi_0 \mathbb{1}$ encodes in its spectrum the optimal estimator $\hat{\phi}$ for the optimal measurement, which leads to the average error, cf. Eq. (1.17),

$$\text{AME}(\bar{D}_\rho) = \int_\Phi d\phi g(\phi) (\phi - \phi_0)^2 - \text{Tr} \left(\bar{\rho} \bar{D}_\rho^2 \right). \quad (1.19)$$

1.1.3 Ultimate precision limits and quantum correlations

From now on we consider local and asymptotic strategies, where the Fisher information, (1.6), and the quantum Fisher information, (1.7), can be used to quantify the quality of a metrology setup.

Standard scaling. Consider parameter estimation using a quantum system consisting of N identical subsystems, e.g. N two-level atoms. A state $\rho_\phi^{\otimes N}$ with *no correlations* between subsystems leads to the QFI *linear* in N , cf. (1.7), as it corresponds to N independent experiments using just one subsystem, and thus mean square errors scale $\propto N^{-1}$, so called *standard (shot-noise) limit*, cf. Eq. (1.11). Furthermore, precision of estimation setup using any *separable* state can be shown to be bounded by $N \max_\rho F(\Lambda_\phi(\rho))$ due to convexity of the QFI [1, 2]. On the other hand, an entangled state of a quantum system exhibits stronger than classical correlations, which has been exploited in

quantum computation and communication protocols [7]. Those quantum correlations can also result in fast evolution in the quantum states space, which makes entangled states very sensitive to changes in dynamics parameters and therefore potentially useful for metrology [1, 2, 62]. Entanglement has been indeed demonstrated to enhance the precision of estimating unknown phase (optical shift) in optical setups (first considered in [3]) and unknown magnetic field via spectroscopy (first discussed in [4], for experiments see [5, 6]) when system dynamics is unitary.

Heisenberg scaling in phase and frequency estimation. Let us briefly consider the example of *unitary* estimation with the maximally correlated Greenberger-Horne-Zeilinger (GHZ) state $\frac{1}{\sqrt{2}}(|\text{GHZ}\rangle = |0\rangle^{\otimes N} + |1\rangle^{\otimes N})$ consisting of N qubits (e.g. N photons with $|0\rangle, |1\rangle$ representing modes in two arms in an interferometer, in which case such a state is called the NOON state, or N two-level atoms with $|0\rangle, |1\rangle$ describing the ground and the excited states of an atom). When dynamics introduces a relative phase difference ϕ between $|0\rangle$ and $|1\rangle$, we obtain the evolved state $|\text{GHZ}_\phi\rangle = \frac{1}{\sqrt{2}}(|0\rangle^{\otimes N} + e^{-iN\phi}|1\rangle^{\otimes N})$ which effectively encodes the phase $N\phi$, the phase estimation precision for the optimal measurement (parity measurement) will scale $\propto N^{-2}$, and indeed it can be easily shown that the QFI equals $F(|\text{GHZ}_\phi\rangle) = N^2$, which is actually the maximum value of the QFI for such unitary dynamics. This is referred to as *Heisenberg limit* or *scaling* in N [3]. On the other hand, the uncorrelated state of N atoms, $\frac{1}{\sqrt{2^N}}(|0\rangle + e^{-i\phi}|1\rangle)^{\otimes N}$, the QFI equals only N .

In general, for any phase encoding with unitary dynamics, i.e., $\rho_\phi = U_\phi \rho U_\phi^\dagger$ where $U_\phi = e^{-i\phi H}$, we obtain that the QFI is independent of ϕ value, $F_\phi(\rho_\phi) = F(\rho)$, as the optimal measurements for different $\phi_1 \neq \phi_2$ are simply related by the unitary $U_{\phi_2 - \phi_1}$. Furthermore, from convexity of the QFI, the optimal initial state is pure. For any pure initial state $|\psi\rangle$, we simply have that the QFI is proportional to the Hamiltonian variance, $F(|\psi\rangle) = 4\Delta^2 H$. Therefore, when the Hamiltonian is *local* with respect to subsystems, $H = \sum_{j=1}^N \mathbb{1}^{\otimes(j-1)} \otimes h \otimes \mathbb{1}^{\otimes(N-j)}$, the

maximum QFI equals $N^2(h_{\max} - h_{\min})^2$ and is achieved for a GHZ-like state consisting of the extreme eigenvectors of h corresponding to eigenvalues h_{\max} , h_{\min} , whereas for separable states the QFI reaches at most $N(h_{\max} - h_{\min})^2$. For frequency ω estimation in spectroscopy, i.e., the encoded phase being $\phi = \omega t$, it simply follows that the maximum QFI is $N^2 t^2$, while for the uncorrelated state $N t^2$, see [4].

We note that the Heisenberg scaling can be beaten for states with a fluctuating number of subsystems, e.g. for states composed of different number of photons, and there is no ultimate bound as the QFI can even be infinite [82]. When Gaussian states are considered, however, the Heisenberg scaling is recovered as the limit, due to the fluctuations of the number of subsystems being bounded, see e.g. [83, 84].

It should be noted that except for very particular forms of ρ_ϕ , the optimal measurement given by D_{ρ_ϕ} is usually difficult to engineer. Nevertheless, its SNR equals the QFI, $F_\phi(\rho_\phi)$, and thus bounds the (asymptotic) precision of any measurement that can be performed in practice. Therefore, it provides an *ultimate* benchmark against which performance of measurements currently used in experiments can be checked, see e.g. [85]. Moreover, as we discuss in the next subsection on quantum metrology in the presence of noise, when $F(\rho_g)$ is optimised over all possible preparations ϕ , it can be determined whether there is at all possibility of enhancement in scaling using entangled states of N subsystems.

QFI as a witness of multipartite entanglement. As we discussed above, when an estimated parameter is encoded via unitary dynamics with a local Hamiltonian, the corresponding QFI for a separable state is necessarily limited to linear scaling, $F_{\text{sep}} = N(h_{\max} - h_{\min})^2$. Therefore, if there is a way of determining the QFI for a given state ρ experimentally, or at least a lower bound for the QFI, it serves as a *witness of multipartite entanglement* whenever the measured value is higher than F_{sep} [10, 11]. Moreover, this criterium can be refined by considering limits of

the QFI for k -producible states (a mixture of tensor products of at most k -subsystem states), $F_{k\text{-prod}} = N k (h_{\max} - h_{\min})^2$ [10, 86]. Experimental schemes to obtain a QFI value or its lower bound have been proposed e.g. in [87–89].

It is known, however, that for mixed states there can be quantum correlations present, so called quantum discord [90], even if the state is not entangled, i.e., separable. It can be shown that those quantum correlations can be useful for certain metrological scenarios where the Hamiltonian encoding a parameter to be estimated is unknown [91].

1.1.4 Metrology in the presence of noise

In the previous section we discussed how an entangled initial state preparation can lead to Heisenberg scaling in estimation precision [2]. This quantum enhancement in precision, however, may be significantly limited in the presence of additional noise - *decoherence* [15, 16, 92].

When the system is interacting with external environments, quantum correlations may be significantly reduced and thus the quantum enhancement in precision may be limited for open quantum systems. This is especially visible in the case when the noise effects commute with the phase encoding, i.e., $\Lambda_\phi(\rho) = e^{-i\phi H} \Lambda(\rho) e^{i\phi H}$, since it effectively limits the set of possible initial states from ρ to $\Lambda(\rho)$. This is the case in the optical interferometry in the presence of photon losses which reduce the precision scaling to the *standard limit* [13, 14]. It was shown later in that similar results hold for dephasing noise [15, 16, 92].

Markovian noise in frequency estimation. In a frequency estimation setup, an initial system state ρ evolves for time t so that frequency can be encoded in phases of the evolved state, $\rho_{\omega,t} = \Lambda_{\omega,t}(\rho)$, and accessed by a subsequent measurement. For a total time T given for estimation, the single experiment is repeated $n = \frac{T}{t}$ times, assuming negligible preparation and measurement times. Single experiment time t is chosen so that the corre-

sponding estimation errors are minimal, e.g. for local perturbation estimation so that $\max_{t \leq T} \frac{1}{t} F_{\omega}(\rho_{\omega,t})$ is achieved, cf. (1.11). In order to do so, the quantum channel $\Lambda_{\omega,t}$ needs to be specified as a function of time t . When interactions between the system and environments are weak and the noise correlation time is much shorter than the characteristic time of the system ω^{-1} , environments can be assumed to have no memory and the quantum channel has a semigroup structure $\Lambda_{\omega,(t_1+t_2)} = \Lambda_{\omega,t_2} \circ \Lambda_{\omega,t_1}$, which corresponds to a time-homogenous master equation for system dynamics [8, 9], see also derivation in Sec. 2.1.1. For the interaction leading to local Markovian dephasing, it was shown in [12] that the GHZ and uncorrelated states provide exactly the same precision, and together with generalized Ramsey spectroscopy schemes have standard scaling, see Fig. 1.4 and [93]. It was proved later, also for other local Markovian noise usually encountered in spectroscopy experiments (depolarisation, spontaneous emissions/amplitude damping), that the standard scaling indeed holds for any atom preparation and measurement, and the quantum enhancement is limited to just a constant [15, 94]. Nevertheless, there are realistic Markovian models in which the standard scaling can be beaten [95, 96] or even the Heisenberg scaling can be restored using error correction methods [97–99] or due to spatial-correlations in non-local noise [100].

Non-Markovian noise in frequency estimation and new precision limits. Markovian noise models are an approximation of the system dynamics and not all noise models can be described within this approximation, resulting in so called *non-Markovian models with noise correlated in time*. For example, in magnetic field sensing using the GHZ state in the presence of semi-classical dephasing due to unaccounted stationary magnetic fields has infinite correlation time, the precision of magnetic field sensing scales $\propto N^{-3/2}$ [21, 101]. Furthermore, joint unitary dynamics of the system and an environment impose an initial *quadratic decay* of the probability of observing the system in its initial state, which leads to the quantum Zeno effect [17–20], whereas

the semi-group structure of Markovian models imposes a faster exponential decay of this probability. The authors of [22, 23] showed that the precision of frequency estimation in the Zeno-dynamics regime with the atoms prepared in the GHZ state scales $\propto N^{-3/2}$ for numerous local non-Markovian dephasing models. It was also argued that the *Zeno scaling* $\propto N^{-3/2}$ should be a limit valid for any system preparation and any local dephasing model, as the scaling enhancement for the GHZ state in comparison to the Markovian noise is due to the slower increase of the noise strength in the Zeno-dynamics regime.

In Sec. 1.4 we derive a bound for the precision of frequency estimation in the presence of general local dephasing. For dephasing featuring the initial Zeno dynamics, we prove that the Zeno scaling is indeed the best possible precision scaling for all atom preparations and measurements, and can be achieved *only* for experiments performed within the Zeno dynamics-regime, whereas for other regimes the precision scaling is necessary standard and thus non-Markovian revivals *are not a resource for metrology* asymptotically. Moreover, using already earlier derived bounds [15, 94], the Zeno scaling can be shown to be the limit for frequency estimation with non-Markovian depolarisation and damping models. These results have been published in [24]. The authors of the later work [102] prove that the Zeno scaling is the precision limit for all models of noise commuting with phase ωt encoding, $\Lambda_{\omega,t}(\rho) = U_{\omega t} \Lambda_t(\rho) U_{\omega t}^\dagger$, which feature initial Zeno dynamics.

Spatial correlations in noise and limits in phase estimation precision. In Sec. 1.3 we present a bound for semi-classical model of Gaussian dephasing derived in [27] which crucially depends on the noise correlations and thus bridges the gap between usually considered local noise [13, 15, 16, 94] and fully correlated noise [84, 103]. In particular depending on the correlation length in the noise we observe transition between *linear* and *constant* scaling of the Fisher information for phase estimation and Markovian frequency estimation. The bound [27] is later

used to prove the Zeno scaling in [24]. In [100] the frequency estimation using atoms interacting with electromagnetic fields via electric quadrupole moments was considered. For the case of the dephasing noise with the spatial correlation length increasing linearly with the number N of atoms, it was shown that the Heisenberg scaling is restored in the limit of an infinite number of subsystems, $N \rightarrow \infty$.

Unitary noise. If the parameter being estimated is not encoded simply as a phase, the precision scaling may be limited, even when there is no interaction with an environment and the system dynamics is unitary, e.g. for $U_\phi = e^{-i(\phi H + \phi H')}$ and two terms in the Hamiltonian not commuting, $[H, H'] \neq 0$ [104–106]. This is due to the fact that the parameter ϕ is effectively encoded with a parameter-dependent Hamiltonian given by $H_{\phi, \phi} = \int_0^\phi d\phi' e^{-i\phi'(H + \frac{\phi}{\phi'} H')} H e^{i\phi'(H + \frac{\phi}{\phi'} H')}$. In particular, for frequency estimation, t^2 -scaling of the QFI may not be present asymptotically [105]. When both H and H' are local, however, the best possible scaling in the number N of subsystems is still the Heisenberg limit [104, 106].

Estimation of noise parameters. For the optimal estimation of a noise parameter, see [94] for bounds and [107] for an example of temperature estimation.

1.1.5 Resources in metrology

In frequency estimation there is an additional parameter of time t , which can be optimised to lower estimation errors, when total time T of experiments is given as a *resource*. In the case of phase estimation with N subsystems, *local phase encoding*, $\Lambda_\phi^{(N)} = \Lambda_\phi^{\otimes N}$, can be thought as *parallel* application of N encoding operations Λ_ϕ . In such situations enhancement can come from the initial entangled preparation usually requiring also an entangled measurement to retrieve the value of ϕ [1], cf. the SLD in (1.8). On the other hand, consider applying N encoding

operations *sequentially* to one subsystem, Λ_ϕ^N , so called *multi-pass interferometry*, which for unitary phase estimation leads to Heisenberg scaling with N *without multipartite entanglement* between subsystems or entangled measurement [73, 74]. One can further consider a general framework treating encoding operations as a resource, which includes the above two. One considers N encoding operations are applied to a finite number of initially uncorrelated subsystems, some of which may play role of *ancillas* (Λ_ϕ is not applied), and interspersed with additional operations possibly entangling the subsystems, leading to an entanglement-assisted scenario [2, 108, 109]. For the unitary case, the solution is known [108], but when Λ_ϕ is noisy, a hierarchy of scenarios is known only for special types of noise, like dephasing and erasure, see [109] for proofs and a general conjecture.

We note here, when a considered scenario is entanglement-assisted, i.e., additional operations used beyond the local encodings, entangle the subsystems, their implementation cost should be also taken into account as they are usually difficult to perform experimentally, possibly within a proper resource theory framework [110].

Furthermore, we note that usually the above scenarios are considered with respect to local estimation, cf. Sec. 1.1.2.2. When there is no initial knowledge about the estimated parameter ϕ , it has been shown for the unitary multiple-passes intereferometry scenario with a single subsystem, or equivalently the parallel scenario using the GHZ states, that the Heisenberg scaling of errors can be indeed achieved [73, 74]. For general (possibly noisy) scenarios, however, it is not known whether the precision achievable locally can be also achieved in the asymptotic sense. Note that the standard scenario using separable states and parallel strategies, simply corresponds to $n = N$ independent experiments and thus the local precision is achievable also asymptotically, cf. Sec. 1.1.2.2.

Non-linear phase estimation. The Heisenberg scaling is a consequence of unitary encoding, $U_\phi = e^{-i\phi H}$, with a local Hamil-

tonian H . When there are interactions in the encoding Hamiltonian H , so called non-linear/many-body encoding, first proposed in [111], the corresponding QFI can feature faster than quadratic (even exponential) scaling, in the number of subsystems N used, which can be remedied by careful counting of resources as $\text{Tr}(H\rho) - E_0$, where E_0 is the ground energy in H [112]. Nevertheless, again a question arises about asymptotic attainability of the corresponding bounds on precision, but the answer seems to be negative [113].

1.1.6 Multi-parameter estimation

Quantum technology applications require precise characterisation of their components via quantum tomography [114], where the density matrix ρ describing a system state is reconstructed from measurement outcomes, and system identification [37, 115], where system dynamics is determined. These tasks require estimation of usually more than a single parameter.

Multi-parameter Cramér-Rao bound. Consider m parameters $\boldsymbol{\phi} = (\phi^{(1)}, \dots, \phi^{(m)})^\top$, whose unknown value is to be estimated. The Cramér-Rao inequality [63] states that the covariance matrix $\Sigma_{\boldsymbol{\phi}}(\hat{\boldsymbol{\phi}})$ of errors of locally unbiased estimators, $\hat{\boldsymbol{\phi}} = (\hat{\phi}^{(1)}, \dots, \hat{\phi}^{(m)})^\top$, is bounded from below by the inverse of the *Fisher information matrix* $I_{\boldsymbol{\phi}}$, cf. (1.6),

$$\begin{aligned} \Sigma_{\boldsymbol{\phi}}(\hat{\boldsymbol{\phi}}) &\geq I_{\boldsymbol{\phi}}^{-1}, \quad \text{where} & (1.20) \\ (\Sigma(\hat{\boldsymbol{\phi}}))_{jk} &= \text{Cov}(\hat{\phi}^{(j)}, \hat{\phi}^{(k)}) = \mathbb{E}(\hat{\phi}^{(j)} - \phi^{(j)})(\hat{\phi}^{(k)} - \phi^{(k)}) \quad \text{and} \\ (I_{\boldsymbol{\phi}})_{jk} &= \sum_{\mathbf{x}} p_{\boldsymbol{\phi}}(\mathbf{x}) \left(\partial_{\phi^{(j)}} \log(p_{\boldsymbol{\phi}}(\mathbf{x})) \right) \left(\partial_{\phi^{(k)}} \log(p_{\boldsymbol{\phi}}(\mathbf{x})) \right). \end{aligned}$$

Moreover, in the quantum metrology setup, where parameters to be estimated are encoded by a quantum channel, $\rho_{\boldsymbol{\phi}} = \Lambda_{\boldsymbol{\phi}}(\rho)$, we further have that the Fisher information matrix is bounded

from above by the *quantum Fisher information matrix* [64, 65], $F_{\Phi}(\rho_{\Phi})$, and thus

$$\begin{aligned} \Sigma_{\Phi}(\hat{\Phi}) &\geq I_{\Phi}^{-1} \geq F_{\Phi}(\rho_{\Phi})^{-1} \quad \text{where} & (1.21) \\ (F_{\Phi}(\rho_{\Phi}))_{jk} &= \frac{1}{2} \text{Tr} \left(\left\{ D_{\rho_{\Phi}}^{(j)}, D_{\rho_{\Phi}}^{(k)} \right\} \rho_{\Phi} \right) \quad \text{and} \\ \frac{1}{2} \left\{ D_{\rho_{\Phi}}^{(k)}, \rho_{\Phi} \right\} &= \partial_{\phi^{(k)}} \rho_{\Phi}. \end{aligned}$$

Note however, that the QFI matrix corresponds in general to m different projective measurements on the eigenbases of the SLDS, $D_{\rho_{\Phi}}^{(k)}$, $k = 1, \dots, m$ and thus may not be attainable. The condition of commutation of all SLDS, $[D_{\rho_{\Phi}}^{(j)}, D_{\rho_{\Phi}}^{(k)}] = 0$, $j, k = 1, \dots, m$ is sufficient for the bound to be achievable in local estimation. In Sec. 1.2 we discuss finding a single optimal measurement so that in the multi-parameter estimation, the trace of the classical Fisher information matrix I_{Φ} , Eq. (1.20), is maximal. Asymptotically, the estimation precision is bounded in the Holevo bound [116]. The Holevo bound has been proven to be achievable recently [117] by methods of Local Asymptotic Normality, where $\rho_{\Phi}^{\otimes N}$ is shown to correspond asymptotically to (in general non-commuting) Gaussian modes. Moreover, the Holevo bound corresponds to the precision of the optimal (usually not projective) POVM performed on the modes, and a collective measurement on $\rho_{\Phi}^{\otimes N}$. When the Gaussian modes commute, the Holevo bound is simply given by the QFI matrix (1.21). This takes place when all the SLDS commute on average, $\text{Tr}([D_{\rho_{\Phi}}^{(j)}, D_{\rho_{\Phi}}^{(k)}] \rho_{\Phi}) = 0$, for $j, k = 1, \dots, m$. For the case of a pure states ρ_{Φ} , the condition of commuting on average was shown to be necessary in order to achieve the QFI already in [118].

Types of parameters. In quantum imaging, an image is described by m phases corresponding to m independent modes, which we refer to as *unitary parameters*. In [119] it has been shown for unitary encoding and pure initial states that optimal multi-parameter estimation yields better results than independent best estimation of each phase, as the total mean square error decreases $\mathcal{O}(m)$ faster when using initial states entangled w.r.t.

all the modes. On the other hand, for system identification also *decoherence parameters* need to be estimated, e.g. losses in optical interferometry. For simultaneous estimation of unitary and decoherence parameters, trade-offs arise due to possible non-commutativity of optimal measurements, for example of optical interferometry see [120–122]. A different setup considers a single *parameter changing in time* according to an unknown function that is to be estimated [123].

For a detailed review of background and recent advances in multi-parameter quantum metrology, see [124].

1.1.7 QFI as a metric

The multi-parameter QFI matrix represents a Riemannian metric on the space of system states [125], which is minimal among monotone metrics [126, 127]. Therefore, it can be used to detect singular changes in the structure of system states corresponding e.g. to quantum phase transitions [128–130] or conversely phase transitions can be used to enhance the estimation precision [107, 131]. In Chapter 2 we will consider the relation between enhanced parameter estimation and dynamical phase transitions [34].

Furthermore, as a metric, the QFI bounds the speed of quantum evolution, in so called *Quantum Speed Limits* [132–135], which can be viewed as a generalisation of the Heisenberg uncertainty for time and energy [136, 137]; for other methods of deriving quantum speed limits see [138–140]. Finally, in turn, the QFI determines also the minimum frequency of the projective measurement on an initial system state, necessary to observe the quantum Zeno effect [141].

In sections below we discuss three aspects of metrology in the presence of decoherence. First in Sec. 1.2, we present a numerical iterative algorithm to find optimal preparation of the initial state ρ and measurement X for a given evolution Λ_ϕ [142].

Secondly, in Sec. 1.3, we deliver bounds on phase estimation precision in the presence of arbitrarily correlated Gaussian dephasing noise showing transition between the standard scaling and the constant scaling [27]. Finally in Sec. 1.4, we prove the Zeno limit $\propto N^{-\frac{3}{2}}$ for frequency estimation in non-Markovian environments [24].

1.2 VARIATIONAL PRINCIPLE FOR QUANTUM FISHER INFORMATION AND NUMERICAL ALGORITHM FOR FINDING OPTIMAL SYSTEM PREPARATION

Since decoherence usually results in a mixed state ρ_ϕ , the maximal quantum Fisher information, $\sup_\rho F_\phi(\rho_\phi)$, is difficult to calculate. In [142] we introduced a variational principle which delivers a convenient numerical algorithm to calculate the maximum QFI for quantum systems of a finite dimension.

1.2.1 Variational principle

Let us consider a quantum metrology setup in which the states used in the estimation are obtained from a quantum channel Λ_ϕ , i.e., $\rho_\phi = \Lambda_\phi(\rho)$, and an observable X is measured on ρ_ϕ in order to retrieve the information about ϕ , see Fig. 1.1. In order to obtain an ultimate limit on precision in local and asymptotic estimation strategies, one optimises the setup in Fig. 1.1 by finding the initial preparation ρ leading to the maximum QFI, $F_\phi^{(\max)} = \sup_\rho F_\phi(\Lambda_\phi(\rho))$.

As we show below, the ultimate limit $F_\phi^{(\max)}$ can be expressed by the following variational principle which includes maximisation w.r.t. both an initial state ρ and an observable X ,

$$F_\phi^{(\max)} = \sup_\rho \sup_X \text{Tr} (G_\phi(X) \rho), \quad \text{where} \quad (1.22)$$

$$G_\phi(X) = -\Lambda_\phi^\dagger (X^2) + 2 (\partial_\phi \Lambda_\phi)^\dagger (X), \quad (1.23)$$

where $\text{Tr} \left((\Lambda_\phi)^\dagger (X) \rho \right) = \text{Tr} (X \Lambda_\phi(\rho))$. A quantum channel Λ_ϕ encoding an unknown value of the parameter ϕ , does not have to be unitary and can represent any decoherence of a state ρ .

Proof of the variational principle. Since $2 \partial_\phi \Lambda_\phi(\rho) = 2 \partial_\phi \rho_\phi = \{D_{\rho_\phi}, \rho_\phi\}$, where $\{\cdot, \cdot\}$ denotes the anti-commutator, cf. (1.8), we have that

$$\begin{aligned} \text{Tr} (G_\phi(X) \rho) &= -\text{Tr} (\rho_\phi X^2) + \text{Tr} (X \{D_{\rho_\phi}, \rho_\phi\}) \\ &= \text{Tr} (\rho_\phi D_{\rho_\phi}^2) - \text{Tr} (\rho_\phi (X - D_{\rho_\phi})^2). \end{aligned}$$

Hence, the first supremum in (1.22) leads to the QFI for $\Lambda_\phi(\rho)$ $\sup_X \text{Tr} (\rho G_\phi(X)) = \text{Tr} (\rho_\phi D_{\rho_\phi}^2) = F(\Lambda_\phi(\rho))$, cf. Eq. (1.7) ■. Note that the parabolic function $G_\phi(X)$, Eq. (1.23), can be replaced by any other function $G'_\phi(X)$ such that for a given initial state ρ , $\text{Tr}(G'_\phi(X) \rho)$ has a global maximum equal to $F(\rho_\phi)$ at $X = D_{\rho_\phi}$.

The value of $F_\phi(\rho, X) := \text{Tr} (\rho G_\phi(X))$ can be viewed as a generalisation of the quantum Fisher information to any projective measurement and a generally biased estimator, encoded in the eigenbasis and the spectrum of an observable X . Note that $F_\phi(\rho, X)$ is a *concave* function of ρ and X , in contrast to the QFI being convex in ρ , cf. (1.10). Furthermore, $F_\phi(\rho, X)$ for given ρ and X provides a *lower bound* for the maximum $F_\phi^{(\max)}$.

Relation to SNR. When the optimisation over X is first done with respect to an optimal linear transformation $\tilde{X} = \alpha X + \beta$ of a given X , it yields $F_\phi(\rho, \tilde{X})$ equal the SNR of X , as $F_\phi(\rho, X)$ is just the difference between twice the signal, $\text{Tr}(\partial_\phi \rho_\phi X)$, and the noise, as $\text{Tr}(\rho_\phi X^2) = \Delta_\phi^2 X + \langle X \rangle_\phi^2$ is minimised when $\langle X \rangle_\phi = 0$ or rather $\beta := -\alpha \langle X \rangle_\phi$. This confirms the inequality between the SNR of any observable and the QFI [68], see Eq. (1.9).

Furthermore, when $F_\phi(\rho, X)$ is optimised only with respect to the choice of X -spectrum and a measurement is fixed as the projective measurement on X -eigenbasis, $F_\phi(\rho, X)$ yields the corresponding Fisher information. In general, for a given POVM measurement $\Pi = \{\Pi_x\}_x$, an analogous variational principle can

be established for the Fisher information corresponding to the optimal initial preparation ρ for that measurement,

$$I_\phi(\Pi) = \sup_{\rho} \sup_{\hat{\phi}} \text{Tr} \left(\rho \left(-\Lambda_\phi^\dagger(X_2) + 2(\partial_\phi \Lambda_\phi)^\dagger(X_1) \right) \right), \quad (1.24)$$

where $\hat{\phi}$ is a used estimator and $X_j := \sum_x \hat{\phi}(x)^j \Pi_x$. When Π is a projective measurement, $X_2 = X_1^2$, and Eq. (1.24) reduces to Eq. (1.23).

Moreover, from the Jensen's inequality for operators [143] it follows that $X_2 = \sum_x \phi(x)^2 \Pi_x \geq (\sum_x \phi(x) \Pi_x)^2 = X_1^2$, where POVM operators $\{\Pi_x\}_x$ play a role of weights, and thus considering more generally the POVM in the variational principle (1.22), also leads to a *projective optimal measurement*.

In the next section we show how the variational principles introduced above can be used to establish numerical iterative algorithms to find optimal initial system preparations.

Example of sequential correlated measurements. Now we show how the variational principle in (1.24) can be used to find an optimal linear estimator, $\hat{\phi}(x) = \sum_{j=1}^n \alpha_j x_j$, in the case when the result of experiment is multidimensional, $x = (x_1, \dots, x_n)$, e.g. corresponding to sequential measurements of the system *during* its dynamics parametrised by ϕ [144] (see also parameter estimation using continuous measurements [37–39]). The signal-to-noise ratio for optimal linear estimator is given by

$$\text{SNR}_\phi^{(\text{linear})} = S_\phi^\top \Sigma_\phi^{-1} S_\phi, \quad (1.25)$$

where $S_\phi = (\partial_\phi \mathbb{E}_\phi x_1, \dots, \partial_\phi \mathbb{E}_\phi x_n)^\top$ is the signal vector, whereas the matrix $\Sigma_\phi = (\mathbb{E}_\phi(x_j x_k) - \mathbb{E}_\phi x_j \mathbb{E}_\phi x_k)_{jk}$ describes correlations between results. This corresponds to the estimator (rescaled for local unbiasedness around ϕ)

$$\hat{\phi}(x_1, \dots, x_n) = \left(\text{SNR}_\phi^{(\text{linear})} \right)^{-1} \sum_{j=1}^n \left(\Sigma_\phi^{-1} S_\phi \right)_j x_j + \phi. \quad (1.26)$$

In the case when the results are i.i.d. we arrive at the optimal estimator being simply proportional to the arithmetic mean of the results, $\hat{\phi}(x) \propto \frac{1}{n} \sum_{k=1}^n x_k$, and corresponding SNR being proportional to n (standard scaling).

We note that the optimal SNR, (1.25), corresponds to the QFI in estimation with correlated Gaussian variables of the same mean ϕ , where we simply have $S_\phi = (1, \dots, 1)^\top$ and thus $\text{SNR}^{(\text{linear})} = \sum_{j,k=1}^n (\Sigma^{-1})_{jk}$ [63]. Moreover, the optimal linear estimator in Eq. (1.26) is optimal among all estimators, furthermore efficient and also globally unbiased.

Derivation. The variational principle (1.24) restricted to linear estimators, $\hat{\phi}(x) = \sum_{j=1}^n \alpha_j x_j + \beta$, and a fixed ρ (or more generally a fixed probability distribution $p_\phi(x)$), yields

$$\begin{aligned} & \max_{\alpha_1, \dots, \alpha_n, \beta} \sum_{x_1, \dots, x_n} \left(p_\phi(x_1, \dots, x_n) \left(\sum_{j=1}^n \alpha_j x_j + \beta \right)^2 \right. \\ & \quad \left. - 2 \partial_\phi p_\phi(x_1, \dots, x_n) \left(\sum_{j=1}^n \alpha_j x_j + \beta \right) \right) \\ & = \max_{\bar{\alpha}, \beta} -\bar{\alpha}^\top \Sigma_\phi \bar{\alpha} - \left(\beta - \bar{\alpha}^\top A_\phi \right)^2 + 2 \bar{\alpha}^\top S_\phi. \end{aligned}$$

Here $\bar{\alpha} = (\alpha_1, \dots, \alpha_n)^\top$ is the vector of coefficients in the linear estimator, and $A_\phi = (\mathbb{E}_\phi x_1, \dots, \mathbb{E}_\phi x_n)^\top$ is the vector of average results. First, the maximum w.r.t. β is achieved when $\beta = \bar{\alpha}^\top A_\phi$. Furthermore, the extremum of the above expression is achieved when the first derivatives w.r.t. $\alpha_1, \dots, \alpha_n$ are 0, which corresponds to

$$\frac{1}{2} \left(\Sigma_\phi^\top + \Sigma_\phi \right) \bar{\alpha} = S_\phi \iff \bar{\alpha} = \Sigma_\phi^{-1} S_\phi,$$

where we used the fact that Σ_ϕ is a symmetric matrix. As the second derivative simply equals minus the correlation matrix, $-\Sigma_\phi \leq 0$, the coefficient vector $\bar{\alpha}$ above indeed corresponds to the optimal choice of a linear estimator. ■

1.2.2 Numerical algorithm to find optimal system preparation

We now introduce an iterative alternating algorithm based on the variational principle in Eq. (1.23). Its construction is based on the observation that the order of two suprema in Eq. (1.23) can be swapped. The convergence of the algorithm to the maximum value of the QFI, $F_\phi^{(\max)}$, is guaranteed for a system of finite-dimension by the *concavity* of $F(\rho, X) = \text{Tr}(G_\phi(X)\rho)$ on the convex sets of system observables X and convex and compact set of initial states ρ . The optimal system preparation is yield by a subsequence of initial states chosen in sequential iterations of the algorithm.

Algorithm. Let $\rho^{(n)}$ be the initial system state considered at n -th step of algorithm. First, we consider the optimal observable X leading to the maximum value of $F_\phi(\rho^{(n)}, X)$. From (1.8) it is attained for the SLD, $X^{(n)} = D_{\rho_\phi^{(n)}}$, and equals the QFI for $\rho_\phi^{(n)}$. Now we *alter* the order of suprema, and choose an initial system state for the next step as the state leading to maximum value of $F_\phi(\rho, D_{\rho_\phi^{(n)}})$. As $F_\phi(\rho, X) = \text{Tr}(G_\phi(X)\rho)$ is *linear* in ρ , we obtain $\rho = \rho^{(n+1)}$ as the *pure* state corresponding to the maximum eigenvalue of $G_\phi(D_{\rho_\phi^{(n)}})$. Note that the quantum Fisher information $F(\rho_\phi^{(n)})$ increases with n ,

$$\begin{aligned} F(\rho_\phi^{(n)}) &= F_\phi\left(\rho^{(n)}, D_{\rho_\phi^{(n)}}\right) \leq F_\phi\left(\rho^{(n+1)}, D_{\rho_\phi^{(n)}}\right) \\ &\leq F_\phi\left(\rho^{(n+1)}, D_{\rho_\phi^{(n+1)}}\right) = F(\rho_\phi^{(n+1)}). \end{aligned} \quad (1.27)$$

The increase in the QFI is thus achieved by alternatively ‘moving’ along two perpendicular ‘directions’ of observables X and initial states ρ . At each step we first go as high as possible in ‘direction’ X and then as high as possible in ‘direction’ ρ . Since $F_\phi(\rho, X)$ is linear w.r.t. ρ , we always choose ρ to be pure, similarly as optimal initial state for a given measurement is always pure due to the convexity of the QFI, cf. Eq (1.10).

In Appendix A.1 we prove that for a system of finite dimension, the algorithm provides the maximum quantum Fisher in-

formation, $\lim_{n \rightarrow \infty} F_{\rho_\phi^{(n)}} = F_\phi^{(\max)}$. In the proof we exploit concavity of $F(\rho, X)$ w.r.t. convex sets of observables X and compact and convex set of initial states ρ . The optimal initial state is given by a subsequence of $\rho^{(n)}$. Although the convergence of the algorithm may not be faster than other algorithms, such as gradient methods, it only requires diagonalising two operators at each step, $\rho_\phi^{(n)}$ and $G_\phi(D_{\rho_\phi^{(n)}})$ and a storage of only one operator at each step.

An analogous algorithm for the variational principle in the case of a fixed POVM, see Eq. (1.24), can be proved to converge as in Appendix A.1. Let us also note that convergence of similar algorithm used in quantum Bayesian estimation [76, 77] can be proved analogously. We note as well that the algorithm is formally similar to the Expectation Maximisation algorithm [145] and similar extensions as in the case of the EM algorithm may be applicable [146].

Restricted set of initial states. If we restrict the set of initial states in Eq. (1.23) to a subset S , e.g. to matrix-product states or Gaussian states, we obtain a variational principle for the maximum quantum Fisher information in S ,

$$\sup_{\rho \in S} F(\rho_\phi) = \sup_{\rho \in S} \sup_X F_\phi(\rho, X) \quad (1.28)$$

Furthermore, when the set S is convex (or at least there exist an open convex neighbourhood around optimal (ρ, D_{ρ_ϕ}) , see Appendix A.1), an analogous alternating iterative algorithm will converge to $\sup_{\rho \in S} F(\rho_\phi)$, which we demonstrate on the following example.

Example of frequency estimation. Consider estimation of the frequency ω of N two-level atom in the presence of collective Markovian dephasing, i.e., $\rho_{\omega, t} = e^{-\frac{i}{2}\omega t \sum_{j=1}^N \sigma_z^{(j)}} \Lambda_t(\rho) e^{\frac{i}{2}\omega t \sum_{j=1}^N \sigma_z^{(j)}}$, where $\sigma_z^{(j)} = -|0^{(j)}\rangle\langle 0^{(j)}| + |1^{(j)}\rangle\langle 1^{(j)}|$ with $|0^{(j)}\rangle$ being the ground and $|1^{(j)}\rangle$ the excited state of j -th atom, whereas Λ_t represents action of dephasing noise. In particular, for fully symmetric

states we have $\langle n|\Lambda_t(\rho)|m\rangle = e^{-\gamma t(n-m)^2}\langle n|\rho|m\rangle$, where γ is dephasing rate and $|n\rangle$ denotes the state of n atoms excited and the rest, $N - n$, in the ground state. In order to fully optimise the estimation setup, one need not only consider an initial state ρ and an observable X , but also possibility of dividing a total time T into $n = \frac{T}{t}$ single experiments each lasting time t , in which case the corresponding total quantum Fisher information equals $F^{(\text{total})} = \frac{T}{t} F(\rho_{\omega,t})$. Fig. 1.2 shows

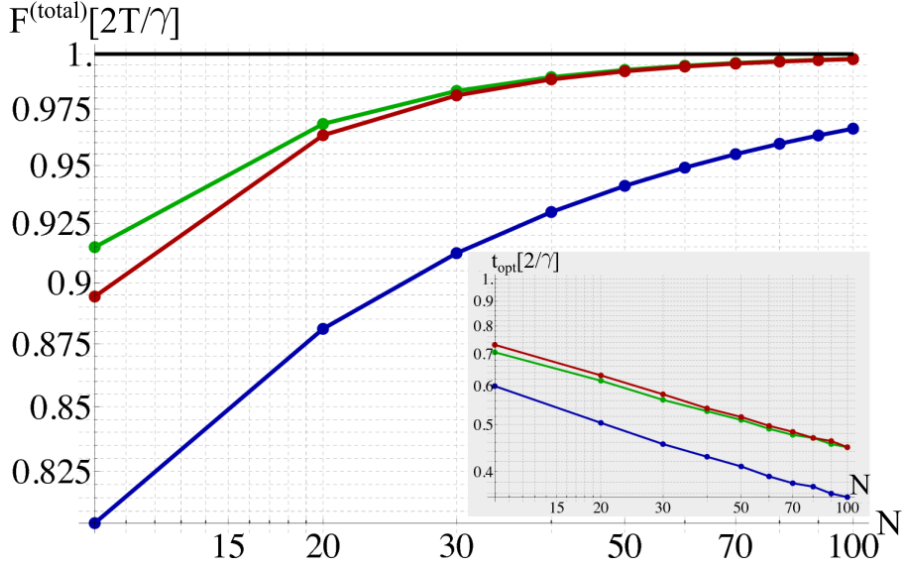


Figure 1.2: **Optimal frequency estimation with collective dephasing:** $F^{(\text{total})}$ for the optimal symmetric states (green) found using the algorithm, the Berry-Wiseman states [75] (red) and the uncorrelated states (blue). Black curve corresponds to the bound $2T/\gamma$ [84]. The inset shows corresponding optimal times of a single experiment.

results for optimal choices of t and symmetric initial state obtained using the algorithm, which achieve an ultimate bound for frequency estimation in the presence of collective dephasing, $F^{(\text{total})} \leq \frac{T}{t} t^2 (N^{-2} + 2\gamma t)^{-1} \leq 2T/\gamma$, which can be derived from a phase-estimation bound in [84]. This confirms that the algorithm indeed converges to $F_{\omega}^{(\text{max})}$. The bound is also approached by the optimal separable states for large N , but the convergence rate is bigger for entangled preparations. One-axis and two-axes squeezed states [28] perform as well as the opti-

mal fully symmetric states for moderate and large N .

Experimental implementation of the algorithm. If diagonalisation of the operators $G_\phi(X)$ and ρ_ϕ is difficult, the algorithm can be generalised as follows. In the n -th step an observable $X^{(n)}$ is fine to be chosen as long as $F_\phi(\rho^{(n)}, X^{(n)}) > F_\phi(\rho^{(n)}, X^{(n-1)})$, and a state for the next step $\rho^{(n+1)}$ when $F_\phi(\rho^{(n+1)}, X^{(n)}) > F_\phi(\rho^{(n)}, X^{(n)})$. This way an increasing sequence $F_\phi(\rho^{(n)}, X^{(n)})$ is obtained. This can be further refined by considering in each step after choice $\tilde{X}^{(n)}$, its linear transformation $\tilde{X}^{(n)}$ leading to $F_\phi(\rho^{(n)}, X^{(n)})$ being its SNR. Furthermore, this generalised algorithm can be actually implemented experimentally or through random sampling techniques *without* any knowledge of X or ρ beyond the signal $\partial_\phi \langle X \rangle_\phi$ and the noise $\Delta_\phi^2 X$ which determine $F_\phi(\rho, X)$, cf. (1.23). Although the series $F_\phi(\rho^{(n)}, X^{(n)})$ does not necessary converge to $F_\phi^{(\max)}$, it provides a way of consistently improving the estimation setup.

1.2.3 Multi-parameter case

Multi-parameter variational principle. Consider quantum dynamics which depends on a vector of m parameters, $\boldsymbol{\phi} = (\phi^{(1)}, \dots, \phi^{(m)})^T$, so that $\rho_\phi = \Lambda_\phi(\rho)$, see Sec. 1.1.6. We introduce a *multi-parameter variational principle* that yields the maximum sum of the Fisher informations w.r.t. a single projective measurement, and thus the trace of the corresponding Fisher information matrix I_ϕ , which is not necessary diagonal, see Eq. (1.20),

$$\sup_{\rho, \Pi} \sum_{k=1}^n I_{\phi^{(k)}}(\rho, \Pi) = \sup_{\rho} \sup_{X, \bar{f}} \sum_{k=1}^m F_\phi^{(k)}(\rho, f^{(k)}(X)), \quad \text{where}$$

$$F_\phi^{(k)}(\rho, X) = \text{Tr} \left(G_\phi^{(k)}(X) \rho \right), \quad (1.29)$$

with the parabolic functions of an observable, similarly as in one-parameter case of Eq. (1.23), are

$$G_\phi^{(k)}(X) = -\Lambda_\phi^\dagger(X^2) + 2(\partial_{\phi_k} \Lambda_\phi(\rho))^\dagger(X), \quad (1.30)$$

and in order to consider any estimator for each parameter corresponding to just one projective measurement given by the eigenbasis of X , we introduce a set of polynomial functions, $\bar{f} = (f^{(1)}, \dots, f^{(m)})^\top$, of an observable X of the order of the system space dimension $d = \dim(\mathcal{H})$,

$$f^{(k)}(X) = \sum_{j=1}^d \alpha_j^{(k)} X^j + \beta^{(k)}. \quad (1.31)$$

Note that in order to be able to reproduce any estimator, we need a non-degenerate spectrum of X . That is why we consider the optimisation w.r.t X and \bar{f} together, cf. $\sup_{X, \bar{f}}$ in (1.30). Note that we consider optimisation with respect to only $d \times m$ more variables than in one-dimensional case. Note that using Lagrange multipliers for commuting observables Y_1, \dots, Y_m corresponding to m parameters, i.e., the variational principle with $\sum_{k=1}^m F_{\Phi}^{(k)}(Y_k, \rho)$, with a condition of all m observables commuting requires $d(d-1)/2 \times m(m-1)/2$ multipliers.

Trade-off in multi-parameter estimation. Note that in the variational principle each term $F_{\Phi}^{(k)}(\rho, X)$ is maximised at in general different $X = D_{\rho_{\Phi}}^{(k)}$, and the principle represents a trade-off between the estimation precision for different parameters, cf. [121, 122].

Optimal projective measurement for a given state. From the supremum over X and polynomials \bar{f} , we can derive the equations for

optimal projective measurement for a given state ρ and dynamics Λ_ϕ as follows.

$$\begin{aligned}
 & - \sum_{k=1}^m \sum_{j=1}^d \alpha_j^{(k)} \left(\sum_{j'=1}^d \alpha_{j'}^{(k)} \sum_{l=1}^{j+j'} X^{l-1} (\rho_\phi) X^{j+j'-l} \right. \\
 & \quad \left. + 2\beta^{(k)} \sum_{l=1}^j X^{l-1} (\rho_\phi) X^{j-l} + \sum_{l=1}^j X^{l-1} (\partial_{\phi_k} \rho_\phi) X^{j-l} \right) = 0, \tag{1.32}
 \end{aligned}$$

$$\text{Tr} \left(X^j \left\{ -f^{(k)}(X) + D_{\rho_\phi}^{(k)}, \rho_\phi \right\} \right) = 0, \quad \text{for } k = 1, \dots, m, \quad j = 1, \dots, d, \tag{1.33}$$

$$\text{Tr} \left(f^{(k)}(X) \rho_\phi \right) = 0, \quad \text{for } k = 1, \dots, m, \tag{1.34}$$

where $D_{\rho_\phi}^{(k)}$ is the SLD corresponding to ϕ_k and above equations corresponds to derivatives w.r.t to X in (1.32), $\alpha_j^{(k)}$ in (1.33), and $\beta^{(k)}$ in (1.34). Note that when there exist k such that $f^{(k)}(X)$ has a non-degenerate spectrum, we can simply choose $f^{(k)}(X) = X$, since X is varied as well.

Iterative alternating algorithm. When Eqs. (1.32-1.34) can be solved, we can also introduce an iterative numerical algorithm to find both the optimal state and the optimal measurement. Again, a generalised algorithm can be performed via experiment/random sampling techniques, without knowing X of ρ only with control over ϕ , but higher moments of X , up to d -th moment, need to be measured, cf. Eq. (1.31).

If we fix X (with non-degenerate spectrum) and consider optimisation with respect to an initial state ρ and polynomials \bar{f} only, we obtain the maximum sum of the Fisher informations for the projective measurement on the eigenbasis of X , cf. (1.24). If instead of polynomials, we simply consider linear transformations, we obtain the maximum sum of the SNRs for the observable X . The latter approach can be useful in the generalised algorithm, in the case when it would take a long time to gather the data to estimate the higher moments of X .

1.2.4 Summary

In this section we presented a variational principle for the maximum quantum Fisher information. This variational principle leads to a computationally efficient iterative algorithm. We illustrated its good performance on the example of frequency estimation in the presence of collective dephasing. Moreover, in the case of multi-parameter estimation, we derived a variational principle maximising the trace of Fisher information matrix w.r.t. to a single projective measurement, and delivered the equations for the optimal projective measurement given a system preparation.

1.3 PRECISION LIMITS FOR PHASE ESTIMATION IN THE PRESENCE OF CORRELATED DEPHASING NOISE

In this section we come back to the simplest quantum metrology setup of interferometry, in which parameter ϕ being estimated is just a phase, cf. Fig. 1.1. We consider a phase encoded by a local Hamiltonian in the presence of dephasing which commutes with the phase encoding, i.e., $\rho_\phi = e^{-i\phi H} \Lambda^{(N)}(\rho) e^{-i\phi H}$, where the Hamiltonian $H = \sum_{j=1}^N H_j$ with $H_j = \mathbb{1}^{\otimes(j-1)} \otimes h \otimes \mathbb{1}^{\otimes(N-j)}$. It is known that for local (independent) dephasing noise, $\Lambda^{(N)} = \Lambda^{\otimes N}$, the scaling of the QFI is at most *standard* in the number N of subsystems [15, 16], while for collective (fully correlated) dephasing, the scaling is at most *constant* [84].

In [27] we derived an upper bound on the QFI for phase estimation in the presence of semi-classical spatially-correlated Gaussian dephasing, see Eq. (1.37), which shows a transition between the standard and the constant scaling, depending on the form of the decay of noise correlations. Below we sketch the derivation and discuss main results of [27].

1.3.1 Semi-classical correlated Gaussian dephasing

Semi-classical dephasing noise can be simply viewed as introducing additional *random phases* $\{\phi_j\}_{j=1}^N$ to the subsystems dynamics, beyond the phase ϕ we want to estimate. Those random phases vary from one experiment to another, and the average state is given by

$$\Lambda_\phi(\rho) = \int d\varphi_1 \dots d\varphi_N g(\varphi_1, \dots, \varphi_N) e^{-i \sum_{j=1}^N (\phi + \varphi_j) H_j} \rho e^{i \sum_{j=1}^N (\phi + \varphi_j) H_j}, \quad (1.35)$$

where we assume a Gaussian distribution of random phases $p(\varphi_1, \dots, \varphi_N) = \sqrt{2\pi \det \Sigma} e^{-\frac{1}{2} \sum_{j,k=1}^N (\varphi_j - \mu_j) (\Sigma^{-1})_{jk} (\varphi_k - \mu_k)}$, which is determined by the covariance matrix of correlations, $\Sigma_{jk} = \mathbb{E}(\varphi_j \varphi_k) - \mu_j \mu_k$, and the means, $\mu_j = \mathbb{E}\varphi_j$, of the random phases. Without loss of generality we can assume $\mu_j = 0$, which corresponds to the measurement of an observable X unitarily transformed as $e^{i \sum_{j=1}^N \mu_j H_j} X e^{-i \sum_{j=1}^N \mu_j H_j}$. When the random phases are independent and identically distributed phases, the dephasing is *local*, whereas the fully correlated phases, $\varphi_j = \varphi_k$, $1 \leq j, k \leq N$, correspond to *collective dephasing*. Correlations in noise can be due to e.g. spatial correlations in unaccounted magnetic fields, or interactions with common baths [100].

1.3.2 Bound on phase estimation precision

Note that there are two contributions to estimation errors.

Firstly, the *quantum noise* related to the fact that phases encoded in a quantum state cannot be observed directly, but can be retrieved only via probabilistically distributed results of measuring an observable X . Even, when system dynamics is unitary, the mean square error is always at least equal to the inverse of the QFI, cf. (1.7), which takes into account available resources, i.e., the number N of subsystems and multipartite correlations in an initial state ρ .

Secondly, in the presence of correlated Gaussian dephasing, even if the phases encoded in the evolved system state could be observed directly and values of $\{\phi + \varphi_j\}_{j=1,\dots,N}$ could be reconstructed, the randomness of $\{\varphi_j\}_{j=1,\dots,N}$ would yield *classical noise* in estimating ϕ given by the minimum error of estimating the mean ϕ of Gaussian random phases $\phi + \varphi_{j=1,\dots,N}$, which error we denote as Δ_Σ^2 .

Using Bayesian estimation tools exploiting knowledge about the random phases distribution, see Sec. 1.1.2.4, we derive a lower bound on the mean square error in phase estimation for all locally unbiased estimators $\hat{\phi}$,

$$\begin{aligned} \Delta_\phi^2 \hat{\phi} &\geq F_\phi(\mathbf{U}_\phi \rho \mathbf{U}_\phi^\dagger)^{-1} + \Delta_\Sigma^2 \\ &\geq N^{-2}(\mathfrak{h}_{\max} - \mathfrak{h}_{\min})^{-2} + \Delta_\Sigma^2. \end{aligned} \quad (1.36)$$

Furthermore, note that this bound corresponds to an upper bound on the QFI,

$$\begin{aligned} F_\phi(\Lambda_\phi(\rho)) &\leq \left(F_\phi(\mathbf{U}_\phi \rho \mathbf{U}_\phi^\dagger)^{-1} + \Delta_\Sigma^2 \right)^{-1} \\ &\leq \left(N^{-2}(\mathfrak{h}_{\max} - \mathfrak{h}_{\min})^{-2} + \Delta_\Sigma^2 \right)^{-1}. \end{aligned} \quad (1.37)$$

The bound is tight for weak decoherence, since it recovers the Heisenberg scaling as dephasing strength decreases to 0. We will exploit this feature in the next Sec. 1.4, in order to derive limits on the frequency estimation in the presence of non-Markovian dephasing noise. As we demonstrate in the examples below, for fully correlated random phases the bound yields a constant limit [84], which is also the case whenever the correlations do not decay to 0. For i.i.d. random phases we obtain the standard limit, as earlier derived in [15, 16], and this limit is also preserved for exponentially decaying correlations, see Fig. 1.3.

Universality of the bound. Although in the derivation of the bound (1.36) we consider semi-classical dephasing model, in which Gaussian random phases are introduced to subsystems

dynamics while encoding a phase ϕ , the bound is not necessary limited only to this model.

First, let us consider the case of the i.i.d. phases with variance σ^2 , in which case the dephasing is local and fully determined by its action on a single subsystem. In particular, for subsystem of a qubit and $h = \frac{1}{2}\sigma_z$, we obtain (in the eigenbasis of σ^z)

$$\Lambda_\phi(\rho) = \begin{pmatrix} \rho_{00} & \rho_{01} e^{i\phi - \frac{\sigma^2}{2}} \\ \rho_{10} e^{-i\phi - \frac{\sigma^2}{2}} & \rho_{11} \end{pmatrix}, \text{ where } \rho = \begin{pmatrix} \rho_{00} & \rho_{01} \\ \rho_{10} & \rho_{11} \end{pmatrix}, \quad (1.38)$$

which is a general structure of any dephasing channel acting on a qubit. Furthermore, in phase estimation, the ultimate precision of measuring a state $\Lambda_\phi(\rho)$, given by the inverse of QFI, depends only the state ρ , and thus depends on the noise only via the strength value $\sigma^2/2$, not any other details of the model. As the variance σ^2 is not limited for uncorrelated Gaussian random phases in the semi-classical model, any other model of local dephasing can be mimicked by this model, and thus the bound (1.36) holds true.

Furthermore, for a system consisting of N subsystems undergoing correlated dephasing described by the following Lindblad master equation [8, 9],

$$\begin{aligned} \frac{d}{dt}\rho_\omega(t) &= -i\omega \left[\sum_{j=1}^N H_j, \rho_\omega(t) \right] \\ &+ \frac{1}{2} \sum_{j,k=1}^N \Sigma(t)_{jk} \left(H_j \rho_\omega(t) H_k - \frac{1}{2} \{H_j H_k, \rho_\omega(t)\} \right), \end{aligned} \quad (1.39)$$

the resulting system dynamics at time t is identical to that of a semi-classical Gaussian model with the covariance matrix $\int_0^t du \Sigma(u)$ and the average $\phi = \omega t$. Therefore, the bound (1.36) is also true for such a class of dephasing noise. For example of such a quantum noise model derived from unitary dynamics of subsystems interacting with baths, see [100].

Derivation. Let us first consider a thought experiment in which phases encoded in an evolved system state can be accessed directly in each realisation of the experiment, i.e., the phases of the state $e^{-i \sum_{j=1}^N (\phi + \varphi_j) H_j} \rho e^{i \sum_{j=1}^N (\phi + \varphi_j) H_j}$. Furthermore, let us assume that we can reconstruct all the values $\{\phi + \varphi_j\}_{j=1, \dots, N}$, in contrast to e.g. an initial state ρ chosen as the GHZ state that encodes only the phase $N\phi + \sum_{j=1}^N \varphi_j$. We have that $\tilde{\varphi}_j = \phi + \varphi_j$, $j = 1, \dots, N$, are Gaussian variables with the covariance matrix Σ and identical means ϕ . From Eqs. (1.25) and (1.26), the mean ϕ is then efficiently estimated with a linear estimator $\varphi_\Sigma = \sum_{j=1}^N \gamma_j \tilde{\varphi}_j$, where $\gamma_j = \sum_{k=1}^N (\Sigma^{-1})_{jk} / \sum_{j,k=1}^N (\Sigma^{-1})_{jk}$ gives the unbiased estimator as $\sum_{j=1}^N \gamma_j = 1$. The mean square error of this estimator is $\Delta_\Sigma^2 = \sum_{j,k=1}^N (\Sigma^{-1})_{jk}$. Note that this linear estimator φ_Σ itself is just a random phase whose distribution is Gaussian with mean ϕ and variance Δ_Σ^2 , and it contains all the information about ϕ therefore giving so called *sufficient statistics* [63].

In a real estimation experiment, however, phases in an evolved system state cannot be accessed directly, but only through a POVM measurement performed on the state. Nevertheless, as we know the Gaussian distribution of random phases $\{\varphi_j\}_{j=1}^N$, in order to estimate $\phi = \phi_0 + \delta\phi$ from a measurement result x , we first use Bayesian estimation to construct optimal estimators of $\{\tilde{\varphi}_j\}_{j=1}^N$ (assuming their means equal ϕ_0), which we denote as $\{\tilde{\varphi}_j(x)\}_{j=1}^N$, and then simply use the linear estimator, $\hat{\phi}(x) = \sum_{j=1}^N \gamma_j \tilde{\varphi}_j(x)$, to estimate ϕ . From Bayesian estimation, we have $\sum_x p_{\phi_0}(x) \hat{\phi}(x) = \phi_0$. Moreover, this estimator is *optimal* (up to a linear transformation guaranteeing local unbiasedness around $\phi = \phi_0$),

$$F_{\phi_0} = \text{SNR}_{\phi_0}(\hat{\phi}) = \frac{(\partial_\phi|_{\phi=\phi_0} \mathbb{E}_\phi \hat{\phi})^2}{\Delta_{\phi_0}^2 \hat{\phi}} = (\Delta_\Sigma^2)^{-2} \Delta_{\phi_0}^2 \hat{\phi}, \quad (1.40)$$

where we also used the fact that the signal $\partial_\phi|_{\phi=\phi_0} \mathbb{E}_\phi \hat{\phi} = (\Delta_\Sigma^2)^{-1} \Delta_{\phi_0}^2 \hat{\phi}$ (for all derivations see Appendix A.2.2).

On the other hand, $\hat{\phi}$ is also the optimal Bayesian estimator for the phase φ_Σ (see Appendix A.2.1). Hence, from Eq. (1.17) we have that its average mean square error

$$\text{AME}(\hat{\phi}) = \Delta_\Sigma^2 - \Delta_{\phi_0}^2 \hat{\phi}. \quad (1.41)$$

The estimator necessary obeys the van Trees inequality [79, 80], see Eq. (1.14),

$$\text{AME}(\hat{\phi}) \geq \left((\Delta_\Sigma^2)^{-1} + \int_{\mathbb{R}} d\varphi_\Sigma p(\varphi_\Sigma) F_{\varphi_\Sigma} \right)^{-1}, \quad (1.42)$$

where we used the easy fact that for Gaussian distribution of φ_Σ we have $I_{\text{prior}} = (\Delta_\Sigma^2)^{-1}$. Moreover, φ_Σ indeed plays a role of a *phase* and is encoded in the system state via the same Hamiltonian H (see Appendix A.2.3). Thus, the Fisher information F_{φ_Σ} for any measurement can be shown to be no more than the QFI with unitary dynamics, $F_{\varphi_\Sigma} \leq F(\mathbf{U}_\phi \rho \mathbf{U}_\phi^\dagger)$.

Therefore, combining Eqs. (1.41) and (1.42) we arrive at

$$\Delta_{\phi_0}^2 \hat{\phi} \leq \Delta_\Sigma^2 - \left((\Delta_\Sigma^2)^{-1} + F_{\phi_0}(\mathbf{U}_{\phi_0} \rho \mathbf{U}_{\phi_0}^\dagger) \right)^{-1}, \quad (1.43)$$

which together with Eq. (1.40) yields the main result

$$F_{\phi_0} \leq \left(F_{\phi_0}(\mathbf{U}_{\phi_0} \rho \mathbf{U}_{\phi_0}^\dagger)^{-1} + \Delta_\Sigma^2 \right)^{-1}. \quad (1.44)$$

Optimisation with respect to a performed POVM measurement leads to Eq. (1.36). ■

1.3.3 Examples

Let us consider two examples of correlated dephasing with covariance matrices given by

$$\Sigma_1 = \sigma^2 \begin{pmatrix} 1 & \alpha & \cdots & \alpha \\ \alpha & 1 & \alpha & \cdots & \alpha \\ \vdots & \ddots & \ddots & \ddots & \vdots \\ \alpha & \cdots & \alpha & 1 & \alpha \\ \alpha & \cdots & \alpha & \alpha & 1 \end{pmatrix}, \quad (1.45)$$

$$\Sigma_2 = \sigma^2 \begin{pmatrix} 1 & \alpha & \alpha^2 & \cdots & \alpha^{N-1} \\ \alpha & 1 & \alpha & \cdots & \alpha^{N-2} \\ \vdots & \ddots & \ddots & \ddots & \vdots \\ \alpha^{N-2} & \cdots & \alpha & 1 & \alpha \\ \alpha^{N-1} & \cdots & \alpha^2 & \alpha & 1 \end{pmatrix}, \quad (1.46)$$

which leads to

$$\Delta_{\Sigma_1}^2 = \sigma^2 \left(\alpha + \frac{1-\alpha}{N} \right), \quad \Delta_{\Sigma_2}^2 = \sigma^2 N^{-1} \frac{1+\alpha}{1-\alpha + \frac{\alpha}{N}}. \quad (1.47)$$

Therefore, from Eq. (1.36), for any value $0 < \alpha < 1$, for constant correlations, Σ_1 , the lower bound on the mean square error converges to a constant, $\sigma^2 \alpha$, whereas for exponentially decaying correlations, Σ_2 , we obtain asymptotically the standard scaling $\sim \sigma^2 N^{-1} \frac{1+\alpha}{1-\alpha}$, see Fig. 1.3. Note that, both for Σ_1 and Σ_2 , the case $\alpha = 1$ corresponds to collective dephasing and

$$\Delta_{\phi}^2 \hat{\phi} \geq \left(\sigma^2 + \frac{1}{F(\mathbf{U}_\phi \rho \mathbf{U}_\phi^\dagger)} \right) \geq \left(\sigma^2 + N^{-2} \right), \quad (1.48)$$

where in the second inequality we assumed $(h_{\max} - h_{\min})^2 = 1$, as is the case in the two-arm interferometry. An analogous bound was derived for two-arm interferometry with Gaussian

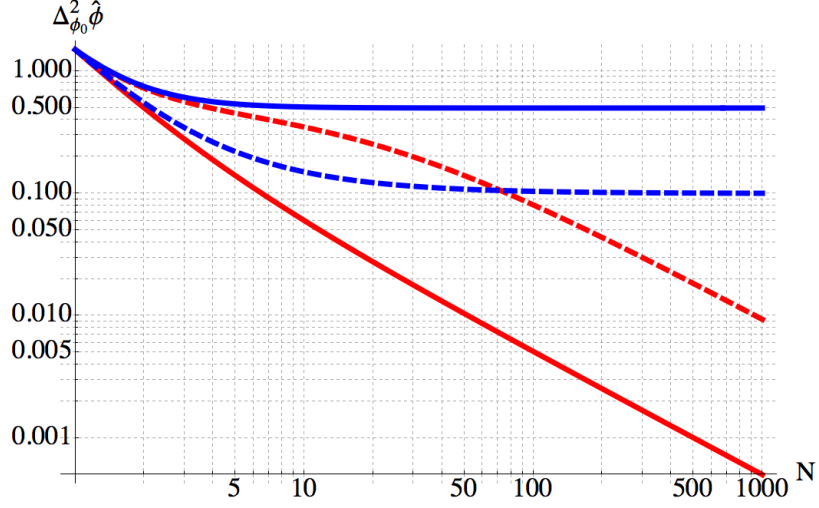


Figure 1.3: **Error scaling in phase estimation with correlated dephasing** Lower bounds on the errors in phase estimation using N two-level atoms, cf. Eq. (1.36). The difference in scaling with N , between independent $\propto N^{-1}$ (red solid) and collective dephasing $\propto 1$ (blue solid) is clearly visible. Exponentially decaying correlations preserve the $\propto N^{-1}$ scaling (red dashed; $\alpha = 0.9$), whereas non-decaying correlations limit the precision scaling to a constant error (blue dashed; $\alpha = 0.2$). Dephasing strength $\sigma^2 = 0.5$.

state of photons [84]. The case of $\alpha = 0$ corresponds to independent random phases and local dephasing with

$$\Delta_{\phi}^2 \hat{\phi} \geq N^{-1} \left(\sigma^2 + \frac{N}{F(U_{\phi} \rho U_{\phi}^{\dagger})} \right) \geq N^{-1} (\sigma^2 + N^{-1}). \quad (1.49)$$

In [16] a different bound has been derived, $\Delta_{\phi_0}^2 \hat{\phi} \geq N^{-1} (e^{\sigma^2} - 1)$, which works better for strong dephasing, $e^{\sigma^2} - 1 \gg N^{-1}$, but does not provide the Heisenberg scaling for weak noise when $\sigma^2 \rightarrow 0$. Both bounds show the standard scaling $\propto N^{-1}$ when $N \rightarrow \infty$.

1.3.4 Comments and summary

Derivation of the bounds (1.48) and (1.49) lends a simple explanation to the constant and linear precision scaling with the collective [84] and local dephasing noise [16], respectively. For

fully correlated random phases, leading to collective dephasing noise, all the subsystems experience a shift by *the same* random phase $\phi + \varphi$, and therefore noise of φ cannot be eliminated, leading to the estimation error bounded by the random phase variance, σ^2 . Only by repeating the experiment n times when there are no correlation in the noise between experiments, one can further reduce the errors to σ^2/n . On the other hand, N i.i.d. random phases leading to local dephasing noise, always give a contribution to estimation errors that scales as N^{-1} due to the Central Limit Theorem (CLT) for the classical noise.

In this section we derived a bound on phase estimation precision in the presence of correlated Gaussian dephasing noise, cf. Eq. (1.36), which delivers the standard limit for exponentially decaying correlations, while for correlations not decaying to 0 asymptotically, imposes the constant limit. In derivation of the bound, we exploited the fact that the dephasing channel Λ_ϕ can be represented as an average over a Gaussian distribution of unitary channels, cf. Eq. (1.35). Therefore, this bound should extend to other channels by modifying the *local classical simulation* method of deriving bounds on the QFI [16], in which the encoding channel is also represented as an average over a probability distribution over the space of quantum channels. This way, new bounds on the QFI in the presence of other correlated noise can be found, and such bounds will be tight for weak decoherence.

1.4 PRECISION LIMITS FOR FREQUENCY ESTIMATION WITH NON-MARKOVIAN DEPHASING, DAMPING AND DEPOLARISING NOISE

An entangled state can be very sensitive to changes introduced to its dynamics and thus can be used as a precise sensor of dynamics parameters. For unitary dynamics of N entangled two-level atoms, precision in frequency estimation is Heisenberg-limited and scales as N^{-2} , whereas uncorrelated states give only the standard-limited precision that scales as N^{-1} . How-

ever, when interactions with external environment lead to local Markovian noise ¹ such as dephasing, depolarisation or amplitude damping, the precision scales at most as N^{-1} for all atom preparations and the quantum enhancement is limited just to a constant [12, 15, 16, 93, 94], see discussion in Sec. 1.1.4.

In this section we discuss frequency estimation in the presence of non-Markovian noise [22, 23, 27, 102]. Markovian dynamics are defined by their semi-group structure, which together with complete positivity of the dynamics leads to their characterisation by a Lindblad master equation [8, 9], see also Sec. 2.1.1. Such a general description, which is a consequence of approximation of weak system-environment interaction and much shorter environment timescales, is missing, however, when those approximations do not hold and system dynamics are non-Markovian. Nevertheless, using a universal bound on phase estimation precision in the presence of local dephasing derived in the previous section, for models featuring initial Zeno dynamics, we show that the *Zeno limit* $\propto N^{-3/2}$ in frequency precision is indeed the best possible scaling for all atom preparations and measurements [27]. This limit was demonstrated for system initially prepared in the GHZ state and the parity measurement [22, 23]. Furthermore, the Zeno limit can be achieved only for experiments performed within the Zeno dynamics-regime, whereas for longer experiments the precision scaling is necessarily standard. Moreover, using similar arguments as given for dephasing noise below, we can show that the Zeno limit also holds for local non-Markovian models of depolarisation or amplitude damping noise. In [102], the Zeno limit result was proven for all noise models commuting with frequency encoding.

¹ Here the Markovian noise refers to time-homogenous Markovian noise, so that $\Lambda_{t_1+t_2} = \Lambda_{t_2} \circ \Lambda_{t_1}$, and any other case we refer to as non-Markovian. We remark that in the literature on non-Markovianity it is common to consider any *divisible dynamics* to be Markovian, i.e., $\Lambda_{t_1+t_2} = \tilde{\Lambda}_{t_2,t_1} \circ \Lambda_{t_1}$, where $\tilde{\Lambda}_{t_2,t_1}$ represents some quantum dynamics, and in general $\tilde{\Lambda}_{t_2,t_1} \neq \Lambda_{t_2}$.

1.4.1 Frequency estimation

Let us recall that a frequency estimation experiment with a system of N two-level atoms consist of three stages: system preparation in an initial state ρ , evolution into $\rho_{\omega,t} = \Lambda_{\omega,t}^{(N)}(\rho)$ within time t and measurement of an observable X on $\rho_{\omega,t}$, which leads to estimation precision given by the inverse of the SNR, $((\partial_{\omega}\langle X \rangle_{\omega,t})^2 / \Delta_{\omega,t}^2 X)^2$, see Fig. 1.4 for an example of Ramsey interferometry. Within total time T , this single experiment is repeated $\frac{T}{t}$ times, assuming that preparation and measurement times are negligible, which leads to total precision $(\frac{T}{t} (\partial_{\omega}\langle X \rangle_{\omega,t})^2 / \Delta_{\omega,t}^2 X)^{-1}$ when the experiments are independent.

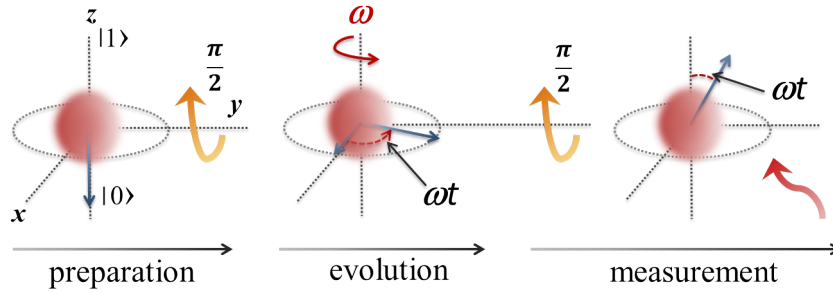


Figure 1.4: **Ramsey spectroscopy** [4, 147]. N two-level atoms in the ground state $|0\rangle^{\otimes N}$ are prepared using the Ramsey $\frac{\pi}{2}$ pulse, which drives each atom into the superposition of the ground and excited states, $\frac{1}{\sqrt{2}}(|0\rangle + |1\rangle)^{\otimes N}$. Next, the atoms evolve for time t , each gaining a relative phase $\phi = \omega t$. Finally, to retrieve ϕ , another $\frac{\pi}{2}$ pulse is applied and the excited state population is measured via stimulated emission, $X = J_x$. SNR equals Nt^2 when the dynamics is unitary and $\phi = \frac{\pi}{2}$. This figure originally appeared in [24].

We want to establish an *ultimate limit* to the estimation precision, by optimising the system preparation ρ , a measurement X and time t of a single experiment, for frequency estimation using N atoms within total time T . Firstly, for a given initial state ρ and time t of dynamics, the optimal X is a linear function of the SLD, $D_{\rho_{\omega,t}}$, see Eqs. (1.8) and (1.7), so that the correspond-

ing SNR equals QFI, $F_\omega(\rho_{\omega,t})$. Secondly, the optimal initial state is the one leading to the maximum QFI, $\max_\rho F_\omega(\rho_{\omega,t})$. Finally, by optimizing time t of a single time, we arrive at the limit,

$$\Delta_\omega^2 \hat{\omega} \geq \min_{t \leq T} \left(\frac{T}{t} \sup_\rho F_\omega(\rho_{\omega,t}) \right)^{-1}. \quad (1.50)$$

Relation to phase estimation. Consider unitary dynamics given by $\rho_{\omega,t} = e^{-i\omega t H} \rho e^{-i\omega t H}$, where the Hamiltonian is given as $H = \frac{1}{2} \sum_{j=1}^N (-|0^{(j)}\rangle\langle 0^{(j)}| + |1^{(j)}\rangle\langle 1^{(j)}|)$ with $|0^{(j)}\rangle$, $|1^{(j)}\rangle$, being the ground and the excited state of j -th atom, respectively. In this case, the bound in Eq. (1.50) reduces to

$$\Delta_\omega^2 \hat{\omega} \geq N^{-2} T^{-2}. \quad (1.51)$$

This limit corresponds to the optimal GHZ preparation encoding effectively a *relative phase* $N\phi$, where $\phi = \omega T$, see discussion in Sec. 1.1.3. Moreover, for any system preparation followed by the unitary dynamics, the frequency ω is encoded in $\rho_{\omega,t}$ always via the phase $\phi = \omega t$. Therefore, we have $F_\omega(\rho_{\omega,t}) = t^2 F_\phi(e^{-i\phi H} \rho e^{i\phi H})$, and moreover, the QFI $F_\phi(e^{-i\phi H} \rho e^{i\phi H})$ is independent from ϕ value and we denote $F_\phi(e^{-i\phi H} \rho e^{i\phi H}) =: F(\rho)$. It simply follows that the optimal time of a single experiment is $t = T$, when the encoded phase ϕ is the largest.

Consider now dynamics with local noise, $\Lambda_{\omega,t}^{(N)} = \Lambda_{\omega,t}^{\otimes N}$, which commutes with frequency encoding, so that the frequency ω is again encoded via the phase, $\rho_{\omega,t} = e^{-i\omega t H} \Lambda_t^{\otimes N}(\rho) e^{i\omega t H}$ and the corresponding QFI equals $t^2 F(\Lambda_t^{\otimes N}(\rho))$. In this case the optimal time of frequency estimation will result from the trade-off between the phase $\phi = \omega t$ growing with time and coherence in the state $\Lambda_t^{\otimes N}(\rho)$ being suppressed with the increasing noise strength.

1.4.2 Universal bounds on frequency estimation precision

The above discussed connection between frequency estimation and phase estimation, enables us to address the question of

the optimal estimation setup by using bounds on the phase estimation precision.

First, consider local dephasing noise. We will use the bound in Eq. (1.37) derived for semi-classical correlated Gaussian dephasing, which in the local independent takes the form of Eq. (1.49). We obtain

$$\Delta_{\omega}^2 \hat{\omega} \geq \min_{t \leq T} \left(\frac{1}{N^2} + \frac{2 \operatorname{Re} \gamma(t)}{N} \right) / T t, \quad (1.52)$$

where $\gamma(t)$ describes the dephasing noise strength. The estimation errors are bounded by the *quantum noise*, $1/N^2 T t$, which bounds the precision of frequency estimation using N atoms when the atoms dynamics is unitary, and the *classical noise*, $2 \operatorname{Re} \gamma(t)/N T t$, which represents the errors caused by random phases introduced to atom dynamics in the semi-classical noise model, and would be present even if the system state could be read out directly.

Note that for any local dephasing noise, due to locality, dynamics of N atoms are determined just by dynamics of a single atom, $\Lambda_{\omega,t}^{(N)} = \Lambda_{\omega,t}^{\otimes N}$, where

$$\Lambda_{\omega,t}(\rho) = \begin{pmatrix} \rho_{00} & \rho_{01} e^{i\omega t - \gamma(t)} \\ \rho_{10} e^{-i\omega t - \gamma(t)^*} & \rho_{11} \end{pmatrix}, \quad (1.53)$$

and $\operatorname{Re} \gamma(t)$ determines the dephasing strength, whereas $\operatorname{Im} \gamma(t)$ effectively shifts the phase $\phi = \omega t$. The precision in phase estimation depends on the noise model only via $\gamma(t)$, not any other details of the model, as measurements are performed on the system alone. Note that for a given time t , the action of any local dephasing model can be mimicked by the independent semi-classical Gaussian model, and therefore, the bound in Eq. (1.52) is valid for all dephasing models.

Similarly, for non-Markovian noise models of local depolarisation or spontaneous emission, we can modify bounds on frequency estimation precision in the presence of Markovian noise derived with Channel Extension method in [15, 94]. As those

types of noise commute with frequency encoding, in derivation of the bounds, bounds on phase estimation precision are established first. These bounds do not explicitly assume Markovian dynamics and are valid for non-Markovian models as well, see Tab. 1.1. Note that for a given local dephasing model, the

Noise	CE bound
Dephasing	$(\eta(t)^{-2} - 1 + \frac{1}{N}) / NTt$
Depolarisation	$[(\eta(t)^{-2} + \eta(t)^{-1} - 2) + \frac{2}{N}] / 2NTt$
Spon. Emission	$(\eta(t)^{-1} - 1 + \frac{4}{N}) / 4NTt$

Table 1.1: Channel Extension bounds on frequency estimation precision for local noise [15, 94]. We have $0 \leq \eta(t) \leq 1$, for dephasing $\eta(t) = |e^{\gamma(t)}| = e^{\text{Re}\gamma(t)}$.

bound (1.52) can be used to determine the best possible precision scaling with N by finding the optimal experiment time t_{opt} . In Fig. 1.5 we consider the quantum dephasing model solved in [148] and discussed in [22], in which interaction of atoms with bosonic baths with the cut-off frequency ω_c and at inverse temperature β , leads to local dephasing, $\gamma(t) = \ln(1 + \omega_c^2 t^2) + 2 \ln(\frac{\sinh(\pi t \beta^{-1})}{\pi t \beta^{-1}})$. The optimal precision asymptotically scales as $\propto N^{-3/2}$, the *Zeno limit* [22, 23]. Below we show that this result holds for all local dephasing models featuring initial Zeno dynamics [17–20].

1.4.3 Zeno limit

Quantum models of noise are derived assuming that global dynamics of the system and environment is unitary and the initial state of the system and environment is a tensor product. Local decoherence models originate from the situation where each subsystem, in our case a single atom, interacts with a different environment, so that the global Hamiltonian is a sum of individual Hamiltonians for N subsystem-environment pairs. For identical subsystems and environments this leads to $\rho_{\omega,t} = \Lambda_{\omega,t}^{\otimes N}(\rho)$. Furthermore, the initial behaviour of any quantum model is characterised by a quadratic decay of the proba-

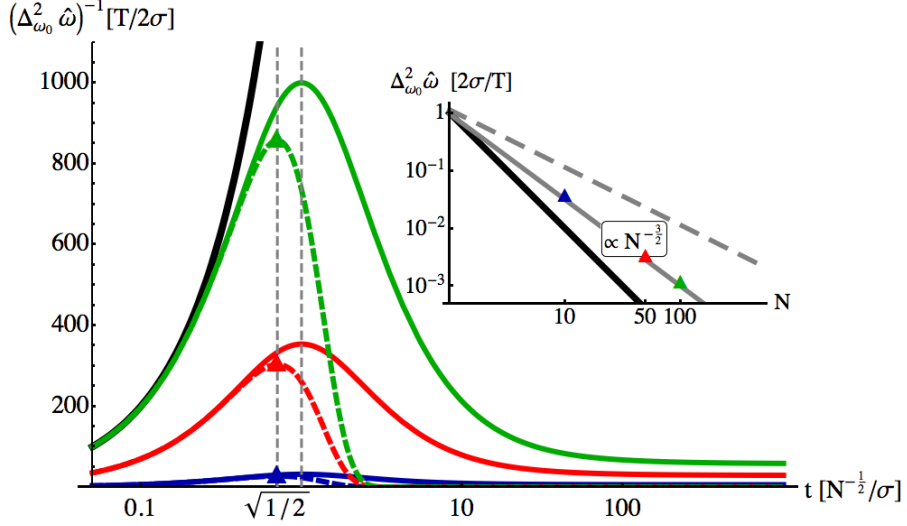


Figure 1.5: **Frequency estimation with non-Markovian dephasing** from [148]. Main plot: bound (1.52) (continuous lines) is compared to GHZ state performance (short-dashed lines), for different experiment times t and number of atoms $N = 10$ (blue), 50 (red), 100 (green). Optimal values both for the bound and GHZ state are achieved at $t \propto N^{-1/2}$ inside Zeno-dynamics regime, but noise strength is not negligible leading to worse precision than in unitary case (for $N=100$ see continuous black line). Inset: optimal precision for different number N of atoms. Precision in the bound (continuous gray) and for GHZ state (triangles) scales $\propto N^{-3/2}$ in contrast to standard scaling for uncorrelated state (long-dashed gray) and unitary Heisenberg scaling (continuous black). Plot parameters were chosen $\omega_c = \frac{\pi}{\sqrt{3}}\beta^{-1}$, which leads to $\beta^{-1} = \frac{\sqrt{3}}{2\pi}\sigma$. This figure originally appeared in [24].

bility of observing the system in its initial state, so called survival probability, $\langle \psi | \rho_{\omega, t} | \psi \rangle = 1 - \frac{c}{2}t^2 + \mathcal{O}(t^3)$, which enables the quantum Zeno effect [17–20]. We refer to this time regime this quadratic decay takes place as Zeno dynamics regime. In the case of local dephasing noise, the dynamics is parametrised by $\gamma(t)$, see Eq. (1.53), which by construction does not depend on N , but on the interaction details [22, 23]. We now show how the initial behaviour of $\gamma(t)$ is fully determined by the quadratic

decay of the survival probability. Consider a single atom initially in the state $|\psi\rangle = \frac{1}{\sqrt{2}}(|0\rangle + |1\rangle)$, we have

$$\langle \psi_0 | \rho_{\omega,t} | \psi_0 \rangle = \frac{1}{2} \left[1 + e^{-\text{Re} \gamma(t)} \cos(\omega t - \text{Im} \gamma(t)) \right],$$

which, when expanded around small t , implies

$$\text{Re} \gamma(t) = \frac{\sigma^2}{2} t^2 + \mathcal{O}(t^3) \quad \text{and} \quad (1.54)$$

$$\text{Im} \gamma(t) = -\mu t + \mathcal{O}(t^2), \quad (1.55)$$

where σ corresponds to the fastest energy scale in the bath dynamics [22, 23]. Let τ be chosen so that for $t < \tau$ the above approximation is valid. Note that σ , μ and τ do not depend on N , as $\gamma(t)$ does not. The general characterization of initial dynamics given in Eq. (1.54) will allow us now to derive the Zeno limit $\propto N^{-3/2}$ for frequency estimation precision in the presence of any non-Markovian dephasing noise with initial Zeno dynamics. Moreover, as we show in Tab. (1.2), the quadratic decay of the survival probability allows for similar characterisation of initial dynamics in noise models of depolarisation and spontaneous emission.

For local semi-classical models of dephasing, random classical fields independently acting on atoms are considered. For a random field h , $e^{-\gamma(t)} = \mathbb{E} e^{i \int_0^t h(s) ds}$ [22], where \mathbb{E} is the average over the field probability distribution. When h is Gaussian, $\gamma(t)$ depends only on the field correlations in time. Constant correlations lead to $\gamma(t) = \frac{\sigma^2}{2} t^2 - i\mu t$, where σ^2 , μ are simply the variance and mean of the time-independent field $h(t) = h(0)$ [149]. Such behaviour of $\gamma(t)$ is analogous to Zeno dynamics regime in quantum models. When there are no time correlations (white noise), we obtain the linear behaviour, $\gamma(t) = \gamma t$.

The linear behaviour is a characteristic feature of Markovian models, where dynamics obey a master equation [8, 9] and a semi-group structure, $\Lambda_{\omega, t_1+t_2}(\rho) = \Lambda_{\omega, t_2}(\Lambda_{\omega, t_1}(\rho))$, thus imposing $\gamma(t) = \gamma t$ [12].

Let us now consider the following time regimes in atom dynamics with non-Markovian dephasing: the quantum regime when the classical noise is much smaller than the quantum noise, i.e., $2 \operatorname{Re} \gamma(t)/N \ll 1/N^2$, the quantum-classical regime when the noises are of the same order, and the classical regime when the classical noise dominates. From now on we will consider a large number N of atoms. When $N \rightarrow \infty$, in the quantum-classical regime the dephasing strength gets arbitrarily small, $\operatorname{Re} \gamma(t) \approx 1/N \rightarrow 0$. For models without complete revivals in which $\operatorname{Re} \gamma(t) = 0$ only at $t = 0$, this implies that in the quantum-classical regime time $t \rightarrow 0$ as $N \rightarrow \infty$ and thus, for large enough N one must enter the Zeno-dynamics regime, where $\operatorname{Re} \gamma(t) = \frac{\sigma^2}{2} t^2 + \mathcal{O}(t^3)$.

For experiments in the quantum time regime, the frequency estimation precision is just like in the unitary case, see Fig. 1.5, as initial quantum correlations are preserved. The phase $\phi = \omega t$ encoded in the state is, however, very small due to the short experiment time t leading to,

$$\Delta_{\omega}^2 \hat{\omega} \gtrsim \min_{t \ll N^{-1/2}/\sigma} N^{-2}/T t \gg N^{-3/2} \sigma/T. \quad (1.56)$$

For experiments in the classical time regime, the precision obeys the standard scaling, which is a consequence of suppression of quantum correlations in the dephased system state $\Lambda_t^{(N)}(\rho)$,

$$\Delta_{\omega}^2 \hat{\omega} \gtrsim \min_{t \gg N^{-1/2}/\sigma, t \leq T} N^{-1} 2 \operatorname{Re} \gamma(t)/T t = N^{-1} C/T. \quad (1.57)$$

The quantum-classical regime is optimal when $N \rightarrow \infty$, as it lays asymptotically in the Zeno-dynamics regime and Eq. (1.52) reduces to Zeno limit

$$\begin{aligned} \Delta_{\omega}^2 \hat{\omega} &\geq \min_{t=\mathcal{O}(N^{-1/2}/\sigma)} \left(\frac{1}{N^2} + \frac{\sigma^2 t^2 + \mathcal{O}(t^3)}{N} \right) / T t \\ &= N^{-3/2} 2\sigma/T + \mathcal{O}(N^{-2}), \end{aligned} \quad (1.58)$$

where the minimum is achieved at $t_{\text{opt}} = N^{-1/2}/\sigma$. The bound in Eq. (1.58) is also valid for semi-classical models whose dy-

namics within the random field correlation time τ is analogous to the Zeno dynamics, for examples see [22].

Let us recall from [22, 23] the results on frequency estimation in the presence of non-Markovian dephasing using atoms prepared in the GHZ state and the parity measurements. The total precision for optimal locally unbiased estimator is

$$\Delta_{\omega}^2 \hat{\omega} = \min_{t \leq T} N^{-2} e^{2N \operatorname{Re} \gamma(t)} / T t = N^{-3/2} \sqrt{2e} \sigma / T, \quad (1.59)$$

where we used the fact that for large N , the optimal time enters the Zeno-dynamics and $t_{\text{opt}} = N^{-1/2}/\sigma$. This proves that the *Zeno limit is achievable*. Note that the GHZ state performs optimally for experimental times $t \lesssim 0.4 N^{-1/2}/\sigma$, see Fig. 1.5, but it may not be optimal as the constant in the bound (1.58) is not achieved.

Markovian dephasing noise. For Markovian dephasing the noise strength increases faster for initial times, as $\gamma(t) = \gamma t$. Consequently, phases encoded in the system state in the quantum-classical regime are so small that the scaling remains standard,

$$\Delta_{\omega}^2 \hat{\omega} \geq \frac{2 \operatorname{Re} \gamma}{T} N^{-1}. \quad (1.60)$$

Other types of noise. By considering a modification of the bounds on frequency estimation precision in the presence of Markovian noise, derived with Channel Extension method in [15, 94], see Tab. 1.1, one analogously arrives at the Zeno limit $\propto N^{-3/2}$ for depolarisation and spontaneous emission, as long as a noise model features initial Zeno dynamics, see Tab. 1.2. In [102] it was shown that the Zeno limit holds for all noise models that commute with frequency encoding and feature initial Zeno dynamics.

Noise	$\langle \psi \rho_{\omega,t} \psi \rangle$	$\eta(t)$ at $t < \tau$	$\eta(t)$ Markov
Dephasing	$(1 + \eta(t) \cos(\omega t))/2$	$1 - \frac{\sigma^2}{2} t^2 + \mathcal{O}(t^3)$	$e^{-\gamma t}$
Depolarisation	$(1 + \eta(t) \cos(\omega t))/2$	$1 - \frac{2\sigma^2}{3} t^2 + \mathcal{O}(t^3)$	$e^{-\frac{4}{3}\gamma t}$
Spon. Emission	$\eta(t) (1 + \cos(\omega t))/2$	$1 - 4\sigma^2 t^2 + \mathcal{O}(t^3)$	$e^{-8\gamma t}$

Table 1.2: The survival probability for an initial state $|\psi\rangle = \frac{1}{\sqrt{2}}(|0\rangle + |1\rangle)$ of a single atom and parametrisations of noise in the Zeno regime and with Markovian assumption that lead to bounds (1.58) and (1.60).

1.4.4 Non-Markovianity is (not) a resource

Let us note that the fact that the bound in Eq. (1.57) proving the standard scaling of frequency estimation precision in the classical time regime, has important consequences for regarding non-Markovianity as a resource. It shows that no matter what type of non-Markovian dynamics takes place after the initial Zeno dynamics it does not lead to enhancement in the precision scaling for estimation in the presence of dephasing noise. In particular, any revivals in coherence or in quantum correlations, usually considered as a signature of non-Markovian dynamics [25, 26], *will asymptotically not enhance* the precision scaling with the number N of subsystems used, for example see Fig. 1.6. This is due to the fact that choosing a revival time t_r , which is independent of N , leads to a finite strength of the local noise and thus the standard scaling. Choosing t_{opt} as above, which approaches $t = 0$ as the number of subsystems grows, however, can reduce the noise strength with N due to a slow quadratic increase of noise strength in the Zeno regime, cf. Eqs. (1.54), in contrast to much the faster linear growth in the case of Markovian noise [12]. See also the discussion in [102].

1.4.5 Summary and outlook

Summary. The Zeno limit $\propto N^{-3/2}$ in the precision of frequency estimation was first demonstrated for the GHZ state [22, 23]. In this section we presented the results of [27], where the Zeno

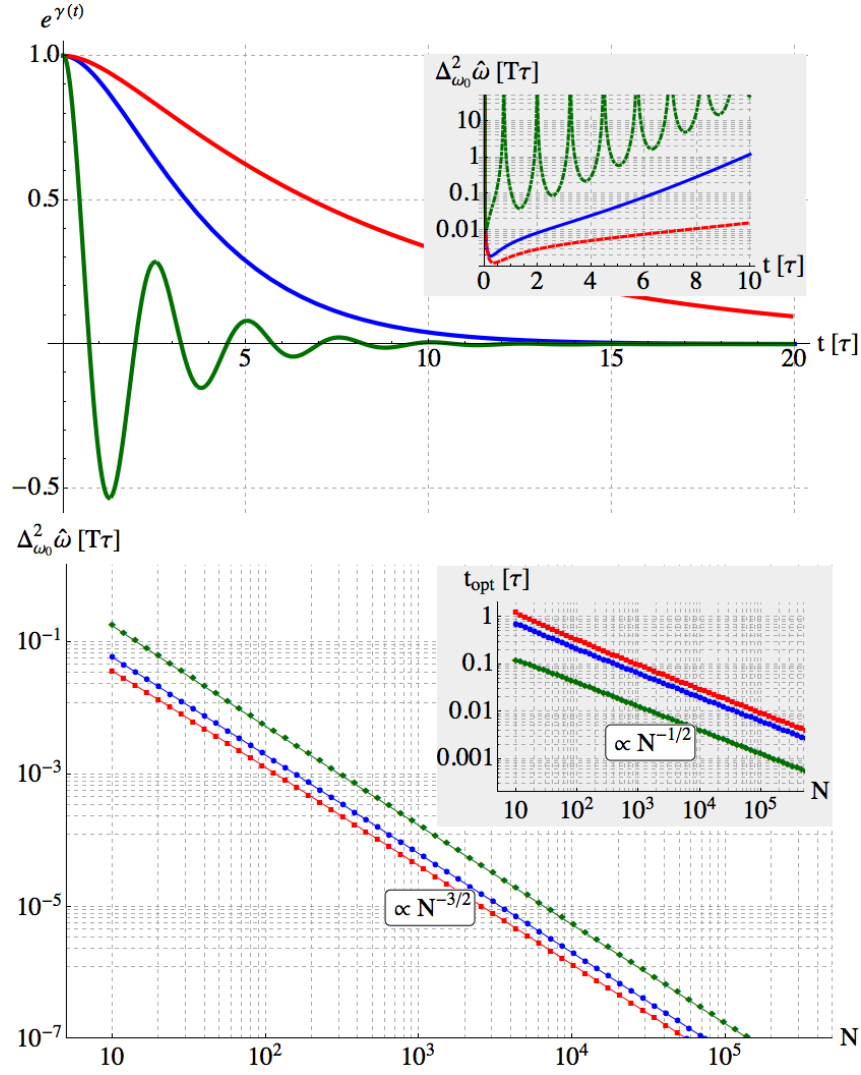


Figure 1.6: **Asymptotic irrelevance of non-Markovian revivals in frequency estimation.** *Upper panel:* Example of non-Markovian dephasing channel from [150], where $e^{\gamma(t)} = e^{-\frac{t}{2\tau}} \left(\cos(\mu \frac{t}{2\tau}) + \frac{1}{\mu} \sin(\mu \frac{t}{2\tau}) \right)$ and $\mu = \sqrt{(4a\tau)^2 - 1}$, where a is system-bath coupling strength and τ determines preferred interaction frequencies, $\mu = i\tau$ (red), $\mu = 0$ (blue), $\mu = 10\tau$ (green). The inset depicts dependence of the bound from Tab. 1.1 for $N = 100$ on the single experiment time t . *Lower panel:* Numerical optimisation of t in all time regimes. For large N the Zeno limit in precision, $N^{-\frac{3}{2}}2\sigma/T$, and $t_{\text{opt}} = N^{-\frac{1}{2}}/\sigma$ (inset) is obtained. Note that not only τ , but also μ determines $\sigma = \sqrt{2 + |\mu|^2}/2\tau$ for this model and thus the optimal times are different for the chosen parameters.

limit has been proven to hold for any frequency estimation experiments in the presence of local dephasing noise featuring initial Zeno dynamics. Moreover, the Zeno scaling can be achieved only for experiments performed in the Zeno-dynamics regime and for other regimes the precision is standard-limited.

Future work. In this section and other works on frequency estimation in the presence of non-Markovian noise [22, 23, 102], the noise was assumed to be independent in individual experiments, so that the signal to noise ratio of $n = T/t$ experiments lasting time t is simply n times the SNR of a single-experiment, cf. Eq. (1.25). In general, however, one should consider correlations between measurements results due to correlations in time of random fields in semi-classical models, or perturbations in the environment state introduced by measurements on the system evolving coherently with the environment. Those perturbations, together with correlations created between the system and its environments, are two core ingredients of the parent definition of non-Markovian dynamics [151, 152], and should not be easily discarded.

Interestingly, in the quantum metrology setup, the scenario simplifies as follows. Of course, the evolved and then measured system state is replaced by a new initial preparation in each experiment, thus removing the correlations between the system state and its environments, but due to exactly those correlations created in the coherent system-environment, the evolved environment state is in general different from its initial state. As, in every individual experiment, the system is assumed to be initialised in the same state that is uncorrelated with the environment, this imposes *Markovian* dynamics of the environment. Asymptotically, for large total time T of experiments, the environment will approach the stationary state of that Markovian dynamics, which will in general depend on time t and an initial state of the system [153]. In turn, the system dynamics should be considered as a collection of quantum channels indexed by the single experiment time t [152], as a consequence of different stationary states of the environment. Furthermore,

bounds on frequency estimation precision should be derived for that collection of system quantum channels. We intend to apply this idea to non-Markovian models in which the system couples strongly to a part of the environment, while dynamics with respect to the rest of the environment obeys the Markovian approximation [154].

2

DYNAMICAL PHASE TRANSITIONS AS A RESOURCE FOR QUANTUM ENHANCED METROLOGY

The estimation of unknown parameters is a crucial task for quantum technology applications such as state tomography [114], system identification [115], and quantum metrology [1, 2, 4–6, 59].

In the previous chapter 1 we discussed how the enhancement in the estimation precision can be achieved by using highly correlated/entangled quantum states which encode the unknown parameter, like the GHZ state $|\text{GHZ}\rangle = \frac{1}{\sqrt{2}}(|0\rangle^{\otimes N} + e^{-iN\phi}|1\rangle^{\otimes N})$ constructed out of N qubits and encoding an unknown phase ϕ . Since the phase effectively encoded in the state is $N\phi$, the estimation errors obey the Heisenberg scaling $\propto N^{-2}$ [3], instead of the standard $\propto N^{-1}$ scaling for a separable state $(|0\rangle + e^{-i\phi}|1\rangle)^{\otimes N}$. For large N , however, such highly correlated *pure* states are challenging to prepare in practice [155], either as the ground state of a closed many-body system, or as the stationary state of some dissipative dynamics [156, 157], which typically requires careful system engineering, since generic open quantum systems have *mixed* rather than pure stationary states, see Sec 2.1.1.

The key property that makes correlated states such as $|\text{GHZ}\rangle$ useful for enhanced metrology is that they can be thought of as “bimodal”, in the sense that the probability of an appropriate observable is peaked in two (or more) “phases” (the states $|0\rangle^{\otimes N}$ and $|1\rangle^{\otimes N}$ in the case of $|\text{GHZ}\rangle$). This bimodality is reminiscent of what occurs near a first-order phase transition. In fact, en-

hanced estimation of parameters in a system Hamiltonian can be achieved with a pure ground state at quantum phase transitions [130, 131]. In this chapter we discuss how to exploit the dynamics of open quantum systems (for example, driven atomic or molecular ensembles emitting photons [31], or quantum dots [32]) to generate states for quantum enhanced metrology. This can be achieved by using both the system and its output when the system dynamics is in proximity of a *dynamical* phase transition, which is characterised by singular changes in dynamical observables on the output, in contrast to static observables on the system, see [34] and Sec. 2.1.2. In particular, we show how using an intermittent system near a dynamical first-order transition for preparation of a photonic state, quantum enhancement in optical phase-shift estimation can be achieved [29].

2.1 BACKGROUND

Before presenting the results of [29], we first sketch a derivation of Markovian dynamics [8, 9] and introduce the input-output formalism [30]. This is followed by a short introduction to dynamical phase transitions [34] in Sec. 2.1.2, which notion we later generalise. Finally, as we will quantify the precision using the quantum Fisher information (QFI), in Sec. 2.1.4 we recall a convenient way of its calculation using the fidelity of quantum states.

2.1.1 *Markovian dynamics of open quantum system and input-output formalism*

Our goal is to explore open quantum systems as resources for parameter estimation. We consider systems whose reduced dynamics, after tracing out the environment, is given by a Markovian master equation [8, 9],

$$\frac{d\rho}{dt} = \mathcal{L}\rho = -i[H, \rho] + \sum_j \left(J_j \rho J_j^\dagger - \frac{1}{2} \{J_j^\dagger J_j, \rho\} \right), \quad (2.1)$$

where H is the system's Hamiltonian, and J_j are so called jump operators describing the interaction with the environment¹.

Sketch of derivation (based on [30]). Markovian dynamics is a result of three approximations [8, 9]. We consider the joint unitary dynamics governed by Hamiltonian $H = H_S \otimes \mathbb{1}_E + \mathbb{1}_S \otimes H_E + H_{SE}$, where an initial system-environment state is independent, $\rho_{SE}(t) = \rho_S(0) \otimes \rho_E$, and the interaction between the system and its environment, H_{SB} , is weak. In the interaction picture with respect to the non-interacting dynamics, $H_{\text{int}}(t) = e^{it(H_S \otimes \mathbb{1}_E + \mathbb{1}_S \otimes H_E)} H_{SE} e^{-it(H_S \otimes \mathbb{1}_E + \mathbb{1}_S \otimes H_E)}$, we have

$$\begin{aligned} \frac{d}{dt} \rho_{SE}^{(\text{int})}(t) &= -i \left[H_{\text{int}}(t), \rho_{SE}^{(\text{int})}(t) \right], \quad \text{which gives} \\ \rho_{SE}^{(\text{int})}(t) &= \rho_{SE}^{(\text{int})}(0) - i \int_0^t dt' \left[H_{\text{int}}(t'), \rho_{SE}^{(\text{int})}(t') \right], \quad \text{and thus} \\ \frac{d}{dt} \rho_{SE}^{(\text{int})}(t) &= -i \left[H_{\text{int}}(t), \rho_{SE}^{(\text{int})}(0) \right] - \int_0^t dt' \left[H_{\text{int}}(t), \left[H_{\text{int}}(t'), \rho_{SE}^{(\text{int})}(t') \right] \right]. \end{aligned}$$

We are interested now in the reduced state of the system, $\rho_S(t) = \text{Tr}_E(\rho_{SE}) = e^{-itH_S} \text{Tr}_E(\rho_{SE}^{(\text{int})}) e^{itH_S}$. In *Born approximation* the joint state of the system and environment is assumed to factorise, $\rho_{SE}(t) = \rho_S(t) \otimes \rho_E$, and the environment state to be stationary w.r.t. H_E . This is motivated by the fact that environment state is perturbed weakly by the interaction and its is assumed significantly bigger than the system and thus less affected. We obtain

$$\frac{d}{dt} \rho_S^{(\text{int})}(t) = - \int_0^t dt' \text{Tr}_E \left(\left[H_{\text{int}}(t), \left[H_{\text{int}}(t'), \rho_S^{(\text{int})}(t') \otimes \rho_E \right] \right] \right),$$

where we assumed the first-order term to be 0 (which can be done by redefining H_S). In *Markov approximation*, the correlations in the environment dynamics depending on ρ_E are further assumed to disappear much faster than the rate at which system state changes, thus giving

$$\frac{d}{dt} \rho_S^{(\text{int})}(t) = - \int_0^\infty dt'' \text{Tr}_E \left(\left[H_{\text{int}}(t), \left[H_{\text{int}}(t-t''), \rho_S^{(\text{int})}(t) \otimes \rho_E \right] \right] \right),$$

¹ The calligraphic font denotes super-operators, such as the generator \mathcal{L} , while the Roman font denotes normal operators, such as the Hamiltonian H or the jump operators J_j .

where $t'' = t - t'$. We have thus arrived at an equation in which the change in a system state depends only on its present state, and thus dynamics is *Markovian*. Furthermore, when the correlations depend only on the time difference, t'' , due to stationarity of ρ_E (and usually within the *rotating wave approximation*), this equation becomes *time-homogeneous* and leads to Eq. (2.1), where for simplicity we dropped the lower index S . Note that Eq. (2.1) yields a dynamical semi-group, i.e., $\mathcal{T}_{t_1+t_2}(\rho) = \mathcal{T}_{t_2}(\mathcal{T}_{t_1}(\rho))$, where $\mathcal{T}_t(\rho) = \rho(t)$ is the solution of (2.1) for an initial state ρ of the system. It can be shown that Eq. (2.1) defines actually the most general form of completely positive dynamical semi-group, see e.g. [158]. ■

Input-output formalism. In this chapter we consider initial states of the system being *pure*, as so are the optimal states for quantum parameter estimation. Moreover, we are interested in systems where the system-environment interaction leads to emissions of quanta to the environment, and corresponding jumps operators J_j acting on the system. Such quanta do never again interact with the system, due to Markovian approximation, but can be detected, e.g. as in quantum optics one can perform a continuous measurement on an output field. This assumption is crucial, as in order to achieve enhanced parameter estimation we aim to exploit not only open quantum systems, but especially their outputs.

When the environment (input) is initially in the vacuum, we can represent the system evolution as a superposition of all possible emission records and corresponding conditional states of the system, with respective probability amplitudes of observing such an emission record in a continuous measurement [30],

$$\begin{aligned}
|\Psi(t)\rangle = & \sum_{m=0}^{\infty} \sum_{j_1, \dots, j_m} \int_0^t dt_1 \int_{t_1}^t dt_2 \cdots \int_{t_{m-1}}^t dt_m \\
& \times \left(e^{-i(t-t_m)H_{\text{eff}}} J_{j_m} e^{-i(t_m-t_{m-1})H_{\text{eff}}} \right. \\
& \left. \cdots J_{j_2} e^{-i(t_2-t_1)H_{\text{eff}}} J_{j_1} e^{-it_1 H_{\text{eff}}} |\chi\rangle \right) \\
& \otimes |(j_1, t_1), (j_1, t_2), \dots, (j_m, t_m)\rangle. \quad (2.2)
\end{aligned}$$

A sequence of m quantum jumps $\{j_1, \dots, j_m\}$ that happen at times $\{t_1, \dots, t_m\}$ corresponds to an output state $|(j_1, t_1), (j_1, t_2), \dots, (j_m, t_m)\rangle$. The probability of the sequence depends on an initial pure state of the system $|\chi\rangle$, waiting times between the jumps, when the evolution is governed by the effective non-Hermitian Hamiltonian, $H_{\text{eff}} = H - \frac{i}{2} \sum_j J_j^\dagger J_j$, and types of jumps/emitted quanta. The term $m = 0$ in the first sum corresponds to no jumps/no emissions, when the output state remains unchanged in the input vacuum, and the corresponding probability, so called *waiting time probability*, is given by dynamics only with H_{eff} . The structure of the *joint system and output state* in Eq. (2.2) is a continuous matrix product state (CMPS) [35, 128, 159–161].

For simplicity, the CMPS can be approximated by a regular matrix product state (MPS) by discretising time into time steps of length δt , see [35, 128, 159, 160],

$$|\Psi(t)\rangle = \sum_{j_n \dots j_1} K_{j_n} \cdots K_{j_1} |\chi\rangle \otimes |j_1, \dots, j_n\rangle, \quad (2.3)$$

where $n = t/\delta t$ and the Kraus operators

$$\begin{aligned} K_0 &= e^{-i\delta t H} \sqrt{\mathbb{1} - \delta t \sum_j J_j^\dagger J_j}, \\ K_{j>0} &= e^{-i\delta t H} \sqrt{\delta t} J_j. \end{aligned} \quad (2.4)$$

Here the output state $|j_1, \dots, j_n\rangle$ describes the time record of type of jumps or no jumps that happened at each time step δt , as sketched in Fig. 1(a).

2.1.2 Dynamical phase transitions

A state of a quantum system can be accessed only by performing a measurement. For example, a system state described by a density matrix ρ can be fully reconstructed in quantum tomography [114], where the set of system observables being measured constitutes a basis in the space of observables, so that all the information about ρ is retrieved.

Static phase transitions. Consider the system interacting *weakly* with an environment, so that the system dynamics can be approximated as Markovian, see Sec. 2.1.1. For any initial state the system asymptotically approaches the stationary state, ρ_{ss} such that $\mathcal{L}\rho_{\text{ss}} = 0$, e.g. a thermal equilibrium state when interacting with a thermal bath. When parameters of dynamics are varied, e.g. the system Hamiltonian or the temperature of the bath, such a stationary state can undergo singular changes — *static* phase transitions — which correspond to a cumulant of a system observable diverging faster than linearly with the increasing system size. For a first-order phase transition, the expected value of such an observable, e.g. spin magnetisation, constitutes an *order parameter*. In the case, when the stationary state is thermal and at zero temperature, it corresponds to a ground state of the system Hamiltonian and its transitions are referred to as *quantum* phase transitions [162].

Dynamical phase transitions [34–36, 163, 164]. For Markovian systems whose dynamics features an output, for example photon emissions from atoms corresponding to their decay from higher to lower energy, one can consider performing a *continuous measurement* of the output, e.g. counting of emitted photons. Let $\mathbb{P}_t(\Lambda)$ be the probability of observing in time t , Λ photons associated with the jump J_1 . In this case the cumulant generating function (CGF) can be related to a deformation of the master operator \mathcal{L} [34],

$$\Theta_t(s) = \log \left(\sum_{\Lambda} e^{-s\Lambda} \mathbb{P}_t(\Lambda) \right) = \log \text{Tr}(e^{t\mathcal{W}_s} \rho_{\text{in}}), \quad \text{where} \quad (2.5)$$

$$\mathcal{W}_s \rho = \mathcal{L} \rho + (e^{-s} - 1) J_1 \rho J_1^\dagger. \quad (2.6)$$

For examples of CGF for homodyne and heterodyne continuous measurement see [164]. We have $\langle \Lambda(t) \rangle = -\partial_s \Theta_t(s)|_{s=0}$ and $\Delta^2 \Lambda(t) = \partial_s^2 \Theta_t(s)|_{s=0}$. When we are interested in the asymptotic behaviour of the $\Lambda(t)$ cumulants, we consider the long time limit of the CGF,

$$\theta(s) = \lim_{t \rightarrow \infty} \frac{1}{t} \Theta_t(s). \quad (2.7)$$

This function plays the role of a density of *dynamical free-energy* for the ensemble of records (trajectories) of photon emissions [34]. When $\theta(s)$ is differentiable, the distribution of photon number $\Lambda(t)$ obeys *Large Deviations Principle*, i.e., its tails decay exponentially,

$$\mathbb{P}_t(\Lambda(t) > \Lambda) \approx e^{-t\varphi(\frac{\Lambda}{t})} \quad \text{for } \Lambda \geq \mu t, \quad (2.8)$$

$$\mathbb{P}_t(\Lambda(t) < \Lambda) \approx e^{-t\varphi(\frac{\Lambda}{t})} \quad \text{for } \Lambda \leq \mu t, \quad (2.9)$$

where $\mu = \lim_{t \rightarrow \infty} \langle \Lambda(t) \rangle / t$ is the asymptotic emission rate, and $\varphi(\lambda) = -\inf_s (\lambda s + \theta(s))$, see Gärtner-Ellis theorem in [165, 166]. The function $\varphi(\lambda)$ acts as an *entropy density* for ensemble of emission records and its minimum corresponds to $\mu = \lim_{t \rightarrow \infty} \langle \Lambda(t) \rangle / t$. Moreover, when $\varphi(\lambda)$ is twice differentiable around $\lambda = \mu$, $d\Lambda(t)$ obeys CLT [166] with asymptotic variance given by $\frac{d^2}{d\lambda^2} \varphi(\lambda)|_{s=\mu}^{-1}$. For CLT in continuous measurements statistics see also [37, 39].

A singularity of $\theta(s)$ at some s_c is an indication of a *phase transition* in the ensemble of quantum jump trajectories. When $s_c = 0$, we have a singular change in the actual dynamics of the open system, which we term a dynamical phase transition (DPT). This singular behaviour in n -th derivative corresponds to divergence of the n -th cumulant of $\Lambda(t)$ and is necessary associated with the vanishing spectral gap of $\mathcal{L} \equiv \mathcal{W}_0$ [34, 35]. Note that a dynamical transition of higher than the first order does not have to be accompanied by a static transition in the stationary state [36]. For a finite quantum system with a single stationary state, $\theta(s)$ is simply the maximal eigenvalue of \mathcal{W}_s , and thus the perturbation theory for linear operators [167] w.r.t. s , implies analyticity of $\theta(s)$ at $s = 0$ and the asymptotic linear behaviour in time of all $\Lambda(t)$ cumulants.

We note that there are other definitions of dynamical phase transitions in the literature, see e.g. [168–170].

2.1.3 *Parameter estimation using both system and output*

Ability to access not only the system, but also the output, allows for improved precision of estimating parameters of the master equation \mathcal{L} . This is due to the fact that the effective “size” of the system and output is now Nt , where t is the observation time and N is the system size. Furthermore, considering both the system and the output provides the ultimate bound on estimation precision by considering the most general measurement exploiting all the available resources, see recent work on parameter estimation with single stationary states of open quantum systems [37–39]. Later in this chapter, we present results of [29] where estimation of dynamical parameters is enhanced near or at a DPT, similarly as estimation of Hamiltonian parameters at quantum phase transitions [131]. We show that at a first-order DPT [34, 36], the QFI of the system-and-output may become quadratic in t giving rise to the *Heisenberg scaling*, while away from the transition point the Heisenberg scaling is present for times shorter than the correlation time of the dynamics, and asymptotically standard scaling is recovered. Moreover, both a first and a second-order DPT correspond to diverging correlation time in dynamics, which is related to closing of the master operator gap [35]. Those correlations correspond to multipartite entanglement in the system-output state, since it is pure, and can be exploited to achieve enhanced parameter estimation of extrinsic parameters encoded on the output, which is the main result of this chapter. We illustrate this idea with a simple example of enhanced estimation of optical phase-shift encoded on photons emitted by an intermittent system near a first-order DPT.

2.1.4 *Fidelity of pure states and QFI*

Considering a pure joint state of system and output circumvents a problem of calculating the best possible precision of pa-

parameter estimation for mixed states, which is usually difficult, except for particular cases such as thermal states [69].

Quantum Fisher information. Let us recall essential aspects of quantum parameter estimation introduced in Chapter 1. We are interested in estimating a parameter g , not necessary a phase, encoded in a state ρ_g . By measuring an observable X , the asymptotic estimation precision is given by the inverse of the signal to noise ratio (SNR) [68], which is always bounded by the quantum Fisher information,

$$\text{SNR}_g(X) = (\partial_g \langle X \rangle_g)^2 / \Delta_g^2 X \leq F_g(\rho_g) = \Delta_g^2 D_g, \quad (2.10)$$

$$\text{where} \quad \frac{1}{2} \{D_g, \rho_g\} = \partial_g \rho_g, \quad (2.11)$$

and the symmetric logarithmic derivative D_g is the optimal observable [64, 65, 67]. Although generically D_g is difficult to engineer, its SNR given by the QFI, $F_g(\rho_g)$, bounds the precision of any measurement that can be performed in practice.

QFI for pure states and fidelity. For a pure state, $|\psi_g\rangle$, the QFI can be obtained from the fidelity $\langle \psi_{g_1} | \psi_{g_2} \rangle$ [39, 130, 131] according to,

$$F(|\psi_g\rangle) = 4 \partial_{g_1} \partial_{g_2} \log \langle \psi_{g_1} | \psi_{g_2} \rangle \Big|_{g_1=g_2=g}, \quad (2.12)$$

see Appendix B.1 for the proof². A simple situation, which will turn out to be relevant for the results of this chapter, is when the parameter g is encoded as a phase in a unitary transformation on a pure state, $|\psi_g\rangle = e^{-igG}|\psi\rangle$. Here the fidelity $\langle \psi_{g_1} | \psi_{g_2} \rangle$ is the characteristic function of G at $g_1 - g_2$, and the QFI is given by its variance, $F(|\psi_g\rangle) = 4\Delta_g^2 G$. Note that while the QFI is given by the variance of both D_g and G , these two operators play very different roles. The optimal measurement to recover the parameter g is D_g , and its SNR is maximal, $\text{SNR}_g(D_g) = F_g(|\psi_g\rangle)$. In

² We refer here to the scalar product $\langle \psi_{g_1} | \psi_{g_2} \rangle$ instead of the absolute value $|\langle \psi_{g_1} | \psi_{g_2} \rangle|$ as the fidelity. The phase $\phi(g_1, g_2)$ of $\langle \psi_{g_1} | \psi_{g_2} \rangle = e^{i\phi(g_1, g_2)} |\langle \psi_{g_1} | \psi_{g_2} \rangle|$ does not contribute to the result of the differentiation in Eq. (2.12), as it is an antisymmetric function, $\phi(g_1, g_2) = -\phi(g_2, g_1)$.

contrast, G encodes g in the quantum state, but measuring it provides no information about g since $\text{SNR}_g(G) = 0$.

For the example of the GHZ state $|\text{GHZ}\rangle$ and the generator $G = \sum_j (1 + \sigma_z^{(j)})/2$, the optimal measurement is $D_g = \bigotimes_{j=1}^N e^{-igG} \sigma_y^{(j)} e^{igG}$, where $\sigma_a^{(j)}$ are Pauli operators acting on qubit j . The QFI for the GHZ state then obeys Heisenberg scaling, $F_g(|\text{GHZ}_g\rangle) = N^2$, which is related to the fact that the distributions of both G and D_g are bimodal. In contrast, the QFI of the uncorrelated state is standard, $F_g((|0\rangle + e^{-ig}|1\rangle)^{\otimes N}) = N$, given by the fact that the corresponding distributions of G and D_g are unimodal, which is a consequence of the CLT. We show below that an analogous change from bimodal to unimodal also accompanies a change in the scaling with time of the QFI when approaching a first-order DPT.

Fidelity and generalised phase transitions. As the fidelity corresponds to Bures distance on the space of quantum states [7], defined as $D_B(|\phi_{g_1}\rangle, |\phi_{g_2}\rangle) = \sqrt{2(1 - |\langle\phi_{g_1}|\psi_{g_2}\rangle|)}$, it can be used to capture singularities of the state $|\psi_g\rangle$ with respect to the parameter g [128–130]. In particular, singularities of the fidelity may allow for identification of quantum phase transitions of ground states in situation where typical observables do not feature any singularities, e.g. the ground state energy is constant, $E_g = E_0$ [128]. Therefore, considering the joint system-output, Eq. (2.2), as a resource, not only allows to find the best achievable estimation precision, but also provides a generalisation to the definition of DPT, cf. Sec. 2.1.2, as we discuss in detail in Sec. 2.5.

After this short introduction to concepts of Markovian open quantum dynamics, an output of open quantum system and dynamical phase transitions, let us present the results on the enhanced parameter estimation in the presence of dynamical phase transitions. First, in Sec. 2.2 we discuss an example of enhanced optical-shift estimation for a system with intermittent photon emissions. In this example the Heisenberg enhance-

ment in precision is a consequence of a macroscopic optical phase-shift effectively encoded in the joint system-output state as a consequence of bimodal distribution of photon statistics. In Sec. 2.3 we discuss estimation of a general parameter and show how enhanced estimation precision is again related to a bimodal distribution of an observable distinguishing the dynamical phases at a first-order DPT, and also to a static transition in the stationary state of the system. In Sec. 2.4, we discuss possibility of enhancement for certain classes of parameters, features of the corresponding optimal measurement and influence of noise on the estimation precision. Finally, in Sec. 2.5, we finish the chapter by discussing the generalised DPTs and ways of detecting their signatures in experiments. Derivations of the results of this chapter are presented in Appendix B.

2.2 INTERMITTENCY AND ENHANCED ESTIMATION OF OPTICAL SHIFT

Here we present a simple example of the relation between dynamical phase transitions and enhanced metrology. We discuss a scheme for enhanced optical-shift estimation using a photon output of a quantum system near a first-order DPT in photon emissions.

Consider a setup in which an unknown value ϕ of optical shift is unitarily encoded on photons emitted from a quantum system initially in a pure state, see Fig. 2.1. This transforms the MPS $|\Psi(t)\rangle$ of the system and the output as follows, $|\Psi_\phi(t)\rangle = e^{-i\phi\Lambda(t)}|\Psi(t)\rangle$, where $\Lambda(t)$ is the operator that counts the number of photons emitted up to time t . The optimal estimation precision is given by the inverse of the QFI, which in turn, for pure states, is related to the second derivative of logarithm of the fidelity, see Eq. (2.12). In the case of optical shift, the fidelity corresponds simply to the characteristic function of the number of photons emitted,

$$\langle\Psi_{\phi'}(t)|\Psi_\phi(t)\rangle = \langle\Psi(t)|e^{-i(\phi-\phi')\Lambda(t)}|\Psi(t)\rangle$$

and, thus, the QFI is proportional to its variance,

$$F(|\Psi_\phi(t)\rangle) = 4\Delta^2\Lambda(t). \quad (2.13)$$

Note that the QFI is the same for any value of ϕ . Eq. (2.13) shows the relation between the photon counting problem and the optical-shift estimation precision using an open quantum system initially in a pure state. In the next subsections we discuss the behaviour of the variance $\Delta^2\Lambda(t)$ away, at and near a DPT, and thus the QFI for initial pure state.

2.2.1 Away from a DPT

For a finitely dimensional open quantum system with a unique stationary state, ρ_{ss} , both the average and the variance of the total number of photons, $\Lambda(t)$, can be shown to asymptotically scale *linearly* in time, which is a consequence of the Local Asymptotic Normality (a quantum analogue of the CLT) for photon counting [37, 39]. Therefore, the enhancement in estimation precision is only limited to a *constant*. In Appendix B.2 we derive the linear limits of the photon emission average (μ) and variance (ν), and thus QFI, which turn out to be independent from the initial system state,

$$\mu = \lim_{t \rightarrow \infty} \frac{\langle \Lambda(t) \rangle}{t} = \text{Tr} \left\{ J_1^\dagger J_1 \rho_{ss} \right\} \quad (2.14)$$

$$\begin{aligned} \nu = \lim_{t \rightarrow \infty} \frac{\Delta^2 \Lambda(t)}{t} = & \text{Tr} \left\{ J_1^\dagger J_1 \rho_{ss} \right\} \\ & - 2 \text{Tr} \left\{ J_1^\dagger J_1 \left[\mathcal{L}^{-1} \right]_{\mathcal{J}-\mathcal{P}_{ss}} \left(J_1 \rho_{ss} J_1^\dagger \right) \right\} \end{aligned} \quad (2.15)$$

where $[\cdot]_{\mathcal{J}-\mathcal{P}_{ss}}$ restricts a superoperator to the complement of the stationary state and it was assumed for simplicity that photon emissions are associated with the jump operator J_1 . Note that the second line in Eq. (2.15) describes the photon emission correlations in otherwise Poissonian distribution, see Appendix B.3.1.

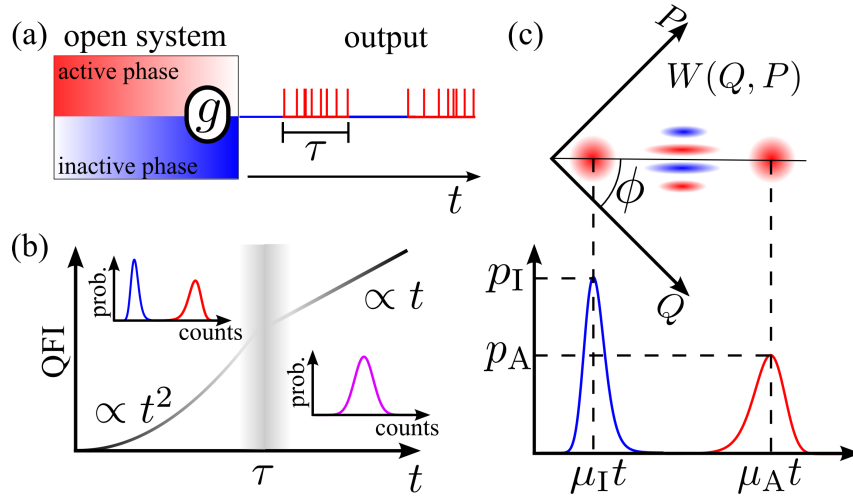


Figure 2.1: **General scheme of enhanced quantum metrology using output of system near a DPT** (a) Open quantum system with dynamics that depends on the unknown parameter g in the vicinity of a first-order DPT with two dynamical phases differing in activity. The output shows strong intermittency with active/inactive periods of length determined by the correlation time τ . (b) The QFI of the combined system-output state scales quadratically for observation times $t \ll \tau$. In the example of optical phase-shift, this regime features a bimodal photon count distribution corresponding to two dynamical phases, while for $t \gg \tau$ the distribution becomes unimodal and consequently, the QFI scales linearly with t . (c) Wigner distribution $W(Q, P)$ of the state (2.41) after being projected on an appropriate system state ($|I\rangle + |A\rangle$). The two peaks are located at radii that corresponds to the square root of the count rates $\mu_{I,A}$ of the inactive/active phase. The homodyne measurement is not optimal, however, as the highly oscillatory fringe pattern [with period $\propto [t(\mu_A - \mu_I)]^{-1}$] between the peaks, characteristic for a Schrödinger cat state, is simply rotated by ϕ . This figure originally appeared in [29].

2.2.2 At a first-order DPT in photon emissions

For a system at a first-order DPT, the gap of the master operator \mathcal{L} closes, i.e., $\lambda_2 = 0$, which for a finite system causes the asymptotic state to be no longer unique and the linear limit ν of the variance may diverge (see Eq. (2.15)). Below we show that the variance scales *quadratically* with with time for a first-order DPT

in photon emissions.

For two-fold degeneracy of 0-eigenvalue of \mathcal{L} , there exist two stationary states, $\tilde{\rho}_A$ and $\tilde{\rho}_I$, supported within orthogonal subspaces $\mathcal{H}_A, \mathcal{H}_I$ of the system Hilbert space, $\mathcal{H}_A \oplus \mathcal{H}_I \subset \mathcal{H}$. Let us further assume that there is no decay subspace, i.e., $\mathcal{H}_A \oplus \mathcal{H}_I = \mathcal{H}$ (for a general case see Sec. 2.3). In this case dynamics leave these subspaces invariant, i.e., the jump and Hamiltonian operators in Eq. (2.1) are block-diagonal in this decomposition, $H = H^A \oplus H^I$ and $J_j = J_j^A \oplus J_j^I$. As we consider a first-order DPT in photon emissions, we assume that the dynamics within \mathcal{H}_A corresponds to a higher average number of emissions per unit of time than dynamics within \mathcal{H}_I , and term the respective dynamics “active” and “inactive”.

Let us consider the system initially in a pure state supported both in \mathcal{H}_A and \mathcal{H}_I with probability weights p_A and p_I , i.e., $|\chi\rangle = \sqrt{p_A}|\chi_A\rangle + \sqrt{p_I}|\chi_I\rangle$, where $|\chi_A\rangle \in \mathcal{H}_A$ and $|\chi_I\rangle \in \mathcal{H}_I$. The corresponding MPS at time t is a *macroscopic superposition* $|\Psi(t)\rangle = \sqrt{p_A}|\Psi_A(t)\rangle + \sqrt{p_I}|\Psi_I(t)\rangle$ of the orthogonal states $|\Psi_A(t)\rangle$ and $|\Psi_I(t)\rangle$, as the system state within $|\Psi_{A,I}(t)\rangle$ is supported only on $\mathcal{H}_{A,I}$ due to the Hamiltonian H and jumps $\{J_j\}_j$ preserving the subspaces. Moreover, as the photon emission number $\Lambda(t)$ is an observable on the output state only, the system states remain orthogonal, and there is no interference between $|\Psi_A(t)\rangle$ and $|\Psi_I(t)\rangle$ in the photon emission statistics, which is just a *mixture* of distributions for $|\Psi_A\rangle$ and $|\Psi_I\rangle$. Thus, the leading terms in the average and the variance of the photon emission number are

$$\langle \Lambda(t) \rangle = t(p_A \mu_A + p_I \mu_I) + \mathcal{O}(1) \quad (2.16)$$

$$\begin{aligned} \Delta^2 \Lambda(t) &= p_A \Delta_A^2 \Lambda(t) + p_I \Delta_I^2 \Lambda(t) \\ &\quad + p_A p_I (\langle \Lambda(t) \rangle_A - \langle \Lambda(t) \rangle_I)^2 \\ &= t^2 p_A p_I (\mu_A - \mu_I)^2 + \mathcal{O}(t), \end{aligned} \quad (2.17)$$

where $\langle \Lambda(t) \rangle_{A,I}$ and $\Delta_{A,I}^2 \Lambda(t)$ are the average and variance, respectively, of the number of emissions for the system initially in

the state $|\chi_{A,I}\rangle$. Note that the leading terms in (2.16) and (2.17) depend on the initial state only via the probabilities p_A and p_I . For a DPT in photon emissions, the emission rates within \mathcal{H}_A and \mathcal{H}_I are different, $\mu_A > \mu_I$, and the variance grows *quadratically* in time. The photon statistics are *bimodal* and do not follow the CLT. Note that in the case of higher-degeneracy of the 0-eigenvalue of \mathcal{L} , the photon statistics may feature more than two modes, but the variance will again scale quadratically with time. Finally, the quadratic scaling of variance of photon emissions corresponds to different averages of a system observable $M = J_1^\dagger J_1$ in two stationary states (see Eq. (2.14)) and thus, to a *stationary* first-order phase transition.

Macroscopic optical shift. The quadratic scaling of the photon number variance implies that the QFI in optical-shift estimation using photons emitted from the system initially in the pure state, also scales quadratically, see Eq. (2.13). In the case of a first-order DPT, this is a consequence of a *macroscopic* optical-shift difference effectively encoded on the two states $|\Psi_A(t)\rangle$ and $|\Psi_I(t)\rangle$ in the superposition of the MPS $|\Psi_\phi(t)\rangle$. In the first order of ϕ , the difference in complex phase is $t(\mu_A - \mu_I)\phi$. This, analogously as in the case of optical-shift estimation with the GHZ state, leads to the *Heisenberg scaling* in time.

2.2.3 Near a first-order DPT in photon emissions

Generically, open quantum system dynamics feature a single stationary state, ρ_{ss} , and thus photon counting statistics obeys the central limit theorem, and both the variance of photon emissions and the QFI scale linearly in time, see Eq. (2.15). The emission records, however, can be *intermittent* with dynamics switching between long periods with distinct emission characteristics [32–34, 36], see also Fig. 2.1 (b). Below we explain that intermittency corresponds to proximity to a first-order DPT. Furthermore, it leads to *bimodal* photon emission statistics with the *quadratically* growing variance for times shorter than the corre-

lation time τ of the dynamics [36].

Regime of quadratic scaling in photon emission variance. The average length τ_A , τ_I of “active” and “inactive” periods in the dynamics is the longest (observed) timescale in the dynamics. Let us assume that there does not exist any other (direct or continuous) measurement on the system demonstrating a longer timescale. Then τ_A , τ_I is necessary proportional to the dynamics correlation time $\tau = (-\lambda_2)^{-1}$, given by the inverse of the lowest-lying eigenvalue of the master operator \mathcal{L} . For times much shorter than the correlation time τ — and thus τ_A and τ_I — photon emission records are mostly inside “active” or “inactive” periods. The photon statistics is approximately bimodal, see also Fig. 2.1 (b) and [36]. This implies a quadratic increase of the variance with time, and thus also of the QFI,

$$\Delta^2 \Lambda(t) \approx t^2 p_A p_I (\mu_A - \mu_I)^2 + \mathcal{O}(t). \quad (2.18)$$

Here μ_A and μ_I are the average counting rates in “active” or “inactive” periods, while p_A and p_I are probabilities of observing an “active” or “inactive” period. For $t \ll \tau$ there is a macroscopic, $\propto t$, difference between the number of photons observed in emission records. When the photon output is used for optical-shift estimation, this will lead to encoding in the MPS, $|\Psi_\phi(t)\rangle$, the macroscopic parameter $t(\mu_1 - \mu_2)\phi$, and thus to the quadratic scaling of the QFI with time.

For times much longer than τ , in each emission record the dynamics switch between periods of distinct emission rates many times, giving rise to the intermittent behaviour [34, 36]. The eventual distribution of the photon count is *unimodal* centered around the overall average with the variance scaling *linearly* in time, cf. Fig. 2.1 (b) and Fig. 2.2. There is no macroscopic optical shift encoded in the MPS anymore.

In Fig. 2.2 we show the QFI for optical-shift estimation using photon output of a 3-level system, with a Hamiltonian $H = \Omega_1 H_1 + \Omega_2 H_2$, where $H_j = |j\rangle\langle 0| + |0\rangle\langle j|$, $j = 1, 2$, and a single jump operator $J = \sqrt{\kappa} |0\rangle\langle 1|$ that corresponds to an emission of

a photon. When $\Omega_2 \ll \Omega_1$, system trajectories can be “shelved” for long times in $|2\rangle$, giving rise to intermittency in observed quantum jumps [33]. The intermittency can be seen as the proximity to a first-order DPT [34] and is a consequence of a small gap in the master operator \mathcal{L} [35]. In Fig. 2.2 the estimation precision is enhanced as long as initial state evolves into mixtures of “active” and “inactive” records, cf. Eq. (2.35). Furthermore, in the quadratic regime of the QFI, the resource used – average number of photons – scales linearly with time, see the inset of Fig. 2.2.

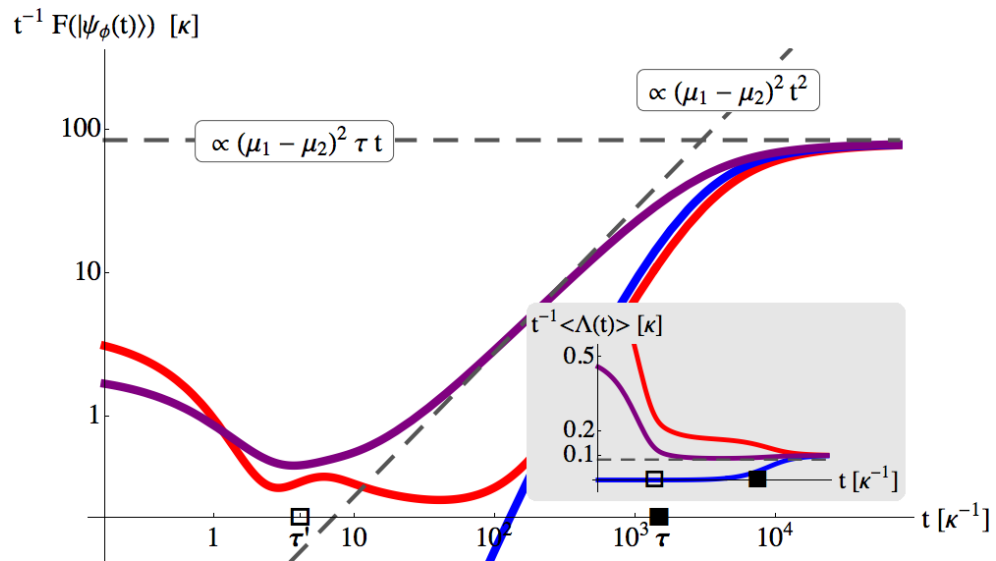


Figure 2.2: **Enhanced estimation of optical phase-shift using intermittent 3-level system:** The precision is enhanced quadratically in the regime $\tau' \ll t \ll \tau$ for the initial state $\frac{1}{\sqrt{2}}(|1\rangle + |2\rangle)$ (purple), while for initial states $|1\rangle$ (red) and $|2\rangle$ (blue), it is absent. This corresponds to the initial state $\frac{1}{\sqrt{2}}(|1\rangle + |2\rangle)$ evolving into mixture of active and inactive records, see the average photon number in the inset for the initial states and Eq. (2.18). At times $t \gg \tau$ a linear scaling of the QFI is recovered, cf. Eq. (2.15). The parameters were chosen as $\Omega_1 = 4\kappa$ and $\Omega_2 = \Omega_1/50$.

Intermittency as proximity to a DPT in photon emissions. For intermittent records of photon emissions, the correlation time τ is much longer than any other timescales, e.g. time between individual emissions in “active” periods. This implies a separation of the eigenvalues of the master operator \mathcal{L} , which determine all the dynamics timescales. In particular, for two distinct emis-

sion characteristics appearing in a record, $-\lambda_2 = \tau^{-1} \ll -\text{Re}\lambda_3$. Therefore, \mathcal{L} has a small gap, which is necessary to be near a DPT.

At times much longer than the correlation time, $t \gg \tau$, the system reaches the stationary state ρ_{ss} and the initial state is forgotten. However, correlations in photon emissions records do not disappear. The correlation between numbers of photons emitted in different time intervals $[t_1, t_1 + \Delta t]$, $[t_2, t_2 + \Delta t]$ depends only on the time $|t_1 - t_2|$ between them, due to stationarity of the system state, $\rho(t) = \rho_{ss}$, and decays approximately as $e^{\lambda_2|t_1 - t_2|}$ for the interval length chosen as $(-\text{Re}\lambda_3)^{-1} \ll \Delta t \ll \tau$. Since the variance of the total number of photons emitted up to time t is simply the double integral over the correlations, for $t \gg \tau$ we have

$$\Delta^2 \Lambda(t) \approx \sum_{k,j=1}^{t/\Delta t} \Delta^2 \Lambda(\Delta t) e^{\lambda_2|k-j|\Delta t},$$

where $\Delta^2 \Lambda(\Delta t)$ is the variance of the number of photons emitted within Δt for the system in the stationary state. Together with Eq. (2.18) this gives a leading contribution to the asymptotic linear behaviour

$$v = \lim_{t \rightarrow \infty} \frac{\Delta^2 \Lambda(t)}{t} \approx 2 \tau p_A^{ss} p_I^{ss} (\mu_A - \mu_I)^2, \quad (2.19)$$

where p_A^{ss} , p_I^{ss} are probabilities of observing an "active" or "inactive" period for the observation time $\Delta t \ll \tau$ and the system in the stationary state. Thus, the variance diverges as the correlation time τ , see also Eq. (2.15) and Fig. 2.2. This demonstrates that an intermittent system dynamics is indeed near a DPT in photon emissions. As only finitely many eigenvalues of \mathcal{L} are close to 0-eigenvalue (in the case above only λ_2), the intermittent dynamics manifests proximity to a first-order DPT.

The relation of parameter estimation to second-order DPTs, which can only appear in the thermodynamic limit of the sys-

tem size as well as to transitions in ensembles of trajectories, will be discussed in the next subsection.

2.2.4 Optical-shift encoding and deformation of master dynamics

The MPS of the system and the output is an unravelling of the system master dynamics, which purifies a mixed state of the system. Note that the MPS represents the perfect knowledge on the joint system-environment evolution, as there exist various gauge choices of H , and $\{J_j\}$ leading to the same master dynamics \mathcal{L} , but different MPSS.

As the optical-shift encoding is an operation that can be implemented sequentially in time, it can be included as a part of the joint system-environment evolution. For simplicity let a photon emission event be associated with the jump operator J_1 . The MPS with the encoded optical shift ϕ , $|\Psi_\phi(t)\rangle = e^{-i\phi\Lambda(t)}|\Psi(t)\rangle$, is identical to the MPS for the master dynamics with the jump $J_{1,\phi} := e^{-i\phi}J_1$ now depending on the optical shift, and the Hamiltonian H and the other jump operators as before, $H_\phi = H$, $J_{j,\phi} = J_j$, $j > 1$. Note that although the jump operator $J_{1,\phi}$ depends on the parameter ϕ , the master dynamics of the system state $\mathcal{L}_\phi = \mathcal{L}$ remains unchanged, as the optical shift is encoded on the output only. Optical-shift encoding is thus an example of a *gauge* transformation of \mathcal{L} , i.e., a transformation of H and L that do not alter the master operator \mathcal{L} itself, for other examples see Appendix B.3.3.

The fidelity between the MPSS with different optical-shift values can be expressed on the system level as

$$\langle \Psi_{\phi'}(t) | \Psi_\phi(t) \rangle = \text{Tr} \left(e^{t\mathcal{L}_{\phi',\phi}} |\chi\rangle\langle\chi| \right), \quad \text{with} \quad (2.20)$$

$$\mathcal{L}_{\phi',\phi}\rho = -i[H, \rho] + e^{-i(\phi-\phi')}J_1\rho J_1^\dagger + \sum_{j>1} J_j \cdot J_j^\dagger - \frac{1}{2} \sum_j \{J_j^\dagger J_j, \rho\} \quad (2.21)$$

being a *deformation* of the master operator \mathcal{L} , which is not trace-preserving (for the derivation see the next Sec. 2.3). In the case

of a single stationary state, from Eq. (2.24), the QFI is related to $\mathcal{L}_{\phi_1, \phi_2}$ as follows

$$\lim_{t \rightarrow \infty} \frac{1}{t} F(|\Psi_\phi(t)\rangle) = 4 \left. \partial_{\phi_1} \partial_{\phi_2} \lambda_1(\phi_1, \phi_2) \right|_{\phi_1 = \phi_2 = \phi}, \quad (2.22)$$

where $\lambda_1(\phi_1, \phi_2)$ is the eigenvalue of $\mathcal{L}_{\phi_1, \phi_2}$ with the maximal real part.

More on relation to photon counting. In the case of optical-shift encoding the fidelity corresponds to a characteristic function of the number of photons emitted up to time t and thus its logarithm encodes the cumulants of the photon number statistics. As we discussed in Sec. 2.1.2, the cumulants can also be encoded in the CGF, $\Theta_t(s)$, and its long-time limit, $\theta(s)$, which are given by dynamics with a deformation \mathcal{W}_s of the master operator \mathcal{L} , see Eqs. (2.5), (2.7) and (2.6). Note that \mathcal{W}_s is the same as $\mathcal{L}_{\phi', \phi}$ with $(\phi - \phi') = -is$. As the QFI is related to the variance of the photon emission number (2.13), we arrive at

$$\lim_{t \rightarrow \infty} \frac{1}{t} F(|\Psi_\phi(t)\rangle) = 4 \left. \partial_s^2 \theta(s) \right|_{s=0}. \quad (2.23)$$

For a DPT in photon emissions of a first or second order (which happens only in the limit of the infinite system size), the QFI scaling with time will be enhanced and no longer linear. For a transition in the ensemble of quantum jump trajectories, when the function $\theta(s)$ has a first- or second-order singularity at some $|s_c|$, although the QFI necessary scales linearly, the constant enhancement in Eq. (2.23) can be large when $|s_c| \approx 0$. Note that from Eq. (2.15), this can be also seen as a consequence of the fact that the gap in \mathcal{L} must be small when $|s_c| \approx 0$.

2.3 GENERAL PARAMETER ESTIMATION AND DPTS

In the previous section 2.2 we discussed optical-shift estimation using a photon output of an open quantum system, see Fig. 2.1. We showed how the corresponding QFI can be enhanced from a linear to a quadratic scaling in time for the system at a first-

order DPT in photon emissions. Moreover, we demonstrated that near such a first-order DPT, when the photon emissions are intermittent, although the asymptotic scaling is linear, there exist an intermediate time regime when the QFI scales quadratically with time. Furthermore, the constant in the linear scaling of the QFI diverges as one approaches the transition due to increasing correlations in photon emissions. In this section we show that analogous results hold for a general parameter estimation.

We consider estimation of a parameter g in the joint system-and-output evolution, such as g being an *intrinsic* parameter of the system dynamics or a *extrinsic* parameter encoded locally in time on the output. Thus, we assume that the Hamiltonian, H_g , and jump operators, $L_{j,g}$ may depend on g *analytically*, but the type of emitted quanta does not depend on g . It follows that the MPS representing the system-output state, $|\Psi_g(t)\rangle$, also depends on g , see Eqs. (2.2) and (2.3). In contrast, the master operator \mathcal{L}_g , Eq. (2.1), depends on g only when varying g changes the actual system dynamics. This is not the case for encoding a parameter on the output, which is a gauge transformation of \mathcal{L} .

2.3.1 Parameter estimation and deformation of master dynamics

In order to consider optimal precision of the estimation, we investigate the QFI related to the fidelity, $\langle \Psi_{g'}(t) | \Psi_g(t) \rangle$, see Eq. (2.12). Similarly, as in the case of the optical shift encoded on a photon output, the fidelity can be expressed on the level of the system state as

$$\langle \Psi_{g'}(t) | \Psi_g(t) \rangle = \text{Tr} \left(e^{t\mathcal{L}_{g',g}} |\chi\rangle \langle \chi| \right), \quad (2.24)$$

where $\mathcal{L}_{g',g}$ is a deformation of the master operator

$$\begin{aligned} \mathcal{L}_{g',g}\rho &= -iH_g\rho + i\rho H_{g'} \\ &+ \sum_j \left[J_{j,g}\rho J_{j,g'}^\dagger - \frac{1}{2} \left(J_{j,g}^\dagger J_{j,g}\rho + \rho J_{j,g'}^\dagger J_{j,g'} \right) \right]. \end{aligned} \quad (2.25)$$

Note that the operator $\mathcal{L}_{g',g}$ in general is not trace-preserving and thus, it does not explicitly correspond to any system dynamics, but nonetheless can be (indirectly) realised experimentally, for details see Sec. 2.5.2.

Proof. In order to prove Eq. (2.24), let us consider the discrete MPS in (2.3). We have

$$\begin{aligned} \langle \Psi_{g'}(t) | \Psi_g(t) \rangle &= \text{Tr}_S \text{Tr}_O (|\Psi_g(t)\rangle \langle \Psi_{g'}(t)|) \\ &= \text{Tr}_S \left\{ \sum_{j_n, \dots, j_1} K_{j_n, g} \cdots K_{j_1, g} |\chi\rangle \langle \chi| K_{j_n, g'}^\dagger \cdots K_{j_1, g'}^\dagger \right\}, \end{aligned}$$

where $\text{Tr}_{S,O}$ stands for the trace over the space of the system (S) or output (O). In the rest of this chapter we will simplify the notation and use Tr instead of Tr_S .

In the limit $\delta t \rightarrow 0$, we obtain Eq. (2.24) analogously as the discretisation in the master dynamics converges to the continuous dynamics given by \mathcal{L}_g ,

$$\begin{aligned} \rho_g(\mathbf{n}) &= \sum_{j_n, \dots, j_1} K_{j_n, g} \cdots K_{j_1, g} |\chi\rangle \langle \chi| K_{j_n, g}^\dagger \cdots K_{j_1, g}^\dagger \\ &\xrightarrow{\delta t \rightarrow 0} \rho_g(t) = e^{t\mathcal{L}_g} |\chi\rangle \langle \chi|. \end{aligned}$$

The result in Eq. (2.24) has been already discussed in [38, 39]. ■

2.3.2 Linear scaling of QFI away from a DPT

For dynamics with a single stationary state, the QFI asymptotically scales *linearly* with time with the constant enhancement related the largest eigenvalue $\lambda_1(g_1, g_2)$ of \mathcal{L}_{g_1, g_2} [38, 39], as from Eqs. (2.12) and (2.24) it follows that

$$\lim_{t \rightarrow \infty} t^{-1} F(|\Psi_g(t)\rangle) = 4 \partial_{g_1} \partial_{g_2} \lambda_1(g_1, g_2) |_{g_1=g_2=g}. \quad (2.26)$$

Eq. (2.26) can be expressed via the master operator \mathcal{L} as follows (see Appendix B.2 or non-hermitian perturbation theory in [38]),

$$\lim_{t \rightarrow \infty} t^{-1} F(|\Psi_g(t)\rangle) = 4 \text{Tr} (\partial_{g_1} \partial_{g_2} \mathcal{L}_{g_1, g_2} \rho_{ss}) \quad (2.27)$$

$$- 8 \text{Re Tr} \left(\partial_{g_1} \mathcal{L}_{g_1, g} \left[\mathcal{L}_g^{-1} \right]_{\mathcal{J}-\mathcal{P}_{ss}} \partial_{g_2} \mathcal{L}_{g, g_2} \rho_{ss} \right)_{g_1 = g_2 = g},$$

where $[\cdot]_{\mathcal{J}-\mathcal{P}_{ss}}$ restricts a superoperator to the complement of the stationary state. One can already see that something interesting may occur as the system approaches a DPT when the gap in \mathcal{L}_g closes at some g , and $[\mathcal{L}_g^{-1}]_{\mathcal{J}-\mathcal{P}_{ss}}$ diverges as $(\lambda_2)^{-1}$. Consequently, closing of the gap in \mathcal{L}_g may cause $\lambda_1(g_1, g_2)$ to be *non-analytic* at $g_1 = g_2 = g$.

2.3.3 Quadratic scaling of QFI, bimodality and first-order DPTs

Regime of quadratic scaling of QFI near a first-order DPT. Near a first-order DPT the gap of the master operator \mathcal{L}_g is necessary small [35], i.e., there is a separation in real parts of the \mathcal{L}_g spectrum, e.g. $-\lambda_2 \ll -\text{Re}\lambda_3$. Therefore, there exist an intermediate time regime $\tau' \ll t \ll \tau$, where τ is the dynamics correlation time given by the gap, $\tau = (-\text{Re} \lambda_2)^{-1}$, while τ' is the longest timescale associated with the rest of the spectrum, $\tau' = (-\text{Re} \lambda_3)^{-1}$. In this regime the slowest second dynamical mode appears stationary whereas the contribution from all the other eigenmodes in \mathcal{L}_g can be neglected. This further leads to the QFI being quadratic in time (see Appendix B.2 for the derivation),

$$F(|\Psi_g(t)\rangle) = 4t^2 \left(- \left| \partial_{g_1} \text{Tr} (\mathcal{L}_{g_1, g} \mathcal{P}|\chi\rangle\langle\chi|) \right|^2 \quad (2.28)$$

$$+ \partial_{g_1} \partial_{g_2} \text{Re Tr} (\mathcal{L}_{g_1, g} \mathcal{P} \mathcal{L}_{g, g_2} \mathcal{P}|\chi\rangle\langle\chi|) \right)_{g_1 = g_2 = g}$$

$$+ t^2 \mathcal{O}(t\lambda_2) + \mathcal{O}(t),$$

where \mathcal{P} is a projection onto the eigenmatrices of \mathcal{L}_g corresponding to the eigenvalues within the gap, e.g. for $-\lambda_2 \ll -\text{Re}\lambda_3$, \mathcal{P} projects onto first two eigenvectors of \mathcal{L}_g . At a first-order DPT, the gap closes, $\lambda_2 \rightarrow 0$ and Eq. (2.28) becomes valid for all times $t \gg \tau'$ with the projection \mathcal{P} becomes the projection on the stationary manifold \mathcal{P}_0 of two stationary states $\tilde{\rho}_1, \tilde{\rho}_2$ supported in orthogonal subspaces $\mathcal{H}_1, \mathcal{H}_2$.

Quadratic scaling and bimodality. We will now show that the *quadratic* scaling with time of the QFI, corresponds to *bimodal statistics* of an observable acting on both the system and the output. The way the MPS $|\Psi_g(t)\rangle$ changes with g is encoded in the observable (see Sec. 2.5.1 for the precise definition)

$$G_g(t) |\Psi_g(t)\rangle := i \partial_{g'} |\Psi_{g'}(t)\rangle|_{g'=g}. \quad (2.29)$$

From Eq. (2.12) it follows that the QFI is again simply proportional to the variance of $G_g(t)$ when measured on the MPS $|\Psi_g(t)\rangle$,

$$F(|\Psi_g(t)\rangle) = 4\Delta^2 G_g(t). \quad (2.30)$$

This establishes the relation between the precision of parameter g estimation with a system initially in a *pure* state and statistics of an observable on the joint system-output state.

The generator $G_g(t)$ is a *stochastic integral* of an observable *local* in time, see Sec. 2.5.1. Therefore, it follows that the finite-time interval before the system relaxes to its asymptotic state, $t \lesssim \tau$, contributes negligibly to the asymptotic behaviour of leading terms in $G_g(t)$ cumulants. Note that in general, at a first-order DPT with two stationary states, for a system state ρ_{in} with initial coherences between the subspaces $\mathcal{H}_1, \mathcal{H}_2$, the coherences will persist in the joint system-output MPS and lead to interferences in statistics of $G_g(t)$. Since coherences are absent in the asymptotic state of the system, $\lim_{t \rightarrow \infty} \rho(t) = p_1 \tilde{\rho}_1 + p_2 \tilde{\rho}_2$, leading orders in the average, variance of $G_g(t)$ will not,

however, depend on the coherences, but on the probabilities p_1 and p_2 .

We first discuss the average of $G_g(t)$. We have

$$\begin{aligned} \langle G_g(t) \rangle &= -i \partial_{g'} \langle \Psi_{g'}(t) | \Psi_g(t) \rangle_{g'=g} = -i \partial_{g'} \text{Tr}(e^{t\mathcal{L}_{g',g}} |\chi\rangle \langle \chi|)_{g'=g} \\ &= -i \int_0^t du \text{Tr}(\partial_{g'} \mathcal{L}_{g',g} \rho(u))_{g'=g} \quad \text{and} \end{aligned} \quad (2.31)$$

$$\mu_g = \lim_{t \rightarrow \infty} \frac{1}{t} \langle G_g(t) \rangle = -i \text{Tr}(\partial_{g'} \mathcal{L}_{g',g} \mathcal{P}_0 |\chi\rangle \langle \chi|)_{g'=g} \quad (2.32)$$

Note that the *instant rate* at which $G_g(t)$ is accumulated is given by $-i \text{Tr}(\partial_{g'} \mathcal{L}_{g',g} \rho(t))_{g'=g}$. Moreover, this result holds also for mixed initial states ρ_{in} . In the case of the single stationary state $\mathcal{P}_0 = \rho_{\text{ss}} \text{Tr}(\cdot)$ and thus the average of $G_g(t)$ per unit time, $\mu_g = -i \text{Tr}(\partial_{g'} \mathcal{L}_{g',g} \rho_{\text{ss}})_{g'=g}$, is independent from the initial state. In the case of two-fold degeneracy of the 0-eigenvalue of \mathcal{L}_g , the asymptotic rate

$$\mu_g = p_1 \mu_1 + p_2 \mu_2, \quad (2.33)$$

where $p_{1,2}$ are probabilities in the asymptotic state, $p_1 \tilde{\rho}_1 + p_2 \tilde{\rho}_2$, and μ_1, μ_2 are asymptotic rates of $G_g(t)$ for initial states relaxing to \mathcal{H}_1 and \mathcal{H}_2 , respectively. Note that the asymptotic rate indeed does not depend on the initial coherences between \mathcal{H}_1 and \mathcal{H}_2 which are absent for times $t \gg \tau'$.

Let us now discuss the variance of $G_g(t)$. For the case of the single stationary state, the variance $\Delta^2 G_g(t)$ necessarily scales linearly in time for $t \gg (-\lambda_2)^{-1}$, cf. Eq. (2.27). In contrast, when the master operator \mathcal{L}_g has a degenerate 0-eigenvalue, the asymptotic scaling of the variance may become quadratic in time, see Eq. (2.28). For two-fold degeneracy of 0-eigenvalue, the leading quadratic term of the variance, similarly as the average, will not depend on the coherences (see Appendix B.3.1)

$$\Delta^2 G_g(t) = t^2 p_1 p_2 (\mu_1 - \mu_2)^2 + \mathcal{O}(t). \quad (2.34)$$

For the system state relaxing only to one of the subspaces \mathcal{H}_1 or \mathcal{H}_2 (for example initialised in those subspaces), the variance scales linearly as in the case of dynamics with a single stationary state. In particular, when there is no decay subspace, the linear and constant terms are given exactly as in Eqs. (2.27), (B.6), with $\mathcal{J} - \mathcal{P}_{ss}$ replaced by $\mathcal{J}_{\mathcal{H}_{1,2}} - \mathcal{P}_{ss}^{(1,2)}$. For a general initial state the linear terms in Eq. (2.34) will also depend also on initial coherences between \mathcal{H}_1 and \mathcal{H}_2 , see Appendix B.3.2.

We have shown that quadratic scaling of $\Delta^2 G_g(t)$ for dynamics featuring two stationary states, Eq. (2.34), is a consequence of bimodal statistics of the observable $G_g(t)$. In the case of a higher than two-fold degeneracy of the 0-eigenvalue of \mathcal{L}_g , the $G_g(t)$ statistics may feature several modes, but the variance scaling will be always at most quadratic with time, cf. derivation of Eq. (2.28) in Appendix B.2. For higher-fold degeneracy some of the initial coherences in the system may not decay, in which case the leading quadratic term may crucially depend also on those initial coherences. For general discussion of enhanced parameter estimation in the case of higher-fold degeneracy, see Appendix D.3.

Quadratic scaling and macroscopic phase-shift. We have shown that for a pure initial state of the system the quadratic scaling of QFI is related to the bimodality of variance of the observable $G_g(t)$, (2.29). The observable $G_g(t)$ encodes the parameter via a "phase" in the MPS state

$$|\Psi_{g'}(t)\rangle = \mathcal{T} e^{-i \int_g^{g'} dh G_h(t)} |\Psi_g(t)\rangle,$$

where \mathcal{T} is the g -ordering (cf. time-ordering) operator, see also [104, 105, 171]. The quadratic behaviour of the QFI can be associated with a *macroscopic phase shift* encoded via $G_g(t)$ in the MPS, since, in the first order with respect to $\Delta g := g' - g$, two parts of the MPS initialised in \mathcal{H}_1 and \mathcal{H}_2 differ in the complex phase by a macroscopic *effective* parameter $t(\mu_1 - \mu_2)\Delta g$. For a finite system, it is this macroscopic phase-shift that leads to the *Heisenberg scaling* in time, similarly as in the case of GHZ states.

No quadratic scaling for classical systems. Let us note that the t^2 -scaling of the QFI is an intrinsically quantum feature. This behaviour cannot occur in finitely dimensional systems for which the associated MPS is real, as the average of the observable $G_g(t)$ is 0, $\langle G_g(t) \rangle = -i \partial_{g'} \langle \Psi_{g'}(t) | \Psi_g(t) \rangle \in i\mathbb{R} \cap \mathbb{R} = \{0\}$, and thus also the rate $\mu_g = 0$. Therefore, only terms linear in t will survive in Eq. (2.34). In other words, the parameter g cannot be encoded via unitary transformation of the MPS and there cannot be any macroscopic phase shift.

Bimodal statistics near a first-order DPT. We assume that the master operator \mathcal{L}_g with a single stationary state features a small gap, i.e., there is a split in its spectrum. This leads to a separation of dynamics timescales which manifest itself in the system dynamics as a broad intermediate time regime, $\tau' \ll t \ll \tau$, when the system state $\rho(t)$ appears stationary before eventually relaxing to the true stationary state ρ_{ss} at times $t \gg \tau$.

In the time regime $\tau' \ll t \ll \tau$, the instant rate of $G_g(t)$, $\mu_g(t) = \text{Tr}(\partial_{g'} \mathcal{L}_{g',g} \rho(t))_{g'=g}$, is approximately constant. Therefore, for times t towards the end of the regime, the average is dominated by $\langle G_g(t) \rangle \approx t \text{Tr}(\partial_{g'} \mathcal{L}_{g',g} \rho(t))_{g'=g}$. Since the instant rate depends on the initial system state via $\rho(t)$, let consider the initial states leading to the maximal μ_1 and the minimal μ_2 instant rate for the metastable regime $\tau' \ll t \ll \tau$, and thus also the extremal averages $\langle G_g(t) \rangle_1$ and $\langle G_g(t) \rangle_2$. Furthermore, the initial states can be chosen pure, $|\chi_1\rangle$ and $|\chi_2\rangle$. In the case of one-low lying eigenvalue in the \mathcal{L}_g spectrum, i.e., $-\lambda_2 \ll -\text{Re}\lambda_3$, for the system initially in a *superposition* of those initial states, $|\chi\rangle = \sqrt{p_1} |\chi_1\rangle + \sqrt{p_2} |\chi_2\rangle$, the statistics of $G_g(t)$ can be shown to be bimodal as follows. The system state in the intermediate regime can be well described by an approximately stationary contribution of the second dynamical mode — one degree of freedom — while all the other modes are negligible. Thus, the initial coherences can no longer be present in $\rho(t)$. Consequently, as the statistics of $G_g(t)$ for time t at the end of the regime is dominated by the contribution during the regime, the statistics is necessary close to that of the system initially in

a *mixture* of the two initial states, $\rho_{\text{in}} = p_1|\chi_1\rangle\langle\chi_1| + p_2|\chi_2\rangle\langle\chi_2|$. Therefore, the statistics of $G_g(t)$ for times $\tau' \ll t \ll \tau$ is *bimodal* and its variance scales *quadratically* with time,

$$\Delta^2 G_g(t) \approx t^2 p_1 p_2 (\mu_1 - \mu_2)^2 + \mathcal{O}(t). \quad (2.35)$$

Moreover, for *any* initial state the instant rate in the intermediate regime can be expressed as $p_1\mu_1 + p_2\mu_2$ for some probabilities $p_1, p_2 = 1 - p_1$. As this fixes the only degree of freedom in this regime, the corresponding system state in the intermediate regime can be approximated by the system state initialised in a *mixture* $\rho_{\text{in}} = p_1|\chi_1\rangle\langle\chi_1| + p_2|\chi_2\rangle\langle\chi_2|$. It follows that the statistics $G_g(t)$ is *bimodal* and the variance can be expressed as in (2.35) for any initial state of the system. For a formal proof of correspondence between Eqs. (2.28) and (2.35) see Appendix D.1.

Note that for *classical systems* the instant rate is always 0, and thus there is *no quadratic regime* in the variance scaling.

The quadratic scaling of the variance in (2.35) is related to correlations in the dynamics which disappear as $\exp(-\lambda_2 t)$ and thus in the intermediate regime are approximately constant. As the observable $G_g(t)$ is a stochastic integral (see Sec. 2.5.1), let us consider it as a sum of contributions from time intervals Δt within the intermediate regime length, $\tau' \ll \Delta t \ll \tau$. As after $t \gg \tau$ the system is in the stationary state the asymptotic variance can be approximated well as (see also Appendix B.3.2)

$$\Delta^2 G_g(t) \approx \sum_{k,j=1}^{t/\Delta t} \Delta^2 G_g(\Delta t) e^{\lambda_2 |k-j|\Delta t},$$

where $\Delta^2 G_g(\Delta t)$ is the variance for the system in the stationary state. Together with Eq. (2.35) this gives a leading contribution to the asymptotic linear scaling of the variance

$$\nu_g = \lim_{t \rightarrow \infty} \frac{\Delta^2 G_g(t)}{t} \approx 2 \tau p_1^{\text{ss}} p_2^{\text{ss}} (\mu_1 - \mu_2)^2. \quad (2.36)$$

where p_1^{ss}, p_2^{ss} are probabilities determined by the asymptotic rate $\mu_g = -i\text{Tr}(\partial_{g'}\mathcal{L}_{g',g}\rho_{ss})_{g'=g} = p_1^{ss}\mu_1 + p_2^{ss}\mu_2$. Thus, the linear limit of the variance diverges as the correlation time τ , see also Eq. (2.27) and the formal proof in Appendix D.1.

In Chapter 3 we discuss *metastability* in Markovian open quantum systems. We argue how this phenomena is related to a separation in the spectrum of a master operator and how it manifests itself in the dynamics on the level of the system and output observables. In particular, we show how, in the case of one low-lying eigenvalue of the master operator, i.e., $-\lambda_2 \ll -\text{Re}\lambda_3$, one can observe *intermittent* system dynamics. Furthermore, in Appendix D.1 we prove that the system states in the metastable regime which lead to the extremal averages of $G_g(t)$, correspond to extreme metastable states — *metastable phases*. Moreover, the quadratic scaling of the QFI with time for a pure initial state of the system, is also related to a macroscopic phase-shift encoded in the MPS state during the metastable regime, see Appendix D.1. As we discuss in the next section, the instant rate of $G_g(t)$ corresponds to an expected values of a system observable, see Eq. (2.37). Therefore, if metastability of a finite system is a consequence of a first-order static transition occurring in the thermodynamic limit of the system size, so that $\lim_{N\rightarrow\infty} \frac{\mu_1}{N} \neq \lim_{N\rightarrow\infty} \frac{\mu_2}{N}$, the QFI displays also the *Heisenberg scaling in the system size*, $F(|\Psi_g(t)\rangle)N^2 \propto t^2N^2$, cf. Eq. 2.36 and see example of photon emissions corresponding to spin magnetisation in a dissipative Ising chain with transverse field [36, 172].

2.4 ESTIMATION SCHEMES

In this section we discuss enhancement in optimal parameter estimation for several class of parameters, we consider parameter regimes in which such enhancement is present and study features of any efficient measurement that can exploit this enhancement.

2.4.1 Parameters

Here we discuss enhancement in parameter estimation near a first-order dynamical phase transition for parameters in the free system dynamics, strength of system-environment interaction and output parameters.

Let us first note that for a general parameter g the instant rate of $G_g(t)$ observable, $\mu_g = -i\text{Tr}(\partial_{g'}\mathcal{L}_{g',g}\rho(t))$, corresponds to the average, $\mu_g = \text{Tr}(M_g\rho(t))$, of the *system observable*

$$M_g = H'_g + \frac{i}{2} \sum_j \left[J_{j,g}^\dagger J'_{j,g} - (J'_{j,g})^\dagger J_{j,g} \right], \quad (2.37)$$

where we have introduced the notation $X'_g = \partial_{g'}X_g|_{g'=g}$. The quadratic behaviour of QFI at a DPT is a consequence of difference in the rates for two stationary states, $\mu_1 = \text{Tr}(M_g\tilde{\rho}_1) \neq \mu_2 = \text{Tr}(M_g\tilde{\rho}_2)$, see Eq. (2.34). Therefore, M_g can be used to determine the multiplicative constant in the quadratic scaling of QFI with time. Furthermore, for a system near a DPT, the observable M_g determines the quadratic scaling of the QFI in the intermediate regime $\tau' \ll t \ll \tau$, see (2.30) and (2.35). This criterion can be further simplified, as it is sufficient to check whether $\langle M_g \rangle$ is different for metastable phases discussed in Chapter 3, see Appendix D.1.

We consider the following class of parameters of the system-output dynamics, see Eq. (2.1),

- Coupling constants Ω in free system dynamics.

We consider the Hamiltonian $H_\Omega = H_0 + \Omega H_1$. We simply obtain

$$M_\Omega = H_1. \quad (2.38)$$

- Strength of the system-environment interaction.

We assume $J_{j,\kappa_j} = \sqrt{\kappa_j} J_j$, where $\kappa_j \geq 0$. Since

$$M_{\kappa_j} = 0 \quad \forall j, \quad (2.39)$$

the corresponding rate for any state is always 0 and thus there is no quadratic term in (2.34). Hence, there is *no enhancement* in estimation of the strength of the system-environment interaction. This is a consequence of the fact that κ_j is encoded in the MPS, $|\Psi_{\kappa_j}(t)\rangle$, as a *classical* parameter, which when varied, changes only the absolute values of amplitudes in the MPS, not their phase, cf. Eq. (2.2). Therefore, there is *no macroscopic phase* encoded on the MPS, similarly as in the case of a classical system. Furthermore, the QFI takes a simple form, cf. Appendix B.2,

$$F(|\Psi_{\kappa_j}(t)\rangle) = \left(t \operatorname{Tr} \left(J_j^\dagger J_j \rho_{ss} \right) + \operatorname{Tr} \left(J_j^\dagger J_j \left[\frac{e^{t\mathcal{L}_g} - \mathbb{J}}{\mathcal{L}_g} \right]_{\mathcal{J} \rightarrow \mathcal{P}_{ss}} |\chi\rangle\langle\chi| \right) \right), \quad (2.40)$$

which corresponds to the variance of the uncorrelated Poissonian statistics of jumps J_j .

- A phase in a unitary transformation of the output that can be implemented locally in time.

Here we can consider a gauge transformation of the master dynamics, when all H_g and $\{J_{j,g}\}_j$ can depend on g , but $\mathcal{L}_g \equiv \mathcal{L}$. In particular, the generator may be independent from the parameter value, $G_g(t) = G(t)$, in which case also its instant rate $\mu_g = \mu$, as the observable $M_g = M$.

In the example of the *optical shift* ϕ encoded on photons emitted by the system, we have $J_{1,\phi} := e^{-i\phi} J_1$ and the system observable is independent from ϕ , $M = J_1^\dagger J_1$. Similarly, for the parameter encoded by the *homodyne current* associated with photon emissions J_1 , we have the operators $J_{1,g} := J_1 - ig e^{-i\phi}$ and $H_g := H + \frac{g}{2} \left(e^{-i\phi} J_1 + e^{i\phi} J_1^\dagger \right)$ which leads to $M = e^{-i\phi} J_1 + e^{i\phi} J_1^\dagger$ being related to the average current rate, see Appendix B.3.3 for derivation. Note, however, that for the $g = \phi$ being the angle associated with the homodyne measurement, we have $J_{1,\phi} := J_1 - ie^{-i\phi}$ and $H_\phi := H + i \frac{e^{-i\phi} J_1 - e^{i\phi} J_1^\dagger}{2}$. This again leads

to the average current rate given by the observable $M_\phi = e^{-i\phi} J_1 + e^{i\phi} J_1^\dagger$, which in this case depends on the parameter ϕ , as so does the generator G_ϕ .

In Fig. 2.3 we show the QFI for estimation of the intrinsic parameters in dynamics of the 3-level system (see the upper inset) $\Omega_1, \Omega_2, \kappa$. The quadratic enhancement is absent due to no difference in the extreme rates μ_1, μ_2 , cf. Eq. (2.35). In contrast, for a parameter encoded as an amplitude (g) or an angle (ϕ) of homodyne current, cf. Appendix B.3, the quadratic scaling is present for $\phi \neq k\pi, k \in \mathbb{Z}$, see the inset of Fig. 2.3, which is analogous to enhancement in the optical phase-shift estimation in Fig. 2.2.

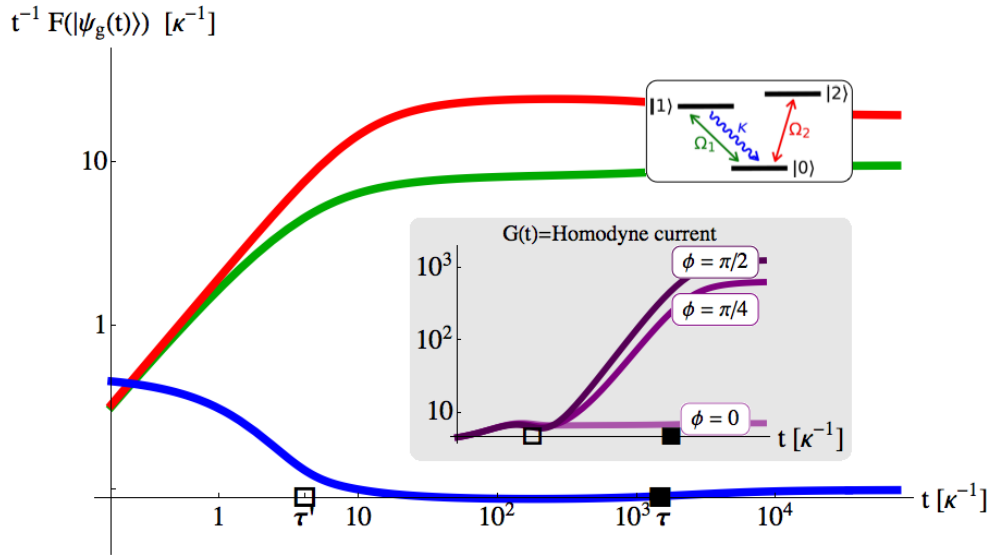


Figure 2.3: **Estimation of intrinsic dynamical parameters in 3-level system:** The quadratic enhancement is absent for Ω_1 (green), Ω_2 (red), and the classical parameter - decay rate κ (blue), and the asymptotic linear scaling is obtained at earlier timescales $\tau' = (-\text{Re}\lambda_3)^{-1} \ll \tau = (-\text{Re}\lambda_2)^{-1}$, as the lowest-lying mode does not contribute to the asymptotic precision. In contrast, for a parameter g encoded as the amplitude or the angle of homodyne current, the enhancement in precision is present for $\phi \neq k\pi, k \in \mathbb{Z}$ (for $\phi = k\pi$ we have that M_g equals $M_{\Omega_1} = H_1$ up to a linear transformation, see Appendix B.3.3). The initial state was chosen as $|\chi\rangle = \frac{1}{\sqrt{2}}(|1\rangle + |2\rangle)$ and the Rabi frequencies as $\Omega_1 = 4\kappa$ and $\Omega_2 = \Omega_1/50$.

2.4.2 Sensitivity over broad parameter range

In order to use an open quantum system and its output as a resource for enhanced parameter estimation, the sensitivity of the joint system-and-output state should be present over a broad parameter range. Otherwise, the system-output MPS can be used to mark a fixed point in the parameter range. This is analogous to requirements for classical sensors, e.g. thermometers, which should give an accurate temperature prediction over a broad range of temperatures, between fixed points usually given by thermal phase transitions in various classical systems [173]. Note that at those fixed points the accuracy can scale better than linear with the size of a classical system, as the accuracy for a thermal state $\rho_T = e^{-\frac{H}{k_B T}} / \text{Tr}(e^{-\frac{H}{k_B T}})$ is proportional to the variance of the system Hamiltonian, $\Delta^2 H$ [131]. Away from the transition, however, the accuracy scaling is necessary linear from the very definition of a phase transition.

Extrinsic parameters. Consider an *extrinsic parameter* g encoded as a phase by an *output observable* $O(t)$, $|\Psi_g(t)\rangle = e^{igO(t)}|\Psi(t)\rangle$, so that the corresponding system state does not change $\rho_g(t) \equiv \rho(t)$. Let us further assume that $O(t)$ is an integral of local-in-time quantity, i.e., an observable representing a continuous measurement, e.g. a total number of photons or an integrated homodyne current. In this case the MPS $|\Psi_g(t)\rangle$, can be expressed as the MPS obtained for dynamics with parameter dependent operators: the Hamiltonian H_g and the jump operators $\{J_{j,g}\}_{j=1}^k$. The master dynamics of the system, however, will be independent from the value of g , $\mathcal{L}_g \equiv \mathcal{L}$, as is the reduced state of the system obtained from $|\Psi_g(t)\rangle\langle\Psi_g(t)|$ by tracing out the output degrees of freedom. This emphasizes that the *resource* used for the estimation for all values of g is the same MPS, on which an unknown value of g is encoded.

Let system dynamics be close to a first-order DPT, so that \mathcal{L} features a separation in spectrum which leads to $\Delta^2 O(t)$ scaling linearly in time with a large constant, see Eq. (2.27), which is

directly related to quadratic scaling in the regime $\tau' \ll t \ll \tau$ due to distinct instant rates of $O(t)$. As the QFI is the same for all g , cf. (2.30), the optimal estimation precision is enhanced for the whole range of g . Therefore, a system near such a first-order DPT can be used as a resource for enhanced estimation of the parameter g .

For a general parameter g encoded by a stochastic integral, i.e., $|\Psi_g(t)\rangle = e^{iO_g(t)}|\Psi(t)\rangle$, where $O_g(t) \neq gO(t)$, we have $G_g(t) = \partial_g O_g(t)$. When at $g = g_0$ dynamics is close to a DPT with $\Delta^2 G_{g_0}(t)$ scaling linearly in time with a large constant, there exist a finite range of g , where, in spite of varying g , the extremal rates of $G_g(t)$ in the regime $\tau' \ll t \ll \tau$ stay non-negligibly different, $(\mu_1 - \mu_2) \gg (-\lambda_2)$. In this parameter range the QFI features the quadratic scaling regime and the constant of the asymptotic linear scaling is large (see (2.35) and (2.36)).

Intrinsic parameters. Let us now consider an intrinsic parameter g of dynamics such that the master operator \mathcal{L}_g depends on the value of g . We distinguish two types of intrinsic parameters.

Parameters driving a transition. When a parameter g drives a stationary or dynamical phase transition at $g = g_0$, the corresponding MPS undergoes a singular change at $g = g_0$. It is this singularity that allows for estimating with high precision the value of g in the vicinity of g_0 , and in the case of a first-order DPT, it manifests itself as a regime of quadratic scaling of the QFI (2.35). Varying g in broader range, however, takes system away from the transition point and increases the gap in \mathcal{L}_g thus shortening the quadratic regime, which further leads to a moderate constant in linear scaling of the QFI (2.27). Although such open dynamics cannot be used for estimation of g in a broad regime, it can be used to mark a fixed point $g = g_0$.

Other parameters for which varying a parameter in \mathcal{L}_g does not move the system away from a phase transition or increase the gap significantly, but changes the properties of the stationary state and the low-lying modes analytically. On the phase diagram this is manifested by a horizontal or a vertical line of the phase coexistence. As the gap is not changed significantly

by varying g in some finite range, the estimation precision may be enhanced due to persisting long correlation time in the dynamics. Similarly as in the case of an extrinsic parameter, this requires the extremal instant rates μ_1, μ_2 in the regime $\tau' \ll t \ll \tau$, to be non-negligibly different, see Eqs. (2.35) and (2.36).

Example I. Let us consider a finite open quantum system with two-fold degeneracy of 0-eigenvalue in \mathcal{L}_{g_0} and estimation of the field g in the system Hamiltonian $H_g = gH$. It follows that $g_0H = H_{g_0}^{(1)} \oplus H_{g_0}^{(2)}$ and $J_j = J_j^{(1)} \oplus J_j^{(2)}$ for the decomposition $\mathcal{H} = \mathcal{H}_1 \oplus \mathcal{H}_2$. This implies that \mathcal{H}_1 and \mathcal{H}_2 are invariant for all values of g , since $H_g = \frac{g}{g_0} (H_{g_0}^{(1)} \oplus H_{g_0}^{(2)})$. Furthermore, when two stationary states $\tilde{\rho}_{1,g}, \tilde{\rho}_{2,g}$ supported within $\mathcal{H}_1, \mathcal{H}_2$ correspond to different rates $\text{Tr}(H\tilde{\rho}_{1,g}) \neq \text{Tr}(H\tilde{\rho}_{2,g})$, the value of g can be estimated with the QFI scaling quadratically in time, see Eq. (2.34). This is due to the fact that the macroscopic phase encoded in the MPS, is actually here a global phase on the system, which can be resolved only when the output is accessed, and thus the quadratic scaling is absent when measurements are considered on the system only, see also Appendix D.3.

Example II. Let \mathcal{L}_{g_0} feature $m \geq 4$ eigenvalues with real part 0 (but possibly non-zero imaginary parts). When asymptotic states preserve some initial coherences, there is a part of the system space where dynamics is unitary — a decoherence free subspace (DFS) [40–43] or a noiseless subsystem (NSS) [44–46], see also Sec. 3.1.3. Let g be a coupling constant in the Hamiltonian $H'_g = gH'$ governing such a unitary evolution inside a DFS or NSS. The corresponding QFI for the reduced system state, $\rho_g(t)$, is independent from g . Moreover, for an initial state being a superposition of H' eigenvectors with different eigenvalues, the QFI scales quadratically in times, as phases growing linearly with time t are encoded in the coherences of $\rho_g(t)$, therefore it is enough to use just the system to achieve enhanced estimation. Using the output as well can provide a higher constant in quadratic scaling, see Appendix D.3 for details.

Example III. Consider \mathcal{L}_{g_0} with all eigenvalues with 0 real part corresponding just to a single DFS or a NSS. As the output statistics is the same for all states in DFS/NSS due to no infor-

mation leak from the inside guaranteed by unitary evolution, there is *no quadratic enhancement* in estimation of any parameter encoded on the output. It is the difference in the output states corresponding to different stationary states that may lead to multiple modes in statistics of an output observable and further to quadratic scaling in the QFI for parameter encoded using such an observable.

2.4.3 Optimal measurement

We have shown that near a DPT the system-output state can have a large QFI. In order to exploit this, and achieve quantum enhanced sensitivity, it is necessary to measure an appropriately chosen observable. The optimal observable is known to be the SLD D_g defined as the solution of (2.11). For pure states this can be solved and $D_g = 2\partial_g|\psi_g\rangle\langle\psi_g|$. However, the measurement of D_g will be difficult to engineer in most practical situations. One needs therefore to find an alternative which is both practical and whose SNR is as close as possible to the QFI. Despite the fact that the intricacy of the optimal measurement makes it impractical, we can still formulate general characteristics for a measurement that achieves enhanced precision.

Support of measurement observable. The first consideration is whether the measurement should be on the system or output, or both. Consider \mathcal{L}_g with 2 low-lying eigenvalues, i.e., close to the two-fold degeneracy of 0-eigenvalue. In this case, in the regime of quadratic scaling the optimal measurement whose precision is given by the QFI involves measuring *both system and output*. This is a consequence of the fact that the macroscopic phase $t(\mu_1 - \mu_2)g$ encoded in the MPS during this regime is present neither in the reduced state of the system or the output, as they act as a reference for each other. In particular, at a DPT the precision achievable by measuring only the output is bounded by $p_1 F(|\Psi_g^{(1)}(t)\rangle) + p_2 F(|\Psi_g^{(2)}(t)\rangle)$, which scales *linearly* in time, see Appendix B.2. Here $|\Psi_g^{(1,2)}(t)\rangle$ are the MPSS

associated to two stationary states, and $p_{1,2}$ are their probabilities. This last result is the precision of an idealised protocol given by a first measurement of the system to project onto one of the subspaces associated with the competing stationary states, followed by an optimal measurement of the conditioned system-output state $|\Psi_{1,2}(t)\rangle$. On the other hand, the precision of a measurement performed just on the system is asymptotically a function of the stationary state, $F(\lim_{t \rightarrow \infty} \rho_g(t))$ and therefore is *constant*. A similar situation holds for dynamics featuring multiple stationary states, but not preserving any initial coherences. For a higher degeneracy than three-fold, however, the dynamics can be unitary on a part of the system space, thus preserving some initial coherences. This corresponds to a DFS or a NSS. In this case the asymptotic state of the system may depend on time via this unitary evolution, possibly leading to quadratic scaling of the precision of a measurement performed just on the system, see Example II in the previous subsection and Appendix D.3.

Optimal measurement time. The second consideration is what should be the time extension t of a single measurement run.

Here we imagine that the total time available to the experiment is T and one performs $n = \frac{T}{t}$ independent repetitions of the optimal system-output measurement of the state $|\Psi_g(t)\rangle$. This corresponds to a measurement of the joint state $|\Psi_g(t)\rangle^{\otimes n}$, and the optimal time t is that which maximises the QFI of the joint state, $F(|\Psi_g(t)\rangle^{\otimes n}) = n F(|\Psi_g(t)\rangle) = \frac{T}{t} F(|\Psi_g(t)\rangle)$.

For dynamics at a first-order DPT, when the QFI asymptotically has quadratic, linear and constant terms, see Eq. (2.34) and Appendix B.2, and the quadratic behaviour is due to non-decaying correlations in the MPS. All correlations present are exploited by the choice $t = T$, which is confirmed by a positive derivative of the QFI for times $t \gg \tau'$. Near a DPT the quadratic regime is limited to $t \ll \tau$, when the correlations do not decay, cf. Eq. (2.35). The optimal time t is necessary longer than the metastable regime in order to fully exploit correlations in the dynamics $t \approx \mathcal{O}(\tau)$, see Fig. 2.2 and the inset of Fig. 2.3, but

longer experiments with $t \gg \tau$ cannot provide significant enhancement.

Optimal measurement in optical phase-shift estimation. For the case of optical phase-shift estimation at a DPT, the bimodality of the system-output state in the counting statistics means that it is essentially of the form of a ‘‘Schrödinger cat’’ state. Assuming for simplicity that the competing stationary states are pure and the photon emission statistics from each stationary state is Poissonian, it reads,

$$|\Psi_\phi(t)\rangle = \sqrt{p_I} |I\rangle \otimes |\alpha_I(\phi)\rangle + \sqrt{p_A} |A\rangle \otimes |\alpha_A(\phi)\rangle \quad (2.41)$$

where $|\alpha_{I,A}(\phi)\rangle$ are coherent states with amplitudes $\alpha_{I,A}(\phi) = e^{i\phi} \sqrt{t \mu_{I,A}}$, where $\mu_{I,A}$ are the photon emission rates of the dynamical phases, see Eqs. (2.19) and Fig. 2.1 (c). In fact, as shown in Ref. [174], the state (2.41) is approximately a GHZ state with an effective parameter $t(\mu_A - \mu_I)\phi$. Note that for (2.41) neither counting nor homodyne measurements achieve Heisenberg scaling, which highlights the general challenge of identifying optimal measurements, see also Fig. 2.1 c). However, one might think of instead employing interferometric protocols, related to the ones put forward in Refs. [174–176] for superpositions of coherent states, in order to exploit the enhanced precision scaling.

Optical-shift estimation in the presence of noise. It is known that for the optical-shift estimation in the presence of Markovian noise typically arising in experiments, i.e., dephasing or photon losses, the QFI scales necessary *linearly* in the mean number of photons in the interferometer [12–16]. Therefore, the quantum enhancement is limited just to a constant. In the numerical study [161] it was shown, however, that MPSs perform optimally in the presence of losses, i.e., achieve the optimal constant in the linear scaling of the QFI. This can be understood as follows using the sequential structure of MPS [35, 128, 159]. For photon loss occurring at rate η , the average waiting time for a pho-

ton loss to occur is η^{-1} , therefore for correlations in the MPS of a shorter length $\tau \ll \eta^{-1}$, are not affected by the noise. This corresponds to bounds of [15, 94] approaching the Heisenberg scaling in that regime. Moreover, this argument generalises to other local noise models such as local dephasing.

2.5 GENERALISED DPTS

When changing a parameter g of the system dynamics, the joint system-output state $|\Psi_g(t)\rangle$ can undergo a singular change. This could correspond to a static phase transition in the stationary state of the system or to a dynamical phase transition that happens in the output. Both kinds of transitions can be detected by discontinuities in the average or a higher cumulant of an observable; in the case of a static transition, the observable should act on the system, whereas for a dynamical transition — a continuous measurement should be performed on the output. Yet, it is not obvious how to choose such an observable or a continuous measurement. More generally, however, the changes in the structure of any state $|\psi_g\rangle$ with varying g , can be captured by the way the distance between states $|\psi_{g'}\rangle$ and $|\psi_g\rangle$ changes when g and g' are varied. Let us consider \bar{g} being a vector of state parameters. The information-geometric approach [125] using Bures distance, which is based on the fidelity between states, $D_B(|\psi_{\bar{g}'}\rangle, |\psi_{\bar{g}}\rangle) = \sqrt{2(1 - |\langle \Psi_{\bar{g}'} | \Psi_{\bar{g}} \rangle|)}$, establishes a Riemannian metric on the quantum state space. The singularities of the metric in the thermodynamics limit of the system size going to infinity, have been successfully used to identify transitions in ground states of many classes of Hamiltonians, also in the cases when the corresponding ground state energy does not feature any singularities with respect to the parameters \bar{g} [129, 130]. Moreover, the metric determines the state distinguishability, as it is proportional to the QFI matrix for the parameters \bar{g} [127], see Eq. (1.21), thus bounding the optimal precision in the multi-parameter estimation of \bar{g} [131]. In particular, the information-geometric approach has been ap-

plied to Hamiltonians with ground states being matrix-product states [177] (note the difference in the normalisation to the joint system-output state in (2.3)).

The results presented in this chapter and [29] extend the geometric approach to open quantum systems with accessible outputs, thus *generalising* the notion of dynamical phase transitions [34–36, 163, 164]. The thermodynamic limit of infinite system size is replaced by the limit of infinite time t . In the one-parameter case the asymptotic metric is simply given by $\lim_{t \rightarrow \infty} F(|\Psi_g(t)\rangle) / 4t = \partial_{g_1} \partial_{g_2} \lambda_1(g_1, g_2)|_{g_1=g_2=g}$, cf. (2.26). In the multi-parameter case of a vector \bar{g} of parameters, it is the matrix of second derivatives of the maximal eigenvalue in the modified master operator $\mathcal{L}_{\bar{g}', \bar{g}}$, see also [178]. The notion of phase transitions in the metric, although more general and better suited for theoretical investigations than singularities of observable cumulants, does not give a recipe for detection of such a transition in an experiment. In the section 2.3 we have introduced the observable $G_g(t)$, (2.29), whose variance corresponds to the metric, cf. (2.30). Below we characterise $G_g(t)$ as a stochastic integral, and consider the necessary conditions under which measuring $G_g(t)$ could be used to detect the generalised DPTs of the first and the second-order. Furthermore, we discuss some experimental approaches in which the maximal eigenvalue $\lambda_1(g_1, g_2)$ of the modified operator \mathcal{L}_{g_1, g_2} in Eq. (2.25) can be accessed directly, and also the limit $\lim_{t \rightarrow \infty} t^{-1} \log(\langle \Psi_{g_1}(t) | \Psi_{g_2}(t) \rangle)$.

2.5.1 Observable distinguishing dynamical phases

The generator $G_g(t)$ characterises how the system-output MPS changes when g is varied. We have shown that for a finite system the variance $\Delta^2 G_g(t)$ scales linearly except a phase transition point when the stationary state is degenerate and the scaling may be quadratic, in which case measuring rates of $G_g(t)$ distinguishes two dynamical phases, cf. (2.34). Here we discuss the structure of the generator in detail. We note that an analogous notion to the generator $G_g(t)$ has been introduced in [130]

for a general family of states $|\psi_{\bar{g}}\rangle$, but, as we discuss below, the generator can be used to detect a phase transition only if it itself features finite correlations.

Generator as a stochastic integral. Let us first consider the case of a closed system with parameter $g = \Omega$ being a coupling constant in the Hamiltonian, i.e., $H_{\Omega} = H_0 + \Omega H_1$ and $J_j = 0$, which corresponds to all D^2 eigenvalues of \mathcal{L}_g having real part 0, where D is the system space dimension. In this case we have (see also [104, 105])

$$\begin{aligned} G_{\Omega}(t)|\psi_{\Omega}(t)\rangle &= \int_0^t du e^{-i(t-u)H_{\Omega}} H_1 e^{-iuH_{\Omega}} |\psi(0)\rangle \quad (2.42) \\ &= \int_0^t du e^{-i(t-u)H_{\Omega}} H_1 e^{i(t-u)H_{\Omega}} |\psi_{\Omega}(t)\rangle, \end{aligned}$$

so that $G_{\Omega}(t) = \int_0^t du e^{-i(t-u)H_{\Omega}} H_1 e^{i(t-u)H_{\Omega}}$ is an integrated observable. We note, however, that t^2 -scaling of the corresponding QFI, $F(|\psi_{\Omega}(t)\rangle)$, is not always present when H_0 and H_1 do not commute [105].

In the case of an open quantum system which can be described by the input-output formalism the evolution is no longer unitary, but can be described by stochastic unitaries, which will lead to $G_g(t)$ being a stochastic integral. Let us first consider dynamics discretised by δt , see Eq. (2.3), where the joint system and output MPS can be described by a co-cycle $U_g(n, 0)$,

$$|\Psi_g(n)\rangle = U_g(n, 0) |\chi\rangle \otimes |\text{vac}\rangle = U_{n,g} \cdots U_{1,g} |\chi\rangle \otimes |\text{vac}\rangle, \quad (2.43)$$

where $n = t/\delta t$, and $U_{i,g}$ is the unitary acting on the system and a part of the input at time $t = i\delta t$, and as the identity on the the output. $U_{i,g}$ can be expressed by the evolution Kraus operators,

(2.4), as $U_{i,g}|\chi\rangle \otimes |\text{vac}(i)\rangle = \sum_j K_{j,g}|\chi\rangle \otimes |j\rangle$. We therefore arrive at the discrete generator, cf. [171],

$$\begin{aligned} G_g(n)|\Psi_g(n)\rangle &= i \sum_{l=1}^n U_{n,g} \cdots U_{l+1,g} U'_{l,g} U_{l-1,g} \cdots U_{1,g} |\chi\rangle \otimes |\text{vac}\rangle \\ &= i \sum_{l=1}^n U_{n,g} \cdots U_{l,g} U_{l,g}^\dagger U'_{l,g} U_{l,g}^\dagger \cdots U_{n,g}^\dagger |\Psi_g(n)\rangle \\ &= \sum_{l=1}^n U_g(n, l-1) G_{l,g} U_g(n, l-1)^\dagger |\Psi_g(n)\rangle, \end{aligned} \quad (2.44)$$

where $U'_g(l) := \partial_{g'} U_{g'}(l)|_{g'=g}$ and $G_{l,g} := i U_g(l)^\dagger U'_g(l)$. Note that Eq. (2.44) is analogous to Eq. (2.42). In the continuous time $U_g(t, 0)$ is a stochastic unitary

$$dU_g(t, 0) = \left[-iH_g dt + \sum_{j=1}^k \left(J_{j,g} dA_{j,t}^\dagger - J_{j,g}^\dagger dA_{j,t} - \frac{1}{2} J_{j,g}^\dagger J_{j,g} dt \right) \right] U_g(t, 0) \quad (2.45)$$

In order to mimic the structure of the co-cycle in the discrete case, let us introduce

$$\begin{aligned} dU_{t,g} &= U_g(t+dt, t) = U_g(t+dt, 0) U_g(t, 0)^\dagger \\ &= [U_g(t, 0) + dU_g(t, 0)] U_g(t, 0)^\dagger \\ &= \mathbb{1} - iH_g dt + \sum_j \left(J_{j,g} dA_{j,t}^\dagger - J_{j,g}^\dagger dA_{j,t} - \frac{1}{2} J_{j,g}^\dagger J_{j,g} dt \right), \end{aligned} \quad (2.46)$$

which leads to

$$\begin{aligned}
dG_{t,g} &= i dU_{g,t}^\dagger dU'_{g,t} \\
&= i \left[\mathbb{1} + iH_g dt + \sum_j \left(J_{j,g}^\dagger dA_{j,t} - J_{j,g} dA_{j,t}^\dagger - \frac{1}{2} J_{j,g}^\dagger J_{j,g} dt \right) \right] \\
&\quad \times \left[-iH'_g dt + \sum_j \left(J'_{j,g} dA_{j,t}^\dagger - (J_{j,g}^\dagger)' dA_{j,t} - \frac{1}{2} (J_{j,g}^\dagger J_{j,g})' dt \right) \right] \\
&= \left[H'_g + \frac{i}{2} \sum_j \left(J_{j,g}^\dagger J'_{j,g} - (J_{j,g}^\dagger)' J_{j,g} \right) \right] dt \\
&\quad + i \sum_j \left(J'_{j,g} dA_{j,t}^\dagger - (J_{j,g}^\dagger)' dA_{j,t} \right), \tag{2.47}
\end{aligned}$$

where the last equality is due to $dA_{j,t} dA_{j,t}^\dagger = dt$ and all the other cross terms disappearing according to the *quantum Ito rule*, see e.g. [39]. Furthermore, note that the term which acts on the system only is the observable $M_g dt$, (2.37). This is the only term that will contribute to the average $\langle G_g(t) \rangle$ (see Appendix B.3.1), which is consistent with (2.31). The generator $G_g(t)$ is a stochastic integral

$$G_g(t) = \int_0^t U_g(t, u) dG_{u,g} U_g(t, u)^\dagger \tag{2.48}$$

and thus its variance of $\Delta^2 G_g(t)$ is an integral of *correlations* (covariance) between $dG_{u,g}$ and $dG_{v,g}$, $0 \leq u, v \leq t$, see Appendix B.3.1 for discussion. We therefore see that if the Hamiltonian H_g and jumps $\{J_{j,g}\}_j$ depend analytically on g , also $G_g(t)$ is well-behaved.

In particular, for Ω being a coupling constant in the system Hamiltonian, $H_\Omega = H_0 + \Omega H_1$, we obtain

$$G_\Omega(t) = \int_0^t du U_\Omega(t, u) H_1 U_\Omega(t, u)^\dagger, \tag{2.49}$$

which is analogous to Eq. (2.42).

Let us finally note that the generator $G_g(t)$ is not fully determined by Eq. (2.29), since the matrix product states for all

initial system states, with respect to which the generator is defined, do not span the whole system and output state space. In particular, any dC_t such that $dJ_t|\Psi(t)\rangle = 0$ on any MPS $|\Psi(t)\rangle$ leads to equivalent definitions of the generator with $d\tilde{G}_{t,g} = dG_{t,g} + dC_t$. Moreover, Eq. (2.47) can be used to solve the inverse problem of identifying H_g and $\{J_{j,g}\}_j$ for a given generator $G_g(t)$, see Appendix B.3.3 for the example of $G_g(t)$ being the homodyne current of the output.

Using the generator to detect a DPT. We see that in the case of a first-order DPT measuring rates of $G_g(t)$ distinguishes two dynamical phases and can be also related to the variance $\Delta^2 G_g(t)$ scaling quadratically.

In order to use $G_g(t)$ as an observable measured to detect a DPT, all its cumulants, in particular the variance, must scale at most linearly with t for any MPS — not only $|\Psi_g(t)\rangle$ — that corresponds to dynamics with a single stationary state on the same system-output space, e.g. $|\Psi_{g'}(t)\rangle$ at $g' \neq g$ as long as $\mathcal{L}_{g'}$ has non-degenerate 0-eigenvalue. This corresponds to infinite differentiability of the long-time limit of its CGF, which result is not known in general. Moreover, even a weaker result of the Central Limit Theorem, which states that the distribution shifted by minus its average and rescaled by \sqrt{t} asymptotically converges to a Gaussian distribution, is not yet established apart from the case of a continuous measurement of the output where results following from the Local Asymptotic Normality (LAN) [37, 39, 171], which we explain below.

The LAN theorem states that for the finite system dynamics with single stationary state the asymptotic behaviour of the fidelity is asymptotically Gaussian,

$$\lim_{t \rightarrow \infty} \langle \Psi_{g+\frac{v}{\sqrt{t}}}(t) | \Psi_{g+\frac{u}{\sqrt{t}}}(t) \rangle = e^{-\frac{(u-v)^2}{2\nu_g}}, \quad (2.50)$$

where ν_g is the linear limit of the variance $\Delta^2 G_g(t)$, cf. (2.27) and (2.30). For the phase encoded unitarily on the output or in the amplitude of homodyne current (see Appendix B.3.3), the

fidelity corresponds to a characteristic function of the respective integrated continuous measurement, $G_g(t)$. Therefore, the Local Asymptotic Normality result yields the CLT for that measurement performed on $|\Psi_g(t)\rangle$. Moreover, since for g encoded as a phase of the output observable, the generator does not depend on g , $G_g(t) \equiv G(t)$, and all its cumulants measured on $|\Psi_g(t)\rangle$ are the same for all g . Thus, the CLT holds for measuring any joint system-output state corresponding to a single stationary state.

Measuring the generator. Nevertheless, let us assume for now that $G_g(t)$ is well-behaved when measured on any MPS corresponding to single-stationary-state dynamics. We now discuss further aspects of relation between measurement of $G_g(t)$ and DPTs.

In the case of a system near a first-order dynamical transition, due to the small gap, dynamics exhibits *metastability*, which can be observed as a broad time-regime where the average of the system observable M_g , (2.37), appears stationary before relaxing to the value corresponding to the true stationary state ρ_{ss} . Approximate stationarity of $\langle M_g \rangle$ implies a quadratic regime in the variance $\Delta^2 G_g(t)$ and a large constant in its asymptotic linear scaling, see (2.35) and (2.36). This highlights the relation of first-order dynamical phase transitions to first-order stationary phase transitions [36]. In general, however, approximate stationarity of a particular system observable in some broad time-regime does not imply separation in the spectrum of the master operator, as that observable may not capture behaviour of all dynamical modes or, even if the separation is present, the metastable dynamics may not be related to a DPT.

Therefore, in order to observe signatures of being in proximity of first-order or higher-order DPTs, it is necessary to consider not only the system, but also the output. For a DPT corresponding to a diverging cumulant of a continuous measurement, the fidelity of states with parameter g encoded with that measurement as a generator, is simply the characteristic function of the generator and thus a DPT corresponds to singular-

ities of $\log\langle\Psi_{g'}(t)|\Psi_g(t)\rangle$ with respect to g' . For a general parameter g , such singularities will correspond to diverging behaviour of *time-ordered* cumulants of $G_g(t)$, see Appendix B.3.1 and it is left to investigate whether diverging behaviour of time-ordered cumulants implies the divergence of cumulants defined in standard fashion. However, instead of measuring $G_g(t)$, the long-time limit $\lim_{t\rightarrow\infty} t^{-1} \log\langle\Psi_{g'}(t)|\Psi_g(t)\rangle$ can also be accessed in the experiments, and thus the time-ordered cumulants, see Sec. 2.5.2.

Generalised transitions in ensembles of quantum trajectories. Beyond dynamical phase transitions, a notion of transitions in ensembles of dynamical trajectories has been introduced for continuous measurements, such as photon counting [34] or heterodyne/homodyne measurement [164]. Furthermore, a similar notion has been introduced for time-integrated observables of a closed quantum system [179]. Here we introduce a generalised notion of the transitions in ensembles of open quantum system trajectories.

We have discussed how cumulants of a continuous measurement can be encoded in a characteristic function corresponding to the fidelity between quantum states. The cumulants can be also encoded in the CGF associated to a modified master operator [34, 164], see also Sec. 2.1.2. The long-time limit of such CGF corresponds to "free energy" density, whose singularities at $s \neq 0$ manifest non-analytic features among the continuous measurement records, referred to as *transitions in the ensemble of quantum trajectories*. In the case of a closed quantum system one can consider cumulants of a time-integrated system observable and investigate the singularities of the related long time-limit CGF [179]. We now *extend* this approach to the case of an open quantum system and a system observable X , and consider cumulants of $G(t) = \int_0^t du U(t,u) X U(t,u)^\dagger$, analogous to the generator associated with encoding of a coupling constant of the

system Hamiltonian ($H_1 = X$ and $\Omega = 0$ in (2.49)), as follows. We define

$$\begin{aligned}\Theta_t(s) &= \log \langle \Psi(t) | e^{-\int_{-s/2}^{s/2} dh G_h(t)} | \Psi(t) \rangle \\ &= \log \langle \Psi_{i\frac{s}{2}}(t) | \Psi_{-i\frac{s}{2}}(t) \rangle \\ &= \log \text{Tr}(e^{t\mathcal{W}_s} |\chi\rangle \langle \chi|),\end{aligned}\quad (2.51)$$

where (see Eq. (2.25) for $g = \Omega$ being a coupling constant in the Hamiltonian H)

$$\mathcal{W}_s(\rho) := \mathcal{L}_{i\frac{s}{2}, -i\frac{s}{2}}(\rho) = \mathcal{L}(\rho) - \frac{s}{2}\{X, \rho\}. \quad (2.52)$$

$\Theta_t(s)$ is related to $G(t)$ via derivatives w.r.t. s up to the second cumulant, and to higher cumulants up to time ordering, exactly as it is the case for the fidelity, see Appendix B.3.1 for detailed discussion. This is also the case (but not mentioned) for the closed case in [179] and full counting statistics approach [180]. Asymptotically, $\Theta_t(s) \approx t\theta(s)$, where $\theta(s)$ is the maximal eigenvalue of \mathcal{W}_s . A singularity of $\theta(s)$ at $s \neq 0$ will correspond to a new type of transition in ensemble of quantum trajectories. Moreover, this transition can be observed experimentally, see Sec. 2.5.2.

The notion can be extended even further to the case of a general parameter g as follows,

$$\begin{aligned}\Theta_t(s) &:= \log \text{Tr} \left(e^{t\mathcal{L}_{g+i\frac{s}{2}, g-i\frac{s}{2}}} |\chi\rangle \langle \chi| \right) \\ &= \log \langle \Psi_{g+i\frac{s}{2}}(t) | \Psi_{g-i\frac{s}{2}}(t) \rangle \\ &= \log \langle \Psi_g(t) | \mathcal{T} e^{-\int_{-s/2}^{s/2} dh G_h(t)} | \Psi_g(t) \rangle.\end{aligned}\quad (2.53)$$

2.5.2 Direct measurement of fidelity

Here we present two experimental schemes obtaining the values of the fidelity between two MPSs, $\langle \Psi_{g'}(t) | \Psi_g(t) \rangle$ or $\Theta_t(s)$ defined in (2.51). From the experimental results the numerical derivatives can be further determined, in particular the second

derivative corresponding to the QFI (cf. (2.12) and (2.30)).

Interferometry with two-level ancilla (proposed in [181, 182]). We consider an *extended* master dynamics \mathcal{L}_{SA} of the system and a two-level ancilla in which the ancilla controls the system dynamics as follows

$$H^{SA} = \begin{pmatrix} H_g & 0 \\ 0 & H_{g'} \end{pmatrix}, \quad J_j^{SA} = \begin{pmatrix} J_{j,g} & 0 \\ 0 & J_{j,g'} \end{pmatrix}, \quad j = 1, \dots, k, \quad (2.54)$$

where matrices are expressed in the ancilla basis $|0\rangle_A, |1\rangle_A$. For example, for the ancilla initially in the state $|1\rangle_A$ the system dynamics is given by $\mathcal{L}_{g'}$, whereas for the initial state $|0\rangle_A$ the system evolves with \mathcal{L}_g . For the system and ancilla initially in a separable state $|\chi\rangle_S \otimes (|0\rangle_A + |1\rangle_A)/\sqrt{2}$ we have

$$\rho^{SA}(t) = \begin{pmatrix} e^{t\mathcal{L}_g}(|\chi\rangle\langle\chi|) & e^{t\mathcal{L}_{g,g'}}(|\chi\rangle\langle\chi|) \\ e^{t\mathcal{L}_{g',g}}(|\chi\rangle\langle\chi|) & e^{t\mathcal{L}_{g'}}(|\chi\rangle\langle\chi|) \end{pmatrix}. \quad (2.55)$$

Note that the off-diagonal term in the joint system-ancilla state ρ_{10}^{SA} corresponds to the modified master dynamics $\mathcal{L}_{g',g}$ in (2.25). Furthermore, the corresponding off-diagonal term in the ancilla state $\rho_{10}^A = \text{Tr}_A(\rho^{SA}(t)\sigma_-^A) = \text{Tr}_S(e^{t\mathcal{L}_{g,g'}}(|\chi\rangle\langle\chi|))$ yields exactly the MPS fidelity $\langle\Psi_{g'}(t)|\Psi_g(t)\rangle$, cf. (2.24). Therefore, the modified dynamics is simply encoded in the dephasing strength and the rotation experienced by the ancilla atom. As $\langle\sigma_-^A\rangle$ can be determined via measurements of Pauli operators σ_x^A and σ_y^A on the ancilla, $\sigma_-^A = \sigma_x^A - \sigma_y^A$, this interferometric scheme provides a direct access to the value of the fidelity, from which its numerical derivatives can be further determined.

Waiting time distribution. For a parameter being a coupling constant in the free system dynamics, e.g. Ω with $H_\Omega = H_0 + \Omega H_1$, the fidelity can be related to the modified master operator \mathcal{W}_s , analogously as a characteristic function is related to a CGF, cf. Eqs. (2.51) and (2.52). Although the operator \mathcal{W}_s is not trace-

preserving, it can be related to physical dynamics of \mathcal{L} , but with additional jumps operators corresponding to interactions with more modes of the environment, as follows. For $s \geq 0$, without loss of the generality, let us assume that the observable X is positive, $X \geq 0$, as the shift by a constant will not change the (time-ordered) cumulants of its time-integral. We consider a master operator

$$\begin{aligned}\tilde{\mathcal{W}}_s(\cdot) &:= \mathcal{L}(\cdot) + \sum_{j'} \left(s \tilde{J}_{j'}(\cdot) \tilde{J}_{j'}^\dagger - \frac{s}{2} \{ \tilde{J}_{j'}^\dagger \tilde{J}_{j'}(\cdot) \} \right) \quad (2.56) \\ &= \mathcal{W}_s(\cdot) + s \sum_{j'} \tilde{J}_{j'}(\cdot) \tilde{J}_{j'}^\dagger\end{aligned}$$

where we have only assumed that the additional jump operators $\{\tilde{J}_{j'}\}_{j'}$ obey $\sum_{j'} \tilde{J}_{j'}^\dagger \tilde{J}_{j'} = X$ for $s > 0$, and when $s < 0$ we consider X shifted by a constant so that $X \leq 0$. In the case of physical dynamics generated by $\tilde{\mathcal{W}}_s(\cdot)$, $\Theta_t(s) = \text{Tr}(e^{t\tilde{\mathcal{W}}_s} \rho_{\text{in}})$ is logarithm of the probability of observing *none* of the additional jumps $\{\tilde{J}_{j'}\}_{j'}$ up to time t for the system initially in the state ρ_{in} , cf. the effective Hamiltonian H_{eff} in (2.2). Note that the waiting time distribution, and thus $\text{Tr}(e^{t\tilde{\mathcal{W}}_s} \rho_{\text{in}})$, can be accessed in an experiment with dynamics given by $\tilde{\mathcal{W}}_s$ or in Monte Carlo simulations of that dynamics. We note that this approach has been originally proposed for closed systems, i.e., $\mathcal{L}\rho = -i[H, \rho]$, in [179].

Continuous measurements. For a parameter encoded as a phase of output observable, i.e., a continuous measurement, the fidelity corresponds simply to a characteristic function of that observable and can be reconstructed from moments of the measurement statistics.

2.6 CONCLUSIONS

We have shown that, close to a first-order dynamical phase transition, the output of an open quantum system can be seen as a resource for quantum metrology applications, in which the

parameter to be estimated is encoded on the output state. For times of the order of the dynamics correlation time, the system-output QFI scales quadratically with time, while in the long time limit, the QFI scales linearly in time with the multiplicative constant that diverges when the spectral gap closes, as in a DPT. Furthermore, the precision of estimating intrinsic parameters of the system dynamics may also be enhanced, but only around the parameter values corresponding to dynamics being in the proximity to a DPT. The regime of the quadratic scaling of the QFI in time, corresponds to a bimodal distribution of the dynamical observable encoding the parameter, and thus a macroscopic relative phase encoded in the joint system-output state. Asymptotically, the distribution becomes unimodal and the relative phase is lost, which results in the linear scaling of the QFI. It remains an open issue what experimentally realisable measurement can exploit the large QFI of the system-output close to a DPT. Finally, exploiting the fact that the QFI corresponds to a metric on the space of quantum states, we have discussed how its singularities for the joint system-output state correspond to generalised DPTs.

3

METASTABILITY IN MARKOVIAN OPEN QUANTUM SYSTEMS

In Chapter 2 we explored the possibility of quantum enhancement in parameter estimation by using Markovian open quantum systems together with their output. The crucial property we exploited was a small or zero (at a DPT) gap in the spectrum of the Markovian master operator governing the system dynamics.

In this chapter we show that a splitting in the spectrum results in the separation of timescales of the system dynamics, corresponding to initial partial relaxation into long-lived states, with subsequent decay to true stationarity occurring at much longer times. This phenomenon is referred to as *metastability* and has evident experimental manifestations, for example in two-step decay of time correlation functions of system observables [183].

Metastability is a common occurrence in classical stochastic many-body systems often displaying complex and slow relaxation, including classical soft matter [54], glasses being the paradigmatic example [55, 56]. On the other hand, in the non-equilibrium dynamics of quantum many-body systems, both closed and open, questions about timescales and partial versus full relaxation play central roles in issues such as thermalisation [184–187], many-body localisation [188–190], and an aging and glassy behaviour [183, 191–195].

Given this broad range of problems, it would be highly desirable to have a unified theory of quantum metastability. In this chapter we present results of [196], where we lay grounds

for such a theory for the case of open quantum systems with Markovian dynamics. By generalising concepts from classical stochastic systems [47–53], we develop an approach for quantum Markovian systems based on the spectral properties of the generator of the dynamics. We show how to exploit its spectral structure to obtain a low-dimensional approximation to the dynamics in terms of motion in a manifold of metastable states constructed from the low-lying eigenmatrices of the generator, and consider the associated behaviour of time correlations. Based on perturbative calculations for finite systems, we argue that the manifold of metastable states is in general composed of disjoint states, decoherence-free subspaces (DFSS) [40–43] and noiseless subsystems (NSSs) [44–46]. We illustrate these possibilities with simple examples.

Let us note that from the quantum information perspective, decoherence free subspaces and noiseless subsystems, where parts of the Hilbert space are protected against external noise, are ideal scenarios for implementing quantum information processing [7]. Since experiments are performed in finite time, however, it is sufficient to consider a larger class of systems whose coherence is only stable over experimental timescales, i.e., metastable.

3.1 BACKGROUND

Before discussion of the results for metastability in Markovian open quantum systems, we briefly review the notion of metastability in classical equilibrium systems. Next, we sketch the basics of the metastability theory for classical Markovian dynamics [48, 51]. We also recall the general structure of manifolds of stationary states in Markovian open quantum systems.

3.1.1 Phenomenology of metastability in classical equilibrium systems

A finite classical system at equilibrium with a bath of certain temperature, can be described by its free-energy functional, which determines the probability of observing a given (usually collective) configuration (a *microstate*) [197]. For a large system size, the minimum of the free-energy functional corresponds to the *macrostate* observed on average in experiments (up to thermal fluctuations, which disappear in the thermodynamic limit). Due to thermal fluctuations, the system undergoes stochastic dynamics between configurations. When the dynamics is time-reversible, the difference of free-energy functional for two configurations, i and j , determines the ratio between the escape rates in *detailed balance* condition, $w_{jk}/w_{kj} = e^{-\beta(f(j)-f(k))}$, where w_{jk} is the escape rate from the configuration k to j , $f(j)$ is the free energy of j -configuration, and β is the inverse temperature rescaled by the Boltzmann constant k_B .

Let us consider an example of a classical ferromagnet at low temperatures, where metastability is a dynamical consequence of the static features of the system. In the thermodynamic limit, this system features a first-order static phase transition at zero magnetic field (and the Landau free energy w.r.t. the spin magnetisation features two equal minima). If the ferromagnet is close to the coexistence point (e.g. at small positive magnetic field), but initially at a state belonging to the unfavoured phase (in this case with negative magnetisation corresponding to local minimum of Landau free-energy) there will be an initial fast relaxation within this phase, before a much longer relaxation to the eventual equilibrium state within the stable phase (of positive magnetisation corresponding to global minimum of Landau free-energy). This occurs due to the existence of a large, but finite, free-energy barrier that needs to be crossed from the metastable phase to the stable phase due to small thermal fluctuations. The barrier height is related to the surface tension of creating domains of the stable phase in the background of the other. At the zero field there is a strict coexistence be-

tween the phases of positive and negative magnetisation, and dynamics is no longer ergodic. At finite size, however, the phase transition is absent and the dynamics is necessarily metastable, with the metastable states being those of non-zero magnetisation, and the true equilibrium state being paramagnetic, due to intermittent dynamics between two metastable phases [197]. In this sense, metastability does not require the presence of a phase transition, only that the distinct states are long lived and only weakly connected by dynamics, which is exactly the case of many-body systems with complex collective dynamics and slow relaxation, such as glasses [55, 56].

In Sec. 3.3 we show that for an open quantum system with small gap, i.e., a single low-lying master operator eigenvalue close to 0, the system dynamics always features two metastable phases and the long-time dynamics corresponds to a *classical* motion between two minima of a free-energy functional separated by a barrier, although the underlying system dynamics is quantum.

3.1.2 Metastability in classical stochastic systems

Let us now recall the metastability theory for classical Markovian systems of finite size, developed by B. Gaveau and L. S. Schulman [48, 51]. As Markovian dynamics in general does not obey detailed balance nor their stationary states are thermal, the metastability theory [48, 51] comprises also large class of non-equilibrium dynamics that can be approximated as Markovian.

Consider a Markovian master equation for a vector of probabilities $\bar{p} = (p_1, \dots, p_d)^T$, ($p_k \geq 0$, $k = 1, \dots, d$, $\sum_{k=1}^d p_k = 1$) on a discrete space of d system configurations,

$$\frac{d}{dt}\bar{p} = \mathcal{W}\bar{p}. \quad (3.1)$$

As dynamics preserves positivity of \bar{p} , the off-diagonal entries of the master operator \mathcal{W} are positive $w_{jk} := (\mathcal{W})_{jk} \geq 0$, and

correspond to escape rates from j -th to k -th configuration, $j \neq k = 1, \dots, d$. Furthermore, as the total probability is conserved, $\sum_{k=1}^d p_k = 1$, we also have that $\sum_{j=1, j \neq k}^d w_{jk} = -w_{kk}$, $k = 1, \dots, d$, and hence the diagonal entries are negative. The differential equation in (3.1) can be solved formally as $\bar{p}(t) = e^{t\mathcal{W}}\bar{p}_{\text{in}}$ by finding the eigenmodes of the master operator \mathcal{W} . In particular, when \mathcal{W} is diagonalisable, we have $\bar{p}(t) = \sum_{k=1}^d e^{t\lambda_k} r_k l_k^T \bar{p}_{\text{in}}$, where r_k and l_k are right and left eigenvectors of \mathcal{W} corresponding to an eigenvalue λ_k (ordered with decreasing real part). When dynamics are ergodic, we have that $\text{Re}(\lambda_k) < 0$ for $k = 2, \dots, d$ and the first eigenvalue equals 0, $\lambda_1 = 0$, which corresponds to the stationary probability distribution, $r_1 = \bar{p}_{\text{ss}}$, and $l_1^T = (1, 1, \dots, 1)$.

In [48, 51] \mathcal{W} is considered to have a *separation* in real parts of eigenvalues. This implies that there exists metastable time regime when only low-lying eigenmodes contribute to the dynamics of the probability distribution, $\bar{p}(t)$, and their decay is negligible. In this regime it can be shown that any metastable system state is simply a mixture of multiple phases characterised by approximately disjoint probability distributions, which is a structure analogous to that at a first-order transition.

Sketch of the proof. Consider m low-lying eigenmodes and assume that in the metastable regime their decay is negligible, so that $p(t) \approx \sum_{k=1}^m e^{t\lambda_k} r_k l_k^T \bar{p}_{\text{in}}$ is determined by so called *observable representation of state space*, i.e., the coefficients $c_k = l_k^T \bar{p}_{\text{in}}$, $k = 2, \dots, m$, ($c_1 = 1$ for all \bar{p}_{in}), where the low-lying spectrum has been assumed real and without Jordan blocks. It will be shown that the set C of $\bar{c} = (c_2, \dots, c_m)$ for all possible initial distributions \bar{p}_{in} is approximately a *simplex*, i.e., a convex set whose interior points uniquely represent probability distributions on m vertices via barycentric coordinates. Moreover, the vertices can be uniquely associated with disjoint sets of initial configurations — basins of attraction — evolving into metastable states with the coefficients \bar{c} close to a given vertex. Finally, each vertex represents one of m metastable phases, which

are approximately proportional to \bar{p}_{ss} on the respective basins of attraction.

Consider m extreme points in the set C , such that the point $(0, \dots, 0)$ corresponding to the stationary distribution \bar{p}_{ss} can be represented as their convex combination. The dynamics of $\bar{p}(t)$ for any initial system configuration, will feature decay of the low-lying modes, i.e., time-dependent $\bar{c}(t)$, but due to separation in the spectrum during metastable regime the decay is small, $\bar{c}(t) - \bar{c} =: \mathcal{O}(\delta)$ (including the initial system configurations corresponding to the chosen extreme points, with respective $\delta_l, l = 1, \dots, m$). For a given extreme point, \bar{c}_l , one can choose an affine transformation such that the given extreme point is the origin of the new *local* (in general non-orthogonal) coordinates, and all points in C have non-negative coordinates. This is possible since C is a subset of a cone originating at \bar{c}_l as C consists of finitely many, at most d , extreme points. Consider a set $X_l(a_l)$ of initial system configurations s.t. the corresponding coefficients \bar{c} are not further away, in the local coordinates, from \bar{c}_l than a_l . One can show that probability $p_l(t)$ corresponding to the extreme point \bar{c}_l , is supported on configurations belonging to $X_l(a_l)$ up to $m \frac{\delta_l}{a_l}$. As one does not want to choose sets $X_l(a_l)$ overlapping for different l , we need an assumption (I), so called *separation hypothesis*, that the m extreme points, $\bar{c}_1, \dots, \bar{c}_m$, are separated by $\mathcal{O}(1)$, when the left eigenvectors $l_k, k = 1, \dots, m$, of \mathcal{W} are normalised in the max norm. Furthermore, this separation needs to be maintained also in the local coordinates (assumption II). In such a case one can choose a_l s.t. $\delta_l \ll a_l \ll \mathcal{O}(1)$, which guarantees $X_l(a_l)$ to capture the supports of $p_l(t)$ up to $m \frac{\delta_l}{a_l}, l = 1, \dots, m$, and be disjoint. Moreover, \bar{p}_{ss} is supported on $\bigcup_{l=1}^m X_l(a_l)$ up to $m \times \max_{l=1, \dots, m} \frac{\delta_l}{a_l}$, and this is also the case for any metastable state.

Furthermore, assuming that in the inverse affine transformation from the local coordinates back to the original coordinates of the coefficients \bar{c} , distances are only changed by order $\mathcal{O}(1)$ (assumption III), one also obtains that the left eigenvectors $l_k, k = 1, \dots, m$, are constant on each $X_l(a_l)$ up to corrections of the order $\mathcal{O}(a_l)$. This leads, for any initial configuration y , to the

corresponding coefficients, $\bar{c}(y)$, being a convex combination of the m extreme points \bar{c}_l , up to corrections of the $\mathcal{O}(\alpha_l)$, and thus the corresponding probability distribution being simply a mixture of the extreme probability distributions $p_l(t)$, $l = 1, \dots, m$. This finally proves that C is approximately a simplex and the choice of the extreme points is unique up to $\mathcal{O}(\alpha_l)$. ■.

In [51] the effective long-time dynamics is obtained as *coarse-graining of the space* of system configurations over disjoint basins defined above, and necessary corresponds to transition between metastable phases. As we show in this chapter for quantum systems, such transitions can be observed in *coarse-graining in time* of quantum jump trajectories of the Markovian open quantum system, although such dynamics may not be ergodic and thus coarse-graining in space does not have clear interpretation.

We finally note here that the observable representation have been utilised to define *dynamical distance* between system configurations, which can be further used in pattern recognition in classical stochastic trajectories, see [52, 198].

3.1.3 Stationary manifolds of quantum semi-group dynamics

In the previous subsection, we recalled the results of [48, 51] stating that metastable states of classical Markovian systems can be represented as a probabilistic mixture of approximately disjoint metastable phases. This resembles the general situation at a first-order phase transition when more phases are stable than just a single one, which for Markovian systems corresponds to non-uniqueness of a stationary probability distribution.

Let us now present the general structure of degenerate stationary states in Markovian open quantum dynamics [199]. We consider dynamics of a finite quantum system with the Hilbert space \mathcal{H} , described by a Lindblad master equation [8, 9], so that

the system state $\rho(t)$ obeys $\frac{d}{dt}\rho(t) = \mathcal{L}\rho(t)$, with the generator of the dynamics \mathcal{L} ,

$$\mathcal{L}\rho = -i[H, \rho] + \sum_j \left(J_j \rho J_j^\dagger - \frac{1}{2} \{J_j^\dagger J_j, \rho\} \right), \quad (3.2)$$

where H is the system Hamiltonian, and J_j quantum jump operators describe the system interaction with an environment. Any stationary state of such dynamics, $\mathcal{L}\rho_{ss} = 0$, is in general of the following form [199],

$$\rho_{ss} = 0_{\mathcal{H}_0} \oplus \bigoplus_{l=1}^{m'} p_l \tilde{\rho}_l \otimes \omega_l, \quad (3.3)$$

where the system space is divided into orthogonal subspaces $\mathcal{H} = \mathcal{H}_0 \oplus \bigoplus_{l=1}^{m'} \mathcal{H}_l \otimes \mathcal{K}_l$, and $\tilde{\rho}_l$ are fixed full-rank states on \mathcal{H}_l , while arbitrary states ω_l on \mathcal{K}_l and probabilities p_l depend on an initial state of the system. When $\dim(\mathcal{K}_l) > 1$ and $\dim(\mathcal{H}_l) = 1$, \mathcal{K}_l is a decoherence free subspace (DFS) protected from the noise [40–43]. When $\dim(\mathcal{K}_l) > 1$ and $\dim(\mathcal{H}_l) > 1$, \mathcal{K}_l is also protected from noise, but in general the corresponding state $\tilde{\rho}_l \otimes \omega_l$ cannot be pure, and \mathcal{K}_l is termed a noiseless subsystem (NSS) [44–46]. When $\dim(\mathcal{K}_l) = 1$ there are no coherences preserved in $\mathcal{H}_l \otimes \mathcal{K}_l$. The subspace \mathcal{H}_0 corresponds to the decay subspace, which is not supported asymptotically, see also [199, 200]. In general the master dynamics within DFSs and NSSs is unitary and corresponds to purely imaginary eigenvalues of \mathcal{L} [199].

Idea of the proof for the case of no decay (based on [158], for the general case see [199]). One may ask about the structure of stationary observables, which always include $\mathbb{1}_{\mathcal{H}}$ due to trace-preservation. It can be easily shown that when an operator commutes with all the operators appearing in the master equations: with the Hamiltonian, H , and the jumps operators (both J_j and J_j^\dagger), it is stationary. A set of such operators is a von Neumann algebra, i.e., all linear combinations of such operators and their conjugates commute as well. When there is no

decay, $\dim(\mathcal{H}_0) = 0$, it can be shown that there are no other stationary operators. It is known that any von Neumann algebra on a finite Hilbert space \mathcal{H} has a general form

$$M_{ss} = \bigoplus_{l=1}^{m'} \mathbb{1}_{\mathcal{H}_l} \otimes M_l, \quad (3.4)$$

where M_l is an arbitrary operator on \mathcal{K}_l and $\mathcal{H} = \bigoplus_{l=1}^{m'} \mathcal{H}_l \otimes \mathcal{K}_l$. Conversely, the algebra generated by H and $\{J_j, J_j^\dagger\}_j$ (which becomes a von Neumann algebra by including $\mathbb{1}_{\mathcal{H}}$) necessarily commutes with the stationary operators. Therefore, we arrive at the decomposition of the Hamiltonian and jump operators as

$$H = \bigoplus_{l=1}^{m'} H^{(l)} \otimes \mathbb{1}_{\mathcal{K}_l} \quad \text{and} \quad J_j = \bigoplus_{l=1}^{m'} J_j^{(l)} \otimes \mathbb{1}_{\mathcal{K}_l}, \quad (3.5)$$

leading to the stationary states of the form given in Eq. (3.3). ■

From, Eq. (3.3), we see that the asymptotic state of the system depends on its initial state not only via probabilities between the disjoint stationary states, but also initial coherences preserved within DFSS and NSSs. This much richer structure allows us to anticipate that the metastability theory in such systems should be more complex than in the classical case reviewed in Sec. 3.1.2.

3.2 TOWARDS METASTABILITY THEORY IN OPEN QUANTUM SYSTEMS WITH MARKOVIAN DYNAMICS

The aim of this chapter is to lay ground for metastability theory for the case of open quantum systems evolving with Markovian dynamics. Our starting point is a well-established approach for metastability in classical stochastic systems [47, 48, 50–52, 201] we reviewed in Sec. 3.1.2. We develop an analogous method for quantum Markovian systems based on the spectral properties of the generator of the Markovian dynamics.

First we show that metastability, which is a manifestation of separation of timescales, requires a splitting in the generator spectrum. Using this spectral division allows us further to construct a low-dimensional description of metastable states from the low-lying eigenmatrices of the generator. Moreover, we show that the long-time dynamics reduce to a low-dimensional effective motion in the metastable manifold (MM). We also show how both the metastability and the effective motion can be probed by considering the behaviour of time correlations in results of measurements performed sequentially on the system.

In the next Sec. 3.3 we show that in the case of two low-lying modes, which we also discussed in Chapter 2, the structure of the MM is classical and it is composed of two metastable phases. Consequently, the effective long-time dynamics is classical stochastic – consisting of jumps between the metastable phases. We argue how intermittency of continuous measurement records corresponds directly to that effective dynamics and is therefore a signature of metastability.

In Sec. 3.4 we move on to considering higher-dimensional metastable manifolds. First, we demonstrate that for the class of systems perturbed away from a degenerate stationary manifold, the metastable manifold is in general composed of disjoint states, noiseless subsystems and decoherence-free subspaces. We also provide the metastable regime and the effective long-time dynamics, which is trace-preserving and approximately completely positive. The complementary derivations can be found in Appendix C, while in Appendix D we show how such metastability can be exploited for enhanced parameter estimation.

In general case of higher-dimensional metastable manifolds, e.g. for a class of system dynamics in which metastability emerges with increasing system size, it is not yet known what is the structure of the MM, but based on perturbative results, we formulate a conjecture. We finish this chapter by discussing possible methods of unfolding classical and quantum components of a general structure of the MM, and extensions of the metastability theory to non-Markovian and closed quantum system dynamics.

3.2.1 *Review of spectral properties*

We consider a finite open quantum system evolving under Markovian dynamics, so that the system state $\rho(t)$ obeys Lindbladian master equation $\frac{d}{dt}\rho(t) = \mathcal{L}\rho(t)$ [8, 9], where the generator of the dynamics \mathcal{L} is given by Eq. (3.2). As the generator \mathcal{L} is a linear operator on the system state $\rho(t)$, the formal solution of Eq. (3.2) is simply given by $\rho(t) = e^{t\mathcal{L}}\rho_{\text{in}}$, where ρ_{in} is an initial state of the system. Therefore, when the eigendecomposition of the generator \mathcal{L} can be found, the system dynamics can be expressed into exponentially decaying, possibly oscillatory, dynamics of the eigenmodes, which we elaborate on below using basic linear algebra.

While in general the generator \mathcal{L} is not diagonalisable, one can find its eigenvalues $\{\lambda_k, k = 1, 2, \dots\}$, each corresponding to an eigenspace or a Jordan block (generalised eigenspace). We order the eigenvalues by decreasing real part, i.e., $\text{Re}\lambda_k \geq \text{Re}\lambda_{k+1}$. Let us first note that \mathcal{L} generates a trace-preserving dynamics of $\rho(t)$, and thus there is an eigenvalue $\lambda_1 = 0$ with the corresponding left eigenmatrix being the identity, $L_1 = \mathbb{1}$ and $L_1\mathcal{L} = \lambda_1 L_1 = 0$. Moreover, together with positivity-preserving, it further implies the corresponding right eigenmatrix $R_1, \mathcal{L}R_1 = \lambda_1 R_1 = 0$, can be chosen positive [158], $R_1 \geq 0$, which yields the stationary state of the dynamics, $R_1 = \rho_{\text{ss}}$ after normalisation $\text{Tr}(R_1) = 1$. Generically, the stationary state is unique and the 0-eigenvalue is non-degenerate. In the case when there are more eigenvalues with real part equal 0, the associated Jordan blocks are only 1-dimensional and the basis of the (right) 0-eigenspace can be chosen as consisting of only positive matrices, cf. Sec. 3.1.3. Here, for simplicity of the presentation, we assume the 0-eigenvalue to be non-degenerate. The other right (generalised) eigenmatrices, $\{R_k\}_{k>1}$, corresponding to the eigenvalues with $\text{Re}\lambda_k \neq 0$, cannot be positive due to orthogonality between the left and the right (generalised) eigenmatrices of different eigenvalues, in this case $\text{Tr}(L_1 R_k) = \text{Tr}(R_k) = 0$ for $k > 1$. Hence, dynamics preserving positivity of $\rho(t)$ requires $\text{Re}\lambda_k < 0$, so that the R_k eigenmatrices represent exponentially decay-

ing eigenmodes with the relaxation rates $(-\text{Re } \lambda_k)$ (or exponentially damped polynomial time-dependence for non-trivial Jordan blocks).

Although the generator \mathcal{L} is in general not Hermitian, $\mathcal{L} \neq \mathcal{L}^\dagger$ and thus $L_k \neq R_k$, it is Hermiticity-preserving, i.e., $(\mathcal{L}\rho)^\dagger = \mathcal{L}\rho^\dagger$. Therefore, the complex eigenvalues necessarily come in conjugate pairs, i.e., when $\mathcal{L}R_k = \lambda_k R_k$ and $L_k \mathcal{L} = \lambda_k L_k$, we also have $\mathcal{L}R_k^\dagger = \lambda_k^* R_k^\dagger$ and $L_k^\dagger \mathcal{L} = \lambda_k^* L_k^\dagger$ ¹. As we are interested in the dynamics of Hermitian matrices, we notice that on top of the exponential decay there will be oscillations with a frequency $\omega_k = \text{Im } \lambda_k$, between the Hermitian $R_k + R_k^\dagger$ and the anti-Hermitian part $-i(R_k - R_k^\dagger)$ of the (generalised) eigenmatrix R_k . Moreover, when the real part of an eigenvalue is non-degenerate, it must be real, $\lambda_k = \text{Re } \lambda_k$, and we can choose the corresponding left and right eigenmatrix to be Hermitian. Finally, we normalise the left and right (generalised) eigenmatrices so that $\text{Tr}(L_j R_k) = \delta_{jk}$.

The real parts of eigenvalues $\{\lambda_{k>1}\}$ determine the timescales of relaxation of the modes of the system dynamics. In particular, the second eigenvalue λ_2 determines the *spectral gap*, whose inverse is related to the longest timescale τ of the relaxation of the system to the stationary state, i.e., $\|\rho(t) - \rho_{\text{ss}}\| \sim e^{-t/\tau}$ with $\tau \sim (-\text{Re } \lambda_2)^{-1}$ (where $\|A\| := \text{Tr}\sqrt{A^2}$).

3.2.2 Metastability and separation in generator spectrum

Metastability manifests itself as a long time regime when the system appears stationary, before eventually relaxing to ρ_{ss} . A quantum state of the system can be probed by measuring an observable M in repeated realisation of the same experiment in order to obtain the average value $\langle M(t) \rangle = \text{Tr}(M \rho(t))$, and at different times t after the initialisation of the system in a state ρ_{in} to get the average dependence on time t . When metastabil-

¹ In the case of a generalised eigenmatrix R_k , we have $\mathcal{L}R_k = \lambda_k R_k + R_{k-1}$, and thus also $\mathcal{L}R_k^\dagger = \lambda_k^* R_k^\dagger + R_{k-1}^\dagger$.

ity occurs, there will be a plateau in $\langle M(t) \rangle$ when the system state $\rho(t)$ is metastable for any observable M .

As we show below, metastability will occur *if and only if* the low-lying eigenvalues of \mathcal{L} become separated from the rest of the spectrum in terms of their real part.

Let us first assume that this separation takes place between the m -th mode and the rest, that is, $(-\text{Re } \lambda_m) \ll (-\text{Re } \lambda_{m+1})$. The system evolution from an initial state ρ_{in} is then

$$\rho(t) = e^{t\mathcal{L}} \rho_{\text{in}} = \rho_{\text{ss}} + \sum_{k=2}^m e^{t\lambda_k} c_k R_k + \left[e^{t\mathcal{L}} \right]_{\mathcal{J}-\mathcal{P}} \rho_{\text{in}}, \quad (3.6)$$

where $c_k = \text{Tr}(L_k \rho_{\text{in}})$ are coefficients of the initial state decomposition into the eigenbasis of \mathcal{L} , and we have introduced the projection \mathcal{P} on the subspace of the first m eigenmatrices, $\mathcal{P}\rho := \rho_{\text{ss}} \text{Tr}(\rho) + \sum_{k=2}^m R_k \text{Tr}(L_k \rho)$, and $[e^{t\mathcal{L}}]_{\mathcal{P}} := \mathcal{P}e^{t\mathcal{L}}\mathcal{P}$. In Eq. (3.6) we have assumed there are no Jordan blocks in the low-lying spectrum relevant for our analysis, which assumption is motivated by the structure of the 0-eigenspace, cf. Sec. 3.1.3, as non-trivial Jordan blocks would lead to an unbounded norm of $\rho(t)$ in the limit of gap $\rightarrow 0$ [158]. More precisely, Jordan blocks may be considered as long as they do not contribute significantly, so that Eq. (3.7) holds true with appropriately redefined corrections being small (see also discussion in Sec. 3.4).

Expanding the exponentials in the sum, and assuming $\lambda_1, \dots, \lambda_m$ are real, Eq. (3.6) can be rewritten as,

$$\begin{aligned} \rho(t) = & \rho_{\text{ss}} + \sum_{k=2}^m c_k R_k \\ & + \mathcal{O}(\| [t\mathcal{L}]_{\mathcal{P}} \|) + \mathcal{O}\left(\left\| \left[e^{t\mathcal{L}} \right]_{\mathcal{J}-\mathcal{P}} \right\| \right), \end{aligned} \quad (3.7)$$

where the norm $\|\cdot\|$ of a super-operator \mathcal{S} , is the norm induced by the trace norm, $\|A\| := \text{Tr}\sqrt{A^2}$, of Hermitian matrices A on which \mathcal{S} acts $\|\mathcal{S}\| := \sup_{\|A\|=1} \text{Tr}\|\mathcal{S}A\|$. Dynamics will appear stationary for *any* initial state ρ_{in} when the last two terms in Eq. (3.7) are small. This defines a time regime $\tau'' \ll t \ll \tau'$ where metastability occurs. Intuitively, the last term in (3.7) can

be discarded if $\tau'' \sim (-\text{Re} \lambda_{m+1})^{-1}$ and the overlap of the initial state with the suppressed modes is not too large, so that the sum over many modes of small amplitude can still be neglected. Thus, for times $\tau'' \ll t$ the system relaxes into a state determined by decomposition into the low-lying eigenmodes, $\rho(t) = \rho_{\text{ss}} + \sum_{k=2}^m e^{t\lambda_k} c_k R_k + \mathcal{O} \left(\left\| [e^{t\mathcal{L}}]_{\mathcal{J}-\mathcal{P}} \right\| \right)$. Apparent stationarity of this state further requires $\| [t\mathcal{L}]_{\mathcal{P}} \| \ll 1$, which defines the upper limit of the metastable interval, $\tau' \sim (-\text{Re} \lambda_m)^{-1}$ (for m not too large) and yields the corresponding metastable state as $\rho_{\text{MS}} = \rho_{\text{ss}} + \sum_{k=2}^m c_k R_k$.

More generally, eigenvalues λ_k , $k = 2, \dots, m$, can be complex, appearing in conjugate pairs, $\lambda_{k_1} = \lambda_{k_2}^*$, with imaginary parts that cannot be discarded, i.e., $|\text{Im}(\lambda_k)| \gg (-\text{Re} \lambda_k)$. Taking this into account, a state ρ_{MS} in the MM would read in general,

$$\rho_{\text{MS}} = \rho_{\text{ss}} + \sum_k^m c'_k(t) R'_k. \quad (3.8)$$

When λ_k is real, we simply keep $c'_k(t) := c_k$ and $R'_k := R_k$. For conjugate pairs, $\lambda_{k_1} = \lambda_{k_2}^*$, we introduce pairs of Hermitian operators, $R'_{k_1} := R_{k_1} + R_{k_1}^\dagger$ and $R'_{k_2} := i(R_{k_1} - R_{k_1}^\dagger)$, between which the oscillations with frequency $\omega_{k_1} := \text{Im} \lambda_{k_1}$ take place as follows, $c'_{k_1}(t) := |c_{k_1}| \cos(\omega_{k_1} t + \delta_{k_1})$ and $c'_{k_2}(t) := |c_{k_1}| \sin(\omega_{k_1} t + \delta_{k_1})$ with $\delta_{k_1} := \arg(c_{k_1})^2$. Due to the remaining time dependence in (3.8) the state ρ_{MS} is in general not stationary in the metastable regime, $\tau'' \ll t \ll \tau'$, defined above. However, the set of ρ_{MS} for all initial conditions ρ_{in} – the metastable manifold – remains invariant, as the time dependence in Eq. (3.8) simply constitutes rotations within the MM. Therefore, Eq. (3.8) corresponds to non-dissipative evolution for $\tau'' \ll t \ll \tau'$, which we further discuss in Sec. 3.4.

Note that In Eq. (3.8) we have discarded the second line of Eq. (3.7) where $\| [t\mathcal{L}]_{\mathcal{P}} \|$ by $\| \sum_{k=2}^m \text{Re} \lambda_k R_k \text{Tr}(L_k \cdot) \|$ corresponding to the real part of the low-lying spectrum. Note that truncating of the terms in Eqs. (3.7), (3.8) leads ρ_{MS} to be approximately pos-

² The orthonormalised choice of the left basis will be $L'_{k_1} := (L_{k_1} + L_{k_1}^\dagger)/2$ and $L'_{k_2} := (L_{k_1} - L_{k_1}^\dagger)/2i$, but note $c'_k(t) \neq \text{Tr}(L'_k \rho_{\text{in}})$ in general.

itive with its negative part bounded by the corrections to the invariance of the MM.

In order to prove that separation in the real parts of the \mathcal{L} spectrum is *necessary*, consider the opposite case of no pronounced separation in the spectrum. For the choice of an observable $M = L_k$, where for simplicity we assume $\lambda_k \in \mathbb{R}$ and thus L_k is Hermitian, we have $\langle M(t) \rangle = e^{t\lambda_k} \text{Tr}(\mathcal{L}_k \rho_{\text{in}})$ (with an extra polynomial term for a generalised eigenmatrices L_k, R_k). This shows it is possible to single out dynamics of each eigenmode. Hence, when there is no separation in the spectrum, one cannot find an approximately stationary regime valid for all the modes and for any initial state ρ_{in} . Therefore, the system dynamics *cannot* be metastable, which proves that separation in the real parts of the \mathcal{L} spectrum is necessary.

Note that if the set of observables which can be measured in a given experiment is limited to $\{M_j\}_j$, one can observe *effective metastability* when the observables couple only to a subset of modes, i.e., R_k such that $\exists_j \text{Tr}(M_j R_k) \neq 0$, and the eigenvalues in that subset are separated in their real parts.

Similarly, when preparation of only some initial system states ρ_{in} is feasible, some modes may never be present in the dynamics, i.e., $\text{Tr}(L_k \rho_{\text{in}}) = 0$. In particular, for $\rho_{\text{in}} = \rho_{\text{ss}}$, we simply have $\langle M(t) \rangle = \langle M \rangle_{\text{ss}} = \text{Tr}(\mathcal{L}_k \rho_{\text{ss}})$ and there is no dynamics in measurement averages. Note however, that performing a measurement usually changes the system state, and thus dynamics can be unfolded by correlations of sequential measurements, even for $\rho_{\text{in}} = \rho_{\text{ss}}$, which we present in detail in Sec. 3.2.5.

3.2.3 Geometrical description of quantum metastable manifold

The MM can be described geometrically by generalising the classical method of Refs. [48, 50, 51, 53].

In the metastable regime, the system state is well approximated by a linear combination of the m low-lying modes, see Eq. (3.7). Hence, a metastable state ρ_{MS} in Eq. (3.7) is deter-

mined by a vector of the coefficients (c'_2, \dots, c'_m) that belongs to \mathbb{R}^{m-1} . Thus, the MM is $(m - 1)$ -dimensional, although each point on this manifold (approximately) represents a d^2 density matrix ρ_{MS} , where $d = \dim(\mathcal{H})$ is the dimension of the Hilbert space \mathcal{H} of the system. This effective dimensional reduction due to a separation of timescales will be exploited in next sections to unfold the structure of the metastable states and the long-time dynamics. Note that the coefficients (c'_2, \dots, c'_m) represent $(m - 1)$ degrees of freedom preserved for times $t \ll \tau'$. As we show in Sections 3.3 and 3.4 those can correspond to both to classical probabilities and quantum coherences.

Since the MM is an image of the linear projection \mathcal{P} of the convex set of initial states ρ_{in} , it is itself convex. The coefficients $\{c'_k\}_{k=2}^m$ are bounded by the maximum and the minimum eigenvalues of $\{L'_k\}_{k=2}^m$, respectively, and thus the MM is also bounded.

3.2.4 Effective long-time dynamics

For times $t \gtrsim \tau'$, only the first m modes contribute significantly to the system dynamics,

$$\rho(t) = e^{t\mathcal{L}} \rho_{in} = \rho_{ss} + \sum_{k=2}^m e^{t\lambda_k} c_k R_k + \mathcal{O} \left(\left\| \left[e^{t\mathcal{L}} \right]_{\mathcal{J}-\mathcal{P}} \right\| \right). \quad (3.9)$$

Therefore, dynamics takes place essentially only inside the MM, $\rho(t) \approx [e^{t\mathcal{L}}]_{\mathcal{P}} \rho_{in} = e^{t[\mathcal{L}]_{\mathcal{P}}} (\mathcal{P} \rho_{in})$. The MM contracts exponentially towards the stationary state ρ_{ss} , which is reached at times $t \gg \tau$. Note that this low-dimensional evolution in the MM is well described by an effective generator $\mathcal{L}_{eff} := [\mathcal{L}]_{\mathcal{P}}$. The knowledge about the structure of the MM gives further interpretation to \mathcal{L}_{eff} as a generator of the dynamics on that structure. For example, in the case of classical MM, the effective long-time dynamics is classical dynamics with probabilities, with \mathcal{L}_{eff} being a generator stochastic transitions between metastable phases, whose trajectories further correspond to coarse-graining in time of continuous measurement records, see Sec. 3.3.2.

3.2.5 Experimental observation of metastability

As we discussed a quantum state of the system $\rho(t)$ can be probed via measurements of the average of an observable M , $\langle M(t) \rangle = \text{Tr}(M\rho(t))$. Observation of the metastability requires non-trivial system dynamics triggered by preparation of the initial state $\rho_{\text{in}} \neq \rho_{\text{ss}}$. In practice, when preparation of a given initial state is difficult, metastability can be observed through the *double-step decay* of correlations [183] in sequential measurements of M , even in the case of the stationary state, $\rho_{\text{in}} = \rho_{\text{ss}}$. We consider the autocorrelation

$$C(t) := \text{Tr}(\mathcal{M}e^{t\mathcal{L}} \mathcal{M}\rho_{\text{ss}}) - \text{Tr}(\mathcal{M}\rho_{\text{ss}})^2, \quad (3.10)$$

where \mathcal{M} is the superoperator describing the action of measuring of M on the system (the average of a result and the corresponding conditional system state); for $M = \sum_{i=1}^d m_i |m_i\rangle\langle m_i|$, we have $\mathcal{M}(\rho) = \sum_{i=1}^d m_i \langle m_i|\rho|m_i\rangle |m_i\rangle\langle m_i|$.

Performing a measurement generically perturbs the stationary state ρ_{ss} , $\mathcal{M}(\rho_{\text{ss}}) \neq \mathcal{M}\rho_{\text{ss}}$, unless the eigenbasis of M and ρ_{ss} coincide. Consider the system state conditioned on a result of the first measurement of M . For time $t \lesssim \tau''$ it relaxes (partially) towards the MM. Since only $(m-1)$ degrees of freedom are preserved, a part of the information about the initial result is erased, which manifests in an initial decay of correlations. During the metastable regime, $\tau'' \ll t \ll \tau'$, in the case when where all low-lying eigenvalues are real, correlations show a plateau, $C(t) \approx \text{Tr}(\mathcal{M}\mathcal{P}\mathcal{M}\rho_{\text{ss}}) - \text{Tr}(\mathcal{M}\rho_{\text{ss}})^2$, due to the approximate stationarity of the dynamics, see Fig. 3.1(e). When low-lying eigenvalues are complex, undamped oscillations of $C(t)$ can occur in the metastable regime, cf. Eq. (3.7), e.g. coherent rotation in Fig. 3.2(d). At later times, when $t \gtrsim \tau'$, dynamics begins to relax back towards ρ_{ss} , further erasing the information about the initial result. This corresponds to the second final decay of correlations governed by the effective dynamics of $m-1$ degrees of freedom, $C(t) \approx \text{Tr}(\mathcal{M} [e^{t\mathcal{L}_{\text{eff}}}]_{\mathcal{P}} \mathcal{M}\rho_{\text{ss}})$. At times

$t \gg \tau$, when any initial state relaxes to ρ_{ss} , all the information is erased and $C(t) \approx 0$.

3.3 BIMODAL CASE OF TWO LOW-LYING MODES

We first consider the case of $m = 2$ low-lying modes and derive the classical structure of the MM with the effective classical dynamics. Note that, since the real part of λ_2 is non-degenerate, it is real, $\lambda_2 \in \mathbb{R}$, and L_2 can be assumed Hermitian. Moreover, we have $\tau' = \tau = (-\text{Re } \lambda_2)^{-1}$.

3.3.1 Classical structure of the metastable manifold

The metastable manifold is 1-dimensional and convex and therefore corresponds to an interval. Indeed, a metastable state, $\rho_{MS} = \rho_{ss} + c_2 R_2$, is determined by the single coefficient $c_2 = \text{Tr}(L_2 \rho_{in})$, whose value is between the maximum c_2^{\max} and minimum c_2^{\min} eigenvalues of L_2 . As $c_2 = p_1 c_2^{\max} + p_2 c_2^{\min}$, where $p_1 = 1 - p_2 \in [0, 1]$, any metastable state is simply a mixture, $\rho_{MS} = p_1 \tilde{\rho}_1 + p_2 \tilde{\rho}_2$, of two *extreme* metastable states,

$$\tilde{\rho}_1 = \rho_{ss} + c_2^{\max} R_2, \quad \tilde{\rho}_2 = \rho_{ss} + c_2^{\min} R_2. \quad (3.11)$$

Note that $\tilde{\rho}_1$ and $\tilde{\rho}_2$ correspond to the metastable states obtained for the system initialised in pure states chosen as the L_2 eigenvectors with the eigenvalues c_2^{\max} and c_2^{\min} , respectively. Consequently, in contrast to the R_2 eigenmode being non-positive with $\text{Tr}(R_2) = 0$, we obtain that the each extreme metastable state (eMS) fulfils $\text{Tr}(\tilde{\rho}_{1,2}) = 1$ and is positive up to corrections of the order of non-stationary terms neglected in the metastable regime, cf. Eq. (3.7). Therefore, $\tilde{\rho}_1, \tilde{\rho}_2$ represent (approximately) quantum states of the system.

The probabilities for any initial state ρ_{in} to evolve during the metastable regime into each of two eMSs are given by $p_{1,2} = \text{Tr}(\tilde{P}_{1,2} \rho_{in})$ (up to corrections in Eq. (3.7)), where the observables

$$\tilde{P}_1 = (L_2 - c_2^{\min} \mathbf{1}) / \Delta c_2, \quad \tilde{P}_2 = (-L_2 + c_2^{\max} \mathbf{1}) / \Delta c_2, \quad (3.12)$$

with $\Delta c_2 := c_2^{\max} - c_2^{\min}$. Note that $\tilde{P}_{1,2} \geq 0$ and $\tilde{P}_1 + \tilde{P}_2 = \mathbb{1}$, and hence two observable \tilde{P}_1, \tilde{P}_2 constitute a POVM, which is a consequence of the MM being a simplex. Finally, as we also have $\text{Tr}(\tilde{P}_i \tilde{\rho}_j) = \delta_{ij}$, $i, j = 1, 2$, the eMSs $\tilde{\rho}_1, \tilde{\rho}_2$ and the observables \tilde{P}_1, \tilde{P}_2 constitute a (right and left) basis of the MM.

Let us note that properties of any metastable state are fully characterised by its decomposition into the two eMSs and their properties. Hence, in analogy with the Maxwell construction in equilibrium classical systems [197], we refer to $\tilde{\rho}_1, \tilde{\rho}_2$ as *metastable phases*. Moreover, when a finite system features two stationary states (phases), it is known their supports are mutually disjoint (see 3.1). It can be shown this is approximately the case also for the metastable phases (see Appendix C.1).

Example I: 3-level system. Consider the 3-level system in Fig. 3.1 (a), with the Hamiltonian $H = \Omega_1 (|1\rangle\langle 0| + |0\rangle\langle 1|) + \Omega_2 (|2\rangle\langle 0| + |0\rangle\langle 2|)$ and a single jump operator $J = \sqrt{\kappa} |0\rangle\langle 1|$. When $\Omega_2 \ll \Omega_1$, dynamics can be “shelved” for long times in $|2\rangle$, giving rise to intermittency in quantum jumps [33], which can be seen as coexistence of “active” and “inactive” dynamical phases [34]. Fig. 3.1 (b) shows the spectrum of \mathcal{L} : the gap is small for $\Omega_2 \ll \Omega_1$, the two leading eigenvalues detach from the rest ($m = 2$), and the dynamics is metastable. The MM for this $m = 2$ case is a one-dimensional simplex, see Fig. 3.1 (c). Fig. 3.1 (d) illustrates the trace distance of the state $\rho(t)$ to the MM starting from $\rho_{\text{in}} \neq \rho_{\text{ss}}$: an initial decay on times of order of τ'' to the nearest point on the MM (in this case to an eMS) is followed by decay to ρ_{ss} on times of order τ described by \mathcal{L}_{eff} .

For the example of metastability with $m = 2$ low-lying modes, appearing as a collective effect with an increasing system size, see the analysis for a dissipative quantum Ising chain with transverse field [172]. In this model there exists a region in parameter space for which there are two metastable phases: ferromagnetic (spins down) and paramagnetic (spins close to the fully mixed state) one.

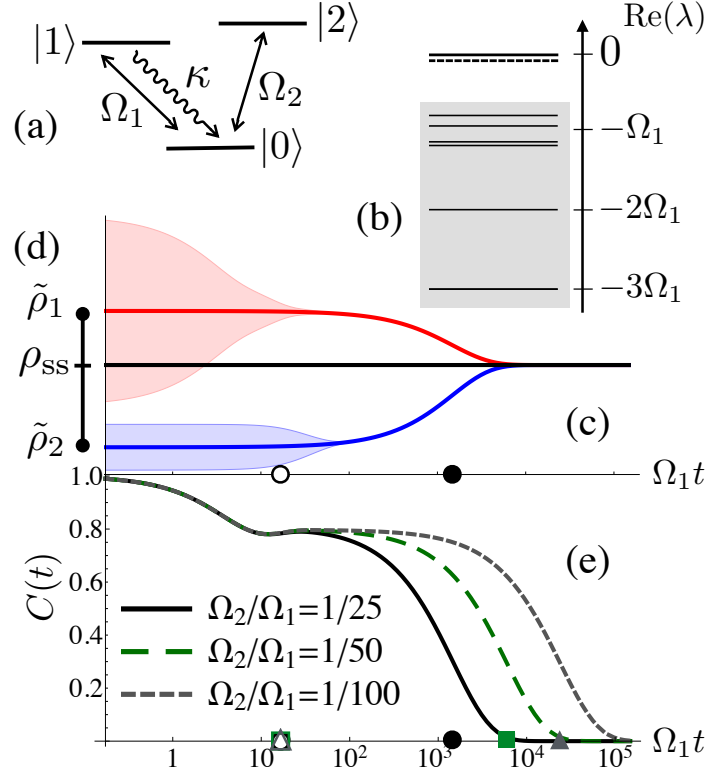


Figure 3.1: **Example of metastability in a 3-level system:** (a) Level scheme and transitions. (b) Spectrum of \mathcal{L} showing separation between eigenvalues (λ_1, λ_2) (full, dashed) and $\{\lambda_{k>2}\}$ (shaded), for the case $\kappa = 4\Omega_1$, $\Omega_2 = \Omega_1/10$. (c) Illustration of the distance of the state, $\rho(t)$, to the MM. We consider $\rho(t)$ starting from pure states corresponding to the eigenvectors of L_2 with maximal (red) and minimal eigenvalues (blue), c_2^{\max} and c_2^{\min} . The full curves indicate the nearest state on the MM, $\rho_{MS}(t)$, to the full state $\rho(t)$. The shaded region indicates the scale of the “approximation” $\|\rho(t) - \rho_{MS}(t)\|$. On times of order τ'' (open circle) the state $\rho(t)$ relaxes to the MM (in this case to the eMSS, $\tilde{\rho}_{1,2}$), as seen by the shaded region decreasing to zero. On times of order τ (filled circle) there an eventual relaxation to the stationary state ρ_{ss} takes place (black line). $\Omega_2 = \Omega_1/25$. (d) The MM is a one-dimensional simplex. (e) Normalised autocorrelation, $C(t)$, of the observable $|1\rangle\langle 1| - |2\rangle\langle 2|$, in ρ_{ss} . For a decreasing ratio of Ω_2/Ω_1 , the gap decreases and the metastable regime between τ'' (open symbols) and τ (filled symbols) is increasingly pronounced. This figure originally appeared in [196].

3.3.2 Effective classical long-time dynamics

For times $t \gtrsim \tau = (-\lambda_2)^{-1}$ only two low-lying eigenmodes, R_2 and ρ_{ss} , contribute non-negligibly to the system dynamics

$$\begin{aligned} \rho(t) &= [e^{t\mathcal{L}}]_{\mathcal{P}} \rho_{\text{in}} + \mathcal{O}\left(\left\| [e^{t\mathcal{L}}]_{\mathcal{J}-\mathcal{P}} \right\|\right). \\ &= \rho_{ss} + e^{t\lambda_2} c_2 R_2 + \mathcal{O}\left(\left\| [e^{t\mathcal{L}}]_{\mathcal{J}-\mathcal{P}} \right\|\right). \end{aligned} \quad (3.13)$$

Thus, long-time dynamics effectively take place only on the metastable manifold, $e^{t\mathcal{L}} \approx [e^{t\mathcal{L}}]_{\mathcal{P}}$, which contracts exponentially towards the steady state ρ_{ss} .

As we have showed above, due to the MM being an interval, and thus a simplex, all metastable states can be represented as the probability distributions (p_1, p_2) between the metastable phases $\tilde{\rho}_1, \tilde{\rho}_2$. Since, the effective long-time dynamics, $[e^{t\mathcal{L}}]_{\mathcal{P}}$, transforms the MM into itself, it necessarily preserves the probability distribution structure: positivity ($p_{1,2}(t) \geq 0$) and total probability ($p_1(t) + p_2(t) = 1$). We indeed have

$$\begin{aligned} \begin{pmatrix} p_1(t) \\ p_2(t) \end{pmatrix} &= [e^{t\mathcal{L}}]_{\mathcal{P}} \begin{pmatrix} p_1 \\ p_2 \end{pmatrix} \\ &= \frac{1}{\Delta c_2} \begin{pmatrix} c_2^{\max} e^{t\lambda_2} - c_2^{\min} & -c_2^{\min} (1 - e^{t\lambda_2}) \\ c_2^{\max} (1 - e^{t\lambda_2}) & c_2^{\max} - c_2^{\min} e^{t\lambda_2} \end{pmatrix} \begin{pmatrix} p_1 \\ p_2 \end{pmatrix}, \end{aligned} \quad (3.14)$$

where $[e^{t\mathcal{L}}]_{\mathcal{P}}$ is expressed in the basis of the metastable phases, see Eqs. (3.11) and (3.12), and the initial probability distribution is $p_{1,2} = \text{Tr}(\tilde{\mathcal{P}}_{1,2}\rho_{in})$. Note that $[e^{t\mathcal{L}}]_{\mathcal{P}}$ features only positive entries (positivity) and its columns sum to 1 (total probability preservation). The asymptotic probability distribution, $(p_1^{ss}, p_2^{ss}) = (\frac{-c_2^{\min}}{\Delta c_2}, \frac{c_2^{\max}}{\Delta c_2})$, corresponds directly to the stationary state ρ_{ss} , see Fig. 3.1 (c-d).

Let us note that although long-time dynamics is classical, the underlying system in general features quantum effects which are present at shorter $t < \tau''$ times, cf. Eq. (3.2).

Classical trajectories. Let us note that the classical dynamics of probabilities given in (3.14) can be viewed as generated by the classical stochastic generator $\mathcal{L}_{\text{eff}} := [\mathcal{L}]_{\mathcal{P}}$,

$$\begin{aligned} \frac{d}{dt} \begin{pmatrix} p_1(t) \\ p_2(t) \end{pmatrix} &= \mathcal{L}_{\text{eff}} \begin{pmatrix} p_1(t) \\ p_2(t) \end{pmatrix} \\ &= \frac{-\lambda_2}{\Delta c_2} \begin{pmatrix} -c_2^{\max} & -c_2^{\min} \\ c_2^{\max} & c_2^{\min} \end{pmatrix} \begin{pmatrix} p_1(t) \\ p_2(t) \end{pmatrix}. \end{aligned} \quad (3.15)$$

The stochastic trajectories generated by \mathcal{L}_{eff} consist of transitions between two metastable phases $\tilde{\rho}_1, \tilde{\rho}_2$.

Note that the dynamics in Eq. (3.15) satisfies the *detailed balance* condition due to the space of effective configurations consisting only of two macrostates, $\tilde{\rho}_1$ and $\tilde{\rho}_2$. Therefore, the decomposition of the stationary state ρ_{ss} between the metastable phases is determined by the ratio of the off-diagonal terms, $-c_2^{\text{min}}/c_2^{\text{max}}$, which is independent from λ_2 . Dynamics of classical trajectories generated by \mathcal{L}_{eff} can be characterised by the mean time a metastable phase survive in a (so called mean exit time), which is given by the inverse of the related diagonal entry, e.g. $(-c_2^{\text{max}}\lambda_2)^{-1} = \tau(c_2^{\text{max}})^{-1}$ for $\tilde{\rho}_1$ and proportional to τ . Therefore, the average ratio of time a trajectory spends in each of the phases is given by the ratio $-c_2^{\text{min}}/c_2^{\text{max}}$, and thus corresponds to the decomposition of the stationary states between two phases, confirming that classical dynamics of \mathcal{L}_{eff} is *ergodic*.

The long-time dynamics obeys detailed balance, although we consider general, including non-equilibrium and driven, Markovian quantum dynamics, see Eq. (3.2).

Finally, let us note the similarity of trajectories of \mathcal{L}_{eff} to the long-time equilibrium dynamics of a particle in a double well potential. This model, although simple, captures dynamics of classical equilibrium systems close to a first-order phase transition featuring two stable phases, such as a ferromagnet at low temperatures, see Sec. 3.1.1. The potential of a particle represents the Landau free-energy functional of the equilibrium system, while the spacial coordinates correspond to configurations of the system. The long-lasting states/probability distributions are represented by two states initially equilibrated within each well ($t \gg \tau''$). Thermal fluctuations allow for particle movement between the wells, but at much longer time scales inversely proportional to the barrier height ($t \sim \tau$), which asymptotically ($t \gg \tau$) leads the system to the final equilibrium state. The division of the equilibrium probability between the two wells depends on the difference of the free energies of the wells,

but not on the barrier height (proportional to τ).

In the next subsection we argue that classical trajectories of \mathcal{L}_{eff} can be viewed as *coarse-graining in time* of quantum trajectories over intervals longer than the initial relaxation time τ'' .

3.3.2.1 *Metastability as intermittence of quantum trajectories*

In the discussion so far we considered the dynamics of the system state described by a density matrix $\rho(t)$, which represents the average state of the system obtained at time t in a given experimental realisation of the dynamics (3.2). Let us consider additional continuous monitoring of the environment state in a given experimental realisation of system dynamics. Results of such a continuous measurement up to time t , can be used to reconstruct a conditional state of the system at all times $t' \leq t$, and thus unravel the system dynamics into *quantum trajectories* [30, 33], see also in the input-output formalism used in Chapter 2.

A quantum trajectory of time t is a record of a system state at all times $t' \leq t$, which state is conditioned on the continuous measurement results. Consider Example I of 3-level system above with an experimental realisation as follows: the levels $|0\rangle, |1\rangle, |2\rangle$, are electronic levels of an atom interacting with surrounding it electromagnetic vacuum and driven by Rabi laser. The interaction with the vacuum leads to photon emissions described by the action of the jump, $J = \sqrt{\kappa}|0\rangle\langle 1|$. Emitted photons can be further detected. Based on the measurement record of photon emission times up to time t , the conditional pure state $|\psi(t')\rangle$ of the system can be reconstructed for all times $t' \leq t$, thus yielding a quantum trajectory. In this case, the density matrix $\rho(t)$ is simply the conditional system state $|\psi(t)\rangle\langle\psi(t)|$ averaged over all possible photon emission records.

Metastability and intermittence. We now discuss how metastability with two phases can manifest itself in intermittence of

quantum trajectories, and thus can be observed also in individual realisations of the experiment.

Consider a state evolving into just one of the metastable phases, $\tilde{\rho}_1, \tilde{\rho}_2$, e.g. the pure states $|1\rangle$ or $|2\rangle$ for the 3-level system. Furthermore let us consider an integrated record $\Lambda(t)$ of a continuous measurement, e.g. total number of photons emitted up to time t by the system. For time t much longer than the initial system relaxation time, $t \gg \tau''$, the main contribution to the integrated observable $\Lambda(t)$ comes from the period after the initial relaxation, when, on average, the system state is metastable ($\rho(t) \approx \tilde{\rho}_{1,2}$). Since the instant rate μ at which $\Lambda(t)$ is accumulated depends only on the system state, and thus corresponds to the mean of a system observable, e.g. $\mu = \text{Tr}(J^\dagger J \rho) = \text{Tr}(|1\rangle\langle 1| \rho)$, the value taken by $\Lambda(t)$ will be on average determined by $\langle \Lambda(t) \rangle = \int_0^t dt' \mu(t') \approx t \mu_{1,2}$, where $\mu_{1,2}$ is the rate for the metastable phase $\tilde{\rho}_{1,2}$. Furthermore, the variance of $\Lambda(t)$ will necessarily scale linearly, as any correlations in dynamics inside a metastable phase support, must decay at most at the timescale τ'' corresponding to the faster eigenmodes R_k , $k > m = 2$. If we now consider the activity $k(t) = \Lambda(t)/t$ of trajectories, we have that its fluctuations $\Delta^2 k(t) \propto t^{-1}$ around its mean, $\mu_{1,2}$, will be small if the metastable regime is long enough. In this case, trajectories/measurement records can be classified as "active" and "inactive" ($\mu_1 \neq \mu_2$). So far we have considered initial states evolving into just one of two metastable phases, but for a general initial state the system evolves into a mixture of two metastable phases, $\rho(t) \approx p_1 \tilde{\rho}_1 + p_2 \tilde{\rho}_2$, and it follows that emission records are a mixture of active and inactive records with probabilities p_1 and p_2 , since the statistics of activity is determined mostly by the contribution from the metastable regime.

Consider now *coarse graining* in time of measurement records, where a record is divided into time bins of a size t_{bin} and photon emissions are replaced by the activity in individual time bins. From the previous paragraph it follows that, the coarse-grained record consist of active and inactive time-bins with activity $k \approx \mu_{1,2}$, when t_{bin} is long enough. Furthermore, the

periods of active and inactive dynamics (so called *dynamical phases* [34, 36, 172]) correspond directly to the two metastable phases of the system, $\tilde{\rho}_1, \tilde{\rho}_2$.

Coarse-grained measurement records and effective trajectories. We now argue that the coarse-grained trajectories are directly related to classical trajectories of \mathcal{L}_{eff} in Eq. (3.15).

Classical trajectories of \mathcal{L}_{eff} are ergodic, with the ratio of the average time spent in metastable phases given by stationary probabilities, $p_1^{\text{ss}}/p_2^{\text{ss}}$. We now argue that this is also true for active and inactive periods in continuous measurement records. Since for times $t \gg \tau$ the system state is stationary, the asymptotic activity is given by the stationary rate, $\langle k \rangle_{\text{ss}} := \lim_{t \rightarrow \infty} \langle k(t) \rangle = \mu_{\text{ss}}$ with fluctuations disappearing as t^{-1} (see also CLT for continuous measurements [37, 39]). Therefore, the ratio of times spent in active ($k \approx \mu_1$) and inactive ($k \approx \mu_2$) periods, must be given approximately by the stationary probabilities, $p_1^{\text{ss}}/p_2^{\text{ss}}$, so that $\langle k \rangle_{\text{ss}} \approx p_1^{\text{ss}}\mu_1 + p_2^{\text{ss}}\mu_2 = \mu_{\text{ss}}$. This implies that measurement records are ergodic with probability 1. In particular, for coarse graining of a single measurement record, a histogram of time-bin activities must be bimodal [36, 172], with probabilities of two modes corresponding to the stationary probabilities p_1^{ss} and p_2^{ss} .

Moreover, the average time of active dynamics (or inactive dynamics rescaled by the ratio $p_1^{\text{ss}}/p_2^{\text{ss}}$) in coarse-grained records is necessary not longer than $\mathcal{O}(\tau)$, as τ is the longest timescale of the system dynamics. It also cannot be shorter, as otherwise the mean activity $\langle k(t) \rangle$ for the initial states evolving into $\tilde{\rho}_1, \tilde{\rho}_2$, would not be given by $\mu_{1,2}$, but values in between. Consequently, the coarse-grained measurement records and classical trajectories of \mathcal{L}_{eff} are *equivalent* (with probability 1).

One can further ask about equivalence of quantum trajectories to the classical dynamics \mathcal{L}_{eff} , i.e., whether time-coarse grained conditional system state, $t_{\text{bin}}^{-1} \int_t^{t+t_{\text{bin}}} dt' |\psi(t')\rangle\langle\psi(t')|$, corresponds to two metastable states for t_{bin} chosen as above. Let us note that this would imply ergodicity of quantum tra-

jectories, i.e., time-averaged state of the system approaching the stationary state, $\lim_{t \rightarrow \infty} t^{-1} \int_0^t dt' |\psi(t')\rangle \langle \psi(t')| = \rho_{ss}$. Conversely, if quantum trajectories were ergodic, as the supports of metastable phases are approximately disjoint (see Appendix C.1), quantum trajectories would be ergodic also inside the phases for long enough metastable regime $\tau'' \ll t \ll \tau$. It is not generally known, however, whether quantum trajectories are ergodic for open Markovian dynamics featuring a unique stationary state.

Beyond activity. The relation of effective dynamics to coarse-graining of measurement records can be extended to the case when metastable phases do not differ in activity, $\mu_1 = \mu_2 = \mu_{ss}$, and there is no apparent intermittency in the records. In that case one needs to consider fluctuations of the integrated observable instead of its activity and double coarse-graining of records. For first coarse-graining we choose $\delta t = n^{-1} t_{\text{bin}} \gg \tau''$ and look at fluctuations, $\Lambda^{(2)}(t + k\delta t) := (\delta t)^{-1} [\Lambda(t + (k + 1)\delta t) - \Lambda(t + k\delta t) - \delta t \mu_{ss}]^2$, $0 \leq k \leq n - 1$. In the second coarse graining we consider time-average of fluctuations over t_{bin} , $\overline{\Lambda^{(2)}}(t) := n^{-1} \sum_{k=0}^{n-1} \Lambda^{(2)}(t + k\delta t)$. Note that $\Delta^2 \overline{\Lambda^{(2)}}(t) \propto n^{-1}$, as the correlations of fluctuations inside metastable phases decay at times $t \sim \tau''$. Hence, for a long enough metastable regime, one observes "intermittency" between small and large fluctuations in measurement records. Using analogous arguments as for activity $k(t)$, we obtain that the ratio of average lengths of those periods is again determined by p_1^{ss}/p_2^{ss} and the average length corresponds to the longest timescale τ .

3.3.3 Biased QJMC - how to investigate metastability without diagonalising master operator

We now show how to use dynamical large-deviation approach [166] to identify dynamically the metastable phases by biasing ensembles of quantum trajectories [34]. These methods can be implemented numerically by generalising classical path sampling

[202] and/or cloning techniques [203]. In particular, for many-body systems where direct diagonalisation of the master operator \mathcal{L} is not feasible, this provides a computational scheme to unfold the classical metastable manifold structure.

We discuss here biasing towards the number of jumps J_1 in a quantum trajectory, e.g. the number of photon emissions in 3-level system. First, let us recall that cumulants of total number of jumps J_1 that happened up to time t , $\Lambda(t)$, are given by the derivatives of the cumulant generating function (CGF) $\Theta_t(s)$ [34],

$$\Theta_t(s) = \log \text{Tr}(e^{t\mathcal{W}_s} \rho_{\text{in}}), \quad (3.16)$$

$$\mathcal{W}_s \rho = \mathcal{L}\rho + (e^{-s} - 1) J_1 \rho J_1^\dagger, \quad (3.17)$$

see also Sec. 2.1.2. The asymptotic linear limits of $\Lambda(t)$ cumulants are given by respective derivatives of

$$\theta(s) = \lim_{t \rightarrow \infty} t^{-1} \Theta(s, t). \quad (3.18)$$

Let us note that, although \mathcal{W}_s is not a master operator for $s \neq 0$, in particular it is *not* trace-preserving, the related evolution preserves positivity of ρ . This can be easily seen from the fact that trajectories of \mathcal{W}_s can be sampled analogously as quantum trajectories of \mathcal{L} in quantum jump Monte Carlo (QJMC) simulations [204], but with probability of the jump J_1 rescaled by e^{-s} , so that $s > 0$ decreases the activity of trajectories, while $s < 0$ enhances it. As $\rho_s(t)/\text{Tr}(\rho_s(t))$, where $\rho_s(t) = e^{t\mathcal{W}_s} \rho_{\text{in}}$, is the average of conditional system state $|\psi_s(t)\rangle\langle\psi_s(t)|$ over all such trajectories, it must be positive. The limiting state $\rho_s = \lim_{t \rightarrow \infty} \rho_s(t)/\text{Tr}(\rho_s(t))$ obtained in biased QJMC is the eigenmatrix of \mathcal{W}_s corresponding to its maximum eigenvalue is exactly

$$\theta(s) = \text{Tr}(\mathcal{W}_s \rho_s). \quad (3.19)$$

State ρ_s as metastable phase. Here we consider the parameter s to be small, and we treat $\mathcal{W}_s - \mathcal{L} = (e^{-s} - 1) J_1 \rho J_1^\dagger$ as a perturbation (for classical Markovian systems see Chapter 5.2 in [53]).

Since the first two eigenmodes of \mathcal{L} are not degenerate ($\lambda_2 < 0$), for the perturbation small in comparison with $-\lambda_2$ we have that [167]

$$\lambda_1(s) = \theta(s) = -\tilde{s} \operatorname{Tr}(J_1^\dagger J_1 \rho_{ss}) + \mathcal{O}(\tilde{s}^2), \quad (3.20)$$

$$\lambda_2(s) = \lambda_2 - \tilde{s} \operatorname{Tr}(L_2 J_1 R_2 J_1^\dagger) + \mathcal{O}(\tilde{s}^2), \quad (3.21)$$

where $\tilde{s} = (1 - e^{-s})$, with the corresponding eigenmodes simply given by $\rho_s = \rho_{ss} + \mathcal{O}(s)$ and $R_2 + \mathcal{O}(s)$. In particular, we recover the asymptotic activity, $\lim_{t \rightarrow \infty} \langle \Lambda(t) \rangle / t = \mu_{ss} = \operatorname{Tr}(J_1^\dagger J_1 \rho_{ss})$.

When the perturbation is larger, $(-\lambda_2) \ll \tilde{s} \kappa_1 \ll (-\operatorname{Re} \lambda_3)$, where $\kappa_1 = \|J_1(\cdot)J_1^\dagger\|$, in order to find the asymptotic CGF, $\theta(s)$, and the corresponding eigenmatrix ρ_s , we need to consider almost degenerate perturbation theory of the first two modes [167],

$$[\mathcal{W}_s]_{\mathcal{P}} = \begin{pmatrix} -\tilde{s} \operatorname{Tr}(J_1^\dagger J_1 \rho_{ss}) & -\tilde{s} \operatorname{Tr}(J_1^\dagger J_1 R_2) \\ -\tilde{s} \operatorname{Tr}(L_2 J_1 \rho_{ss} J_1^\dagger) & \lambda_2 - \tilde{s} \operatorname{Tr}(L_2 J_1 R_2 J_1^\dagger) \end{pmatrix}, \quad (3.22)$$

which in the basis of metastable phases gives, cf. Eqs. (3.11) and (3.12),

$$[\mathcal{W}_s]_{\mathcal{P}} = \mathcal{L}_{\text{eff}} - \tilde{s} \begin{pmatrix} \operatorname{Tr}(\tilde{P}_1 J_1 \tilde{\rho}_1 J_1^\dagger) & \operatorname{Tr}(\tilde{P}_1 J_1 \tilde{\rho}_2 J_1^\dagger) \\ \operatorname{Tr}(\tilde{P}_2 J_1 \tilde{\rho}_1 J_1^\dagger) & \operatorname{Tr}(\tilde{P}_2 J_1 \tilde{\rho}_2 J_1^\dagger) \end{pmatrix}. \quad (3.23)$$

When \tilde{s} is big enough, \mathcal{L}_{eff} is just a perturbation of the second matrix. Furthermore, as we show in Appendix D.2, the off-diagonal terms $\operatorname{Tr}(\tilde{P}_1 J_1 \tilde{\rho}_2 J_1^\dagger)$ and $\operatorname{Tr}(\tilde{P}_2 J_1 \tilde{\rho}_1 J_1^\dagger)$ are of the order $\mathcal{O}(\max(\lambda_2 t, \| [e^{t\mathcal{L}}]_{\mathcal{J}-\mathcal{P}} \|)^{1/2} \times \kappa_1)$, and thus the last matrix is diagonal up to those corrections. Therefore, up to corrections given by \mathcal{L}_{eff} and the off-diagonal terms,

$$\theta(s) \approx \max((e^{-s} - 1)\mu_1, (e^{-s} - 1)\mu_2) \quad \text{and} \quad \rho_s \approx \tilde{\rho}_k \quad (3.24)$$

for $k \in \{1, 2\}$ such that μ_k is chosen in $\theta(s)$. We see that indeed $s > 0$ biases the system dynamics towards less active trajectories with respect to jumps J_1 , while $s < 0$ otherwise, and the

average state ρ_s obtained asymptotically corresponds to a respective metastable phase.

Timescales in biased dynamics. For \mathcal{W}_s with s chosen so that $(-\lambda_2) \ll \tilde{s}\kappa_1 \ll (-\text{Re } \lambda_3)$ the initial relaxation timescale equals τ'' for unbiased dynamics, $W_0 = \mathcal{L}$ (cf. Appendix C.2.2). This is followed by a *metastable regime*, $\tau'' \ll t \ll \tilde{s}^{-1}\kappa_1^{-1}$, due to a persisting separation in spectrum of \mathcal{W}_s , and the asymptotic state ρ_s is achieved for times $t \gg \tilde{s}^{-1}\kappa_1^{-1}$, cf. (3.23). To circumvent those timescales and achieve ρ_s in simulations, one should bias ensembles of quantum trajectories instead of biasing jumps probabilities, which can be implemented numerically by generalising classical path sampling [202] and/or cloning techniques [203].

3.4 HIGHER DIMENSIONAL METASTABLE MANIFOLDS AND THEIR EFFECTIVE DYNAMICS

In the previous section we exploited the fact that for $m = 2$ the convex set of the coefficients, which represent the MM, is one-dimensional and thus a simplex with two eMSs. For $m > 2$, however, the set of possible coefficients can have more than m extreme points. For classical dynamics it has been proven, that this set is well approximated by a $(m - 1)$ -dimensional simplex [51], see Sec. 3.1.2. The simplex vertices correspond to m approximately disjoint eMSs and its barycentric coordinates to the probabilities of a metastable state decomposed as a mixture of the eMSs, cf. Fig. 3.1 (d).

For quantum dynamics and $m > 3$, we expect the structure of the MM to be richer than just a simplex. As we describe below, the MM can in general include decoherent free subspaces (DFSS) [40–43] and noiseless subsystems (NSSs) [44–46], which are protected from dissipation during the metastable regime.

We consider two classes of systems for which the master operator \mathcal{L} has a small gap: (A) finite systems where the gap closes at some limiting values of the parameters in \mathcal{L} (such as $\Omega_2 \rightarrow 0$ in Example I above, and $\Omega_{1,2} \rightarrow 0$ in Example II below);

(B) scalable systems consisting of N subsystems where the gap may close only in the thermodynamic limit of $N \rightarrow \infty$ (such as the dissipative Ising chain with transverse field in Refs. [36] and [172]).

3.4.1 Metastability in class A systems

We first discuss metastability in dynamics of a finite open quantum system for which the gap closes at some value of parameters in the master equation, $\mathcal{L} = \mathcal{L}_0$, see Eq. (3.2). The stationary state ρ_{ss} is no longer unique and has a general structure of Eq. (3.3). Using perturbation theory of linear operators [167], we show that there is a separation in the \mathcal{L} spectrum for dynamics which are close to the degenerate case of \mathcal{L}_0 . We further derive the metastable time regime during which the system state has approximately the structure given in Eq. (3.3) and the long-time effective dynamics, which is trace-preserving and approximately completely positive.

Example II: Collective dissipation and a metastable DFS. Consider a two-qubit system with Hamiltonian $H = \Omega_1 \sigma_1^x + \Omega_2 \sigma_2^x$, and a collective jump operator $J = \sqrt{\gamma_1} n_1 \sigma_2^- + \sqrt{\gamma_2} (1 - n_1) \sigma_2^+$. When $\Omega_{1,2} \ll \gamma_{1,2}$ there is a small gap and the four leading eigenvalues of \mathcal{L} detach from the rest, Fig. 3.2 (a). This is related to the fact that any superposition of $|01\rangle$ and $|10\rangle$ is annihilated by jump J . Fig. 3.2 (b) maps out the MM by randomly sampling all (pure) initial states ρ_{in} from \mathcal{H} and obtaining their corresponding metastable state via Eq. (3.8): the MM is an affinely transformed Bloch ball corresponding to a DFS of a qubit within the metastable regime $\tau'' \ll t \ll \tau'$. It is important to note: (i) this coherent structure is not the consequence of a symmetry, as for $\gamma_1 \neq \gamma_2$ the system dynamics neither has a $U(2)$ nor an up-down nor a permutation symmetry, cf. [205]; (ii) the smallest m for which we can obtain a DFS in class A systems is $m = 4$, as in this case.

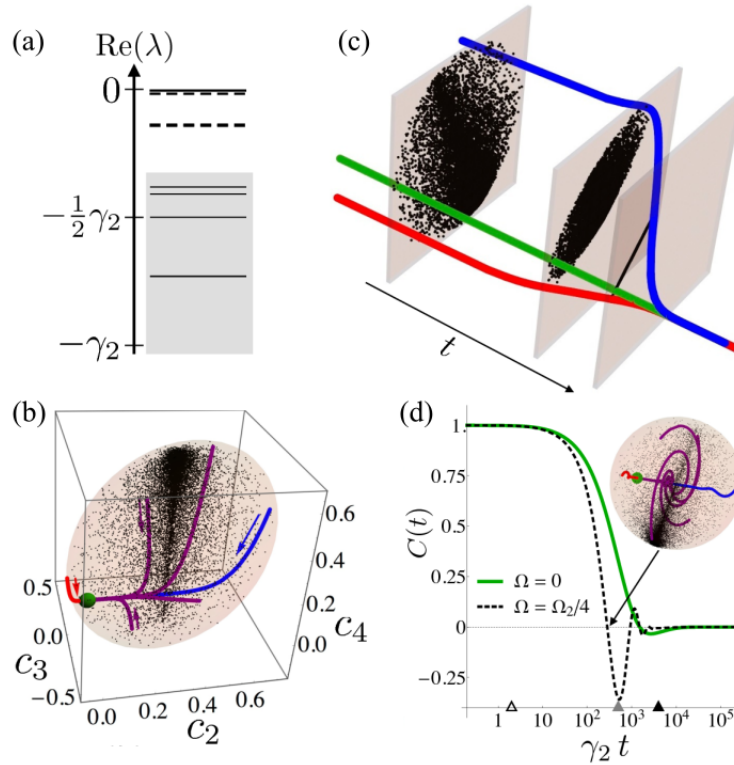


Figure 3.2: **Example of a coherent metastable manifold:** (a) Spectrum of \mathcal{L} for Example II ($\gamma_1 = 4\gamma_2$, $\Omega_1 = 2\Omega_2 = \gamma_2/50$). The first four eigenvalues ($m = 4$) split from the rest (shaded). (b) Dots representing the metastable states reached from random initial pure states map out an affinely transformed Bloch ball (shaded) and the MM is a qubit, see (3.8). The large dot (green) is ρ_{ss} ; curves indicate paths in the MM taken by the states evolving from the extreme eigenvectors of L_2 (red and blue), L_3 and L_4 (purple) towards ρ_{ss} . (c) Time evolution in the MM (affinely transformed to a Bloch ball): the MM contracts towards a one-dimensional simplex before relaxing eventually to ρ_{ss} , due to the splitting of between the first two eigenvalues and the next two, see (a). (d) Normalised auto-correlation $C(t)$ for $\sigma_1^z - \sigma_2^z$ (green/solid). Same for the case with an extra perturbing Hamiltonian $\Delta H = \Omega\sigma_1^x \otimes \sigma_2^x$ that induces a rotation in the MM, manifesting in oscillations of $C(t)$ during the metastable regime (black/dashed). This realises in a metastable system the proposal of [57, 58] for implementing unitary gates. This figure originally appeared in [196].

3.4.1.1 Spectrum of perturbed generator

Consider the dynamics $\mathcal{L}(x)$ with the Hamiltonian $H(x)$ and jumps operators $J_j(x)$, see Eq. (3.2). Let the Hamiltonian $H(x) =$

$H + \chi H^{(1)}$ and the jumps operators $J_j(\chi) = J_j + \chi J_j^{(1)}$ be linear perturbations of the Hamiltonian and jump operators of the degenerate dynamics \mathcal{L}_0 , where $H^{(1)}$ is Hermitian and χ is a dimensionless scale parameter. Results of this section can be easily generalised to the case of analytic perturbation $H(\chi)$, $J_j(\chi)$. The perturbed generator $\mathcal{L}(\chi)$ is then given by

$$\begin{aligned}\mathcal{L}(\chi) &= \mathcal{L}_0 + \chi \mathcal{L}^{(1)} + \chi^2 \mathcal{L}^{(2)}, \quad \text{where} \\ \mathcal{L}^{(1)} \rho &= -i[H^{(1)}, \rho] + \sum_j \left(J_j^{(1)} \rho J_j^\dagger - \frac{1}{2} \{ J_j^\dagger J_j^{(1)}, \rho \} + \text{h.c.} \right) \\ \mathcal{L}^{(2)} \rho &= \sum_j \left(J_j^{(1)} \rho J_j^{(1)\dagger} - \frac{1}{2} \{ J_j^{(1)\dagger} J_j^{(1)}, \rho \} \right),\end{aligned}\quad (3.25)$$

where we fix χ so that $\max(\|\mathcal{L}^{(1)}\|, \|\mathcal{L}^{(2)}\|) = \mathcal{O}(\tau_0^{-1})$, where τ_0 is the relaxation time in \mathcal{L}_0 dynamics (see Eqs. (3.27) and (3.28) for precise definition).

From the perturbation theory of linear operators [167] it is known that the perturbation of \mathcal{L}_0 changes its eigenvalues continuously with respect to χ . Therefore, when λ is an eigenvalue of \mathcal{L}_0 with algebraic multiplicity m , for χ small enough, m eigenvalues of $\mathcal{L}(\chi)$ cluster around the unperturbed value λ , and we refer to these eigenvalues as λ -group. Consider \mathcal{L}_0 with m -fold degeneracy of the stationary state manifold (SSM), cf. Eq. (3.3), and assume that $\text{Im} \lambda_k = 0$ for $k = 1, \dots, m$, so that there are no unitary rotations in the stationary state manifold. For χ small enough, the 0-group clusters around 0 and the separation to the $(m+1)$ -th eigenvalue is maintained, see Fig. 3.2 (a). Moreover, as both \mathcal{L}_0 and $\mathcal{L}(\chi)$ are completely positive trace-preserving (CPTP) generators and there are no Jordan blocks in 0-eigenspace of \mathcal{L}_0 , we show below that

$$\lambda_k(\chi) = \chi \lambda_k^{(1)} + \chi^2 \lambda_k^{(2)} + o\left(\chi^2 \left(\|\mathcal{L}^{(1)}\| + \|\mathcal{L}^{(2)}\|\right)\right), \quad k = 1, \dots, m, \quad (3.26)$$

where $\text{Re} \lambda_k^{(1)} = 0$ and $\text{Re} \lambda_k^{(2)} \leq 0$, so that the spectrum structure of a positive trace-preserving generator is reproduced in the second order. Eq. (3.26) follows from two facts: $\lambda_k^{(1)}$ being

an eigenvalue of $[\mathcal{L}^{(1)}]_{\mathcal{P}(x)}$ that is a unitary generator on the SSM, and $\lambda_k^{(2)}$ being an eigenvalue of a CPTP generator on the SSM.

Derivation. Although the eigenvalues of $\mathcal{L}(x)$ may not be analytic in x and projections on eigenmatrices may feature algebraic poles, projections onto subspace spanned by λ -groups are analytic [167]. In particular, the $\mathcal{P}(x)$ projection on the low-lying modes is analytic and it follows that restriction of $\mathcal{L}(x)$ to this subspace is analytic as well. In particular due to no-Jordan blocks in 0-eigenspace of \mathcal{L}_0 , we have that [167]

$$\mathcal{P}(x) = \mathcal{P}_0 + x \left(-\mathcal{S}\mathcal{L}^{(1)}\mathcal{P}_0 - \mathcal{P}_0\mathcal{L}^{(1)}\mathcal{S} \right) + \mathcal{O}(x^2) \quad (3.27)$$

$$=: \mathcal{P}_0 + x \mathcal{P}^{(1)} + \mathcal{O}(x^2),$$

$$[\mathcal{L}(x)]_{\mathcal{P}(x)} = x [\mathcal{L}^{(1)}]_{\mathcal{P}_0} + x^2 \left([\mathcal{L}^{(2)}]_{\mathcal{P}_0} - \mathcal{P}_0\mathcal{L}^{(1)}\mathcal{S}\mathcal{L}^{(1)}\mathcal{P}_0 + \quad (3.28)$$

$$-\mathcal{S}\mathcal{L}^{(1)}[\mathcal{L}^{(1)}]_{\mathcal{P}_0} - [\mathcal{L}^{(1)}]_{\mathcal{P}_0}\mathcal{L}^{(1)}\mathcal{S} \right) + \mathcal{O}(x^3(\|\mathcal{L}^{(1)}\| + \|\mathcal{L}^{(2)}\|))$$

$$=: x \tilde{\mathcal{L}}^{(1)} + x^2 \tilde{\mathcal{L}}^{(2)} + \mathcal{O}(x^3(\|\mathcal{L}^{(1)}\| + \|\mathcal{L}^{(2)}\|)),$$

where \mathcal{S} is the reduced resolvent of \mathcal{L}_0 at 0, i.e., $\mathcal{S}\mathcal{L}_0 = \mathcal{L}_0\mathcal{S} = \mathcal{I} - \mathcal{P}_0$ and $\mathcal{S}\mathcal{P}_0 = \mathcal{P}_0\mathcal{S} = 0$. Note that the resolvent \mathcal{S} is related to the relaxation time as $\|\mathcal{S}\| = \mathcal{O}(\tau_0)$, as for diagonalisable \mathcal{L}_0 we have $\mathcal{S}(\cdot) = \sum_{k>m} \lambda_k^{-1} \mathbf{R}_k \text{Tr}(\mathbf{L}_k \cdot)$. In Eqs. (3.27) and (3.28) for convenience we *define* the scale x of the perturbation in Eq. (3.25) so that $\max(\|\mathcal{L}^{(1)}\|, \|\mathcal{L}^{(2)}\|) = \|\mathcal{S}\|^{-1}$.

First-order perturbation. As we show in Appendix C.2.1, $\tilde{\mathcal{L}}^{(1)}$ is a CPTP generator on the SSM of \mathcal{L}_0 , and thus its eigenvalues have non-positive real parts. But $\mathcal{L}(-x)$ is a CPTP generator as well and its first-order correction $\tilde{\mathcal{L}}^{(1)}$ is of the opposite sign. Hence, $\tilde{\mathcal{L}}^{(1)}$ eigenvalues must be imaginary, which will correspond to coherent dynamics in the MM during the metastable regime. In [57, 58] it was shown that the first order indeed yields *unitary dynamics* and the corresponding Hamiltonian was derived, see also Fig. 3.2 (d).

Second-order perturbation. The generator $\tilde{\mathcal{L}}^{(1)}$ partially lifts degeneracy of the first m eigenvalues of \mathcal{L}_0 and the higher-order corrections should be considered separately for each eigenspace of $\tilde{\mathcal{L}}^{(1)}$ (cf. *reduction process* in [167]). Since the unitary generator $\tilde{\mathcal{L}}^{(1)}$ features only trivial Jordan blocks, for the eigenspace

\mathcal{P}_l related to its $\lambda_l^{(1)}$ eigenvalue, $l = 1, \dots, m''$, we obtain (cf. Eq. (3.28))

$$\mathcal{P}_l(x) = \mathcal{P}_l + x \left(-\mathcal{P}_l \mathcal{L}^{(1)} \mathcal{S} - \mathcal{S} \mathcal{L}^{(1)} \mathcal{P}_l - \mathcal{P}_l \tilde{\mathcal{L}}^{(2)} \tilde{\mathcal{S}}_l - \tilde{\mathcal{S}}_l \tilde{\mathcal{L}}^{(2)} \mathcal{P}_l \right) + \mathcal{O}(x^2), \quad (3.29)$$

$$[\mathcal{L}(x)]_{\mathcal{P}_l(x)} = x \lambda_l^{(1)} \mathcal{P}_l(x) + x^2 [\tilde{\mathcal{L}}^{(2)}]_{\mathcal{P}_l} + \mathcal{O}(x^3), \quad (3.30)$$

where $\tilde{\mathcal{S}}_l$ is the resolvent of $\tilde{\mathcal{L}}^{(1)}$ at $\lambda_l^{(1)}$ restricted to \mathcal{P}_0 , i.e., $\tilde{\mathcal{S}}_l (\tilde{\mathcal{L}}^{(1)} - \lambda_l^{(1)}) = (\tilde{\mathcal{L}}^{(1)} - \lambda_l^{(1)}) \tilde{\mathcal{S}}_l = \mathcal{P}_0 - \mathcal{P}_l$ and $\tilde{\mathcal{S}}_l \mathcal{P}_l = \mathcal{P}_l \tilde{\mathcal{S}}_l = 0^3$. From (3.30), the restriction of the second-order correction $\tilde{\mathcal{L}}^{(2)}$ to $\lambda_l^{(1)}$ eigenspace, $[\tilde{\mathcal{L}}^{(2)}]_{\mathcal{P}_l}$, further lifts degeneracy in 0-eigenspace of \mathcal{L}_0 . Therefore, the second-order corrections in 0-group eigenvalues are simply given by $x \lambda_l^{(1)} + x^2 \lambda_{l,j}^{(2)} + o(x^2)$, where $\{\lambda_{l,j}^{(2)}\}_j$ are eigenvalues of $[\tilde{\mathcal{L}}^{(2)}]_{\mathcal{P}_l}$, $l = 1, \dots, m''$. In order to argue $\text{Re} \lambda_{l,j}^{(2)} \leq 0$ and thus prove (3.26), we use the fact that $[\tilde{\mathcal{L}}^{(2)}]_{\mathcal{P}_0} = [\mathcal{L}^{(2)}]_{\mathcal{P}_0} - \mathcal{P}_0 \mathcal{L}^{(1)} \mathcal{S} \mathcal{L}^{(1)} \mathcal{P}_0$ is a CPTP generator on the SSM of \mathcal{L}_0 (see Appendix C.2.1) and

$$\sum_{l=1}^{m''} [\tilde{\mathcal{L}}^{(2)}]_{\mathcal{P}_l} = \lim_{t \rightarrow \infty} t^{-1} \int_0^t du e^{-u \tilde{\mathcal{L}}^{(1)}} [\tilde{\mathcal{L}}^{(2)}]_{\mathcal{P}_0} e^{u \tilde{\mathcal{L}}^{(1)}}. \quad (3.31)$$

The generator in (3.31) corresponds to first-order perturbation theory for weak dissipation, where the fast unitary evolution given by $\tilde{\mathcal{L}}^{(1)}$ erases all the contributions of the slow dissipation $[x \tilde{\mathcal{L}}^{(2)}]_{\mathcal{P}_0}$ that would create any coherence with respect to the Hamiltonian of $\tilde{\mathcal{L}}^{(1)}$, see also dynamics in the metastable regime below, see also Fig. 3.2 (d).

Finally, note that when the eigenvalues of $[\tilde{\mathcal{L}}^{(2)}]_{\mathcal{P}_l}$ are non-degenerate, the corresponding eigenvalues in 0-group of $\mathcal{L}(x)$ are analytic, and projections on the corresponding eigenmatrices are analytic as well.

³ Note that the first-order terms in $\mathcal{P}_l(x)$ – the projection on the $\lambda_l^{(1)}$ -group – correspond to the first-order perturbation of all the low-lying modes given by $\mathcal{P}^{(1)}$, and to the first-order perturbation of \mathcal{P}_l inside \mathcal{P}_0 due to $\tilde{\mathcal{L}}^{(1)} + x[\tilde{\mathcal{L}}^{(2)}]_{\mathcal{P}_0}$, respectively. Thus, as $\sum_{l=1}^{m''} \mathcal{P}_l = \mathcal{P}_0$, we recover $\sum_{l=1}^{m''} [\mathcal{L}(x)]_{\mathcal{P}_l(x)} = [\mathcal{L}(x)]_{\mathcal{P}(x)}$ up to $\mathcal{O}(x^3)$.

3.4.1.2 *Initial dynamics and metastable regime*

We now discuss how the perturbations in Eq. (3.25) change the system dynamics. We derive the metastable regime when the system dynamics appears stationary as a consequence of the separation in the $\mathcal{L}(x)$ spectrum discussed above. As in Eq. (3.6) we consider separately the low-lying modes with the projection $\mathcal{P}(x)$ and the rest of modes

$$e^{t\mathcal{L}(x)} = [e^{t\mathcal{L}(x)}]_{\mathcal{P}(x)} + [e^{t\mathcal{L}(x)}]_{\mathcal{J}-\mathcal{P}(x)}. \tag{3.32}$$

Initial relaxation timescale $\tau''(x)$. The metastable regime begins when the contribution from the fast decaying modes of the eigenvalues $\lambda_{m+1}(x), \lambda_{m+2}(x), \dots, \lambda_{d^2}(x)$, given by $[e^{t\mathcal{L}(x)}]_{\mathcal{J}-\mathcal{P}(x)}$ in (3.32), becomes negligible. When λ_{m+1} of \mathcal{L}_0 is non-degenerate, the perturbed eigenvalue $\lambda_{m+1}(x)$ is analytic in x ,

$$\lambda_{m+1}(x) = \lambda_{m+1} + x \text{Tr}(\mathbf{L}_{m+1} \mathcal{L}^{(1)} \mathbf{R}_{m+1}) + \mathcal{O}(x^2 \Delta_{m+1})$$

where $\Delta_k = \max(\|\mathcal{L}^{(2)}\|, \|\mathcal{L}^{(1)}\|^2 \|\mathcal{S}_k\|)$ with \mathcal{S}_k being the reduced resolvent of \mathcal{L}_0 at λ_k , cf. Eq. (3.28). When the system space dimension d is not too large, this implies that *initial relaxation timescale* $\tau''(x)$ is also analytic in x , $\tau''(x) \approx \lambda_{m+1}(x)^{-1} \approx \tau_0 - x \text{Tr}(\mathbf{L}_{m+1} \mathcal{L}^{(1)} \mathbf{R}_{m+1}) + \mathcal{O}(x^2 \Delta_{m+1})$. In fact, it can be shown in general that the choice

$$\tau''(x) = \tau_0, \tag{3.33}$$

leads to corrections $\mathcal{O}(x) + t\mathcal{O}(x^2 \|\mathcal{L}^{(1)}\|)$ in the metastable regime (see Appendix C.2.2 and corrections in Eq. (3.34)), thanks to $[e^{t\mathcal{L}(x)}]_{\mathcal{J}-\mathcal{P}(x)}$ being analytic in x , which is a consequence of both $e^{t\mathcal{L}(x)}$ and $\mathcal{J} - \mathcal{P}(x)$ being analytic in x , cf. Eqs. (3.25) and (3.27).

Unitary dynamics and final relaxation timescale $\tau'(x)$. The metastable manifold given by projection $\mathcal{P}(x)$ is mapped by the dynamics $[e^{t\mathcal{L}(x)}]_{\mathcal{P}(x)}$ into itself. By definition, the longer timescale $\tau'(x)$ of the metastable regime bounds from above time t when the system dynamics leaves the MM approximately invariant. As the first-order correction to the low-lying eigenvalues of

$\mathcal{L}(x)$, (3.26), corresponds to the unitary dynamics with generator $\tilde{\mathcal{L}}^{(1)}$, the timescale $\tau'(x)$ is necessary related to higher-order corrections in x . In Appendix C.2.3 we show that

$$\begin{aligned}
 [e^{t\mathcal{L}(x)}]_{\mathcal{P}(x)} &= e^{t\tilde{\mathcal{L}}^{(1)}}\mathcal{P}_0 + x \left(-\mathcal{S}\mathcal{L}^{(1)}e^{t\tilde{\mathcal{L}}^{(1)}}\mathcal{P}_0 - e^{t\tilde{\mathcal{L}}^{(1)}}\mathcal{P}_0\mathcal{L}^{(1)}\mathcal{S} \right) + \mathcal{O}(x^2) + \\
 &+ t x^2 e^{t\tilde{\mathcal{L}}^{(1)}} \left(t^{-1} \int_0^t du e^{-u\tilde{\mathcal{L}}^{(1)}} [\tilde{\mathcal{L}}^{(2)}]_{\mathcal{P}_0} e^{u\tilde{\mathcal{L}}^{(1)}} \right) + \\
 &+ t \mathcal{O}(x^3 \|\tilde{\mathcal{L}}^{(2)}\|) + t^2 \mathcal{O}(x^4 \|\tilde{\mathcal{L}}^{(2)}\|^2). \tag{3.34}
 \end{aligned}$$

where the corrections to the invariance of the MM are given by the second and third line representing the contribution from the dissipative dynamics in the interaction picture (see also Eq. (3.31)), whereas the first line describes unitary dynamics in the MM (cf. Eq. (3.27)). Thus, the metastable regime is limited to times t for which all the terms in the second and third line of (3.34) are small. As the second line is bounded by $tx^2\|\tilde{\mathcal{L}}^{(2)}\|$, this is satisfied for times $t \ll \tau'(x)$, where

$$\begin{aligned}
 \tau'(x) &= \left(x^{-2} + \mathcal{O}(x^{-1}) \right) \|\tilde{\mathcal{L}}^{(2)}\|^{-1} \\
 &\geq x^{-2} \mathcal{O}(\tau_0) + \mathcal{O}(x^{-1}\tau_0), \tag{3.35}
 \end{aligned}$$

We used Taylor expansion in the first line and $\|\tilde{\mathcal{L}}^{(2)}\| \leq \|\mathcal{L}^{(2)}\| + \|\mathcal{L}^{(1)}\|^2\|\mathcal{S}\|$, cf. Eq. (3.28), together with the definition of the scale x , $\max(\|\mathcal{L}^{(1)}\|, \|\mathcal{L}^{(2)}\|) = \|\mathcal{S}\|^{-1} = \mathcal{O}(\tau_0)^{-1}$, to conclude that $\|\tilde{\mathcal{L}}^{(2)}\| \leq \mathcal{O}(\tau_0)^{-1}$.

In order to find the timescale of approaching the stationary state ρ_{ss} at times $t \gg \tau(x)$, we need to consider effective dynamics $\mathcal{L}_{\text{eff}}(x) := [\mathcal{L}(x)]_{\mathcal{P}(x)}$ in the MM, see below.

No Jordan blocks in the metastable regime. Let us note that no matter whether there are Jordan blocks in the low-lying spectrum of $\mathcal{L}(x)$, they *do not contribute* in the metastable regime, cf. Eqs. (3.34), which motivates our assumption on the low-lying spectrum in the metastability theory for a general open dynamics as in Eq. (3.2).

3.4.1.3 Metastable manifold

We now consider projection of a system state during the metastable regime, $\tau''(x) \ll t \ll \tau'(x)$, onto the MM of low-lying modes, $\rho_{\text{MS}}(t) = \mathcal{P}(x)\rho(t)$. From (3.34) we find

$$\rho_{\text{MS}}(t) = e^{tx\tilde{\mathcal{L}}^{(1)}} \mathcal{P}_0 \rho_{\text{in}} + x \left(-\mathcal{S}\mathcal{L}^{(1)} e^{tx\tilde{\mathcal{L}}^{(1)}} \mathcal{P}_0 - e^{tx\tilde{\mathcal{L}}^{(1)}} \mathcal{P}_0 \mathcal{L}^{(1)} \mathcal{S} \right) + \mathcal{O}(x^2) \quad (3.36)$$

where the imaginary parts of the m low-lying eigenvalues appear in the (non-negligible) first order by means of the unitary dynamics $x\tilde{\mathcal{L}}^{(1)}$ within the MM, compare Eqs. (3.27) and (3.34). Therefore, as $\mathcal{O}(x \|\mathcal{S}\| \|\mathcal{L}^{(1)}\|) = \mathcal{O}(x)$, we have that metastable states are approximately given by a general structure of a manifold of stationary states of open quantum Markovian dynamics [199],

$$\rho_{\text{MS}}(t) = \mathcal{O}_{\mathcal{H}_0} \oplus \bigoplus_{l=1}^{m'} p_l \tilde{\rho}_l \otimes \mathcal{U}_l(\omega_l) + \mathcal{O}(x), \quad (3.37)$$

with \mathcal{H} being the orthogonal sum $\mathcal{H} = \mathcal{H}_0 \oplus \bigoplus_l \mathcal{H}_l \otimes \mathcal{K}_l$, where \mathcal{H}_0 is the decay subspace, $\tilde{\rho}_l$ are fixed states on \mathcal{H}_l (cf. eMS in classical dynamics and the case of $m = 2$), ω_l are arbitrary states on \mathcal{K}_l (representing a DFS/NSS), and p_l are probabilities. Time dependence $\rho_{\text{MS}}(t)$ during the metastable regime is due to the unitary dynamics \mathcal{U}_l inside a DFS/NSS of \mathcal{K}_l , given by $\mathcal{U}_l := \mathbb{1}_{\mathcal{K}_l} e^{tx\tilde{\mathcal{L}}^{(1)}} \mathbb{1}_{\mathcal{K}_l}$, see Fig. 3.2 (b,d), and there is no dynamics for classical case of $\dim(\mathcal{K}_l) = 1$.

Furthermore, let us note the correction in (3.37) is of the same order as the dissipative *corrections to invariance of the MM*, for times $t = \mathcal{O}(x(\|\mathcal{L}^{(1)}\| + \|\mathcal{L}^{(2)}\|)^{-1}) = \mathcal{O}(x^{-1}\tau_0)$ within the metastable regime $\tau''(x) \ll t \ll \tau'(x)$, see Eq. (3.34).

Coefficients of the MM. Note when $\dim(\mathcal{K}_l) = 1$, the l -th block is a disjoint eMS. It is known for classical systems the MM is always approximately a simplex of m disjoint eMSs [51] with probabilities corresponding *classical degrees of freedom*. In quantum open systems this is the case for $m = 2$, where there are two eMSs, $\tilde{\rho}_{1,2}$, with metastable states being mixtures of them.

For class A systems we have that, when $\dim(\mathcal{K}_l) > 1$, ω_l inside a DFS/NSS represents *quantum degrees of freedom* (ω_l), which do not appear in the case of classical dynamics [51]. This is the case in Example II where the MM is a qubit. In general the number of blocks in Eq. (3.37) is $m' \leq m$, with equality occurring only when there are no DFS or NSS. As we show below the $(m-1)$ coefficients (c'_2, \dots, c'_m) that determine ρ_{MS} , see Eq. (3.8), correspond approximately to an *affine transformation* of the m entries of $p_l \omega_l$ ($l = 1, \dots, m'$) in Eq. (3.37), where $\sum_{l=1}^{m'} p_l = 1$. Therefore, the MM approximately represents the degrees of freedom of the classical-quantum space in Eq. (3.37).

Consider the generic case of degeneracy of the first m eigenvalues of \mathcal{L}_0 being lifted in the second-order perturbation theory. In this case the projections on the individual eigenmatrices of \mathcal{L}_0 are analytic and in the 0-th order simply given by projections on the $[\tilde{\mathcal{L}}^{(2)}]_{\mathcal{P}_l}$ eigenspaces, $l = 1, \dots, m''$, where \mathcal{P}_l is a projection on an $\tilde{\mathcal{L}}^{(1)}$ eigenspace. As for a left eigenmatrix $L_{l,j}$ of $[\tilde{\mathcal{L}}^{(2)}]_{\mathcal{P}_l}$ corresponding to an eigenvalue $\lambda_{l,j}^{(2)}$, we have that the left $\mathcal{L}(x)$ eigenmatrix $L_{l,j}(x) \propto L_{l,j} \mathcal{P}_{l,j}(x)$ is analytic in x . When it is further normalised in the spectral norm, or rescaled by the difference of its extreme eigenvalues, thanks to Hermitian perturbation theory for $L_{l,j}(x)$, the coefficient $c'_{l,j}(x) = \text{Tr}(L_{l,j}(x) \rho_{in})$ can be expressed as a series in x (see Appendix C.2.4 for details).

Therefore, for x small enough, the set of coefficients representing the MM is well approximated by the image of an *affine transformation* of the $(m-1)$ degrees of freedom describing the SSM of \mathcal{L}_0 , i.e., the entries of $p_l \omega_l$, $l = 1, \dots, m'$ with $\sum_{l=1}^{m'} p_l = 1$, see Fig. 3.2 (b). This affine transformation is determined by the invertible linear transformation from the basis of the SSM of the entries in $p_l \omega_l$, $l = 1, \dots, m'$, to the right eigenmatrices, $\{R_{l,j}\}_j$, of $[\tilde{\mathcal{L}}^{(2)}]_{\mathcal{P}_l}$, for $l = 1, \dots, m''$, see Fig. 3.2 (b-c).

3.4.1.4 Effective dynamics in metastable manifolds

During the metastable regime the dynamics is approximated by unitary transformation of the MM with generator $\tilde{\mathcal{L}}^{(1)}$, see

Eq. (3.36). For times following the metastable regime, $\tau'(x) \lesssim t \ll x^{-1} \tau'(x) = x^{-3} \mathcal{O}(\tau_0)$, we show in Appendix C.2.5 that effective dynamics in the MM is dissipative and characterised by a CPTP generator on the SSM of \mathcal{L}_0 ,

$$\tilde{\mathcal{L}}(x) := x\tilde{\mathcal{L}}^{(1)} + x^2[\tilde{\mathcal{L}}^{(2)}]_{\mathcal{P}_0}, \quad (3.38)$$

as follows

$$\begin{aligned} [e^{t\tilde{\mathcal{L}}(x)}]_{\mathcal{P}(x)} &= e^{t\tilde{\mathcal{L}}(x)}\mathcal{P}_0 + x \left(-\mathcal{S}\tilde{\mathcal{L}}^{(1)} e^{t\tilde{\mathcal{L}}(x)}\mathcal{P}_0 - e^{t\tilde{\mathcal{L}}(x)}\mathcal{P}_0\tilde{\mathcal{L}}^{(1)}\mathcal{S} \right) + \\ &+ \mathcal{O}(x^2) + t \mathcal{O}(x^3\tau_0^{-1}), \end{aligned} \quad (3.39)$$

see Fig. 3.2 (c). Note that $\|\mathcal{L}_{\text{eff}}(x) - \tilde{\mathcal{L}}(x)\| = \mathcal{O}(x^2\|\tilde{\mathcal{L}}^{(1)}\|)$, see Eq. (3.28), which may seem puzzling when there is non-trivial coherent dynamics during metastable regime, $\tilde{\mathcal{L}}^{(1)} \neq 0$. It follows, however, from Eqs. (3.29-3.30) that this order of the difference is due to first-order corrections outside \mathcal{P}_0 to the eigenspaces of $\tilde{\mathcal{L}}^{(1)}$, represented by the projections $\{\mathcal{P}_l(x)\}_{l=1}^{m''}$, not the difference between the eigenvalues of $\mathcal{L}_{\text{eff}}(x)$ and $\tilde{\mathcal{L}}(x)$, which is of a higher order $\mathcal{O}(x^2(\|\mathcal{L}^{(1)}\| + \|\mathcal{L}^{(2)}\|))$, cf. Eq. (3.26). Therefore, the order $\mathcal{O}(x^2\|\tilde{\mathcal{L}}^{(1)}\|)$ of corrections above, *does not determine* the postmetastable regime when $\tilde{\mathcal{L}}(x)$ is a valid approximation for long-time dynamics⁴ (for details see derivation in Appendix C.2.5). Dynamics generated in the SSM by $\tilde{\mathcal{L}}(x)$ was previously discussed in [206] for the case of a Hamiltonian perturbation and $\tilde{\mathcal{L}}^{(1)} = 0$, cf. Eq. (3.25).

Let us comment on the relation between $\tilde{\mathcal{L}}(x)$ above and the interaction picture appearing in (3.31) and (3.34). Again, the difference in eigenvalues of those two generators is of the higher order $\mathcal{O}(x^2(\|\mathcal{L}^{(1)}\| + \|\mathcal{L}^{(2)}\|))$, so that $\tilde{\mathcal{L}}(x)$ can be replaced by $\tilde{\mathcal{L}}^{(1)} + \sum_{l=1}^{m''} [\tilde{\mathcal{L}}^{(2)}]_{\mathcal{P}_l}$ in Eq. (3.39).

Finally, note that from the fact that $\mathcal{L}(x)$ is trace-preserving, it follows that it features the left eigenmatrix $\mathbb{1}_{\mathcal{H}}$ corresponding to 0-eigenvalue, which, by construction, also holds true for

⁴ When corrections in the eigenvalues are considered with respect to the analytic operator $\mathcal{L}_{\text{eff}}(x) - \tilde{\mathcal{L}}(x)$, they contribute as $\mathcal{L}_{\text{eff}}(x) - x \sum_{l=1}^{m''} \lambda_l^{(1)} \mathcal{P}_l(x)$, which is of the order $\mathcal{O}(x^3(\|\mathcal{L}^{(1)}\| + \|\mathcal{L}^{(2)}\|)) = \mathcal{O}(x^3\tau_0^{-1})$, see Eq. (3.30), which determines the bound where Eq. (3.39) is valid.

$\mathcal{L}_{\text{eff}}(\chi) = [\mathcal{L}(\chi)]_{\mathcal{P}(\chi)}$. Therefore, together with (3.39) it implies that long-time effective dynamics in the MM is trace-preserving and approximately completely-positive. This is a consequence of the effective motion preserving the structure of Eq. (3.37). Note that decoupling of (slower) classical dynamics from (faster) quantum evolution in the MM requires further separation in low-lying eigenvalues of $\mathcal{L}(\chi)$. This is illustrated in Fig. 3.2 (c) for Example II.

Stationary state. We note that a stationary state of the dynamics perturbed away from the degeneracy has been studied in [199]. In the case when the degeneracy of the stationary state is lifted in the second order of the perturbation theory, we have that (cf. Eq. (3.29))

$$\begin{aligned} \rho_{\text{ss}}(\chi) &= \rho_{\text{ss}} + \chi \left(-\mathcal{S} \mathcal{L}^{(1)} \rho_{\text{ss}} - \tilde{\mathcal{S}}_1 \tilde{\mathcal{L}}^{(2)} \rho_{\text{ss}} - \tilde{\mathcal{S}}_{1,1} \tilde{\mathcal{L}}_1^{(3)} \rho_{\text{ss}} \right) + \mathcal{O}(\chi^2), \\ \text{Tr} \rho_{\text{ss}}(\chi) &= 1 + \mathcal{O}(\chi^2), \end{aligned} \quad (3.40)$$

where ρ_{ss} is the unique stationary state of the generator in Eq. (3.31), so that the corresponding eigenvalues $\lambda_1^{(1)} = 0$ and $\lambda_{1,1}^{(2)} = 0$. The linear corrections in $\rho_{\text{ss}}(\chi)$ depend on the way the degeneracy in 0-eigenvalue of \mathcal{L}_0 is lifted, and the three terms represent following contributions. The first term is due to the first-order perturbation of low-lying modes given by $\mathcal{P}^{(1)}$ in (3.27). The second one is a result of the first-order perturbation of 0-eigenspace of $\tilde{\mathcal{L}}^{(1)}$ by $\chi[\tilde{\mathcal{L}}^{(2)}]_{\mathcal{P}_0}$, cf. $\tilde{\mathcal{L}}(\chi)$ above, where $\tilde{\mathcal{S}}_1$ denotes the reduced resolvent of $\tilde{\mathcal{L}}^{(1)}$ at $\lambda_1^{(1)} = 0$ inside \mathcal{P}_0 . Finally, the third term is a linear correction to the 0-eigenmatrix of $[\tilde{\mathcal{L}}^{(2)}]_{\mathcal{P}_1}$ perturbed by the third-order correction in $[\mathcal{L}(\chi)]_{\mathcal{P}_1(\chi)}$ (see Eq. (C.16)), where \mathcal{P}_1 is the projection on the 0-eigenspace of $\tilde{\mathcal{L}}^{(1)}$ and $\tilde{\mathcal{S}}_{1,1}$ denotes the resolvent of $[\tilde{\mathcal{L}}^{(2)}]_{\mathcal{P}_1}$ at $\lambda_{1,1}^{(2)} = 0$ restricted to \mathcal{P}_1 . Therefore, considering analogously the first and third correction for the stationary state of $\tilde{\mathcal{L}}(\chi)$, one obtains $\rho_{\text{ss}}(\chi)$ up to $\mathcal{O}(\chi^2)$. The normalisation of $\rho_{\text{ss}}(\chi)$ follows directly from orthonormality of right and left eigenmatrices of the generator in Eq. (3.31), and $L_{1,1} = \mathbb{1}_{\mathcal{H}}$.

Timescale $\tau(x)$. Let us recall that negative real parts of the low-lying spectrum are recovered in the second order of perturbation theory, cf. Eq. (3.26), and are given by the generator $\sum_{l=1}^{m''} [\tilde{\mathcal{L}}^{(2)}]_{\mathcal{P}_l}$, see Eqs. (3.31,3.34,3.39). Therefore, when the degeneracy of the stationary state is lifted in the second order, the timescale $\tau(x)$ can be approximated by

$$\tau(x) = x^{-2} \left\| \tilde{\mathcal{S}} \right\|, \quad (3.41)$$

where $\tilde{\mathcal{S}}$ is the resolvent for $\sum_{l=1}^{m''} [\tilde{\mathcal{L}}^{(2)}]_{\mathcal{P}_l}$ at 0, i.e., $\tilde{\mathcal{S}} = \sum_{l=1}^{m''} \tilde{\mathcal{S}}_{l,0}$ with $\mathcal{S}_{l,0}$ being the resolvent for $[\tilde{\mathcal{L}}^{(2)}]_{\mathcal{P}_l}$ at 0.

Metastability and oscillations in system measurements. For systems in class A, in the metastable regime, $\tau''(x) \ll t \ll \tau'(x)$, metastable states appear stationary or perhaps rotate within the MM which is then solely a consequence of coherent motion in a DFS/NSS where the matrices ω_l of Eq. (3.37) evolve unitarily in time, see also [57, 58]. In the latter case oscillations of correlations in a system observable, $C(t)$ in (3.10), can occur during the metastable regime. Furthermore, in the case of no oscillations in the metastable regime, those can be induced by additionally perturbing the MM with a scale y , cf. (3.25), such that $1 \gg y \gg x^2$ so that the almost degenerate perturbation theory applies to the perturbed low-lying modes, see Fig. 3.2 (d). Hence, (approximately) unitary gates can be applied to the quantum degrees of freedom in the MM, thus making it useful for quantum computation, analogously to degenerate SSMS in proposals of [57, 58]. For times after the metastable regime, when $t \gtrsim \tau'(x)$, evolution follows approximately CPTP dynamics towards $\rho_{ss}(x)$ and the correlations decay as a sum of exponential contributions, see Fig. 3.2 (d).

3.4.2 Metastability in class B systems

So far we have discussed metastability in systems of a finite size that can feature degenerate stationary manifold for some

parameter values in the master equation, $\mathcal{L} = \mathcal{L}_0$. Now we will focus on scalable systems of size N in which the gap may close only in the thermodynamic limit $N \rightarrow \infty$, i.e., due to the structures of interactions in the system and the dissipation, the system evolution is *irreducible* and features a unique stationary state for any finite N . In this chapter we refer to those dynamics as class B.

The choice to limit ourselves to class B systems is motivated by a question important for classical and quantum Statistical Physics, mainly, what is the structure of metastable states emerging due to collective effects. In classical systems, collective metastable behaviour typically occurs in two distinct situations. The first one is in the dynamics near a usually first-order static phase transition, where metastable dynamics is intimately related to the existence of static phases in the thermodynamic limit, although the transition is avoided either through finite size or due to other kind of fluctuations [197]. The second one is in glass forming systems [54] where metastable behaviour is not obviously related to any static features (see e.g. [55] for various viewpoints). The results by B. Gaveau and L. S. Schulman [47, 48, 51, 201] show that for classical systems whose dynamics can be described by a stochastic master equation, the structure of metastable states is analogous to that of a first-order phase transition, i.e., metastable states are probabilistic mixtures of approximately disjoint metastable phases, see Sec. 3.1.2.

Conjecture for class B systems. For the case of $m = 2$ low-lying modes, also in open quantum systems with dynamics governed by a master equation (3.2), both the metastable manifold and the long-time dynamics are necessary classical, see results in Sec. 3.3 and [36, 172]. On the other hand, from perturbative calculations for finite open quantum systems of class A in Sec. 3.4.1, we know that the manifold of metastable states must in general include disjoint states, noiseless subsystems and decoherence-free subspaces, cf. Eq. (3.37). Therefore, for class B we *conjecture* that the coefficients representing the MM approach degrees of freedom of a classical-quantum space as in

Eq. (3.37), as the separation in the spectrum becomes more and more pronounced when $N \rightarrow \infty$. Note that when the dimensionality of the MM does not change with N , the convergence is well defined. In particular, when a first-order transition occurs in the thermodynamic limit, we expect its structure to be resembled by the metastable manifold of a finite-size system, for dynamics close in parameters to those at which the transition is present. We note, however, that the general structure of first-order phase transition in open quantum systems described by (3.2) is not known [207–209]. Our general conjecture is based on the *necessary condition* that the low-lying spectrum of \mathcal{L} features only trivial Jordan blocks or they do not significantly contribute in the metastable regime, so that Eq. (3.7) holds true with appropriately redefined corrections⁵.

Note that a conjecture of the ρ_{MS} structure being approximately that of stationary states, cf. Eq. (3.37) with disjoint subspaces $\mathcal{H}_1 \otimes \mathcal{K}_1$ and protected subsystems \mathcal{K}_1 , is a stronger claim. Proof of both conjectures for class B appear challenging at this moment, as we explain below.

Note that the convex analysis tools used in the classical proof of [48, 51] (see also Sec. 3.1.2) cannot be used for the quantum case as they rely on the finite number d of system configurations. Note, however, that by using *any* tools of convex analysis for the MM represented by the set of coefficients (c_2, \dots, c_m) , and exploiting (approximate) positivity of the metastable states, one could at most prove the structure of fixed points of positive (cf. completely positive) maps, which is richer than Eq. (3.3), see e.g. [210]. For example, for the degeneracy $m = 3$ of the manifold of fixed points there can exist non-commuting metastable states represented by 2×2 real Hermitian matrices [210], in contrast to $m \geq 4$ required for a smallest DFS/NSS of a qubit, cf. Fig. 3.2 (a-b). In order to exploit complete positivity one would need to work with the dynamics extended to $e^{t\mathcal{L}} \otimes \mathcal{J}_{\mathcal{B}(\mathcal{H})}$, which has $m \times d^2$ low-lying eigenvalues and thus the simplicity of the geometric representation of the MM is lost.

⁵ Non-trivial Jordan blocks would lead to an unbounded norm of $\rho(t)$ when gap $\rightarrow 0$ in the thermodynamic limit [158].

For the latter conjecture determining also the structure of the extreme metastable states, cf. $\tilde{\rho}_1$ in (3.37), the difficulty lies in the fact that the existing proofs of the SSM structure [158, 199] rely on the property that left eigenmatrices corresponding to strictly zero eigenvalue of a CPTP generator \mathcal{L}_0 (or the eigenvalue 1 of a CPTP quantum channel) form a von-Neumann algebra and thus stationary states are of the form given in Eq. (3.3). We cannot rely on the algebra structure of metastable states as for states e.g. with approximately the block structure, this structure will not be preserved with the same approximation for products of them. This corresponds to the corrections to complete positivity of the dynamics (of the same order as the corrections to the stationarity, cf. Eq. (3.7) being progressively accumulated with each multiplication of the eigenmatrices (cf. the proof of the SSM structure in [158]). It is likely one could use a proof such as in [211] deriving Eq. (3.7) by exploiting properties of a projection \mathcal{P}_0 on the SSM, without its multiple applications, so that corrections do not accumulate. Finally, note that such a proof would not exploit the existence of the thermodynamic limit and the quantum-classical structure of Eq. (3.37) would be valid for any open quantum system with the separation in the master operator spectrum being pronounced enough.

Quantum degrees of freedom in the thermodynamic limit and self-correcting topological memories. One can ask whether the quantum structures could occur only due to collective effects in a quantum open systems without underlying symmetry protecting part of the Hilbert space from noise also at a finite size [205]. Is the manifold always classical [36, 172]? To argue the converse, let us recall topological quantum memories, such as Kitaev's code [212], in which a ground state of the system Hamiltonian is degenerate due to topological properties of the system, (for Kitaev's code on a torus, it corresponds to two qubits). In the presence of dissipation, however, the system of a finite size features only single stationary state, but error-correction techniques can be employed to eliminate local errors occurring with frequency under certain threshold ($< 11\%$ for Kitaev's code) so

that the quantum state stored in the ground space of the Hamiltonian is protected. In it is possible to achieve a self-correcting code in 4 dimensions, where the errors are suppressed exponentially in the system size by the Hamiltonian itself, thus providing an example of quantum degrees of freedom featuring in a first-order phase transition appearing only in the thermodynamic limit.

Glassy quantum memories. Metastable behaviour is most prominent in glasses where relaxation times diverge as temperature going to zero, which is widely exploited in glass products made of fastly cooled liquid. There is no obvious transition, however, in the equilibrium state of those systems [54]. For various models both the dimensionality of the metastable manifold (e.g. longest-lived states in the hierarchy $\sim N$) and the relaxation time ($\sim \log(N)$) grows with the system size N [213]. Therefore, it is promising to investigate quantum analogues of glassy models, such as East model or FA model, where not only classical degrees of freedom [35, 193], but also quantum coherences can be long-lived [214]. Finding even richer than classical collective dynamics and possibly glassy DFSs/NSSs would pave a way for a new class of quantum memories.

3.5 SUMMARY AND OUTLOOK

In this chapter we established basics of the metastability theory for Markovian open quantum systems [196] by generalising methods for classical stochastic dynamics [48, 51]. We showed how to construct a low-dimensional description of the metastable manifold by exploiting the separation in the spectrum of the Markovian generator. We further argued how the experimentally observable two-step decay of time correlation functions of system observables corresponds to effective long-time dynamics within the MM. For the case of two low-lying eigenvalues we derived the classical structure of the MM consisting of two approximately disjoint metastable phases, where the effective long-time dynamics corresponds to intermittent dynamics

of quantum trajectories. For general case, based on perturbative calculations for systems with degenerate stationary state, we argued that the MM includes disjoint states, noiseless subsystems, and decoherence-free subspaces and formulated a general conjecture.

Let us briefly propose how using the low-dimensional representation of metastable states for a given system dynamics, in Eq. (3.8), the structure of MM can be unfolded for a given model. Those methods will be extended in future work.

Classical MMs. The classical structure of the MM corresponds to the set of coefficients being approximately a simplex. Therefore, for given dynamics, one could construct a simplex inside the MM that gives the maximum volume and check whether the MM is well approximated as probabilistic mixtures of its vortices. Such a simplex could be constructed from a subset of the coefficients corresponding to the initial states chosen as extreme eigenvectors of the low-lying left eigenmatrices, L_2, \dots, L_m . Furthermore, as the effective dynamics maps the MM into itself, for a classical MM, the effective generator \mathcal{L}_{eff} will correspond to classical stochastic transitions between m metastable phases represented by the simplex vertices, which can be understood as coarse-graining in time of continuous measurement records, exactly as in the case of $m = 2$ in Sec. 3.3.

Coherences in the MM. As discussed in Sec. 3.4.1, perturbing a stationary state manifold that features a DFS or a NSS, may result in coherent oscillations with frequency of the lower order in the perturbation, than the destructive decay of coherences. This corresponds to rotations within the MM during the metastable regime. Therefore, by considering time-averaging of metastable states over the metastable regime, such oscillating coherences can be approximately discarded, which in general reduces the MM solely to classical degrees of freedom that could be further analysed by the former method. For a general case of Markovian dynamics displaying metastability which is not classical, one could consider introducing a random Hamiltonian perturbation in order to mix the low-lying eigenmodes and possibly

induce coherent oscillations.

Metastability in non-Markovian dynamics. We have considered the Lindblad generator with a separation in the spectrum which leads to a metastable regime in the system dynamics. It should be possible to extend our approach to the case of non-Markovian dynamics. In particular, one can formulate non-Markovian evolution in terms of a the time-dependent master equation $\mathcal{L}(t)$, cf. Eq. (3.2), where the system Hamiltonian and the rates of jumps in the master equation are time-dependent (and not necessarily positive at all times).

In the non-Markovian case, despite the non-positive rates, the system evolution \mathcal{T}^t from an initial state to the state at any time t is completely positive (in the Markovian case $\mathcal{T}^t = e^{t\mathcal{L}}$). For a given time t one can consider the spectrum of \mathcal{T}^t in order to identify how many modes contribute to the system state for any initial state, in particular, whether the system state can be described by the reduced number of degrees of freedom $m < d^2$, in analogy with how we define the metastable manifold. We expect that with appropriate conditions on the time-dependence of the master equation, $\mathcal{L}(t)$, a metastable regime could thus be determined. There is an important difference to the Markovian case, as non-Markovian evolution after such a metastable regime could take place outside the metastable manifold, for example when some of the lost coherences are recovered (due to information backflow from the environment).

Interestingly, in [215], metastability for one specific model has been derived from the full Hamiltonian dynamics of the system and an environment.

Metastability in closed systems. A significant challenge is to extend the ideas presented here to study metastability in closed quantum systems. By this we understand conditions under which dynamics of a subsystem in a closed quantum system is metastable. Possible directions here include considering: quantum analogues of classical chaotic systems whose dynamics can be described effectively by a master operator, and quantum sys-

tems with almost degenerate gaps, e.g. due to a perturbation. Results on metastability in closed systems would be relevant to the fundamental problems of thermalisation [185] and many-body localisation [188].

Part III

APPENDIX

A

APPENDIX TO CHAPTER 1

In this appendix we provide a proof for the iterative alternating algorithm introduced in Sec. 1.2, and derivation of the bounds for quantum parameter estimation in the presence of correlated Gaussian dephasing, see Sec. 1.3.

A.1 PROOF OF THE CONVERGENCE OF ITERATIVE ALTERNATING ALGORITHM

We assume $F_\phi^{(\max)}$ to be finite, so the increasing sequence $f_\phi^{(n)} := F_\phi(\rho_\phi^{(n)})$ is bounded from above and therefore converges to a limit f_ϕ^* .

Proof. First, we prove that if the algorithm gets stuck, i.e., $F_\phi(\rho, D_{\rho_\phi}) = F_\phi(\rho', D_{\rho_\phi})$, where $\rho' = |\psi\rangle\langle\psi|$ is chosen as the pure state corresponding to the maximum eigenvalue of $G_\phi(D_{\rho_\phi})$, it follows that ρ is the optimal initial preparation achieving the maximum quantum Fisher information, $F_\phi(\rho_\phi) = F_\phi^{(\max)}$.

Note that we have $F(\rho, D_{\rho_\phi}) = F(\rho', D_{\rho_\phi})$ imposes $\rho = \rho'$, when the maximal eigenvalue eigenspace of $\Lambda^\dagger(G(D_{\rho_\phi}))$ is non-degenerate. For now we assume that the choice of ρ is unique at all the steps of the algorithm (see discussion after the proof). Using this fact we prove now that ρ corresponds to the maxi-

mum, i.e., $F_\phi(\rho_\phi) = F_\phi^{(\max)}$. From the definition of $F_\phi(\rho, X)$ in Eq. (1.23) it follows that

$$\begin{aligned}
F_\phi(\rho + \delta\rho, D_{\rho_\phi} + \delta X) &= \\
&= -\text{Tr}\left((\rho + \delta\rho) \Lambda_\phi^\dagger((D_{\rho_\phi} + \delta X)^2)\right) + 2\text{Tr}\left((\rho + \delta\rho) (\partial_\phi \Lambda_\phi)^\dagger (D_{\rho_\phi} + \delta X)\right) \\
&= -\text{Tr}\left((\rho + \delta\rho) \Lambda_\phi^\dagger(D_{\rho_\phi})\right) + 2\text{Tr}\left((\rho + \delta\rho) (\partial_\phi \Lambda_\phi)^\dagger (D_{\rho_\phi})\right) + \\
&\quad -\text{Tr}\left((\rho + \delta\rho) \Lambda_\phi^\dagger(\{D_{\rho_\phi}, \delta X\})\right) - \text{Tr}\left((\rho + \delta\rho) \Lambda_\phi^\dagger((\delta X)^2)\right) + \\
&\quad + 2\text{Tr}\left(\rho (\partial_\phi \Lambda_\phi)^\dagger(\delta X)\right) + 2\text{Tr}\left(\delta\rho (\partial_\phi \Lambda_\phi)^\dagger(\delta X)\right) \\
&= F_\phi(\rho + \delta\rho, D_{\rho_\phi}) + \mathcal{O}\left(\delta X^2, \delta X \delta\rho \left(\|\partial_\phi \Lambda_\phi\| + \|\Lambda_\phi^\dagger(D_{\rho_\phi})\|\right)\right), \\
&< F_\phi(\rho, D_{\rho_\phi}) + \mathcal{O}\left(\delta X^2, \delta X \delta\rho \left(\|\partial_\phi \Lambda_\phi\| + \|\Lambda_\phi^\dagger(D_{\rho_\phi})\|\right)\right),
\end{aligned}$$

where the inequality follows from ρ being the optimal initial state for $X = D_{\rho_\phi}$. Since $F_\phi(\rho, X)$ is concave w.r.t. to the convex set (ρ, X) , the above inequality implies that $F_\phi(\rho, D_{\rho_\phi})$ is the global maximum $F_\phi^{(\max)}$. Note that for this argument it is enough that there exists an open convex neighbourhood around (ρ, D_{ρ_ϕ}) , note necessary that the considered set of initial states and the observables are convex.

Secondly, consider the case when the algorithm gets stuck, i.e., $f_\phi^{(n)} = F_\phi(\rho^{(n)}, D_{\rho_\phi^{(n)}}) = F_\phi(\rho^{(n+1)}, D_{\rho_\phi^{(n)}})$. We have $f_\phi^{(n)} = F_\phi(\rho^{(n+1)}, D_{\rho_\phi^{(n+1)}}) = f_\phi^{(n+1)}$ and we have arrived at the maximum F^Q , thus ending the proof for this case.

Consider the opposite case in which $f_\phi^{(n)} < f_\phi^{(n+1)}$ for all $n = 1, 2, \dots$ (which requires $F_\phi(\rho^{(n)}, D_{\rho_\phi^{(n)}}) \neq F_\phi(\rho^{(n+1)}, D_{\rho_\phi^{(n)}})$). We assume that the dimension of the system Hilbert \mathcal{H} space is finite from now on. As $\rho^{(n)}$ belong to the set of density matrices, which is compact for a system of a finite dimension, one can choose a convergent subsequence $\{\rho^{(n_m)}\}_{m=1}^\infty$; let ρ^* denote the limit of this subsequence. We further assume that D_{ρ_ϕ} is continuous w.r.t. ρ , then, together with the continuity of $F_\phi(\rho, X)$ w.r.t. (ρ, X) , it implies $F(\rho^*, D_{\rho_\phi^*}) = \lim_{m \rightarrow \infty} F(\rho^{(n_m)}, D_{\rho_\phi^{(n_m)}}) = f_\phi^*$. The eigenvector ρ^* corresponding to the maximum eigenvalue of $G_\phi(D_{\rho_\phi^*})$ is the limit of the shifted subsequence $\{\rho^{(n_m+1)}\}_{m \in \mathbb{N}}$

and thus $\rho'^* = \rho^*$. Therefore, if $G_\phi(D_{\rho_\phi^*})$ has a unique state corresponding to the maximal eigenvalue, we obtain $f_\phi^* = F_\phi(\rho^*, D_{\rho_\phi^*}) = F_\phi^{(\max)}$ according to the first part of the proof.

Therefore, we have proved the convergence to the maximum, i.e., $f_\phi^* = F_\phi^{(\max)}$, as long as, at each step the choice of $\rho^{(n)}$ is unique (see the discussion below). ■

The above proof is based on the Chapter 10.3 in [216], where a proof of convergence is presented for an alternating algorithm in the case of $\sup_{u_1 \in A_1} \sup_{u_2 \in A_2} f(u_1, u_2)$, where f is a strictly concave real-valued function and A_k is a compact and convex subset of \mathbb{R}^{n_k} , $k = 1, 2$. In our case the function $F_\phi(\rho, X)$ is linear w.r.t. ρ and strictly concave w.r.t. X .

Unique choices in the algorithm. As stated above, the unique choice of $\rho^{(n)}$ at each step is crucial, as we show below it is related to unique choice of $D_{\rho_\phi^{(n-1)}}$ in the preceding step. For simplicity we consider here the case of phase encoding commuting with noise, so that $\Lambda_\phi(\rho) = e^{-i\phi H} \Lambda(\rho) e^{i\phi H} = \Lambda(e^{-i\phi H} \rho e^{i\phi H})$, or unitary dynamics.

D_{ρ_ϕ} is uniquely defined only when $\Lambda(\rho)$ has a maximum possible rank, which we argue as follows. Let $\rho_\phi = \sum_{j=1}^{d'} \lambda_j |\lambda_j(\phi)\rangle \langle \lambda_j(\phi)|$, where d' is the rank of ρ_ϕ and $\{|\lambda_j(\phi)\rangle\}_{j=1}^{d'}$ are its orthonormal vectors corresponding to non-zero eigenvalues. The definition of the SLD implies the following form of D_{ρ_ϕ} ,

$$D_{\rho_\phi} = \sum_{j,k=1}^{d'} \left(2 \frac{\lambda_j - \lambda_k}{\lambda_j + \lambda_k} \langle \lambda_j(\phi) | iH | \lambda_k(\phi) \rangle \right) - 2 P_{V^\perp} iH P_V + 2 P_V iH P_{V^\perp} + D_{\rho_\phi}^A, \quad (\text{A.1})$$

where V^\perp is the orthogonal complement of $V = \text{span}(\{|\lambda_j(\phi)\rangle\}_{j=1}^{d'})$, P_V, P_{V^\perp} are the orthogonal projections on V and V^\perp respectively and $D_{\rho_\phi}^A : V^\perp \rightarrow V^\perp$ represents the part of D_{ρ_ϕ} which can be defined arbitrarily. It follows D_{ρ_ϕ} is only uniquely defined when $V = \mathcal{H}$.

If D_{ρ_ϕ} is not uniquely defined, we set $D_{\rho_\phi}^A = 0$ in the algorithm. In the case of a unitary channel Λ , the state $\Lambda(|\psi\rangle\langle\psi|)$ has rank equal to 1. Nevertheless, we observed numerically that as long as the initial state $|\psi_0\rangle$ in the first step in the algorithm, leads to $\Lambda(|\psi_0\rangle\langle\psi_0|)$ having non-zero expansion coefficients in the eigenbasis of H , the algorithm converges to the maximum value $F^{(\max)} = 4 \sup_{|\psi\rangle} (\langle\psi|H^2|\psi\rangle - \langle\psi|H|\psi\rangle^2)$. This condition is related to the fact that when $\rho^{(n)}$ is block-diagonal in the eigenbasis of H , it is preserved by Λ . Thus $D_{\rho_\phi^{(n)}}$ is also block-diagonal according to Eq. (A.1) and, moreover, this is preserved at all the following steps of the algorithm. Assuming the non-degeneracy of the maximal eigenvalue of $G_\phi(D_{\rho_\phi^{(n)}})$, $\rho^{(n+1)}$ is only supported on one of the blocks. Therefore, $D_{\rho_\phi^{(n+1)}}$ is not uniquely defined and, from this point on, the algorithm is effectively restricted to the subspace of \mathcal{H} corresponding to this block. Therefore, in such a case the algorithm will fail to provide the maximum quantum Fisher information $F^{(\max)}$, unless that maximum corresponds to the state which is supported only on this block.

Therefore, we make the following

Proposition. If at each step of the algorithm $\rho^{(n)}$ is irreducible w.r.t. the direct sums of the eigenspaces of H , the algorithm will converge to the maximum value $F^{(\max)}$.

By saying that ρ is irreducible w.r.t. the direct sums of the eigenspaces of H , we understand the following: if for a subspace $V \subset \mathcal{H}$ we have both $\rho V \subset V$ and $HV \subset V$, then either $V = \{0\}$ or $V = \mathcal{H}$.

A.2 DERIVATIONS FOR THE BOUND ON PHASE ESTIMATION
PRECISION IN THE PRESENCE OF CORRELATED GAU-
SIAN DEPHASING

A.2.1 *Reduction from multi-parameter to single-parameter Bayesian estimation*

We are interested in Bayesian estimation a random phase $\varphi_\Sigma = \sum_{j=1}^N \gamma_j \tilde{\varphi}_j$, where the random phases $\{\tilde{\varphi}_1, \dots, \tilde{\varphi}_N\}$ have a multi-dimensional Gaussian distribution with a covariance matrix Σ and the same means equal ϕ , i.e.,

$$g_\phi(\tilde{\varphi}_1, \dots, \tilde{\varphi}_N) = \sqrt{2\pi \det \Sigma} e^{-\frac{1}{2} \sum_{j,k=1}^N (\tilde{\varphi}_j - \phi)(\Sigma^{-1})_{jk}(\tilde{\varphi}_k - \phi)},$$

whereas the coefficients in the phase φ_Σ are given as $\gamma_j = \frac{\sum_{k=1}^N (\Sigma^{-1})_{jk}}{\sum_{j,k=1}^N (\Sigma^{-1})_{jk}}$, $j = 1, \dots, N$. It follows that the distribution of φ_Σ is Gaussian with the variance equal $\Delta_\Sigma^2 = \left(\sum_{j,k=1}^N (\Sigma^{-1})_{jk}\right)^{-1}$ and the mean equal ϕ ; we denote this one-dimensional distribution by $g'_\phi(\varphi_\Sigma)$.

We cannot observe a φ_Σ value directly, but only via a result x of a POVM measurement $\{\Pi_x\}_x$. In a single realisation of an experiment the probability of obtaining a result $x \in X$ depends on all the random phases, $p_{\tilde{\varphi}_1, \dots, \tilde{\varphi}_N}(x) = \text{Tr}(\Pi_x e^{-i \sum_{j=1}^N \tilde{\varphi}_j H_j} \rho e^{i \sum_{j=1}^N \tilde{\varphi}_j H_j})$. The probability of obtaining a result x conditioned on the value of φ_Σ is $\int_{M_{\varphi_\Sigma}} g_\phi(\tilde{\varphi}_1, \dots, \tilde{\varphi}_N) p_{\tilde{\varphi}_1, \dots, \tilde{\varphi}_N} / g'_\phi(\varphi_\Sigma) =: p'_{\varphi_\Sigma}(x)$, where the set $M_{\varphi_\Sigma} = \{\{\tilde{\varphi}_1, \dots, \tilde{\varphi}_N\} \in \mathbb{R}^N : \sum_{j=1}^N \gamma_j \tilde{\varphi}_j = \varphi_\Sigma\}$. Therefore, the optimal Bayesian estimator of φ_Σ is, see Sec. 1.1.2.4,

$$\hat{\varphi}_\Sigma(x) := \frac{\int_{\mathbb{R}} d\varphi_\Sigma g'_\phi(\varphi_\Sigma) p'_{\varphi_\Sigma}(x) \varphi_\Sigma}{\int_{\mathbb{R}} d\varphi_\Sigma g'_\phi(\varphi_\Sigma) p'_{\varphi_\Sigma}(x)} = \sum_{j=1}^N \gamma_j \tilde{\varphi}_j(x), \quad (\text{A.2})$$

where $\tilde{\varphi}_j(x) := \frac{\int_{\mathbb{R}^N} d\tilde{\varphi}_1 \dots d\tilde{\varphi}_N g_\phi(\tilde{\varphi}_1, \dots, \tilde{\varphi}_N) p_{\tilde{\varphi}_1, \dots, \tilde{\varphi}_N}(x) \tilde{\varphi}_j}{\int_{\mathbb{R}^N} d\tilde{\varphi}_1 \dots d\tilde{\varphi}_N g_\phi(\tilde{\varphi}_1, \dots, \tilde{\varphi}_N) p_{\tilde{\varphi}_1, \dots, \tilde{\varphi}_N}(x)}$ is the best Bayesian estimator of a random phase $\tilde{\varphi}_j$ with respect to the multi-dimensional distribution $g_\phi(\tilde{\varphi}_1, \dots, \tilde{\varphi}_N)$.

A.2.2 Bayesian estimator as optimal local estimator

Let us prove that the choice of $\hat{\phi}(x) = \sum_{j=1}^N \gamma_j \tilde{\varphi}_j(x)$, which is the best Bayesian estimator for φ_Σ is optimal for local estimation up to a linear transformation guaranteeing local unbiasedness.

Signal. If in Bayesian estimation of φ_Σ we assume the mean $\phi = \phi_0$ in the distribution of $\tilde{\varphi}_1, \dots, \tilde{\varphi}_N$, see Eq. (1.16), it follows $\mathbb{E}_{\phi_0} \hat{\phi} = \phi_0$. Furthermore, as a consequence of Gaussian distribution of random phases we have

$$\begin{aligned} \partial_\phi|_{\phi=\phi_0} \mathbb{E}_\phi \hat{\phi} &= \sum_x \text{Tr}(\Pi_x \partial_\phi|_{\phi=\phi_0} \Lambda_\phi(\rho)) \hat{\phi}(x), \\ \partial_\phi|_{\phi=\phi_0} \Lambda_\phi(\rho) &= \int_{\mathbb{R}^N} d\tilde{\varphi}_1 \dots d\tilde{\varphi}_N \partial_\phi|_{\phi=\phi_0} g_\phi(\tilde{\varphi}_1, \dots, \tilde{\varphi}_N) \rho_{\tilde{\varphi}_1, \dots, \tilde{\varphi}_N} \\ &= (\Delta_\Sigma^2)^{-1} \int_{\mathbb{R}^N} d\tilde{\varphi}_1 \dots d\tilde{\varphi}_N g_{\phi_0}(\tilde{\varphi}_1, \dots, \tilde{\varphi}_N) \\ &\quad \times \rho_{\tilde{\varphi}_1, \dots, \tilde{\varphi}_N} \left(\sum_{j=1}^N \gamma_j \tilde{\varphi}_j - \phi_0 \right). \end{aligned}$$

Moreover, from the definition of $\hat{\phi}$ as the Bayesian estimator of the phase $\varphi_\Sigma = \sum_{j=1}^N \gamma_j \tilde{\varphi}_j$ we obtain

$$\begin{aligned} \int_{\mathbb{R}^N} d\tilde{\varphi}_1 \dots d\tilde{\varphi}_N g_{\phi_0}(\tilde{\varphi}_1, \dots, \tilde{\varphi}_N) \times \text{Tr}(\Pi_x \rho_{\tilde{\varphi}_1, \dots, \tilde{\varphi}_N}) \left(\sum_{j=1}^N \gamma_j \tilde{\varphi}_j - \phi_0 \right) \\ = (\hat{\phi}(x) - \phi_0) \text{Tr}(\Pi_x \Lambda_{\phi_0}(\rho)), \end{aligned}$$

which leads to

$$\text{Tr}(\partial_\phi \Lambda_\phi(\rho) \Pi_x)|_{\phi=\phi_0} = \text{Tr}(\Pi_x \Lambda_{\phi_0}(\rho)) (\Delta_\Sigma^2)^{-1} (\hat{\phi}(x) - \phi_0). \quad (\text{A.3})$$

Thus, as $\sum_x \text{Tr}(\Pi_x \partial_\phi|_{\phi=\phi_0} \Lambda_\phi(\rho)) = \partial_\phi|_{\phi=\phi_0} \mathbf{1} = 0$, we arrive at

$$\begin{aligned} \partial_\phi|_{\phi=\phi_0} \mathbb{E}_\phi \hat{\phi} &= \sum_x \text{Tr}(\Pi_x \partial_\phi|_{\phi=\phi_0} \Lambda_\phi(\rho)) (\hat{\phi}(x) - \phi_0) \quad (\text{A.4}) \\ &= (\Delta_\Sigma^2)^{-1} \sum_x \text{Tr}(\Pi_x \Lambda_{\phi_0}(\rho)) (\hat{\phi}(x) - \phi_0)^2 = (\Delta_\Sigma^2)^{-1} \Delta_{\phi_0}^2 \hat{\phi}. \end{aligned}$$

Noise. From Eq. (A.3) it also follows that

$$\begin{aligned}\hat{\phi}(\mathbf{x}) - \phi_0 &= \Delta_\Sigma^2 \frac{\text{Tr}(\partial_\phi|_{\phi=\phi_0} \Lambda_\phi(\rho) \Pi_x)}{\text{Tr}(\Pi_x \Lambda_{\phi_0}(\rho))} = \partial_\phi|_{\phi=\phi_0} \log(\text{Tr}(\Pi_x \Lambda_\phi(\rho))), \\ \Delta_{\phi_0}^2 \hat{\phi} &= \sum_x \text{Tr}(\Pi_x \Lambda_{\phi_0}(\rho)) (\hat{\phi}(\mathbf{x}) - \phi_0)^2 = (\Delta_\Sigma^2)^2 F_{\phi_0},\end{aligned}\quad (\text{A.5})$$

where in the last line we used a definition of the Fisher information F_{ϕ_0} , see Eq. (1.6).

Signal-to-Noise Ratio. From Eqs. (A.4) and (A.5) it simply follows that the SNR of $\hat{\phi}$ is equal to the Fisher information F_{ϕ_0} and thus $\hat{\phi}$ is optimal estimator up to a linear transformation guaranteeing local unbiasedness around $\phi = \phi_0$. ■

A.2.3 Phase encoding

Below we prove that the phase φ_Σ is encoded in the system state with the the very Hamiltonian encoding the phase ϕ being estimated locally.

In a single realisation of estimation experiment, we perform a POVM measurement $\{\Pi_x\}_x$ on a system state $\rho_{\tilde{\varphi}_1, \dots, \tilde{\varphi}_N} = e^{-i \sum_{j=1}^N \tilde{\varphi}_j H_j} \rho e^{i \sum_{j=1}^N \tilde{\varphi}_j H_j}$, and the probability of obtaining a result x equals $p_{\tilde{\varphi}_1, \dots, \tilde{\varphi}_N}(\mathbf{x}) = \text{Tr}(\rho_{\tilde{\varphi}_1, \dots, \tilde{\varphi}_N} \Pi_x)$. The probability of obtaining a result x condition on a value of the phase φ_Σ is $p'_{\varphi_\Sigma}(\mathbf{x}) = \int_{M_{\varphi_\Sigma}} g_\phi(\tilde{\varphi}_1, \dots, \tilde{\varphi}_N) p_{\tilde{\varphi}_1, \dots, \tilde{\varphi}_N}$, where the set $M_{\varphi_\Sigma} = \{\{\tilde{\varphi}_1, \dots, \tilde{\varphi}_N\} \in \mathbb{R}^N : \sum_{j=1}^N \gamma_j \tilde{\varphi}_j = \varphi_\Sigma\}$, and thus corresponds to a mixed quantum state

$$\rho'_{\varphi_\Sigma} = (g'_\phi(\varphi_\Sigma))^{-1} \int_{M_{\varphi_\Sigma}} g_\phi(\tilde{\varphi}_1, \dots, \tilde{\varphi}_N) \rho_{\tilde{\varphi}_1, \dots, \tilde{\varphi}_N}.$$

Below we show that $\partial_{\varphi_\Sigma} \rho'_{\varphi_\Sigma} = -i [H, \rho'_{\varphi_\Sigma}]$, where $H = \sum_{j=1}^N H_j$ is the Hamiltonian encoding the phase ϕ estimated locally.

We know that the Fisher information of measuring $\{\Pi_x\}_x$ on ρ'_{φ_Σ} is not smaller than the QFI related to unitary encoding with Hamiltonian on the state $\rho'_0 = e^{i\varphi_\Sigma H} \rho'_{\varphi_\Sigma} e^{i\varphi_\Sigma H}$, which does not depend on the value of φ_Σ and we can choose $\varphi_\Sigma = \phi$. Fur-

thermore, as the quantum Fisher information is convex w.r.t. density matrices, we have

$$\begin{aligned} F_\phi(\rho'_\phi) &\leq (g'_\phi(\phi))^{-1} \int_{M_0} g_0(\varphi_1, \dots, \varphi_N) F_\phi(\rho_{\varphi_1+\phi, \dots, \varphi_N+\phi}) \\ &= F_\phi(\mathbf{U}_\phi \rho \mathbf{U}_\phi^\dagger), \end{aligned}$$

as we have $F_\phi(\rho_{\varphi_1+\phi, \dots, \varphi_N+\phi}) = F_\phi(\mathbf{U}_\phi \rho \mathbf{U}_\phi^\dagger)$.

Proof. As $\sum_{j=1}^N \gamma_j = 1$, we obtain

$$\begin{aligned} \rho'_\phi &= (g'_\phi(\varphi_\Sigma))^{-1} \left(\sum_{j=1}^N \gamma_j \right) \int_{M_{\varphi_\Sigma}} g_\phi(\tilde{\varphi}_1, \dots, \tilde{\varphi}_N) \rho_{\tilde{\varphi}_1, \dots, \tilde{\varphi}_N} \\ &= g'_\phi(\varphi_\Sigma)^{-1} \sum_{j=1}^N \gamma_j \int_{\mathbb{R}^{N-1}} d\tilde{\varphi}_1 \dots d\tilde{\varphi}_{j-1} d\tilde{\varphi}_{j+1} \dots d\tilde{\varphi}_N \\ &\quad \times g_\phi \left(\tilde{\varphi}_1, \dots, \tilde{\varphi}_{j-1}, \gamma_j^{-1} \varphi_\Sigma - \gamma_j^{-1} \sum_{k=1, k \neq j}^N \gamma_k \tilde{\varphi}_k, \tilde{\varphi}_{j+1}, \dots, \tilde{\varphi}_N \right) \\ &\quad \times \rho_{\tilde{\varphi}_1, \dots, \tilde{\varphi}_{j-1}, \gamma_j^{-1} \varphi_\Sigma - \gamma_j^{-1} \sum_{k=1, k \neq j}^N \gamma_k \tilde{\varphi}_k, \tilde{\varphi}_{j+1}, \dots, \tilde{\varphi}_N} \quad \text{and} \\ g'_\phi(\varphi_\Sigma) &= \sum_{j=1}^N \gamma_j \int_{\mathbb{R}^{N-1}} d\tilde{\varphi}_1 \dots d\tilde{\varphi}_{j-1} d\tilde{\varphi}_{j+1} \dots d\tilde{\varphi}_N \\ &\quad \times g_\phi \left(\tilde{\varphi}_1, \dots, \tilde{\varphi}_{j-1}, \gamma_j^{-1} \varphi_\Sigma - \gamma_j^{-1} \sum_{k=1, k \neq j}^N \gamma_k \tilde{\varphi}_k, \tilde{\varphi}_{j+1}, \dots, \tilde{\varphi}_N \right). \end{aligned}$$

Therefore,

$$\begin{aligned}
\partial_{\varphi_\Sigma} \mathbf{g}'_\phi(\varphi_\Sigma) &= \sum_{j=1}^N \gamma_j \int_{\mathbb{R}^{N-1}} d\tilde{\varphi}_1 \dots d\tilde{\varphi}_{j-1} d\tilde{\varphi}_{j+1} \dots d\tilde{\varphi}_N \\
&\quad \times \mathbf{g}_\phi \left(\tilde{\varphi}_1, \dots, \tilde{\varphi}_{j-1}, \gamma_j^{-1} \varphi_\Sigma - \gamma_j^{-1} \sum_{k=1, k \neq j}^N \gamma_k \tilde{\varphi}_k, \tilde{\varphi}_{j+1}, \dots, \tilde{\varphi}_N \right) \\
&\quad \times (-\gamma_j^{-1}) \left(\sum_{k=1, k \neq j}^N (\Sigma^{-1})_{jk} (\tilde{\varphi}_k - \phi) + (\Sigma^{-1})_{jj} \left(\gamma_j^{-1} \varphi_\Sigma - \gamma_j^{-1} \sum_{k=1, k \neq j}^N \gamma_k \tilde{\varphi}_k - \phi \right) \right) \\
&= - \sum_{j=1}^N \int_{\mathcal{M}_{\varphi_\Sigma}} \mathbf{g}_\phi(\tilde{\varphi}_1, \dots, \tilde{\varphi}_N) \sum_{k=1}^N (\tilde{\varphi}_k - \phi) (\Sigma^{-1})_{jk} \\
&= - \int_{\mathcal{M}_{\varphi_\Sigma}} \mathbf{g}_\phi(\tilde{\varphi}_1, \dots, \tilde{\varphi}_N) \sum_{k=1}^N (\tilde{\varphi}_k - \phi) \gamma_k (\Delta_\Sigma^2)^{-1} \\
&= - \int_{\mathcal{M}_{\varphi_\Sigma}} \mathbf{g}_\phi(\tilde{\varphi}_1, \dots, \tilde{\varphi}_N) (\varphi_\Sigma - \phi) (\Delta_\Sigma^2)^{-1} \\
&= -(\Delta_\Sigma^2)^{-1} (\varphi_\Sigma - \phi) \mathbf{g}'_\phi(\varphi_\Sigma).
\end{aligned}$$

Hence,

$$\begin{aligned}
\partial_{\varphi_\Sigma} \rho'_{\varphi_\Sigma} &= (g'_\phi(\varphi_\Sigma))^{-1} \sum_{j=1}^N \gamma_j \int_{\mathbb{R}^{N-1}} d\tilde{\varphi}_1 \dots d\tilde{\varphi}_{j-1} d\tilde{\varphi}_{j+1} \dots d\tilde{\varphi}_N \\
&\quad \times g_\phi \left(\tilde{\varphi}_1, \dots, \tilde{\varphi}_{j-1}, \gamma_j^{-1} \varphi_\Sigma - \gamma_j^{-1} \sum_{k=1, k \neq j}^N \gamma_k \tilde{\varphi}_k, \tilde{\varphi}_{j+1}, \dots, \tilde{\varphi}_N \right) \\
&\quad \times \left[-i \gamma_j^{-1} \mathbf{H}_j, \rho_{\tilde{\varphi}_1, \dots, \tilde{\varphi}_{j-1}, \gamma_j^{-1} \varphi_\Sigma - \gamma_j^{-1} \sum_{k=1, k \neq j}^N \gamma_k \tilde{\varphi}_k, \tilde{\varphi}_{j+1}, \dots, \tilde{\varphi}_N} \right] \\
&+ (g'_\phi(\varphi_\Sigma))^{-1} \sum_{j=1}^N \gamma_j \int_{\mathbb{R}^{N-1}} d\tilde{\varphi}_1 \dots d\tilde{\varphi}_{j-1} d\tilde{\varphi}_{j+1} \dots d\tilde{\varphi}_N \\
&\quad \times g_\phi \left(\tilde{\varphi}_1, \dots, \tilde{\varphi}_{j-1}, \gamma_j^{-1} \varphi_\Sigma - \gamma_j^{-1} \sum_{k=1, k \neq j}^N \gamma_k \tilde{\varphi}_k, \tilde{\varphi}_{j+1}, \dots, \tilde{\varphi}_N \right) \\
&\quad \times (-\gamma_j^{-1}) \left(\sum_{k=1, k \neq j}^N (\Sigma^{-1})_{jk} (\tilde{\varphi}_k - \phi) + (\Sigma^{-1})_{jj} \left(\gamma_j^{-1} \varphi_\Sigma - \gamma_j^{-1} \sum_{k=1, k \neq j}^N \gamma_k \tilde{\varphi}_k - \phi \right) \right) \\
&\quad \times \rho_{\tilde{\varphi}_1, \dots, \tilde{\varphi}_{j-1}, \gamma_j^{-1} \varphi_\Sigma - \gamma_j^{-1} \sum_{k=1, k \neq j}^N \gamma_k \tilde{\varphi}_k, \tilde{\varphi}_{j+1}, \dots, \tilde{\varphi}_N} \\
&- \rho'_{\varphi_\Sigma} (g'_\phi(\varphi_\Sigma))^{-1} \partial_{\varphi_\Sigma} g'_\phi(\varphi_\Sigma) \\
&= -i [\mathbf{H}, \rho'_{\varphi_\Sigma}] - \rho'_{\varphi_\Sigma} (\Delta_\Sigma^2)^{-1} (\varphi_\Sigma - \phi) + \rho'_{\varphi_\Sigma} (\Delta_\Sigma^2)^{-1} (\varphi - \phi) \\
&= -i [\mathbf{H}, \rho'_{\varphi_\Sigma}]. \quad \blacksquare
\end{aligned}$$

B

APPENDIX TO CHAPTER 2

B.1 FIDELITY AND QFI

In this Appendix we prove Eqs. (2.12) and (2.24). We have:

$$\begin{aligned}\partial_{g_1} \partial_{g_2} \log \langle \psi_{g_1} | \psi_{g_2} \rangle |_{g_1=g_2=g} &= \frac{\langle \psi'_g | \psi'_g \rangle}{\langle \psi_g | \psi_g \rangle} - \frac{\langle \psi'_g | \psi_g \rangle \langle \psi_g | \psi'_g \rangle}{\langle \psi_g | \psi_g \rangle^2} \\ &= \langle \psi'_g | \psi'_g \rangle - |\langle \psi_g | \psi'_g \rangle|^2\end{aligned}$$

where $|\psi'_g\rangle := \partial_{g_1} |\psi_{g_1}\rangle |_{g_1=g}$ and we have used the normalisation of the state, $\langle \psi_g | \psi_g \rangle = 1$.

On the other hand, for a family of pure states $\rho_g = |\psi_g\rangle\langle\psi_g|$ the symmetric logarithmic derivative is $D_g = 2(|\psi_g\rangle\langle\psi'_g| + |\psi'_g\rangle\langle\psi_g|)$. Therefore

$$\begin{aligned}F(|\psi_g\rangle) &= \text{Tr}(\rho_g D_g^2) \\ &= 4(\langle \psi'_g | \psi'_g \rangle + \langle \psi'_g | \psi_g \rangle \langle \psi_g | \psi'_g \rangle \\ &\quad + \langle \psi'_g | \psi_g \rangle^2 + \langle \psi_g | \psi'_g \rangle^2) \\ &= 4(\langle \psi'_g | \psi'_g \rangle - |\langle \psi'_g | \psi_g \rangle|^2) \\ &= 4 \partial_{g_1} \partial_{g_2} \log |\langle \psi_{g_1} | \psi_{g_2} \rangle |_{g_1=g_2=g},\end{aligned}$$

where we used $\langle \psi'_g | \psi_g \rangle = -\langle \psi_g | \psi'_g \rangle$ resulting from differentiating $\langle \psi_g | \psi_g \rangle = 1$.

B.2 TIME DEPENDENCE OF QFI

In this section we first discuss the general dependence of the QFI of the MPS $|\Psi(t)\rangle$ on time t . This will enable us to prove

the asymptotic linear behaviour of the QFI for dynamics with a unique stationary state, see Eq. (2.26). Using the general time dependence of the QFI, we then prove the existence of a quadratic scaling regime of the QFI for dynamics near a first-order DPT, cf. Eq. (2.28).

B.2.1 General time dependence of QFI

In order to express the QFI of the MPS $|\Psi(t)\rangle$, we use Eqs. (2.12) and (2.24),

$$F(|\Psi_g(t)\rangle) = 4 \partial_{g_1} \partial_{g_2} \log \text{Tr} \{ e^{t\mathcal{L}_{g_1, g_2}} |\chi\rangle\langle\chi| \}_{g_1=g_2=g},$$

and obtain

$$\begin{aligned} F(|\Psi_g(t)\rangle) = & -4 \left| \text{Tr} \int_0^t dt' \partial_{g_1} \mathcal{L}_{g_1, g} \rho_g(t') \right|_{g_1=g}^2 + \\ & + 4 \text{Tr} \left(\int_0^t dt' \partial_{g_1} \partial_{g_2} \mathcal{L}_{g_1, g_2} \rho_g(t') \right)_{g_1=g_2=g} + \\ & + 8 \text{Re} \text{Tr} \left(\int_0^t dt' \int_0^{t-t'} dt'' \partial_{g_1} \mathcal{L}_{g_1, g} e^{t''\mathcal{L}_g} \partial_{g_2} \mathcal{L}_{g, g_2} \rho_g(t') \right)_{g_1=g_2=g}, \end{aligned} \quad (\text{B.1})$$

where $\rho_g(t) := e^{t\mathcal{L}_g} |\chi\rangle\langle\chi|$, $|\chi\rangle$ is an initial pure state of the system, \mathcal{L}_g is the Master operator, see Eq. (2.12), and \mathcal{L}_{g_1, g_2} is the modified Master operator, see Eq. (2.25). Eq. (B.1) above results from the following calculations. Firstly (cf. Dyson-Philips expansion),

$$\begin{aligned} & \partial_{g_1} \partial_{g_2} \log \text{Tr} \left(e^{t\mathcal{L}_{g_1, g_2}} |\chi\rangle\langle\chi| \right)_{g_1=g_2=g} = \\ & = - \left| \partial_{g_1} \text{Tr} \left(e^{t\mathcal{L}_{g_1, g}} |\chi\rangle\langle\chi| \right)_{g_1=g} \right|^2 + \partial_{g_1} \partial_{g_2} \text{Tr} \left(e^{t\mathcal{L}_{g_1, g_2}} |\chi\rangle\langle\chi| \right)_{g_1=g_2=g}. \end{aligned}$$

Secondly,

$$\begin{aligned}
 \partial_{g_1} \text{Tr} \left(e^{t\mathcal{L}_{g_1,g}} |\chi\rangle\langle\chi| \right)_{g_1=g} &= \\
 &= \text{Tr} \left(\int_0^t dt' e^{(t-t')\mathcal{L}_{g_1,g}} \partial_{g_1} \mathcal{L}_{g_1,g} e^{t'\mathcal{L}_{g_1,g}} |\chi\rangle\langle\chi| \right)_{g_1=g} \\
 &= \text{Tr} \left(\int_0^t dt' \partial_{g_1} \mathcal{L}_{g_1,g} \rho_g(t') \right)_{g_1=g},
 \end{aligned}$$

where the third line results from the operator $e^{t\mathcal{L}_g}$ being trace-preserving. Similarly, the second and third line in Eq. (B.1) correspond to $\partial_{g_1} \partial_{g_2} \text{Tr} \{ e^{t\mathcal{L}_{g_1,g_2}} |\chi\rangle\langle\chi| \}_{g_1=g_2=g}$.

Note that \mathcal{L}_g is a linear operator on the space of matrices acting on the system Hilbert space \mathcal{H} . For clarity of further presentation, we assume that \mathcal{L}_g can be diagonalised with right and left eigenmatrices $\{\mathbb{R}_k\}_{k=1}^{d^2}$, $\{\mathbb{L}_k\}_{k=1}^{d^2}$, ordered s.t. the corresponding eigenvalues $0 = \lambda_1 > \text{Re} \lambda_2 \geq \text{Re} \lambda_3 \geq \dots \geq \text{Re} \lambda_{d^2}$ and normalised $\text{Tr} (\mathbb{L}_j \mathbb{R}_k) = \delta_{jk}$, $j, k = 1, \dots, d^2$, where $d = \dim \mathcal{H}$ and we have explicitly assumed one stationary state $\mathbb{R}_1 = \rho_{ss}$ and from trace-preservation it follows $\mathcal{L}_1 = \mathbb{1}_{\mathcal{H}}$. For convenience, apart from the standard matrix notation, the eigenmatrices will be also denoted as vectors $\{\|\mathbb{R}_k\|\}_{k=1}^{d^2}$, $\{\langle\langle\mathbb{L}_k\|\|\rangle\rangle\}_{k=1}^{d^2}$ in the space of matrices, with the scalar product $\langle\langle\mathbb{L}\|\mathbb{R}\rangle\rangle := \text{Tr} (\mathbb{L} \mathbb{R})$. Note the contrast to vectors (pure states) $|\chi\rangle$ in \mathcal{H} . One can now simply write $\mathcal{L}_g = 0 \|\rho_{ss}\rangle\rangle \langle\langle\mathbb{1}_{\mathcal{H}}\|\| + \sum_{k=2}^{d^2} \lambda_k \|\mathbb{R}_k\rangle\rangle \langle\langle\mathbb{L}_k\|\|$. The discussion below will be similar for a general Jordan decomposition of \mathcal{L}_g .

As Eq. (B.1) involves integrals of $e^{t\mathcal{L}_g}$, we need to consider the 0-eigenspace of \mathcal{L}_g , i.e. the stationary state ρ_{ss} , separately from the rest of eigenmatrices whose eigenvalues differ from 0. We introduce the projection on the stationary state ρ_{ss} , $\mathcal{P}_{ss} = \|\rho_{ss}\rangle\rangle \langle\langle\mathbb{1}_{\mathcal{H}}\|\|$, and its complement $\mathcal{J} - \mathcal{P}_{ss} := \sum_{k=2}^{d^2} \|\mathbb{R}_k\rangle\rangle \langle\langle\mathbb{L}_k\|\|$ and denote the restriction of an operator \mathcal{X} to this complement by $[\mathcal{X}]_{\mathcal{J}-\mathcal{P}_{ss}} := (\mathcal{J} - \mathcal{P}_{ss}) \mathcal{X} (\mathcal{J} - \mathcal{P}_{ss})$.

We now express the finite time behaviour of QFI using derivatives of the modified Master operator and the diagonal decom-

position of the original Master operator \mathcal{L}_g . From Eq. (B.1) it follows

$$\begin{aligned}
 F(|\Psi_g(t)\rangle) = & \\
 & -4 \left| t \text{Tr} (\partial_{g_1} \mathcal{L}_{g_1,g} \rho_{ss}) + \text{Tr} \left(\partial_{g_1} \mathcal{L}_{g_1,g} \left[\frac{e^{t\mathcal{L}_g} - \mathcal{J}}{\mathcal{L}_g} \right]_{\mathcal{J}-\mathcal{P}_{ss}} |\chi\rangle\langle\chi| \right) \right|_{g_1=g}^2 \\
 & +4 \left(t \text{Tr} (\partial_{g_1} \partial_{g_2} \mathcal{L}_{g_1,g_2} \rho_{ss}) + \text{Tr} \left(\partial_{g_1} \partial_{g_2} \mathcal{L}_{g_1,g_2} \left[\frac{e^{t\mathcal{L}_g} - \mathcal{J}}{\mathcal{L}_g} \right]_{\mathcal{J}-\mathcal{P}_{ss}} |\chi\rangle\langle\chi| \right) \right)_{g_1=g_2=g} \\
 & +4 t^2 |\text{Tr} (\partial_{g_1} \mathcal{L}_{g_1,g} \rho_{ss})|^2 \\
 & +8 \text{Re} \text{Tr} (\partial_{g_1} \mathcal{L}_{g_1,g} \rho_{ss}) \text{Tr} \left(\partial_{g_2} \mathcal{L}_{g,g_2} \left[\frac{e^{t\mathcal{L}_g} - \mathcal{J} - t\mathcal{L}_g}{\mathcal{L}_g^2} \right]_{\mathcal{J}-\mathcal{P}_{ss}} |\chi\rangle\langle\chi| \right)_{g_1=g_2=g} \\
 & +8 \text{Re} \text{Tr} \left(\partial_{g_1} \mathcal{L}_{g_1,g} \left[\frac{e^{t\mathcal{L}_g} - \mathcal{J} - t\mathcal{L}_g}{\mathcal{L}_g^2} \right]_{\mathcal{J}-\mathcal{P}_{ss}} \partial_{g_2} \mathcal{L}_{g,g_2} \rho_{ss} \right)_{g_1=g_2=g} \\
 & -8 \text{Re} \text{Tr} \left(\partial_{g_1} \mathcal{L}_{g_1,g} [\mathcal{L}_g^{-1}]_{\mathcal{J}-\mathcal{P}_{ss}} \partial_{g_2} \mathcal{L}_{g,g_2} \left[\frac{e^{t\mathcal{L}_g} - \mathcal{J}}{\mathcal{L}_g} \right]_{\mathcal{J}-\mathcal{P}_{ss}} |\chi\rangle\langle\chi| \right)_{g_1=g_2=g} \\
 & +8 \text{Re} \text{Tr} \left(\partial_{g_1} \mathcal{L}_{g_1,g} \left[\frac{e^{t\mathcal{L}_g}}{\mathcal{L}_g} \left(\int_0^t dt' e^{-t'\mathcal{L}_g} \partial_{g_2} \mathcal{L}_{g,g_2} e^{t'\mathcal{L}_g} \right) \right]_{\mathcal{J}-\mathcal{P}_{ss}} |\chi\rangle\langle\chi| \right)_{g_1=g_2=g} \quad (\text{B.2})
 \end{aligned}$$

where $\mathcal{J} = \sum_{k=1}^{d^2} \|\mathbf{R}_k\rangle\langle\mathbf{L}_k\|$ is an identity operator on the space of matrices on \mathcal{H} and one can show that

$$\begin{aligned}
 & \left[\frac{e^{t\mathcal{L}_g}}{\mathcal{L}_g} \left(\int_0^t dt' e^{-t'\mathcal{L}_g} \partial_{g_2} \mathcal{L}_{g,g_2} e^{t'\mathcal{L}_g} \right) \right]_{\mathcal{J}-\mathcal{P}_{ss}} = \\
 & = t \sum_{k=2}^{d^2} \frac{e^{t\lambda_k}}{\lambda_k} \langle\langle \mathbf{L}_k | \partial_{g_2} \mathcal{L}_{g,g_2} | \mathbf{R}_k \rangle\rangle \|\mathbf{R}_k\rangle\langle\mathbf{L}_k| \\
 & + \sum_{j \neq k, j, k > 1}^{d^2} \frac{e^{t\lambda_j} - e^{t\lambda_k}}{\lambda_k(\lambda_j - \lambda_k)} \langle\langle \mathbf{L}_k | \partial_{g_2} \mathcal{L}_{g,g_2} | \mathbf{R}_j \rangle\rangle \|\mathbf{R}_k\rangle\langle\mathbf{L}_j|.
 \end{aligned}$$

The first line and the second line in Eq. (B.2) correspond to the first and the second line in Eq. (B.1), respectively. All other terms in Eq. (B.2) correspond to the third line in Eq. (B.1). We see that the quadratic contribution $t^2 |\text{Tr} (\partial_{g_1} \mathcal{L}_{g_1,g} \rho_{ss})|^2$ cancels out and for one stationary state there is no explicit quadratic behaviour. Eq. (B.2) will be further used for investigating the

asymptotic and the quadratic time regime of QFI in the next subsections.

We note that as an alternative route, one can use the eigendecomposition of the modified Master operator \mathcal{L}_{g_1, g_2} defined in Eq. (2.25),

$$e^{t\mathcal{L}_{g_1, g_2}} = \sum_{k=1}^{d^2} e^{t\lambda_k(g_1, g_2)} \|\mathbf{R}_k(g_1, g_2)\rangle\rangle \langle\langle \mathbf{L}_k(g_1, g_2) \| . \quad (\text{B.3})$$

From Eqs. (2.12) and (2.24), we obtain for a single stationary state

$$\begin{aligned} F(|\Psi_g(t)\rangle) = & \\ & -4 \left(t^2 |\partial_{g_1} \lambda_1(g_1, g)|^2 + 2 t \operatorname{Re} \partial_{g_1} \lambda_1(g_1, g) \sum_{k=1}^{d^2} e^{t\lambda_k} \partial_{g_2} c_k(g, g_2) + \right. \\ & \left. + \sum_{j,k=1}^{d^2} e^{t(\lambda_k + \lambda_j)} \partial_{g_1} c_j(g_1, g) \partial_{g_2} c_k(g, g_2) \right)_{g_1=g_2=g} + \\ & +4 \left(t^2 |\partial_{g_1} \lambda_1(g_1, g)|^2 + t \partial_{g_1} \partial_{g_2} \lambda_1(g_1, g_2) + \sum_{k=1}^{d^2} e^{t\lambda_k} \partial_{g_1} \partial_{g_2} c_k(g_1, g_2) + \right. \\ & \left. + 2 t \operatorname{Re} \sum_{k=1}^{d^2} e^{t\lambda_k} \partial_{g_1} c_k(g_1, g) \partial_{g_2} \lambda_k(g, g_2) \right)_{g_1=g_2=g} \quad (\text{B.4}) \end{aligned}$$

where $c_k(g_1, g_2) = \operatorname{Tr}(\mathbf{L}_k(g_1, g_2) |\chi\rangle\langle\chi|) \times \operatorname{Tr}(\mathbf{R}_k(g_1, g_2))$ and $c_k = c_k(g, g)$, $\lambda_k = \lambda_k(g, g)$, $k = 1, \dots, d^2$. The first line corresponds to the first line of Eq. (B.2) and the second to the rest of terms in Eq. (B.2). We see again that quadratic terms $t^2 |\partial_{g_1} \lambda_1(g_1, g)|^2$ cancel out and there is no explicit quadratic behaviour. In derivation of Eq. (B.4) we have used the fact that, for a single stationary state, $c_1(g, g) = 1$ and $c_k(g, g) = 0$, $k = 2, \dots, d^2$, which follows from the orthogonality and normalisation of the \mathcal{L}_g eigenbasis, $\langle\langle \mathbf{L}_i \| \mathbf{R}_j \rangle\rangle = \delta_{i,j}$, and as $\mathbf{L}_1 = \mathbb{1}_{\mathcal{H}}$ we have $\operatorname{Tr}(\mathbf{R}_k) = \delta_{1,k}$.

We note that in general the eigenvalues $\lambda_k(g_1, g_2)$ and the related coefficients $c_k(g_1, g_2)$ may not be analytic in g_1 or g_2 , even when \mathcal{L}_{g_1, g_2} is analytic (which we always assume). There

are analytic for example in the case when the corresponding eigenvalue λ_k of \mathcal{L}_g is non-degenerate [167]. In general case, however, all non-analyticities must *cancel out*, as $e^{t\mathcal{L}_{g_1,g_2}}$ is an analytic function of analytic \mathcal{L}_{g_1,g_2} .

B.2.2 Asymptotic QFI for a unique stationary state

When the stationary state is unique, the second eigenvalue of the Master operator \mathcal{L}_g is different from 0, $\lambda_2 \neq 0$. As we have $\lim_{t \rightarrow \infty} [e^{t\mathcal{L}_g}]_{j-\mathcal{P}_{ss}} = 0$, from Eq. (B.2) we obtain an asymptotic *linear* behaviour of the QFI,

$$\begin{aligned} \lim_{t \rightarrow \infty} t^{-1} F(|\Psi_g(t)\rangle) &= 4 \operatorname{Tr} (\partial_{g_1} \partial_{g_2} \mathcal{L}_{g_1,g_2} \rho_{ss}) + \\ &- 8 \operatorname{Re} \operatorname{Tr} \left(\partial_{g_1} \mathcal{L}_{g_1,g} [\mathcal{L}_g^{-1}]_{j-\mathcal{P}_{ss}} \partial_{g_2} \mathcal{L}_{g,g_2} \rho_{ss} \right)_{g_1=g_2=g} =: f_{1,g} \end{aligned} \quad (\text{B.5})$$

and the limit is independent from the initial state. The result (B.5) was also obtained using different methods in [38, 39]. We see that Eq. (B.5) can diverge at a first-order DPT when $\lambda_2 \rightarrow 0$ for $g \rightarrow g_c$, as $[\mathcal{L}_g^{-1}]_{j-\mathcal{P}_{ss}}$ has then a diverging eigenvalue λ_2^{-1} . Analogously we can obtain constant terms in the asymptotic QFI:

$$\begin{aligned} f_{0,g} &:= \lim_{t \rightarrow \infty} (F(|\Psi_g(t)\rangle) - t f_{1,g}) \\ &= -4 \left| \operatorname{Tr} \left(\partial_{g_1} \mathcal{L}_{g_1,g} [\mathcal{L}_g^{-1}]_{j-\mathcal{P}_{ss}} |\chi\rangle\langle\chi| \right) \right|_{g_1=g}^2 \\ &- 4 \operatorname{Tr} \left(\partial_{g_1} \partial_{g_2} \mathcal{L}_{g_1,g_2} [\mathcal{L}_g^{-1}]_{j-\mathcal{P}_{ss}} |\chi\rangle\langle\chi| \right)_{g_1=g_2=g} \\ &- 8 \operatorname{Re} \operatorname{Tr} (\partial_{g_1} \mathcal{L}_{g_1,g} \rho_{ss}) \operatorname{Tr} \left(\partial_{g_2} \mathcal{L}_{g,g_2} [\mathcal{L}_g^{-2}]_{j-\mathcal{P}_{ss}} |\chi\rangle\langle\chi| \right)_{g_1=g_2=g} \\ &- 8 \operatorname{Re} \operatorname{Tr} \left(\partial_{g_1} \mathcal{L}_{g_1,g} [\mathcal{L}_g^{-2}]_{j-\mathcal{P}_{ss}} \partial_{g_2} \mathcal{L}_{g,g_2} \rho_{ss} \right)_{g_1=g_2=g} \\ &+ 8 \operatorname{Re} \operatorname{Tr} \left(\partial_{g_1} \mathcal{L}_{g_1,g} [\mathcal{L}_g^{-1}]_{j-\mathcal{P}_{ss}} \partial_{g_2} \mathcal{L}_{g,g_2} [\mathcal{L}_g^{-1}]_{j-\mathcal{P}_{ss}} |\chi\rangle\langle\chi| \right)_{g_1=g_2=g} \end{aligned} \quad (\text{B.6})$$

We see that the asymptotic constant $f_{0,g}$ depends on the initial system state $|\chi\rangle$ and may diverge at a first-order DPT when

$\lambda_2 \rightarrow 0$.

The asymptotic linear behaviour of the QFI can be also obtained from Eq. (B.4) as

$$f_{1,g} = 4 \partial_{g_1} \partial_{g_2} \lambda_1(g_1, g_2) \Big|_{g_1=g_2=g}, \quad (\text{B.7})$$

$$f_{0,g} = \left(\partial_{g_1} \partial_{g_2} c_1(g_1, g_2) - |\partial_{g_1} c_1(g_1, g)|^2 \right) \Big|_{g_1=g_2=g}. \quad (\text{B.8})$$

cf. Eq. (2.26). Note that the eigenvalue $\lambda_1(g_1, g_2)$ of \mathcal{L}_{g_1, g_2} with maximal real part, and the corresponding $c_1(g_1, g_2)$, are analytic functions for small enough g_1 and g_2 as $\lambda_1(g, g) = 0$ is a non-degenerate eigenvalue of \mathcal{L}_g [167]. By comparing Eqs. (B.5) and (B.7), we see that when the gap closes at g_c , $\lambda_2 = 0$, the maximal eigenvalue of \mathcal{L}_{g_1, g_2} can be *non-analytic* at $g_1 = g_2 = g_c$, which we discuss in detail at the end of the next subsection.

B.2.3 Quadratic time-regime of QFI

In this subsection we describe the quadratic regime in the QFI scaling with time, which can be present for systems at and near a first-order DPT.

Quadratic behaviour near a DPT. For a system near a DPT the gap is much smaller than the gap associated with the rest of the spectrum. For simplicity we consider only one low-lying eigenvalue, i.e. $(-\text{Re}\lambda_2) \ll (-\text{Re}\lambda_3)$, but the discussion is similar for the general case of several low-lying eigenvalues. Note that the eigenvalues of \mathcal{L}_g come in conjugate pairs as \mathcal{L}_g preserves the Hermiticity of a matrix ρ , and thus $(-\text{Re}\lambda_2) \ll (-\text{Re}\lambda_3)$ implies $\lambda_2 \in \mathbb{R}$.

The separation in the eigenvalues introduces the intermediate time regime $(-\text{Re}\lambda_3)^{-1} = \tau' \ll t \ll \tau = (-\lambda_2)^{-1}$. In this regime we expect the second eigenmatrix R_2 of \mathcal{L}_g to be almost stationary and determine, with the stationary state ρ_{ss} , dominant terms in the QFI in Eq. (B.2), whereas other eigenmatrices not to play any significant role. We introduce the projection

$\mathcal{P} := \|\rho_{ss}\rangle\rangle\langle\langle \mathbb{1}_{\mathcal{H}} + \|\mathbf{R}_2\rangle\rangle\langle\langle L_2\|$ on the subspace spanned by the ρ_{ss} and ρ_2 . We also introduce the projection on their complement $\mathcal{J} - \mathcal{P} = \sum_{k=3}^{d^2} \|\mathbf{R}_k\rangle\rangle\langle\langle L_k\|$ and denote by $[\mathcal{X}]_{\mathcal{J}-\mathcal{P}} = (\mathcal{J} - \mathcal{P})\mathcal{X}(\mathcal{J} - \mathcal{P})$ the restriction of an operator \mathcal{X} to this complement.

The general behaviour of the QFI in Eq. (B.2) simplifies to

$$\begin{aligned}
 F(|\Psi_g(t)\rangle) = & \\
 & -4 \left| t \operatorname{Tr} (\partial_{g_1} \mathcal{L}_{g_1,g} \mathcal{P} |\chi\rangle\langle\chi|) - \operatorname{Tr} \left(\partial_{g_1} \mathcal{L}_{g_1,g} [\mathcal{L}_g^{-1}]_{\mathcal{J}-\mathcal{P}} |\chi\rangle\langle\chi| \right) \right|_{g_1=g}^2 \\
 & + 4 \left(t \operatorname{Tr} (\partial_{g_1} \partial_{g_2} \mathcal{L}_{g_1,g_2} \mathcal{P} |\chi\rangle\langle\chi|) - \operatorname{Tr} \left(\partial_{g_1} \partial_{g_2} \mathcal{L}_{g_1,g_2} [\mathcal{L}_g^{-1}]_{\mathcal{J}-\mathcal{P}} |\chi\rangle\langle\chi| \right) \right)_{g_1=g_2=g} \\
 & + 4 t^2 \operatorname{Re} \operatorname{Tr} (\partial_{g_1} \mathcal{L}_{g_1,g} \mathcal{P} \partial_{g_2} \mathcal{L}_{g,g_2} \mathcal{P} |\chi\rangle\langle\chi|)_{g_1=g_2=g} \\
 & - 8 \operatorname{Re} \operatorname{Tr} \left(\partial_{g_1} \mathcal{L}_{g_1,g} \mathcal{P} \partial_{g_2} \mathcal{L}_{g,g_2} \left[\frac{\mathcal{J} + t \mathcal{L}_g}{\mathcal{L}_g^2} \right]_{\mathcal{J}-\mathcal{P}} |\chi\rangle\langle\chi| \right)_{g_1=g_2=g} \\
 & - 8 \operatorname{Re} \operatorname{Tr} \left(\partial_{g_1} \mathcal{L}_{g_1,g} \left[\frac{\mathcal{J} + t \mathcal{L}_g}{\mathcal{L}_g^2} \right]_{\mathcal{J}-\mathcal{P}} \partial_{g_2} \mathcal{L}_{g,g_2} \mathcal{P} |\chi\rangle\langle\chi| \right)_{g_1=g_2=g} \\
 & + 8 \operatorname{Re} \operatorname{Tr} \left(\partial_{g_1} \mathcal{L}_{g_1,g} [\mathcal{L}_g^{-1}]_{\mathcal{J}-\mathcal{P}} \partial_{g_2} \mathcal{L}_{g,g_2} [\mathcal{L}_g^{-1}]_{\mathcal{J}-\mathcal{P}} |\chi\rangle\langle\chi| \right)_{g_1=g_2=g} \\
 & + t^2 \mathcal{O}(\lambda_2 t) \mathcal{O} \left(c_2 (c_2 + 1) C_1^2 \right) \\
 & + t \left\{ \mathcal{O}(\lambda_2 t) \left[\mathcal{O} \left(c_2 C_1^2 C_2 \right) + \mathcal{O} \left(c_2 C_3 \right) \right] + \right. \\
 & \quad \left. + \mathcal{O} \left((1 + c_2) C_1^2 C_2 \left\| \left[e^{t \mathcal{L}_g} \right]_{\mathcal{J}-\mathcal{P}} \right\| \right) + \mathcal{O} \left(c_2 C_1^2 C_2 \right) \mathcal{O} \left(\frac{\lambda_2}{\lambda_3} \right) \right\} \\
 & + \mathcal{O}(\lambda_2 t) \mathcal{O} \left(c_2 C_1^2 C_2^2 \right) + \mathcal{O} \left((1 + c_2) C_1^2 C_2^2 \left\| \left[e^{t \mathcal{L}_g} \right]_{\mathcal{J}-\mathcal{P}} \right\| \right) \\
 & + \mathcal{O} \left(C_2 C_3 \left\| \left[e^{t \mathcal{L}_g} \right]_{\mathcal{J}-\mathcal{P}} \right\| \right) + \mathcal{O} \left(c_2 C_1^2 C_2^2 \right) \mathcal{O} \left(\frac{\lambda_2}{\lambda_3} \right) \\
 & + \mathcal{O} \left(C_1 \left\| \sum_{j \neq k, j, k > 2}^{d^2} \frac{e^{t \lambda_j} - e^{t \lambda_k}}{\lambda_k (\lambda_j - \lambda_k)} \|\mathbf{R}_k\rangle\rangle\langle\langle L_k\| \partial_{g_2} \mathcal{L}_{g,g_2} \|\mathbf{R}_j\rangle\rangle\langle\langle L_j\| \right\| \right)_{g_2=g}, \quad (\text{B.9})
 \end{aligned}$$

where corrections in the approximation are given by $c_2 = \|\mathbf{R}_2\rangle\rangle\langle\langle L_2\|$, $C_1 = \|\partial_{g_1}|_{g_1=g} \mathcal{L}_{g_1,g}\|$, $C_2 = \left\| [\mathcal{L}_g^{-1}]_{\mathcal{J}-\mathcal{P}} \right\|$, $C_3 = \|\partial_{g_1} \partial_{g_2}|_{g_1=g_2=g} \mathcal{L}_{g_1,g_2}\|$. The above-introduced norm $\|\mathcal{X}\|$ is an operator norm for \mathcal{X} acting on matrices ρ on the system Hilbert space \mathcal{H} , induced by the trace-norm of the matrices, $\|\rho\| := \operatorname{Tr}\{\sqrt{\rho^\dagger \rho}\}$, i.e., $\|\mathcal{X}\| := \sup_{\rho} \|\mathcal{X}\rho\| / \|\rho\|$. We note that the estimate of the approxima-

tion error in Eq. (B.9) is very rough and implies strong conditions on the Master dynamics near a DPT, i.e. when the corrections are negligible. For a given model one should check the approximation by comparing to the exact results of Eq. (B.2).

Assuming that the corrections in Eq. (B.9) are negligible, there are *quadratic*, linear and constant terms in Eq. (B.9). In particular, the quadratic terms in Eq. (B.9) correspond to Eq. (2.28).

Let us note that using Eq. (B.4) does not provide clear results for the regime $\tau' \ll t \ll \tau$. From comparing Eq. (B.7) to Eq. (B.5), we see that when the gap $\lambda_2 \rightarrow 0$, many terms in Eq. (B.4) diverge. Thus, in order to simplify (B.4) when $(-\lambda_2) \ll (-\text{Re}\lambda_3)$ one needs to go back to the operators $\partial_{g_1} \mathcal{L}_{g_1,g}|_{g_1=g}$ and $\partial_{g_1} \partial_{g_2} \mathcal{L}_{g_1,g_2}|_{g_1=g_2=g}$ and to Eqs. (B.2) and (B.9).

Quadratic behaviour at a first-order DPT. At a first-order DPT we have $\lambda_2 = 0$ and the considered time-regime is infinitely long, $\tau = \infty$. Moreover, in the limit of long time t all the corrections in Eq. (B.9) are 0. Therefore, Eq. (B.9) gives asymptotic *quadratic* behaviour of the QFI, see also Eq. (2.28) in the main text,

$$\lim_{t \rightarrow \infty} t^{-2} F(|\Psi_g(t)\rangle) = -4 |\text{Tr} (\partial_{g_1} \mathcal{L}_{g_1,g} \mathcal{P}_0 |\chi\rangle\langle\chi|)|_{g_1=g}^2 + \quad (\text{B.10}) \\ + 4 \text{Re Tr} (\partial_{g_1} \mathcal{L}_{g_1,g} \mathcal{P}_0 \partial_{g_2} \mathcal{L}_{g,g_2} \mathcal{P}_0 |\chi\rangle\langle\chi|)_{g_1=g_2=g} =: f_{2,g},$$

where \mathcal{P}_0 is projection on the stationary manifold of \mathcal{L}_g consisting of two disjoint stationary states [199]. This formula can be further simplified this structure, see Appendix B.3.2 and Eq. (B.19).

The linear and constant terms in the asymptotic behaviour of QFI are given by

$$\begin{aligned}
 f_{1,g} &:= \lim_{t \rightarrow \infty} t^{-1} \left(F(|\Psi_g(t)\rangle) - t^2 f_{2,g} \right) \\
 &= 4 \operatorname{Tr} \left(\partial_{g_1} \partial_{g_2} \mathcal{L}_{g_1, g_2} \mathcal{P}_0 |\chi\rangle\langle\chi| \right)_{g_1=g_2=g} \\
 &\quad - 8 \operatorname{Re} \operatorname{Tr} \left(\partial_{g_1} \mathcal{L}_{g_1, g} \left[\mathcal{L}_g^{-1} \right]_{j-\mathcal{P}_0} \partial_{g_2} \mathcal{L}_{g, g_2} \mathcal{P}_0 |\chi\rangle\langle\chi| \right)_{g_1=g_2=g} \\
 &\quad - 8 \operatorname{Re} \operatorname{Tr} \left(\partial_{g_1} \mathcal{L}_{g_1, g} \mathcal{P}_0 \partial_{g_2} \mathcal{L}_{g, g_2} \left[\mathcal{L}_g^{-1} \right]_{j-\mathcal{P}_0} |\chi\rangle\langle\chi| \right)_{g_1=g_2=g} \\
 &\quad + 8 \operatorname{Re} \operatorname{Tr} \left(\partial_{g_1} \mathcal{L}_{g_1, g} \mathcal{P}_0 |\chi\rangle\langle\chi| \right) \operatorname{Tr} \left(\partial_{g_2} \mathcal{L}_{g, g_2} \left[\mathcal{L}_g^{-1} \right]_{j-\mathcal{P}_0} |\chi\rangle\langle\chi| \right)_{g_1=g_2=g} \quad (\text{B.11})
 \end{aligned}$$

and

$$\begin{aligned}
 f_{0,g} &:= \lim_{t \rightarrow \infty} \left(F(|\Psi_g(t)\rangle) - t^2 f_{2,g} - t f_{1,g} \right) \\
 &= -4 \left| \operatorname{Tr} \left(\partial_{g_1} \mathcal{L}_{g_1, g} \left[\mathcal{L}_g^{-1} \right]_{j-\mathcal{P}_0} |\chi\rangle\langle\chi| \right) \right|_{g_1=g}^2 \\
 &\quad - 4 \operatorname{Tr} \left(\partial_{g_1} \partial_{g_2} \mathcal{L}_{g_1, g_2} \left[\mathcal{L}_g^{-1} \right]_{j-\mathcal{P}_0} |\chi\rangle\langle\chi| \right)_{g_1=g_2=g} \\
 &\quad - 8 \operatorname{Re} \operatorname{Tr} \left(\partial_{g_1} \mathcal{L}_{g_1, g} \mathcal{P}_0 \partial_{g_2} \mathcal{L}_{g, g_2} \left[\mathcal{L}_g^{-2} \right]_{j-\mathcal{P}_0} |\chi\rangle\langle\chi| \right)_{g_1=g_2=g} \\
 &\quad - 8 \operatorname{Re} \operatorname{Tr} \left(\partial_{g_1} \mathcal{L}_{g_1, g} \left[\mathcal{L}_g^{-2} \right]_{j-\mathcal{P}_0} \partial_{g_2} \mathcal{L}_{g, g_2} \mathcal{P}_0 |\chi\rangle\langle\chi| \right) \\
 &\quad + 8 \operatorname{Re} \operatorname{Tr} \left(\partial_{g_1} \mathcal{L}_{g_1, g} \left[\mathcal{L}_g^{-1} \right]_{j-\mathcal{P}_0} \partial_{g_2} \mathcal{L}_{g, g_2} \left[\mathcal{L}_g^{-1} \right]_{j-\mathcal{P}_0} |\chi\rangle\langle\chi| \right)_{g_1=g_2=g} \quad (\text{B.12})
 \end{aligned}$$

Let us note that linear and constant terms in the asymptotic behaviour QFI depend not only on the asymptotic state $\mathcal{P}_0 (|\chi\rangle\langle\chi|)$, but also on the initial state, which corresponds to the contributions from decaying eigenmodes of \mathcal{L}_g . For detailed discussion of dependence on initial state and its coherences see Appendix B.3.2.

The asymptotic quadratic behaviour of the QFI can be also obtained from Eq. (B.4) as

$$\begin{aligned}
 F(|\Psi_g(t)\rangle) &\approx 4 t^2 c_1 c_2 \left| \partial_{g_1} \lambda_1(g_1, g) - \partial_{g_1} \lambda_2(g_1, g) \right|_{g_1=g}^2 \\
 &+ 4 t (c_1 \partial_{g_1} \partial_{g_2} \lambda_1(g_1, g_2) + c_2 \partial_{g_1} \partial_{g_2} \lambda_2(g_1, g_2))_{g_1=g_2=g} \\
 &+ 8 t \operatorname{Re} (c_2 \partial_{g_1} c_1(g_1, g) - c_1 \partial_{g_1} c_2(g_1, g)) \\
 &\quad \times (\partial_{g_2} \lambda_1(g, g_2) - \partial_{g_2} \lambda_2(g, g_2))_{g_1=g_2=g} \\
 &+ 4 \partial_{g_1} \partial_{g_2} (c_1(g_1, g_2) + c_2(g_1, g_2))_{g_1=g_2=g} \\
 &- 4 \left| \partial_{g_1} c_1(g_1, g) + \partial_{g_1} c_2(g_1, g) \right|_{g_1=g'}^2, \tag{B.13}
 \end{aligned}$$

where $\lambda_1(g_1, g_2), \lambda_2(g_1, g_2)$ are first two eigenvalues of the modified master operator \mathcal{L}_{g_1, g_2} with the largest real part and $L_1(g_1, g_2), L_2(g_1, g_2), R_1(g_1, g_2), R_2(g_1, g_2)$ are the corresponding left and right eigenmatrices, and $c_{1,2}(g_1, g_2) := \operatorname{Tr}(L_{1,2}(g_1, g_2) |\chi\rangle\langle\chi|) \times \operatorname{Tr}(R_{1,2}(g_1, g_2))$ with $c_{1,2} := c_{1,2}(g, g)$.

We note that the 0-eigenspace of \mathcal{L}_g is two-fold degenerate, $\lambda_1(g, g) = \lambda_2(g, g)$. When this degeneracy is lifted in the first order of perturbation theory (i.e. by $\mathcal{P}_0 \partial_{g_1}|_{g_1=g} \mathcal{L}_{g_1, g} \mathcal{P}_0$ or equivalently the Hermitian conjugate $\mathcal{P}_0 \partial_{g_2}|_{g_2=g} \mathcal{L}_{g, g_2} \mathcal{P}_0$) $\lambda_{1,2}(g_1, g_2)$ and also $c_{1,2}(g_1, g_2)$ are analytic in g_1 or g_2 [167]. In the next section we show that this is indeed the case, and moreover $\mathcal{P}_0 \partial_{g_1}|_{g_1=g} \mathcal{L}_{g_1, g} \mathcal{P}_0$ is diagonal in the basis of the disjoint stationary states $\tilde{\rho}_1$ and $\tilde{\rho}_2$, which further gives $c_{1,2} = p_{1,2}$ with $p_{1,2}$ being the asymptotic probabilities, $\lim_{t \rightarrow \infty} \rho(t) = p_1 \tilde{\rho}_1 + p_2 \tilde{\rho}_2$.

Higher-fold degeneracy of stationary state. In general, the degeneracy of 0-eigenspace of \mathcal{L}_g can be higher than two-fold. This may correspond not only to more disjoint stationary states, but also to some of initial coherences being preserved asymptotically within decoherence free subspaces (DFSS) or noiseless subsystems (NSSs), see Sec. 3.1.3 for derivation of general structure of stationary state manifold (SSM). The asymptotic behaviour of the QFI is in general quadratic and again given by Eqs.(B.10-B.12) with \mathcal{P}_0 being the projection on the SSM. Due to the structure of the SSM, cf. Eq. 3.3, the QFI behaviour can further understood in terms of unitary rotations, see Appendix D.3. More-

over, for \mathcal{L}_g with a separation in its spectrum, $-\text{Re } \lambda_m \ll -\text{Re } \lambda_{m+1}$, we have that Eqs. (B.10-B.12) hold in the time regime $(-\text{Re } \lambda_{m+1})^{-1} \ll t \ll (-\text{Re } \lambda_m)^{-1}$, with \mathcal{P}_0 replaced by projection \mathcal{P} on m low-lying eigenmodes and with appropriate corrections, cf. Eq. (B.9).

B.3 STOCHASTIC GENERATOR OF PARAMETER ENCODING

In this section we focus on the generator of the parameter encoding $G_g(t)$, see Eq. (2.29). We study its average and variance, see B.3.1 and their asymptotic behaviour B.3.2. Furthermore, in B.3.3 we show how for a generator being a continuous measurement to find the corresponding parameter dependence of system-output dynamics.

B.3.1 Average and variance of the stochastic generator

Here we discuss the average and variance of the stochastic integral $G_g(t)$ defined in Eqs. (2.47) and (2.48).

We have that, cf. Eq. (2.31),

$$\begin{aligned} \langle G_g(t) \rangle &= \langle \Psi_g(t) | G_g(t) | \Psi_g(t) \rangle = \int_0^t du \langle \Psi_g(u) | dG_{u,g} | \Psi_g(u) \rangle \\ &= \int_0^t du \langle \Psi_g(u) | \left[H'_g - \frac{i}{2} \sum_j \left(J_{j,g}^\dagger J'_{j,g} - (J_{j,g}^\dagger)' J_{j,g} \right) \right] | \Psi_g(u) \rangle \\ &= \int_0^t du \text{Tr}(M_g \rho_g(t)), \end{aligned}$$

where the second line follows from the fact that $dA_{j,t}$ and $dA_{j,t}^\dagger$ act in the interval $(t, t + dt]$, see Eqs. (2.47) and (2.46), at which

the output of the state $|\Psi_g(t)\rangle$ is still in vacuum. Futhermore, this also simplifies the second moment of $G_g(t)$:

$$\begin{aligned}
 \langle G_g(t)^2 \rangle &= \int_0^t \int_0^t \langle \Psi_g(u) | dG_{u,g} U_g(t, u) U_g(t, v)^\dagger dG_{v,g} | \Psi_g(v) \rangle \\
 &= \int_0^t \int_0^t \langle \Psi_g(u) | dG_{u,g} U_g(t, u) U_g(t, v)^\dagger dG_{v,g} | \Psi_g(v) \rangle \\
 &= \int_0^t \int_0^t \langle \Psi_g(u) | \left(M_g du - i(J_{j,g}^\dagger)' dA_{j,u} \right) U_g(t, u) U_g(t, v)^\dagger \\
 &\quad \times \left(M_g dv + iJ'_{j,g} dA_{j,v}^\dagger \right) | \Psi_g(v) \rangle \\
 &= \int_0^t du \int_0^u dv \left(\langle \Psi_g(u) | M_g U_g(u, v) M_g | \Psi_g(v) \rangle + \right. \\
 &\quad \left. + \langle \Psi_g(v) | M_g U_g(u, v)^\dagger M_g | \Psi_g(u) \rangle \right) \\
 &\quad + \int_0^t du \int_0^u \left(i \langle \Psi_g(u) | M_g U_g(u, v) J'_{j,g} dA_{j,v}^\dagger | \Psi_g(v) \rangle + \right. \\
 &\quad \left. - i \langle \Psi_g(v) | (J_{j,g}^\dagger)' dA_{j,v} U_g(u, v)^\dagger M_g | \Psi_g(u) \rangle \right) \\
 &\quad + \int_0^t du \langle \Psi_g(u) | (J_{j,g}^\dagger)' J'_{j,g} | \Psi_g(u) \rangle, \tag{B.14}
 \end{aligned}$$

where in the last equality we again used the fact that when $u > v$, $U_g(u, v)$ acts on the output on times $(v, u]$ and thus $dA_{j,u}$ acts within times $(u, u + du]$ when the output is in vacuum and thus the contributions $\int_0^t \int_0^u \langle \Psi_g(u) | (J_{j,g}^\dagger)' dA_{j,u} U_g(u, v) dG_{v,g} | \Psi_g(v) \rangle = 0$ and $\int_0^t \int_0^u \langle \Psi_g(v) | dG_{v,g} U_g(u, v)^\dagger J'_{j,g} dA_{j,u}^\dagger M_g | \Psi_g(u) \rangle = 0$. Note that the last term above corresponds to the second line in Eq. (B.1), while the other two terms correspond to the third line of Eq. (B.1), as tracing out the output initially in vacuum, we obtain

$$\begin{aligned}
 \langle G_g(t)^2 \rangle &= 2 \operatorname{Re} \int_0^t du \int_0^u dv \operatorname{Tr} \left(M_g e^{(u-v)\mathcal{L}_g} M_g (e^{v\mathcal{L}_g} \rho_{\text{in}}) \right) \\
 &\quad + 2 \operatorname{Re} \int_0^t du \int_0^u \operatorname{Tr} \left(M_g e^{(u-v)\mathcal{L}_g} i \left(J'_{j,g} (e^{v\mathcal{L}_g} \rho_{\text{in}}) J_{j,g}^\dagger - J_{j,g}^\dagger J'_{j,g} (e^{v\mathcal{L}_g} \rho_{\text{in}}) \right) \right) \\
 &\quad + \int_0^t du \operatorname{Tr} \left((J_{j,g}^\dagger)' J'_{j,g} e^{u\mathcal{L}_g} \rho_{\text{in}} \right), \tag{B.15}
 \end{aligned}$$

where $\rho_{\text{in}} = |\chi\rangle\langle\chi|$ in the second line we used $U_g(u, v) J'_{j,g} dA_{j,v}^\dagger = U_g(u, v + dv) dU_{g,v} J'_{j,g} dA_{j,v}^\dagger = U_g(u, v + dv) (J'_{j,g} dA_{j,v}^\dagger - J_{j,g}^\dagger J'_{j,g} dv)$,

from Eq. (2.46) and the quantum Ito rule (see e.g. [30, 39]).

Variance of the generator as integral of correlations. Note that the first line of (B.14) expresses $\Delta^2 G_g(t)$ as a double integral of the correlations between the system-output observable $dG_{t,g}$, similarly as in the case of a closed system with Hamiltonian depending linearly on Ω , $H_\Omega = H_0 + \Omega H_1$, cf. Eq. (2.42),

$$\begin{aligned} \langle \psi_\Omega(t) | G_\Omega(t)^2 | \psi_\Omega(t) \rangle &= \int_0^t du \int_0^t dv \langle \psi_\Omega(u) | H_1 e^{-i(u-v)H_\Omega} H_1 | \psi_\Omega(v) \rangle \\ &= 2 \operatorname{Re} \int_0^t du \int_0^u dv \langle \psi_\Omega(u) | H_1 e^{-i(u-v)H_\Omega} H_1 | \psi_\Omega(v) \rangle. \end{aligned}$$

Note that the above formula *does not* simply represent, however, a *measurement* of H_1 on the system at successive times v and u and then double integral of such a auto-correlation function, unless H_1 commutes with the evolution, i.e. H_Ω . Both in the closed case of $G_\Omega(t)$ [105] and the open case of $G_g(t)$ of (2.48), however, the correlations decay analogously as the auto-correlations of a measurement performed on the system, cf. Eq. (B.15). This decay is due to information being spread over the whole system (closed case) or also leaking to the environment (open case described by noisy stochastic evolution $U_g(t, 0)$).

Consider the special case of parameter estimation, when the parameter g is encoded by an integrated continuous measurement, and the fidelity plays a role of a characteristic function for that continuous measurement. The variance is a double integral of the correlations in that continuous measurement outcomes [217], which in turn correspond to the correlations of a POVM measurement on the system. For system dynamics close to a first-order DPT, there is a metastable regime where the correlations in system measurements display a plateau before eventual exponential decay to 0, which is exactly the reason for the variance of the integrated continuous measurement to grow quadratically in time during the metastable regime, see Sec. 3.3.2.

Fidelity vs. characteristic function of the generator. When the generator is independent from the encoded parameter value, $G_g(t) \equiv G(t)$, it follows directly from (2.29) that the fidelity is the characteristic function of the generator, $\langle \Psi_{g'}(t) | \Psi_g(t) \rangle = \langle \Psi(t) | e^{i(g'-g)G(t)} | \Psi(t) \rangle$. This is exactly the case for the phase encoded on the output $J_{1,\phi} = e^{-i\phi} J_1$, or the parameter being the amplitude of the homodyne current, see Eqs. (B.24) and (B.23), as we show in the next Sec. B.3.3. Here we show why for other cases, including the case of coupling constants in closed system dynamics, $H_g = H_0 + gH_1$, $J_j = 0$, considered in full counting statistics [180], the fidelity does not simply correspond to the characteristic function of the distribution of the generator $G_g(t)$ measured on $|\Psi_g(t)\rangle$ when higher than second derivatives are considered.

Consider the system-output MPS, $|\Psi_g(t)\rangle = U_g(t, 0) |\chi\rangle \otimes |\text{vac}\rangle$, expressed using the stochastic evolution $U_g(t, 0)$, cf. Eqs. (2.45) and (2.46). First let us consider g being a coupling constant, so that $dG_{t,g} = dG_t = H_1 dt$ is parameter independent and we have (cf. *Dyson expansion*)

$$\begin{aligned}
 (i)^k \partial_g^k U_g(t, 0) &= \\
 &= k! \int_0^t \int_0^{t_k} \dots \int_0^{t_2} U_g(t, t_k) dG_{t_k} U_g(t_k, t_{k-1}) dG_{t_{k-1}} \dots U_g(t_2, t_1) dG_{t_1} U(t_1, 0) \\
 &= k! \int_0^t dt_k \int_0^{t_k} dt_{k-1} \dots \int_0^{t_2} dt_1 U_g(t, t_k) H_1 U_g(t_k, t_{k-1}) H_1 \dots U_g(t_2, t_1) H_1 U(t_1, 0).
 \end{aligned}$$

Note that in all evolution operators $U_g(t_{j-1}, t_j)$ we have $t_{j-1} \geq t_j$. Now, in analogy to the parameter encoded on the output, let us consider the n -th derivative of $\langle \Psi_{g+\frac{\Delta g}{2}}(t) | \Psi_{g-\frac{\Delta g}{2}}(t) \rangle$,

$$\begin{aligned}
 & \left. \partial_{\Delta g}^n \langle \Psi_{g+\frac{\Delta g}{2}}(t) | \Psi_{g-\frac{\Delta g}{2}}(t) \rangle \right|_{\Delta g=0} \\
 &= \frac{1}{2^n} \sum_{k=0}^n (-1)^k \langle \chi | \otimes \langle \text{vac} | \partial_g^{n-k} U_g^\dagger(t, 0) \partial_g^k U_g(t, 0) | \chi \rangle \otimes | \text{vac} \rangle \\
 &= \frac{i^n}{2^n} \sum_{k=0}^n k!(n-k)! \\
 & \int_0^t dt_{k+1} \int_0^{t_{k+1}} dt_{k+2} \dots \int_0^{t_{n-1}} dt_n \int_0^t dt_k \int_0^{t_k} dt_{k-1} \dots \int_0^{t_2} dt_1 \\
 & \langle \chi | \otimes \langle \text{vac} | U_g^\dagger(t_n, 0) H_1 U_g^\dagger(t_{n-1}, t_n) H_1 \dots U_g^\dagger(t_{k+1}, t_{k+2}) H_1 U_g^\dagger(t, t_{k+1}) \\
 & \times U_g(t, t_k) H_1 U_g(t_k, t_{k-1}) H_1 \dots U_g(t_2, t_1) H_1 U(t_1, 0) | \chi \rangle \otimes | \text{vac} \rangle.
 \end{aligned}$$

As for $t \geq t'$ we have $U_g^\dagger(t, t') U_g(t, t') = \mathbb{1}$, we can formally consider $U_g^\dagger(t, t') = U_g(t', t)$ in analogy to closed case. As in general H_1 *does not commute* with $U(t_{j+1}, t_j)$, we can classify all the terms above considering possible patterns of signs in time differences $(t_n - t_{n-1}, \dots, t_2 - t_1)$ appearing in $U(t_k, t_{k-1})$ between H_1 for $n > 1$ (first and the last operator have fixed signs, + and - respectively). The patterns are of the following form: (i) for $0 < k < n$ we have $(\underbrace{-\dots-}_{n-k-1} \pm \underbrace{+\dots+}_{k-1})$, where the middle sign of $t_{k+1} - t_k$ can vary as it corresponds to composition of two stochastic unitaries, $U_g^\dagger(t, t_{k+1}) U_g(t, t_k) = U(t_{k+1}, t_k)$; (ii) $(\underbrace{-\dots-}_{n-1})$ for $k = 0$ and $(\underbrace{+\dots+}_{n-1})$ for $k = n$. Note that we have *time-ordering* in the patterns so that all (+) appear before (-).

On the other hand considering n -th moment of $G_g(t)$ we obtain

$$\begin{aligned}
 & \langle \Psi_g(t) | G_g(t)^k | \Psi_g(t) \rangle = \\
 &= \int_0^t \int_0^t \dots \int_0^t \langle \chi | \otimes \langle \text{vac} | U_g^\dagger(t_n, 0) dG_{t_1, g} U_g^\dagger(t, t_n) \\
 & \times U_g(t, t_{n-1}) dG_{t_{n-1}, g} U_g^\dagger(t, t_{n-1}) \dots U_g(t, t_1) dG_{t_1, g} U(t_1, 0) | \chi \rangle \otimes | \text{vac} \rangle.
 \end{aligned}$$

Note that as the limits in integrals are independent, we obtain all possible patterns of the signs of time differences in $U_g^\dagger(t, t_{k+1})U_g(t, t_k) = U(t_{k+1}, t_k)$, e.g. for $n = 3$ corresponding to the 3-rd moment, there exists a pattern $(+ -)$, which cannot appear in time-ordered derivatives of the fidelity (see above). This is the reason why also for methods in closed system dynamics [179] and for full counting statistics [180], where derivatives of the fidelity are effectively accessed, in general only the first and the second cumulant of an integrated system observable can be recovered, with higher derivatives corresponding to time-ordered moment-like expressions.

Note that for a general parameter g , $dG_{t,g}$ is parameter dependent. Hence, when the n -th derivative of $\langle \Psi_{g_1}(t) | \Psi_{g_2}(t) \rangle$ is considered for $n > 1$, there are additional contributions featuring $\partial_g^k dG_{t,g}$, which lead to even further difference from the n -th moment of $G_g(t)$.

In contrast, for g encoded in the system-output MPS simply as a phase of output observable we have that the encoding commutes with dynamics, i.e. encoding can be done as a modification of the Hamiltonian and jumps operators which leads to a modified MPS $|\Psi_g(t)\rangle$, or as a phase encoded on the already existing MPS, $|\Psi_g(t)\rangle = e^{-igG(t)}|\Psi(t)\rangle$. This leads to the fidelity directly corresponding to a characteristic function.

Therefore, we explained why the fidelity is not simply related to a characteristic function of $G_g(t)$ for a general parameter g in dynamics. We have instead $\langle \Psi_{g_1}(t) | \Psi_{g_2}(t) \rangle = \langle \Psi_g(t) | \mathcal{T} e^{-i \int_{g_1}^{g_2} dg' G_{g'}(t)} | \Psi_g(t) \rangle$.

B.3.2 Asymptotic average and variance

Here we derive the asymptotic expressions for the variance of $G_g(t)$ given in Eq. (2.34) corresponding to Eq. (2.28) at a first-order DPT when the gap closes, $\lambda_2 \rightarrow 0$ leading to two-fold degeneracy of the 0-eigenvalue of \mathcal{L}_g . For higher-order degeneracy see Appendix D.3.

For two-fold degeneracy of the 0-eigenvalue of \mathcal{L}_g , there are two stationary states $\tilde{\rho}_1, \tilde{\rho}_2$ supported on orthogonal subspaces

$\mathcal{H}_1, \mathcal{H}_2$. The projection on the stationary manifold is given by $\mathcal{P}_0(\cdot) = \sum_{k=1,2} \tilde{\rho}_k \text{Tr}(\tilde{\mathbb{P}}_k(\cdot))$ where the positive left eigenmatrices corresponding to 0-eigenspace of \mathcal{L}_g fulfil $\tilde{\mathbb{P}}_k \geq \mathbb{1}_{\mathcal{H}_k}$, $k = 1, 2$, (see e.g. [158]), so that $\text{Tr}(\tilde{\mathbb{P}}_k \tilde{\rho}_l) = \delta_{k,l}$ for $1 \leq k, l \leq 2$. We further have $\tilde{\mathbb{P}}_k = \mathbb{1}_{\mathcal{H}_k}$, $k = 1, 2$, when the system space $\mathcal{H} = \mathcal{H}_1 \oplus \mathcal{H}_2$, in which case the subspaces \mathcal{H}_1 and \mathcal{H}_2 are invariant under action of H_g and $L_{j,g}$, $j = 1, \dots, k$, and there exist a stationary state of full rank, $p\tilde{\rho}_1 + (1-p)\tilde{\rho}_2$ with $0 < p < 1$.

As the master operator \mathcal{L}_g generates trace-preserving dynamics, we have $\tilde{\mathbb{P}}_1 + \tilde{\mathbb{P}}_2 = \mathbb{1}_{\mathcal{H}}$. Moreover, multiplying this equality by positive $\mathbb{1}_{\mathcal{H}_2}$ from both sides, we conclude $[\tilde{\mathbb{P}}_1]_{\mathbb{1}_{\mathcal{H}_2}} = \mathbb{1}_{\mathcal{H}_2} \tilde{\mathbb{P}}_1 \mathbb{1}_{\mathcal{H}_2} = 0$ due to $\tilde{\mathbb{P}}_2 \geq \mathbb{1}_{\mathcal{H}_2}$ and analogously $[\tilde{\mathbb{P}}_2]_{\mathbb{1}_{\mathcal{H}_1}} = 0$. Therefore, for an initial state $|\chi_{1,2}\rangle$ in the subspace $\mathcal{H}_{1,2}$, we have that the asymptotic state is within the same subspace, $\lim_{t \rightarrow \infty} \rho(t) = \tilde{\rho}_{1,2}$. Now we show that initial coherence between \mathcal{H}_1 and \mathcal{H}_2 does not contribute asymptotically to the leading linear term in the average of $G_g(t)$, cf. (2.33). For $|\Psi_g^{(1,2)}(t)\rangle$ being the MPS corresponding to the initial system state $|\chi_{1,2}\rangle$ we have

$$\begin{aligned} \lim_{t \rightarrow \infty} t^{-1} \langle \Psi_g^{(1)}(t) | G_g(t) | \Psi_g^{(2)}(t) \rangle &= i \lim_{t \rightarrow \infty} t^{-1} \partial_{g'} \langle \Psi_g^{(1)}(t) | \Psi_{g'}^{(2)}(t) \rangle_{g'=g} = \\ &= i \lim_{t \rightarrow \infty} t^{-1} \partial_{g'} \text{Tr} \left(e^{t\mathcal{L}_{g',g}} |\chi_2\rangle \langle \chi_1| \right)_{g'=g} \\ &= i \partial_{g'} \text{Tr} (\mathcal{L}_{g',g} \mathcal{P}_0 |\chi_2\rangle \langle \chi_1|)_{g'=g} = 0, \end{aligned} \quad (\text{B.16})$$

where we used $\mathcal{P}_0 |\chi_2\rangle \langle \chi_1| = 0$ which we argue as follows. As positivity of $\tilde{\mathbb{P}}_1$ implies positivity of $[\tilde{\mathbb{P}}_1]_{\mathbb{1}_{\mathcal{H}_1 \oplus \mathcal{H}_2}}$, also the Schur complement w.r.t. \mathcal{H}_1 -block must be positive,

$$[\tilde{\mathbb{P}}_1]_{\mathbb{1}_{\mathcal{H}_2}} - (\mathbb{1}_{\mathcal{H}_2} \tilde{\mathbb{P}}_1 \mathbb{1}_{\mathcal{H}_1}) [\tilde{\mathbb{P}}_1]_{\mathbb{1}_{\mathcal{H}_1}}^{-1} (\mathbb{1}_{\mathcal{H}_1} \tilde{\mathbb{P}}_1 \mathbb{1}_{\mathcal{H}_2}) = - [\tilde{\mathbb{P}}_1 \mathbb{1}_{\mathcal{H}_1} \tilde{\mathbb{P}}_1]_{\mathbb{1}_{\mathcal{H}_2}} \geq 0.$$

But we also have $[\tilde{\mathbb{P}}_1 \mathbb{1}_{\mathcal{H}_1} \tilde{\mathbb{P}}_1]_{\mathbb{1}_{\mathcal{H}_2}} \geq 0$ and hence $\tilde{\mathbb{P}}_1$ is *block-diagonal* w.r.t. \mathcal{H}_1 and \mathcal{H}_2 , and $\mathbb{1}_{\mathcal{H}_2} \tilde{\mathbb{P}}_1 = \tilde{\mathbb{P}}_1 \mathbb{1}_{\mathcal{H}_2} = 0$. Analogously, $\mathbb{1}_{\mathcal{H}_1} \tilde{\mathbb{P}}_2 = \tilde{\mathbb{P}}_2 \mathbb{1}_{\mathcal{H}_1} = 0$.

For the second moment of $G_g(t)$ (cf. Eq. (2.28)) we similarly have no asymptotic contribution from the initial coherence between \mathcal{H}_1 and \mathcal{H}_2 ,

$$\begin{aligned} \lim_{t \rightarrow \infty} t^{-2} \langle \Psi_g^{(1)}(t) | G_g^2(t) | \Psi_g^{(2)}(t) \rangle &= \lim_{t \rightarrow \infty} t^{-2} \partial_{g_1} \partial_{g_2} \langle \Psi_{g_1}^{(1)}(t) | \Psi_{g_2}^{(2)}(t) \rangle_{g_1=g_2=g} \\ &= \partial_{g_1} \partial_{g_2} \operatorname{Re} \operatorname{Tr} (\mathcal{L}_{g_1,g} \mathcal{P}_0 \mathcal{L}_{g,g_2} \mathcal{P}_0 | \chi_2 \rangle \langle \chi_1 |)_{g_1=g_2=g} = 0. \end{aligned} \quad (\text{B.17})$$

The general behaviour of the variance with leading quadratic term given by rates corresponding to $\tilde{\rho}_1$ and $\tilde{\rho}_2$, cf. Eq. (2.34), can be argued as follows. Note that from Eq. (2.28) and $\mathcal{P}_0(\cdot) = \sum_{k=1,2} \tilde{\rho}_k \operatorname{Tr}(\tilde{P}_k(\cdot))$ we can write

$$\begin{aligned} \Delta^2 G_g(t) &= t^2 \left[- (p_1 \mu_1 + p_2 \mu_2)^2 + \right. \\ &\quad \left. -i \left(p_1 \mu_1 \operatorname{Tr}(\tilde{P}_1 \mathcal{L}_g^R \tilde{\rho}_1) + p_2 \mu_2 \operatorname{Tr}(\tilde{P}_2 \mathcal{L}_g^R \tilde{\rho}_2) \right) + \right. \\ &\quad \left. -i \left(p_1 \mu_2 \operatorname{Tr}(\tilde{P}_2 \mathcal{L}_g^R \tilde{\rho}_1) + p_2 \mu_1 \operatorname{Tr}(\tilde{P}_1 \mathcal{L}_g^R \tilde{\rho}_2) \right) \right] + \mathcal{O}(t), \end{aligned} \quad (\text{B.18})$$

where $p_{1,2} = \operatorname{Tr}(\tilde{P}_{1,2} \rho_{\text{in}})$ are the asymptotic probabilities between two stationary states $\tilde{\rho}_1$ and $\tilde{\rho}_2$, $\mu_{1,2} := i \operatorname{Tr}(\mathcal{L}_g^L \tilde{\rho}_{1,2})$ are the rates for $\tilde{\rho}_{1,2}$, and $\mathcal{L}_g^R := \partial_{g'} \mathcal{L}_{g,g'}|_{g'=g} = (\partial_{g'} \mathcal{L}_{g',g})^\dagger_{g'=g} =: (\mathcal{L}_g^L)^\dagger$ are the first-order deformations of the master operator \mathcal{L}_g . Note that in general \mathcal{L}_g^R connects the subspaces \mathcal{H}_1 and \mathcal{H}_2 , where the stationary states $\tilde{\rho}_1$ and $\tilde{\rho}_2$ are supported, especially when $\mathcal{L}_{g'}$ features a unique stationary state at $g' \neq g$. Yet, on average the connection is 0, i.e. $\operatorname{Tr}(\tilde{P}_1 \mathcal{L}_g^R \tilde{\rho}_2) = 0 = \operatorname{Tr}(\tilde{P}_2 \mathcal{L}_g^R \tilde{\rho}_1)$. This is due to the fact that for the MPS $|\Psi_g^{(1)}(t)\rangle$ and the system state $\rho_g^{(1)}(t)$ corresponding to the initial state $|\chi_1\rangle$ inside \mathcal{H}_1 we have

$$\begin{aligned} \left| \operatorname{Tr}(\tilde{P}_2 \mathcal{L}_g^R \tilde{\rho}_1) \right| &= \lim_{t \rightarrow \infty} t^{-1} \left| \partial_{g'} \langle \Psi_{g'}^{(1)}(t) | \tilde{P}_2 \otimes \mathbb{1}_{\text{output}} | \Psi_g^{(1)}(t) \rangle_{g'=g} \right| \\ &\leq \lim_{t \rightarrow \infty} \sqrt{t^{-2} \langle \Psi_g^{(1)}(t) | G_g(t)^2 | \Psi_g^{(1)}(t) \rangle} \sqrt{\operatorname{Tr}(\tilde{P}_2^2 \rho_g^{(1)}(t))} \\ &\leq \sqrt{\partial_{g_1} \partial_{g_2} \operatorname{Re} \operatorname{Tr} (\mathcal{L}_{g_1,g} \mathcal{P}_0 \mathcal{L}_{g,g_2} \tilde{\rho}_1)_{g_1=g_2=g}} \sqrt{\operatorname{Tr}(\tilde{P}_2 \tilde{\rho}_1)} = 0, \end{aligned}$$

where the first inequality is the Schwarz inequality and the second inequality simply follows from $\tilde{P}_2^2 \leq \tilde{P}_2$ due to $0 \leq \tilde{P}_2 \leq \mathbb{1}_{\mathcal{H}}$.

Moreover, since $\tilde{P}_1 + \tilde{P}_2 = \mathbb{1}_{\mathcal{H}}$, we also have $\text{Tr}(\tilde{P}_1 \mathcal{L}_g^R \tilde{\rho}_1) = \text{Tr}(\mathcal{L}_g^R \tilde{\rho}_1) = i\mu_1$ and $\text{Tr}(\tilde{P}_2 \mathcal{L}_g^R \tilde{\rho}_2) = i\mu_2$. Thus, we arrive at

$$\Delta^2 G_g(t) = t^2 p_1 p_2 (\mu_1 - \mu_2)^2 + \mathcal{O}(t), \quad (\text{B.19})$$

as in Eq. (2.34). The above argument can be generalised to the case of \mathcal{L}_g with a unique stationary state, but with small gap, i.e. $0 > \lambda_2 \gg \text{Re}(\lambda_3)$, see derivation in D.1.

Note that the result in Eq. (B.19) can be also obtained when the eigendecomposition of $\mathcal{L}_{g,g'}$ is considered explicitly, see (B.3). Due to a diagonal first-order perturbation, $\mathcal{P}_0 \partial_{g'}|_{g'=g} \mathcal{L}_{g,g'} \mathcal{P}_0$ in $\mathcal{L}_{g,g'}$, for the first moment of $G_g(t)$, we have

$$\begin{aligned} \lim_{t \rightarrow \infty} t^{-1} \langle \Psi_g^{(1)}(t) | G_g(t) | \Psi_g^{(2)}(t) \rangle &= i \lim_{t \rightarrow \infty} t^{-1} \partial_{g'} \text{Tr} \left(e^{t\mathcal{L}_{g',g}} |\chi_2\rangle \langle \chi_1| \right)_{g'=g} = \\ &= i (p_1 \partial_{g'} \lambda_1(g', g) + p_2 \partial_{g'} \lambda_2(g', g))_{g'=g}, \end{aligned}$$

and thus we conclude $\mu_{1,2} = i \partial_{g'} \lambda_{1,2}(g', g)|_{g'=g}$. Finally, the quadratic terms of the variance are simply given by the difference of the first derivatives of the leading \mathcal{L}_{g_1, g_2} eigenvalues, $t^2 p_1 p_2 |\partial_{g'} \lambda_1(g', g) - \partial_{g'} \lambda_2(g', g)|_{g'=g}^2$ (cf. Eq. (B.13)), which gives the result in (B.19). This approach cannot be used, however, to argue the quadratic regime in the variance, when $\lambda_2 < 0$, see Sec. B.2.3.

For $G_g(t)$ corresponding to a continuous measurements, such as photon counting or homodyne current, it can be analogously argued for higher cumulants that the leading terms do not depend on initial coherences between \mathcal{H}_1 and \mathcal{H}_2 , but only on the probabilities in the asymptotic state, $p_1 \tilde{\rho}_1 + p_2 \tilde{\rho}_2$ and the corresponding rates, μ_1 and μ_2 .

Sub-leading terms in asymptotic statistics. Let us now focus on sub-leading linear and constant terms in the asymptotic behaviour of the variance $\Delta G_g^2(t)$ which depend not only at the asymptotic state, but also initial state, see Eqs. (B.11) and (B.12).

Let us first consider constant terms in the average $\langle G_g(t) \rangle$, for an initial state ρ_{in} . We have

$$\begin{aligned}
 & \lim_{t \rightarrow \infty} (\langle G_g(t) \rangle - t(p_1 \mu_1 + p_2 \mu_2)) = \\
 & = i \lim_{t \rightarrow \infty} \left(\text{Tr} \left(\int_0^t dt' \partial_{g'} \mathcal{L}_{g',g} e^{t' \mathcal{L}_g} \rho_{\text{in}} \right) - \text{Tr} \left(\int_0^t dt' \partial_{g'} \mathcal{L}_{g',g} \mathcal{P}_0 \rho_{\text{in}} \right) \right)_{g'=g} = \\
 & = -i \text{Tr} \left(\partial_{g'} \mathcal{L}_{g',g} \left[\mathcal{L}_g^{-1} \right]_{\mathcal{J}-\mathcal{P}_0} \rho_{\text{in}} \right)_{g'=g}. \tag{B.20}
 \end{aligned}$$

Therefore, all the other decaying modes give a constant contributions, as after their decay there do not contribute to the dynamics. In particular, the initial coherence between the subspaces \mathcal{H}_1 and \mathcal{H}_2 asymptotically contributes only to the constant in the average $\langle G_g(t) \rangle$. When there is no decay subspace \mathcal{H}_0 , we can separate the contribution from all coherences between \mathcal{H}_1 and \mathcal{H}_2 , as the structure of $\mathcal{L}_g = \mathcal{L}_g^{(1)} \oplus \mathcal{L}_g^{(2)} \oplus \mathcal{L}_g^{(12)} \oplus \mathcal{L}_g^{(21)}$ separates into blocks (as we have $H = H^{(1)} \oplus H^{(2)}$, $J_j = J_j^{(1)} \oplus J_j^{(2)}$) and the coherences undergo generalised dephasing [199].

For discussion of sub-leading terms in the variance $\Delta^2 G_g(t)$, let us assume that \mathcal{L}_g dynamics features no decay subspace \mathcal{H}_0 . First, consider an initial system state ρ_{in} initially supported within only one of the subspaces \mathcal{H}_1 or \mathcal{H}_2 , so that it evolves into one of the stationary states, ρ_1, ρ_2 , respectively. Note that dynamics is reduced to $\mathcal{L}_g^{(1)}, \mathcal{L}_g^{(2)}$, respectively. Therefore, the variance scales linearly, as in the case of dynamics with a single stationary state, see Eq. (2.27), but with $\mathcal{J} - \mathcal{P}_{\text{ss}}$ replaced by $\mathcal{J}_{\mathcal{H}_{1,2}} - \mathcal{P}_{\text{ss}}^{(1,2)}$, and the constant terms given as in (B.6), cf. Eqs. (B.11) and (B.12). Secondly, for an initial state being a mixture of states supported in \mathcal{H}_1 and \mathcal{H}_2 , $\rho_{\text{in}} = p_1 \rho_{\text{in}}^{(1)} + p_2 \rho_{\text{in}}^{(2)}$, so that it evolves into a mixture of the stationary states, $p_1 \tilde{\rho}_1 + p_2 \tilde{\rho}_2$, we have that the distribution of $G_g(t)$ is just a mixture of the distributions for $\rho_{\text{in}}^{(1)}$ and $\rho_{\text{in}}^{(2)}$. We have

$$\begin{aligned}
 \Delta^2 G_g(t) & = p_1 \Delta_{\rho_{\text{in}}^{(1)}}^2 G_g(t) + p_2 \Delta_{\rho_{\text{in}}^{(2)}}^2 G_g(t) + \\
 & + p_1 p_2 \left(\langle G_g(t) \rangle_{\rho_{\text{in}}^{(1)}} - \langle G_g(t) \rangle_{\rho_{\text{in}}^{(2)}} \right)^2.
 \end{aligned}$$

The variances for $\rho_{\text{in}}^{(1)}$ and $\rho_{\text{in}}^{(2)}$ with probabilities p_1, p_2 gives linear (see the first two lines of (B.11)) and constant contribution and the difference in averages asymptotically leads to quadratic terms as in Eq. (2.34) and additional linear (last two lines of (B.11)) and constant terms (see the first line of (B.12)) when the asymptotic constants in the $G_g(t)$ average are different, cf. Eq. (B.20). When there are initial coherences in ρ_{in} between \mathcal{H}_1 and \mathcal{H}_2 , $\rho_{\text{in}}^{(\text{coh})} = \rho_{\text{in}}^{(12)} + \rho_{\text{in}}^{(21)}$ with $\text{Tr}(\rho_{\text{in}}^{(\text{coh})}) = 0$, as a consequence of interference we have an additional contribution to the linear terms of the variance given by

$$\begin{aligned} & 2 p_2 (\mu_2 - \mu_1) \text{Re Tr} \left(i \mathcal{L}_{g,g'} \left[\mathcal{L}_g^{-1} \right]_{\mathcal{J}-\mathcal{P}_0} \rho_{\text{in}}^{(12)} \right)_{g'=g} \\ & + 2 p_1 (\mu_1 - \mu_2) \text{Re Tr} \left(i \mathcal{L}_{g,g'} \left[\mathcal{L}_g^{-1} \right]_{\mathcal{J}-\mathcal{P}_0} \rho_{\text{in}}^{(21)} \right)_{g'=g} \end{aligned}$$

This additional linear contribution disappears when

$$(\partial_{g'}|_{g'=g} \mathcal{L}_{g,g'} \mathbb{1}_{\mathcal{H}_1}) \mathbb{1}_{\mathcal{H}_2} = 0 = (\partial_{g'}|_{g'=g} \mathcal{L}_{g,g'} \mathbb{1}_{\mathcal{H}_2}) \mathbb{1}_{\mathcal{H}_1},$$

see e.g. in the case of photon counting, see Sec. 2.2.4. The constant contributions due to coherences in order to disappear require also that $\partial_{g_1} \partial_{g_2}|_{g_1=g_2=g} \mathcal{L}_{g_1,g_2}$ is block-diagonal, cf. (B.12).

Higher-fold degeneracy of stationary manifold. We have shown that quadratic scaling of $\Delta^2 G_g(t)$ for dynamics featuring two stationary states, Eq. (2.34), is a consequence of bimodal statistics of the observable $G_g(t)$. In the case of a higher than two-fold degeneracy of the 0-eigenvalue of \mathcal{L}_g , the stationary state might have preserved coherences, see Sec. 3.1.3, but the variance scaling is at most quadratic with time, cf. Eq. (2.28). When there are no coherences preserved, and the stationary manifold is classical composed of m stationary states, $\tilde{\rho}_1, \dots, \tilde{\rho}_m$, supported on orthogonal subspaces, $\mathcal{H}_1 \oplus \mathcal{H}_2 \oplus \dots \oplus \mathcal{H}_m \subset \mathcal{H}$, the $G_g(t)$ statistics can be understood as featuring m modes with the leading orders in the average and variance determined by the asymptotic probabilities, $\lim_{t \rightarrow \infty} \rho(t) = \sum_{l=1}^m p_l \tilde{\rho}_l$ and different rates of m stationary states (due to a first order DPT).

In general, however, the leading quadratic term may crucially depend on initial system coherences that do not decay and quadratically scaling precision may be achieved even when there is no first-order DPT and measurements are performed on the system only, cf. Sec. 2.4.3, which is due to change of g inducing a unitary dynamics of coherences. See Appendix D.3 for further discussion.

B.3.3 Reverse engineering of dynamics for a given stochastic generator

Here we present how the parameter dependence of the Hamiltonian and jump operators in the master equation, see Eq. (2.1), can be found for a given stochastic generator. We consider an example of a parameter g encoded either as the amplitude or the phase in *homodyne current*.

Let us first consider the stochastic equation for the homodyne current on quanta emitted due to a jump J_1 (see e.g. [30, 39]),

$$Z_t = e^{-i\phi} A_{1,t} + e^{i\phi} A_{1,t}^\dagger \quad (\text{B.21})$$

$$dZ_{t,g}^{(\text{out})} = e^{-i\phi} dA_{1,t} + e^{i\phi} dA_{1,t}^\dagger + \left(e^{-i\phi} J_{1,g,t} + e^{i\phi} J_{1,g,t}^\dagger \right) dt \quad (\text{B.22})$$

where $Z_{t,g}^{(\text{out})} = U_g(t,0)^\dagger Z_t U_g(t,0)$ and $J_{1,g,t} = U_g(t,0)^\dagger J_{1,g} U_g(t,0)$ is the *Heisenberg picture*. As in the Heisenberg picture we have that $U_g(t,0)^\dagger G_g(t) U_g(t,0) = \int_0^t U_g(u,0)^\dagger dG_{u,g} U_g(u,0)$, by comparing to the increment in Eq. (2.47), $U_g(t,0) dZ_{t,g}^{(\text{out})} U_g(t,0)^\dagger = dG_{t,g}$, we obtain

$$\begin{aligned} e^{i\phi} &= iJ'_{1,g}, \\ e^{-i\phi} J_{1,g} + e^{i\phi} J_{1,g}^\dagger &= H'_g + \frac{i}{2} \left(J_{1,g}^\dagger J'_{1,g} - (J_{1,g}^\dagger)' J_{1,g} \right) \\ &= H'_g + \frac{1}{2} \left(e^{i\phi} J_{1,g}^\dagger + e^{-i\phi} J_{1,g} \right), \end{aligned}$$

which further leads to

$$H_g = H_0 + \frac{g}{2} \left(e^{i\phi} J_1^\dagger + e^{-i\phi} J_1 \right), \quad (\text{B.23})$$

$$J_{1,g} = J_1 - ig e^{i\phi} \quad (\text{B.24})$$

$$\mathcal{L}_{g,g'} \rho = \mathcal{L}_0 \rho - i(g - g')(e^{i\phi} \rho J_1^\dagger + e^{-i\phi} J_1 \rho) - \frac{(g - g')^2}{2} \rho, \quad (\text{B.25})$$

$$M_g = e^{i\phi} J_1^\dagger + e^{-i\phi} J_1, \quad (\text{B.26})$$

and we see that the chosen parameter encoding corresponds to g encoded as the *amplitude* of the homodyne current. On the other hand, for the choice of the parameter encoded as the *angle* of the homodyne current, $g = \phi$, the generator depends on the parameter value, and we arrive at

$$H_\phi = H_0 - \phi + \frac{i}{2} \left(e^{i\phi} J_1^\dagger - e^{-i\phi} J_1 \right), \quad (\text{B.27})$$

$$J_{1,\phi} = J_1 - ie^{i\phi} \quad (\text{B.28})$$

$$\begin{aligned} \mathcal{L}_{\phi,\phi'} \rho &= \mathcal{L}_0 \rho - (e^{i\phi} - e^{i\phi'}) \rho J_1^\dagger + (e^{-i\phi} - e^{-i\phi'}) J_1 \rho + \\ &\quad - (1 - \cos(\phi - \phi')) \rho, \end{aligned} \quad (\text{B.29})$$

$$M_\phi = e^{i\phi} J_1^\dagger + e^{-i\phi} J_1. \quad (\text{B.30})$$

Note that the first two derivatives of $\mathcal{L}_{\phi,\phi'}$ in both cases of the amplitude g and the angle ϕ are exactly the same, leading to the same QFI for estimation of those parameters. The higher order derivatives, however, disappear for the amplitude, but are non-zero for the angle.

Similarly, consider *counting measurement* associated with quanta emitted as a result of jump J_1 . We have $d\Lambda_{t,\phi}^{(\text{out})} = d\Lambda_t + J_{1,\phi,t}^\dagger dA_{1,t} + J_{1,\phi,t} dA_{1,t}^\dagger + J_{1,\phi,t}^\dagger J_{1,\phi,t} dt$. Note that we can shift $\Lambda_{t,\phi}$ by Λ_t which $\equiv 0$ on the considered MPS states, as they feature the output initially in vacuum. After a short calculation, we arrive at $J_{1,\phi} = e^{-i\phi} J_1$ and the rest of jumps and the Hamiltonian independent from ϕ , exactly as discussed in Sec. 2.2.4.

Let us note that in all three cases $\mathcal{L}_g = \mathcal{L}_0$, which is a consequence of the fact that the parameter g is encoded on the output. The transformation in Eqs. (B.24, B.23) and (B.28, B.27) are examples of a non-unique representation of \mathcal{L} , see also Chapter 7.

in [158].

Purifications and QFI. Different representations of \mathcal{L}_g correspond, via the MPSs $|\Psi_g(t)\rangle$, to different *purifications* of the system state $\rho_g(t)$. In [15, 68] it was demonstrated how the quantum Fisher information of the system state $\rho_g(t)$ can be obtained as a minimum QFI over all possible purifications of $\rho_g(t)$. Note that in the case when the generator is encoded on the output, one can choose the Hamiltonian and jump operators at $g = 0$, which leads to no dependence on the parameter g and thus QFI being exactly 0, reflecting the fact that the system state $\rho_g(t) = \rho(t)$ is independent from the value of g .



APPENDIX TO CHAPTER 3

C.1 METASTABILITY IN BIMODAL CASE

Below we prove that in the bimodal case $m = 2$, the extreme metastable states are approximately disjoint. We show that by constructing a division of the system Hilbert space, $\mathcal{H} = \mathcal{H}_1 \oplus \mathcal{H}_2$, so that each of the two eMS is approximately supported within the respective subspace, $\text{Tr} \left(\mathbb{1}_{\mathcal{H}_{1,2}} \tilde{\rho}_{1,2} \right) \geq 1 - \mathcal{O}(C)$, where C are the corrections to the stationarity in the metastable regime, cf. Eq. (3.8).

Proof. The stationary state ρ_{ss} is a mixture of the two eMS, $\rho_{\text{ss}} = p_1^{\text{ss}} \tilde{\rho}_1 + p_2^{\text{ss}} \tilde{\rho}_2$, with $p_1^{\text{ss}} = -c_2^{\text{min}}/\Delta c_2$ and $p_2^{\text{ss}} = c_2^{\text{max}}/\Delta c_2$. We define the orthogonal subspaces

$$\mathcal{H}_1 = \text{span} \{ |\psi_k\rangle, k = 1, \dots, D : \langle \psi_k | \tilde{\mathcal{P}}_1 | \psi_k \rangle \geq p_1^{\text{ss}} \}, \quad (\text{C.1})$$

$$\mathcal{H}_2 = \text{span} \{ |\psi_k\rangle, k = 1, \dots, D : \langle \psi_k | \tilde{\mathcal{P}}_2 | \psi_k \rangle > p_2^{\text{ss}} \}, \quad (\text{C.2})$$

where $\{ |\psi_k\rangle \}_{k=1}^D$ is the orthonormal eigenbasis of L_2 and also of $\tilde{\mathcal{P}}_1$ and $\tilde{\mathcal{P}}_2 = 1 - \tilde{\mathcal{P}}_1$, cf. (3.12).

Let $|\psi_1\rangle$ and $|\psi_2\rangle$ denote the eigenvectors of L_2 corresponding to the extreme eigenvalues c_2^{max} and c_2^{min} and let $\rho_1(t)$, $\rho_2(t)$ be the system state initially in $|\psi_1\rangle$, $|\psi_2\rangle$, respectively. From the orthogonality of the \mathcal{L} eigenmodes (also in the case of Jordan blocks in $\mathcal{J} - \mathcal{P}$), it follows that

$$\text{Tr} \left(\tilde{\mathcal{P}}_1 \rho_2(t) \right) = p_1^{\text{ss}} (1 - e^{t\lambda_2}), \quad (\text{C.3})$$

$$\text{Tr} \left(\tilde{\mathcal{P}}_2 \rho_1(t) \right) = p_2^{\text{ss}} (1 - e^{t\lambda_2}). \quad (\text{C.4})$$

From positivity of the state $\rho_1(t)$ and the fact that $\mathbb{1}_{\mathcal{H}_1}$ is diagonal in the eigenbasis of $\tilde{\mathcal{P}}_1$, we also have

$$\mathrm{Tr} \left(\tilde{\mathcal{P}}_1 \rho_2(t) \right) \geq \mathrm{Tr} \left(\mathbb{1}_{\mathcal{H}_1} \tilde{\mathcal{P}}_1 \rho_2(t) \right) \geq p_1^{\mathrm{ss}} \mathrm{Tr} \left(\mathbb{1}_{\mathcal{H}_1} \rho_2(t) \right) \quad (\text{C.5})$$

where we used the definition of \mathcal{H}_1 . Together with Eq. (C.3) it follows that

$$\mathrm{Tr} \left(\mathbb{1}_{\mathcal{H}_1} \tilde{\rho}_2 \right) \leq \mathrm{Tr} \left(\mathbb{1}_{\mathcal{H}_1} \rho_2(t) \right) + \mathcal{O}(C) \leq (1 - e^{-t\lambda_2}) + \mathcal{O}(C) = \mathcal{O}(C), \quad (\text{C.6})$$

where C are the corrections to the stationarity in the metastable regime, cf. Eq. (3). Analogously, $\mathrm{Tr} \left(\mathbb{1}_{\mathcal{H}_2} \tilde{\rho}_1 \right) < \mathcal{O}(C)$, which ends the proof. Let us note that this argument is analogous to the case of $m = 2$ in classical systems [48]. ■

C.2 METASTABILITY OF PERTURBED DYNAMICS WITH DEGENERATE STATIONARY MANIFOLD

c.2.1 Complete positivity of dynamics projected on SSM

Here we prove that $[\tilde{\mathcal{L}}^{(2)}]_{\mathcal{P}_0}$ and $\tilde{\mathcal{L}}^{(1)}$, Eq. (3.28), generate CPTP dynamics on the SSM given by \mathcal{P}_0 .

We will use Theorem 3.17 from [218] on convergence of one-parameter semigroups, whose statement we recall here for the special case of finite dimensional spaces. Let $\mathcal{Z}(x)$, \mathcal{Z} be generators of one-parameter semigroups $\mathcal{T}^t(x) := e^{t\mathcal{Z}(x)}$, $\mathcal{T}^t := e^{t\mathcal{Z}}$ on a Banach space \mathcal{B} , and assume that for each Y in a spanning set of \mathcal{B} there exist $Y(x) \in \mathcal{B}$ such that $\lim_{x \rightarrow 0} Y(x) = Y$ and $\lim_{x \rightarrow 0} \mathcal{Z}(x)(Y(x)) = \mathcal{Z}(Y)$. Then for all T the limit $\lim_{x \rightarrow 0} \sup_{t \leq T} \|\mathcal{T}^t(x)(Y) - \mathcal{T}^t(Y)\| = 0$, where $\|\cdot\|$ is the norm in \mathcal{B} .

Proof for $[\tilde{\mathcal{L}}^{(2)}]_{\mathcal{P}_0}$. To prove the CPTP property consider $|\psi\rangle = \frac{1}{\sqrt{D}} \sum_{i=1}^D |e_i\rangle \otimes |e_i\rangle \in \mathcal{H} \otimes \mathcal{H}$, where $\{|e_i\rangle\}_{i=1}^D$ is an orthonormal basis of the system space \mathcal{H} . We choose $Y = (\mathcal{P}_0 \otimes \mathcal{J}) (|\psi\rangle\langle\psi|) \in \mathcal{B}(\mathcal{H} \otimes \mathcal{H})$ and $\mathcal{Z} = [\tilde{\mathcal{L}}^{(2)}]_{\mathcal{P}_0} \otimes \mathcal{J}$ so that $M_t := \mathcal{T}^t(Y)$ is the Choi matrix for $e^{\tilde{\mathcal{L}}^{(2)}} \mathcal{P}_0$. By choosing appropriate CPTP gener-

ators $\mathcal{Z}(x)$ and matrices Y_x we will show that M_t is a limit of Choi matrices of quantum channels. Thus for all t , M_t is positive and $\text{Tr}_1(M_t) = \frac{1}{D} I_{\mathcal{H}}$, where Tr_1 denotes the partial trace over the first subsystem in $\mathcal{H} \otimes \mathcal{H}$, and consequently $\tilde{\mathcal{L}}^{(2)}$ generates CPTP dynamics on the SSM given by \mathcal{P}_0 . To prove this, we choose $\mathcal{Z}(x) = x^{-2}(\mathcal{L}(x) - x[\mathcal{L}^{(1)}]_{\mathcal{P}_0}) \otimes \mathcal{J}$, which is a CPTP generator on $\mathcal{H} \otimes \mathcal{H}$ as $[\mathcal{L}^{(1)}]_{\mathcal{P}_0}$ is a generator of unitary quantum dynamics. By defining $Y(x) = Y + xY^{(1)} + x^2Y^{(2)}$, where $Y^{(1)} = -(\mathcal{S}\mathcal{L}^{(1)} \otimes \mathcal{J}) Y$ and $Y^{(2)} = (\mathcal{S}\mathcal{L}^{(1)}\mathcal{S}\mathcal{L}^{(1)} \otimes \mathcal{J}) Y - (\mathcal{S}\mathcal{L}^{(2)} \otimes \mathcal{J}) Y$ are the first and second order perturbation of Y when $\tilde{\mathcal{L}}^{(1)} = 0$, cf. (3.27), we arrive at the conditions of the theorem 3.17 in [218] with the norm $\|\cdot\|$ being the trace norm. We note that the generator property of $[\tilde{\mathcal{L}}^{(2)}]_{\mathcal{P}_0}$ was previously discussed in [206] for the special case of the Hamiltonian perturbation and $\tilde{\mathcal{L}}^{(1)} = 0$ (see Eq. (3.25)). ■

Proof for $\tilde{\mathcal{L}}^{(1)}$. Similarly, to prove that $\tilde{\mathcal{L}}^{(1)} = [\mathcal{L}^{(1)}]_{\mathcal{P}_0}$ generates CPTP dynamics on the SSM given by \mathcal{P}_0 , we need to choose $Y = (\mathcal{P}_0 \otimes \mathcal{J}) (|\psi\rangle\langle\psi|)$ and $\mathcal{Z} = \tilde{\mathcal{L}}^{(1)} \otimes \mathcal{J}$. By considering $\mathcal{Z}(x) = x^{-1}\mathcal{L}(x) \otimes \mathcal{J}$ and $Y(x) = Y - x(\mathcal{S}\mathcal{L}^{(1)} \otimes \mathcal{J}) Y$ we arrive at the conditions of the theorem 3.17 in [218]. We note that $\tilde{\mathcal{L}}^{(1)}$ was proven to be a unitary generator in [57, 58]. ■

c.2.2 Initial relaxation timescale

Here we prove the initial relaxation timescale $\tau''(x)$ of the metastable regime follows Eq. (3.33).

Proof. Consider the Dyson-Philips expansion for $e^{t\mathcal{L}(x)}$, see also Lemma 7.1 in [158],

$$e^{t\mathcal{L}(x)} = e^{t\mathcal{L}_0} + \int_0^t du e^{(t-u)\mathcal{L}_0} \delta\mathcal{L}(x) e^{u\mathcal{L}(x)}, \quad (\text{C.7})$$

where $\delta\mathcal{L}(x) := \mathcal{L}(x) - \mathcal{L}_0 = s\mathcal{L}^{(1)} + x^2\mathcal{L}^{(2)}$ is considered as a perturbation of \mathcal{L}_0 , cf. Eq. (3.25). As both $\mathcal{L}(x)$ and \mathcal{L}_0 are CPTP generators, and $\|\mathcal{J}\| = 1$ for \mathcal{J} positive and trace-preserving [219],

we have $\|e^{t\mathcal{L}(x)}\| = \|e^{t\mathcal{L}_0}\| = 1$. Using the expression (3.27) for $\mathcal{P}(x)$, we obtain

$$\begin{aligned} [e^{t\mathcal{L}(x)}]_{\mathcal{J}-\mathcal{P}(x)} &= (\mathcal{J} - \mathcal{P}_0) e^{t\mathcal{L}_0} (\mathcal{J} - \mathcal{P}_0) \\ &+ x \left[-(\mathcal{J} - \mathcal{P}_0) e^{t\mathcal{L}_0} \mathcal{P}^{(1)} - \mathcal{P}^{(1)} e^{t\mathcal{L}_0} (\mathcal{J} - \mathcal{P}_0) \right] + \mathcal{O}(x^2) \\ &+ (\mathcal{J} - \mathcal{P}_0) \int_0^t du e^{(t-u)\mathcal{L}_0} \delta\mathcal{L}(x) e^{u\mathcal{L}(x)} (\mathcal{J} - \mathcal{P}_0) + t \mathcal{O}(x^2 \|\mathcal{L}^{(1)}\|). \end{aligned} \quad (\text{C.8})$$

In the second line we used the multiplicativity of the norm, and $\|\mathcal{P}(x) - \mathcal{P}_0\| = \mathcal{O}(x)$. In the third line we bound the integral in Eq. (C.7) by $t \|\delta\mathcal{L}(x)\| \leq t(x\|\mathcal{L}^{(1)}\| + x^2\|\mathcal{L}^{(2)}\|)$ and together with $\|\mathcal{P}(x) - \mathcal{P}_0\| = \mathcal{O}(x)$ we arrive at the correction $t \mathcal{O}(x^2 \|\mathcal{L}^{(1)}\|)$.

We now use the following definition of the relaxation time τ_0 of dynamics \mathcal{L}_0 , as the shortest timescale such that for any initial state ρ_{in} , the system state relaxes to the stationary state as $\|e^{t\mathcal{L}_0}\rho_{\text{in}} - \mathcal{P}_0\rho_{\text{in}}\| \leq 2e^{-t/\tau_0}$, which implies $\|e^{t\mathcal{L}_0}(\mathcal{J} - \mathcal{P})\| \leq 4e^{-t/\tau_0}$ due to multiplicativity of the norm. From Eq. (C.8) we get

$$\begin{aligned} \|[e^{t\mathcal{L}(x)}]_{\mathcal{J}-\mathcal{P}(x)}\| &\leq \|[e^{t\mathcal{L}_0}]_{\mathcal{J}-\mathcal{P}_0}\| + 2x \|[e^{t\mathcal{L}_0}]_{\mathcal{J}-\mathcal{P}_0}\| \|\mathcal{S}\| \|\mathcal{L}^{(1)}\| + \mathcal{O}(x^2) \\ &+ 2 \int_0^t du \|[e^{(t-u)\mathcal{L}_0}]_{\mathcal{J}-\mathcal{P}_0}\| \|\delta\mathcal{L}(x)\| + t \mathcal{O}(x^2 \|\mathcal{L}^{(1)}\|) \\ &\leq 4e^{-t/\tau_0}(1 + 2x) + 8x\tau_0\|\mathcal{L}^{(1)}\| + \mathcal{O}(x^2) + t \mathcal{O}(x^2 \|\mathcal{L}^{(1)}\|) \\ &\leq 4e^{-t/\tau_0}(1 + 2x) + \mathcal{O}(x) + t \mathcal{O}(x^2 \|\mathcal{L}^{(1)}\|). \end{aligned} \quad (\text{C.9})$$

Note that the correction $t \mathcal{O}(x^2 \|\mathcal{L}^{(1)}\|)$ for times $t \ll \tau'(x)$ is of the same order as the leading corrections to the invariance of the MM, cf. Eq. (3.34), and hence does not determine the timescale $\tau''(x)$ of the initial relaxation. Therefore, for times $\tau_0 \ll t \ll \tau'(x)$, the contribution from the fast decaying modes is a sum of terms of the order $\mathcal{O}(x)$ and of the same order as the corrections to the invariance of the MM. Similar results would be obtained for τ_0 defined so that $\int_0^{\tau_0} dt \|e^{t\mathcal{L}_0}\rho_{\text{sup}} - \mathcal{P}_0\rho_{\text{sup}}\| = \sup_{\rho_{\text{in}}} \frac{1}{2} \int_0^\infty dt \|e^{t\mathcal{L}_0}\rho_{\text{in}} - \mathcal{P}_0\rho_{\text{in}}\|$, where ρ_{sup} is ρ_{in} that gives the supremum. ■

Note that iteration of Eq. (C.7) for $e^{u\mathcal{L}(x)}$ leads to Dyson-Philips series in x . This series is analytic, due to $\mathcal{L}(x)$ being analytic, cf. Eq. (3.25). As $I - \mathcal{P}(x)$ is also analytic in x , Eq. (C.8) corresponds to the analytic series in x , which we exploit to show that the initial relaxation timescale for $\mathcal{L}(x)$ can be chosen as $\tau''(x) = \tau_0$.

c.2.3 Effective long-time dynamics timescale

Here we derive Eq. (3.34) which shows the dissipative corrections to the dynamics inside the MM, $[e^{t\mathcal{L}(x)}]_{\mathcal{P}(x)}$, and thus determines the longer timescale $\tau'(x)$ of the metastable regime, see Eq. (3.35).

Derivation. The derivation below is analogous to the results of the appendix in [58]. For times $t \ll \tau'(x)$ the unitary contribution to the dynamics, $tx\tilde{\mathcal{L}}^{(1)} = tx[\mathcal{L}^{(1)}]_{\mathcal{P}_0}$, cannot be neglected (see also [57]). In order to derive the perturbation series in x for $[e^{t\mathcal{L}(x)}]_{\mathcal{P}(x)}$, we consider the Dyson-Philips expansion for $[\mathcal{L}(x)]_{\mathcal{P}(x)}$ with $\delta\tilde{\mathcal{L}}(x) := [\mathcal{L}(x)]_{\mathcal{P}(x)} - x\tilde{\mathcal{L}}^{(1)}$ is treated as a perturbation,

$$\begin{aligned} [e^{t\mathcal{L}(x)}]_{\mathcal{P}(x)} &= \mathcal{P}(x) e^{t[\mathcal{L}(x)]_{\mathcal{P}(x)}} \mathcal{P}(x) \\ &= \mathcal{P}(x) \left(e^{tx\tilde{\mathcal{L}}^{(1)}} + \int_0^t du e^{(t-u)x\tilde{\mathcal{L}}^{(1)}} \delta\tilde{\mathcal{L}}(x) e^{u[\mathcal{L}(x)]_{\mathcal{P}(x)}} \right) \mathcal{P}(x), \end{aligned} \quad (\text{C.10})$$

Using $\mathcal{P}(x) = \mathcal{P}_0 + x\mathcal{P}^{(1)} + \mathcal{O}(x^2)$, see Eq. (3.27), and $e^{x[\mathcal{L}(x)]_{\mathcal{P}(x)}} \mathcal{P}(x) = \mathcal{P}(x) e^{u\mathcal{L}(x)} \mathcal{P}(x)$ we obtain

$$\begin{aligned} [e^{t\mathcal{L}(x)}]_{\mathcal{P}(x)} &= \mathcal{P}_0 e^{tx\tilde{\mathcal{L}}^{(1)}} \mathcal{P}_0 + x \left(\mathcal{P}^{(1)} e^{tx\tilde{\mathcal{L}}^{(1)}} \mathcal{P}_0 + \mathcal{P}_0 e^{tx\tilde{\mathcal{L}}^{(1)}} \mathcal{P}^{(1)} \right) + \mathcal{O}(x^2) + \\ &+ \mathcal{P}_0 \int_0^t du e^{(t-u)x\tilde{\mathcal{L}}^{(1)}} \delta\tilde{\mathcal{L}}(x) \mathcal{P}(x) e^{u\mathcal{L}(x)} \mathcal{P}_0 + t \mathcal{O}(x^3 \|\tilde{\mathcal{L}}^{(2)}\|), \end{aligned} \quad (\text{C.11})$$

where the higher-order corrections are explained below. First, as both $x\tilde{\mathcal{L}}^{(1)}$ and $\mathcal{L}(x)$ are CPTP generators, we have $\|e^{tx\tilde{\mathcal{L}}^{(1)}}\| = \|e^{t\mathcal{L}(x)}\| = 1$ and $\|\mathcal{P}_0\| = 1$ [219]. The first line in Eq. (C.11) corresponds to $\mathcal{P}(x) e^{tx\tilde{\mathcal{L}}^{(1)}} \mathcal{P}(x)$ and the higher-order corrections are

of the order $\|\mathcal{P}(x) - \mathcal{P}_0 - x\mathcal{P}^{(1)}\| \|\mathcal{P}(x)\| + x^2\|\mathcal{P}^{(1)}\|^2 = \mathcal{O}(x^2)$ due to the norm $\|\cdot\|$ being submultiplicative. Furthermore, the corrections in the second line, which corresponds to the integral term in (C.10), are of the order

$$\begin{aligned} & \left\| \int_0^t du e^{(t-u)x\tilde{\mathcal{L}}^{(1)}} \delta\tilde{\mathcal{L}}(x) e^{u\mathcal{L}(x)} \right\| \|\mathcal{P}(x)\| \|\mathcal{P}(x) - \mathcal{P}_0\| \leq \\ & \leq \|\mathcal{P}(x)\| \|\mathcal{P}(x) - \mathcal{P}_0\| \times t \|\delta\tilde{\mathcal{L}}(x)\| \\ & = \mathcal{O}(x) \times t \left(x^2 \|\tilde{\mathcal{L}}^{(2)}\| + \mathcal{O}(x^3 \|\tilde{\mathcal{L}}^{(3)}\|) \right) = t \mathcal{O}(x^3 \|\tilde{\mathcal{L}}^{(2)}\|), \end{aligned}$$

where $\tilde{\mathcal{L}}^{(3)}$ is the third order correction in $[\mathcal{L}(x)]_{\mathcal{P}(x)}$, see (C.15), and we used $\delta\tilde{\mathcal{L}}(x) = x^2\tilde{\mathcal{L}}^{(2)} + \mathcal{O}(x^3\|\tilde{\mathcal{L}}^{(3)}\|)$. Furthermore, it also follows that

$$\begin{aligned} & \mathcal{P}_0 \int_0^t du e^{(t-u)x\tilde{\mathcal{L}}^{(1)}} \delta\tilde{\mathcal{L}}(x) \mathcal{P}(x) e^{u\mathcal{L}(x)} \mathcal{P}_0 = \\ & = x^2 \mathcal{P}_0 \int_0^t du e^{(t-u)x\tilde{\mathcal{L}}^{(1)}} \tilde{\mathcal{L}}^{(2)} \mathcal{P}(x) e^{u\mathcal{L}(x)} \mathcal{P}_0 + t \mathcal{O}(x^3 \|\tilde{\mathcal{L}}^{(3)}\|), \end{aligned}$$

and further

$$\begin{aligned} & x^2 \mathcal{P}_0 \int_0^t du e^{(t-u)x\tilde{\mathcal{L}}^{(1)}} \tilde{\mathcal{L}}^{(2)} \left(\mathcal{P}(x) e^{u\mathcal{L}(x)} \right) \mathcal{P}_0 = \\ & = x^2 \int_0^t du e^{(t-u)x\tilde{\mathcal{L}}^{(1)}} \mathcal{P}_0 \tilde{\mathcal{L}}^{(2)} \mathcal{P}_0 e^{ux\tilde{\mathcal{L}}^{(1)}} \mathcal{P}_0 + t \mathcal{O}(x^3 \|\tilde{\mathcal{L}}^{(2)}\|) + t^2 \mathcal{O}(x^4 \|\tilde{\mathcal{L}}^{(2)}\|^2), \end{aligned}$$

where we have used Eq. (C.10), with corrections being the integral and the unitary evolution outside the SSM given by \mathcal{P}_0 . Finally, we note that $\|\tilde{\mathcal{L}}^{(2)}\| = \mathcal{O}(\|\mathcal{L}^{(2)}\| + \|\mathcal{L}^{(1)}\|^2\|\mathcal{S}\|) = \mathcal{O}(\|\mathcal{L}^{(1)}\| + \|\mathcal{L}^{(2)}\|)$, cf. Eq. (3.28), and similarly $\|\tilde{\mathcal{L}}^{(3)}\| = \mathcal{O}(\|\mathcal{L}^{(1)}\| \|\mathcal{L}^{(2)}\| \|\mathcal{S}\| + \|\mathcal{L}^{(1)}\|^3\|\mathcal{S}\|^2) = \mathcal{O}(\|\mathcal{L}^{(1)}\| + \|\mathcal{L}^{(2)}\|)$, cf. Eq. (C.15)), which completes the proof of Eq. (3.34). ■

c.2.4 Coefficients of the metastable manifold

Consider the generic case of degeneracy of the first m eigenvalues of \mathcal{L}_0 being lifted in the second-order perturbation theory. In this case the projections on the individual eigenmatrices of \mathcal{L}_0 are analytic and in the 0-th order simply given by projec-

tions on the eigenbases of $[\tilde{\mathcal{L}}^{(2)}]_{\mathcal{P}_l}$, $l = 1, \dots, m''$, where \mathcal{P}_l is a projection on the eigenspace of $\tilde{\mathcal{L}}^{(1)}$. Therefore we have

$$\begin{aligned} L_{l,j}(x) &\propto L_{l,j} \mathcal{P}_{l,j}(x) \\ &= L_{l,j} + x \left(-L_{l,j} \mathcal{L}^{(1)} \mathcal{S} - L_{l,j} \tilde{\mathcal{L}}^{(2)} \tilde{\mathcal{S}}_l - L_{l,j} \tilde{\mathcal{L}}_l^{(3)} \tilde{\mathcal{S}}_{l,j} \right) + \mathcal{O}(x^2), \end{aligned} \quad (\text{C.12})$$

where $L_{l,j}$ is a left eigenmatrix of $[\tilde{\mathcal{L}}^{(2)}]_{\mathcal{P}_l}$ with eigenvalue $\lambda_{l,j}^{(2)}$, $\mathcal{P}_{l,j}$ is the corresponding projection, $\tilde{\mathcal{S}}_l$ is the reduced resolvent for $\tilde{\mathcal{L}}^{(1)}$ at $\lambda_l^{(1)}$ restricted to \mathcal{P}_0 , $\tilde{\mathcal{S}}_{l,j}$ is the reduced resolvent for $[\tilde{\mathcal{L}}^{(2)}]_{\mathcal{P}_l}$ at $\lambda_{l,j}^{(2)}$ restricted to \mathcal{P}_l , and $\tilde{\mathcal{L}}_l^{(3)}$ is the third-order correction in $[\mathcal{L}(x)]_{\mathcal{P}_l(x)} - x\lambda_l^{(1)}\mathcal{P}_l(x)$ (see (C.16)), cf. the reduction process in [167] and Eq. (3.29). Note that since the projection $\mathcal{P}_{l,j}(x)$ is of rank 1, the eigenmatrix $L_{l,j}$ can be replaced by any matrix L such that $L \mathcal{P}_{l,j}(x) \neq 0$.

Let us assume $L_{l,j}$ is Hermitian (see Eq.(3.8) and paragraph afterwards on how to choose Hermitian basis from the eigenmatrices), so that the coefficient $c_{l,j} = \text{Tr}(L_{l,j}\rho_{\text{in}})$ is real.

Consider rescaling the coefficient $c_{l,j}(x) = \text{Tr}(L_{l,j}(x)\rho_{\text{in}})$ by the *spectral norm* of the left eigenmatrix $L_{l,j}(x)$, which is defined as $\|L_{l,j}(x)\|_\infty := \max_{|\psi\rangle \in \mathcal{H}, \langle\psi|\psi\rangle=1} |\langle\psi|L_{l,j}(x)|\psi\rangle|$. The spectral norm corresponds to the maximal absolute value of the $L_{l,j}(x)$ eigenvalues and we also have $\|L_{l,j}(x)\|_\infty = \max_{\rho_{\text{in}}} |c_{l,j}(x)|$. From the Hermitian perturbation theory for $L_{l,j}(x)$, the eigenvalues of $L_{l,j}(x)$ are analytic for x small enough [167], but $\|L_{l,j}(x)\|_\infty$ does not have to be differentiable at $x = 0$, which happens only when the extreme eigenvalues of $L_{l,j}$ obey $|c_{l,j}^{\text{max}}| = |c_{l,j}^{\text{min}}|$. Nevertheless, for a given sign of x , $\|L_{l,j}(x)\|_\infty$ is analytic for x small enough. Therefore, we arrive at

$$\begin{aligned} c_{l,j}(x) &= \frac{\text{Tr}(L_{l,j}(x)\rho_{\text{in}})}{\|L_{l,j}(x)\|_\infty} = c_{l,j}(1 - x c_{l,j}^{\text{ex},(1)}) + \\ &\quad - x \text{Tr} \left[\left(L_{l,j} \tilde{\mathcal{L}}_l^{(3)} \tilde{\mathcal{S}}_{l,j} - L_{l,j} \tilde{\mathcal{L}}^{(2)} \tilde{\mathcal{S}}_l - L_{l,j} \mathcal{L}^{(1)} \mathcal{S} \right) \rho_{\text{in}} \right] + \mathcal{O}(x^2), \end{aligned} \quad (\text{C.13})$$

where we assumed $\|L_{l,j}\|_\infty = 1$ and $c_{l,j}^{\text{ex},(1)}$ related to the first-order correction in $c_{l,j}^{\text{min}}(x)$ or $c_{l,j}^{\text{max}}(x)$, with its sign depending on the sign of x . Therefore, for x small enough the set of coefficients representing the MM is simply an affine transformation

of the degrees of freedom of the SSM of \mathcal{L}_0 as given in Eq. (3.37) of the main text.

Consider an alternative case in which the coefficient $c_{l,j}(s)$ is rescaled by the difference of the extreme eigenvalues of $L_{l,j}(x)$, $\Delta c_{l,j}(x) := c_{l,j}^{\max}(x) - c_{l,j}^{\min}(x)$. This is convenient as the range of all coefficients determining the MM is of the same length 1, which is also the case for probabilities in a simplex or a Bloch ball, see Fig. 3.2 (b,d). in the main text. Again, from the Hermitian perturbation theory for $L_{l,j}(x)$ it follows that $\Delta c_{l,j}(x)$ is analytic in x for x small enough and

$$c_{l,j}(x) = \frac{\text{Tr}(L_{l,j}(x)\rho_{\text{in}})}{\Delta c_{l,j}(x)} = c_{l,j}(1 - x(\Delta c_{l,j}^{(1)})^{-1}) + \\ - x \text{Tr} \left[\left(L_{l,j} \tilde{\mathcal{L}}_l^{(3)} \tilde{\mathcal{S}}_{l,j} - L_{l,j} \tilde{\mathcal{L}}_l^{(2)} \tilde{\mathcal{S}}_l - L_{l,j} \mathcal{L}^{(1)} \mathcal{S} \right) \rho_{\text{in}} \right] + \mathcal{O}(x^2), \quad (\text{C.14})$$

where we assumed $\Delta c_{l,j}(0) = 1$ and $\Delta c_{l,j}^{(1)}$ is the difference between first-order corrections in $c_{l,j}^{\max}(x)$ and $c_{l,j}^{\min}(x)$. ■

c.2.5 Effective long-time dynamics

Below we obtain Eq. (3.39) which demonstrates how the effective long times dynamics is approximately CPTP and given by the generator $\tilde{\mathcal{L}}(x) = \tilde{\mathcal{L}}^{(1)} + [\tilde{\mathcal{L}}^{(2)}]_{\mathcal{P}_0}$, cf. Appendix C.2.1.

Derivation. From Eq. (3.28) we write $\mathcal{L}_{\text{eff}}(x) = [\mathcal{L}(x)]_{\mathcal{P}(x)} =: \tilde{\mathcal{L}}(x) + \Delta\mathcal{L}(x)$, with $\Delta\mathcal{L}(x)$ regarded as a perturbation whose size is in general $\|\Delta\mathcal{L}(x)\| = \mathcal{O}(x^2 \|\tilde{\mathcal{L}}^{(1)}\|)$, while in the case when $\tilde{\mathcal{L}}^{(1)} = 0$ we have $\|\Delta\mathcal{L}(x)\| = \mathcal{O}(x^3 (\|\mathcal{L}^{(1)}\| + \|\mathcal{L}^{(2)}\|))$, see the third-order correction for $[\mathcal{L}(x)]_{\mathcal{P}(x)}$ in Eq. (C.15) below. The Dyson-Philips expansion for $\mathcal{L}_{\text{eff}}(x)$ with $\Delta\mathcal{L}(x)$ as the perturbation is

$$[e^{t\mathcal{L}(x)}]_{\mathcal{P}(x)} = \mathcal{P}(x) e^{t\tilde{\mathcal{L}}(x)} \mathcal{P}(x) + \mathcal{P}(x) \int_0^t du e^{(t-u)\tilde{\mathcal{L}}(x)} \Delta\mathcal{L}(x) \mathcal{P}(x) e^{u\mathcal{L}(x)} \mathcal{P}(x),$$

where we used $e^{u\mathcal{L}_{\text{eff}}(x)}\mathcal{P}(x) = \mathcal{P}(x)e^{u\mathcal{L}(x)}\mathcal{P}(x)$. We further have

$$\begin{aligned} [e^{t\mathcal{L}(x)}]_{\mathcal{P}(x)} &= \mathcal{P}_0 e^{t\tilde{\mathcal{L}}(x)}\mathcal{P}_0 + x \left(-\mathcal{S}\tilde{\mathcal{L}}^{(1)} e^{t\tilde{\mathcal{L}}(x)}\mathcal{P}_0 - e^{t\tilde{\mathcal{L}}(x)}\mathcal{P}_0\tilde{\mathcal{L}}^{(1)}\mathcal{S} \right) + \mathcal{O}(x^2) + \\ &\quad + \mathcal{P}_0 \int_0^t du e^{(t-u)\tilde{\mathcal{L}}(x)} \mathcal{P}_0 \Delta\mathcal{L}(x) \mathcal{P}_0 e^{u\mathcal{L}(x)}\mathcal{P}_0 + \\ &\quad + t \mathcal{O}(x^3 \|\tilde{\mathcal{L}}^{(1)}\| + x^4 (\|\mathcal{L}^{(1)}\| + \|\mathcal{L}^{(2)}\|)), \end{aligned}$$

Note that $\|e^{t\tilde{\mathcal{L}}(x)}\| = \|e^{t\tilde{\mathcal{L}}(x)}\mathcal{P} + (\mathcal{I} - \mathcal{P})\| \leq 3$ since $\tilde{\mathcal{L}}(x)$ is a CPTP generator on \mathcal{P}_0 . Due to submultiplicativity of the norm, the second order corrections to $\mathcal{P}(x)e^{t\tilde{\mathcal{L}}(x)}\mathcal{P}(x)$ in the first line are $\mathcal{O}(x^2(\|\mathcal{L}^{(1)}\| \|\mathcal{S}\|)^2) = \mathcal{O}(x^2)$. In the second and the third line corresponding to the integral, the corrections are bounded by $t \mathcal{O}(x \|\mathcal{L}^{(1)}\| \|\mathcal{S}\| \|\Delta\mathcal{L}(x)\|) = t \mathcal{O}(x^3 \|\tilde{\mathcal{L}}^{(1)}\| + x^4 (\|\mathcal{L}^{(1)}\| + \|\mathcal{L}^{(2)}\|))$. Although, $\|\Delta\mathcal{L}(x)\| = \mathcal{O}(x^2 \|\tilde{\mathcal{L}}^{(1)}\| + x^3 (\|\mathcal{L}^{(1)}\| + \|\mathcal{L}^{(2)}\|))$, from Eq. (3.28) we obtain $\|[\Delta\mathcal{L}(x)]_{\mathcal{P}_0}\| = \mathcal{O}(x^3 (\|\mathcal{L}^{(1)}\| + \|\mathcal{L}^{(2)}\|)) = \mathcal{O}(x^3\tau_0^{-1})$ which implies that the leading correction in the second line of the equation above is $\mathcal{O}(x^3\tau_0^{-1})$. Note that this reduction to the higher order is a consequence of the fact that $\tilde{\mathcal{L}}^{(1)} + x\tilde{\mathcal{L}}^{(2)}$ and $\tilde{\mathcal{L}}^{(1)} + x[\tilde{\mathcal{L}}^{(2)}]_{\mathcal{P}_0}$ differ in the norm of the order $\mathcal{O}(x\|\tilde{\mathcal{L}}^{(1)}\|)$ due to the first-order corrections in the $\tilde{\mathcal{L}}^{(1)}$ eigenprojections, cf. Eq. (3.29), but not in the eigenvalues that differ in $\mathcal{O}(x^2(\|\mathcal{L}^{(1)}\| + \|\mathcal{L}^{(2)}\|))$, cf. Eq. (3.26). ■

c.2.6 Higher-order corrections

We have that $[\mathcal{L}(x)]_{\mathcal{P}(x)} = x\tilde{\mathcal{L}}^{(1)} + x^2\tilde{\mathcal{L}}^{(2)} + x^3\tilde{\mathcal{L}}^{(3)} + \mathcal{O}(x^4(\|\mathcal{L}^{(1)}\| + \|\mathcal{L}^{(2)}\|))$, where $\tilde{\mathcal{L}}^{(1)}$ and $\tilde{\mathcal{L}}^{(2)}$ are given in Eq. (3.28) and the third-order correction is [167]

$$\begin{aligned} \tilde{\mathcal{L}}^{(3)} &= -\mathcal{P}_0\mathcal{L}^{(1)}\mathcal{P}_0\mathcal{L}^{(2)}\mathcal{S} - \mathcal{P}_0\mathcal{L}^{(2)}\mathcal{P}_0\mathcal{L}^{(1)}\mathcal{S} - \mathcal{P}_0\mathcal{L}^{(1)}\mathcal{S}\mathcal{L}^{(2)}\mathcal{P}_0 + \\ &\quad - \mathcal{P}_0\mathcal{L}^{(2)}\mathcal{S}\mathcal{L}^{(1)}\mathcal{P}_0 - \mathcal{S}\mathcal{L}^{(1)}\mathcal{P}_0\mathcal{L}^{(2)}\mathcal{P}_0 - \mathcal{S}\mathcal{L}^{(2)}\mathcal{P}_0\mathcal{L}^{(1)}\mathcal{P}_0 + \\ &\quad + \mathcal{P}_0\mathcal{L}^{(1)}\mathcal{P}_0\mathcal{L}^{(1)}\mathcal{S}\mathcal{L}^{(1)}\mathcal{S} + \mathcal{P}_0\mathcal{L}^{(1)}\mathcal{S}\mathcal{L}^{(1)}\mathcal{P}_0\mathcal{L}^{(1)}\mathcal{S} + \mathcal{P}_0\mathcal{L}^{(1)}\mathcal{S}\mathcal{L}^{(1)}\mathcal{S}\mathcal{L}^{(1)}\mathcal{P}_0 + \\ &\quad + \mathcal{S}\mathcal{L}^{(1)}\mathcal{P}_0\mathcal{L}^{(1)}\mathcal{P}_0\mathcal{L}^{(1)}\mathcal{S} + \mathcal{S}\mathcal{L}^{(1)}\mathcal{P}_0\mathcal{L}^{(1)}\mathcal{S}\mathcal{L}^{(1)}\mathcal{P}_0 + \mathcal{S}\mathcal{L}^{(1)}\mathcal{S}\mathcal{L}^{(1)}\mathcal{P}_0\mathcal{L}^{(1)}\mathcal{P}_0 + \\ &\quad - \mathcal{P}_0\mathcal{L}^{(1)}\mathcal{P}_0\mathcal{L}^{(1)}\mathcal{P}_0\mathcal{L}^{(1)}\mathcal{S}^2 - \mathcal{P}_0\mathcal{L}^{(1)}\mathcal{P}_0\mathcal{L}^{(1)}\mathcal{S}^2\mathcal{L}^{(1)}\mathcal{P}_0 + \\ &\quad - \mathcal{P}_0\mathcal{L}^{(1)}\mathcal{S}^2\mathcal{L}^{(1)}\mathcal{P}_0\mathcal{L}^{(1)}\mathcal{P}_0 - \mathcal{S}^2\mathcal{L}^{(1)}\mathcal{P}_0\mathcal{L}^{(1)}\mathcal{P}_0\mathcal{L}^{(1)}\mathcal{P}_0. \end{aligned} \tag{C.15}$$

Due to reduction process for $[\mathcal{L}(x)]_{\mathcal{P}(x)}$ we further obtain that $[\mathcal{L}(x)]_{\mathcal{P}_l(x)} = x\lambda_l^{(1)}\mathcal{P}_l(x) + x^2[\tilde{\mathcal{L}}^{(2)}]_{\mathcal{P}_l} + x^3\tilde{\mathcal{L}}_l^{(3)} + \mathcal{O}(x^4)$, where $\mathcal{P}_l(x)$ is a projection on the $\lambda_l^{(1)}$ -group with $\lambda_l^{(1)}$ being an eigenvalue of $\tilde{\mathcal{L}}^{(1)}$, see Eq. (3.29) and

$$\begin{aligned} \tilde{\mathcal{L}}_l^{(3)} = & [\tilde{\mathcal{L}}^{(3)}]_{\mathcal{P}_l} + \lambda_l^{(1)}\mathcal{P}_l\mathcal{L}^{(1)}\mathfrak{S}^2\mathcal{L}^{(1)}\mathcal{P}_l + \\ & - \mathcal{P}_l\tilde{\mathcal{L}}^{(2)}\mathcal{P}_l\mathcal{L}^{(1)}\mathfrak{S} - \mathfrak{S}\mathcal{L}^{(1)}\mathcal{P}_l\tilde{\mathcal{L}}^{(2)}\mathcal{P}_l + \\ & - \mathcal{P}_l\tilde{\mathcal{L}}^{(2)}\tilde{\mathfrak{S}}_l\tilde{\mathcal{L}}^{(2)}\mathcal{P}_l - \mathcal{P}_l\tilde{\mathcal{L}}^{(2)}\mathcal{P}_l\tilde{\mathcal{L}}^{(2)}\tilde{\mathfrak{S}}_l - \tilde{\mathfrak{S}}_l\tilde{\mathcal{L}}^{(2)}\mathcal{P}_l\tilde{\mathcal{L}}^{(2)}\mathcal{P}_l, \end{aligned} \quad (\text{C.16})$$

for $l = 1, \dots, m''$.

D

APPENDIX

In this appendix we merge results of Chapters 2 and 3, in order to provide proofs that precision of quantum parameter estimation can be enhanced when the system dynamics is metastable. In particular, we consider two metastable phases which differ in activity, so that the system is close to a first-order DPT, see Sec. D.1. Furthermore, we also consider quantum parameter estimation using quantum systems with dynamics close to higher than two-fold degeneracy of the stationary state, see Sec. 3.4.1, and show how the unitary dynamics during the metastable regime is related to the quadratic enhancement in the parameter estimation precision, see Sec. D.3.

D.1 METASTABILITY AS A RESOURCE IN ENHANCED PARAMETER ESTIMATION

Consider a master equation \mathcal{L}_g , see Eq. (3.2), in which the Hamiltonian H_g and jump operators $J_{j,g}$ depend on a parameter g . Furthermore, let us assume that the stationary state dynamics is unique, but the gap of \mathcal{L}_g is small, i.e., there is a separation between the second and the third eigenvalues of \mathcal{L}_g , $0 < -\lambda_2 \ll -\text{Re } \lambda_3$. This leads to metastability in the system dynamics with metastable states being mixtures of two metastable phases $\tilde{\rho}_1, \tilde{\rho}_2$ in the metastable regime $(-\text{Re } \lambda_3)^{-1} = \tau'' \ll t \ll \tau = (-\lambda_2)^{-1}$, see Sec. 3.3.

We are interested in estimating a value of the parameter g using the joint system-output MPS at time t , $|\Psi_g(t)\rangle$, precision of which is quantified by the QFI, cf. Eq. (2.12), see Chapter 2.

Here we provide a proof that during the metastable regime, the QFI can grow *quadratically* with time with a multiplicative constant determined by the two metastable phases, as in (2.35) and (2.15). Furthermore, we show that the asymptotic linear behaviour of the QFI, a consequence of the stationary state being unique, is also determined by the metastable phases and the final relaxation time, as given in (2.36) and in (2.19).

Quadratic scaling of QFI. First, let us recall that the QFI is proportional to the variance of the generator $G_g(t)$ that encoded the parameter g in the joint system-output MPS $|\Psi_g(t)\rangle$, cf. Eqs. (2.29) and (2.30-2.10). Before considering the variance, let us show how the average of the generator $G_g(t)$ in the metastable regime can be approximated by the rate of the corresponding to two metastable phases $\tilde{\rho}_1, \tilde{\rho}_2$, see Eq. (3.11). We have, cf. (2.25),

$$\begin{aligned}
t^{-1} \langle \Psi_g(t) | G_g(t) | \Psi_g(t) \rangle &= i t^{-1} \partial_{g'} \langle \Psi_g^{(1)}(t) | \Psi_g^{(2)}(t) \rangle_{g'=g} = \\
&= i t^{-1} \text{Tr} \left(\partial_{g'} e^{t\mathcal{L}_{g',g}} \rho_{\text{in}} \right)_{g'=g} = i \text{Tr} \left(\partial_{g'} \mathcal{L}_{g',g} \mathcal{P} \rho_{\text{in}} \right)_{g'=g} + \\
&+ i \frac{e^{t\lambda_2} - 1}{t} \text{Tr} \left(\partial_{g'} \mathcal{L}_{g',g} R_2 \right)_{g'=g} \text{Tr} (L_2 \rho_{\text{in}}) + \\
&+ i \text{Tr} \left(\partial_{g'} \mathcal{L}_{g',g} \left[\frac{e^{t\mathcal{L}_g} - \mathcal{J}}{t\mathcal{L}_g} \right]_{\mathcal{J}-\mathcal{P}} \rho_{\text{in}} \right)_{g'=g} = p_1 \mu_1 + p_2 \mu_2 + \\
&+ \mathcal{O} \left(\lambda_2 \|\partial_{g'} \mathcal{L}_{g',g}\|_{g'=g} \right) + \mathcal{O} \left(\|\partial_{g'} \mathcal{L}_{g',g}\|_{g'=g} \left\| \left[\frac{e^{t\mathcal{L}_g} - \mathcal{J}}{t\mathcal{L}_g} \right]_{\mathcal{J}-\mathcal{P}} \right\| \right), \quad (\text{D.1})
\end{aligned}$$

where \mathcal{P} is the projection on the two metastable phases, $\mathcal{P}(\cdot) = \sum_{k=1,2} \tilde{\rho}_k \text{Tr}(\tilde{\rho}_k(\cdot))$, so that $\mathcal{P} \rho_{\text{in}} = p_1 \tilde{\rho}_1 + p_2 \tilde{\rho}_2$, see Eq. (3.12), μ_1, μ_2 are the rates of the metastable phases, $\rho_{\text{in}} = |\chi\rangle\langle\chi|$ is a pure initial state of the system, and R_2, L_2 are the right, left eigenmatrices of \mathcal{L}_g corresponding to λ_2 eigenvalue. The first correction in (D.1) is due to corrections to the stationarity during the metastable regime, and the second correction is the contribution before the metastable regime from faster decaying modes. Note that the latter correction is negligible only when the metastable regime is long enough (cf. corrections $\left\| [e^{t\mathcal{L}_g}]_{\mathcal{J}-\mathcal{P}} \right\|$ to the stationarity in Eq. (3.8)), so that $\left\| [(t\mathcal{L}_g)^{-1}]_{\mathcal{J}-\mathcal{P}} \right\|$ is negligible. From Eq. (D.1) system states leading to the extremal averages of $G_g(t)$

in the metastable regime correspond to metastable phases, see Sec. 2.3.3.

In the case of the variance of the generator $G_g(t)$ encoding g in $|\Psi_g(t)\rangle$, $\Delta^2 G_g(t) := \langle G_g^2(t) \rangle - \langle G_g(t) \rangle^2$, the quadratic terms are given by, cf. (B.9) for corrections,

$$\begin{aligned} \Delta G_g^2(t) &= t^2 \left[- \left| \text{Tr} \left(\mathcal{L}_g^L \mathcal{P} \rho_{\text{in}} \right) \right|^2 + \text{Re} \text{Tr} \left(\mathcal{L}_g^L \mathcal{P} \mathcal{L}_g^R \mathcal{P} \rho_{\text{in}} \right) \right] + \mathcal{O}(t) \\ &= t^2 \left[- (p_1 \mu_1 + p_2 \mu_2)^2 - i \left(p_1 \mu_1 \text{Tr}(\tilde{P}_1 \mathcal{L}_g^R \tilde{\rho}_1) + p_2 \mu_2 \text{Tr}(\tilde{P}_2 \mathcal{L}_g^R \tilde{\rho}_2) \right) + \right. \\ &\quad \left. - i \left(p_1 \mu_2 \text{Tr}(\tilde{P}_2 \mathcal{L}_g^R \tilde{\rho}_1) + p_2 \mu_1 \text{Tr}(\tilde{P}_1 \mathcal{L}_g^R \tilde{\rho}_2) \right) \right] + \mathcal{O}(t), \end{aligned} \quad (\text{D.2})$$

where $\mathcal{L}_g^R := \partial_{g'} \mathcal{L}_{g,g'}|_{g'=g} = (\partial_{g'} \mathcal{L}_{g',g})^\dagger_{g'=g} =: (\mathcal{L}_g^L)^\dagger$ are the first-order deformations of the master operator \mathcal{L}_g . We now show that the cross terms $\text{Tr}(\tilde{P}_1 \mathcal{L}_g^R \tilde{\rho}_2)$, $\text{Tr}(\tilde{P}_2 \mathcal{L}_g^R \tilde{\rho}_1)$ are of the order of a square root of corrections to the stationarity during the metastable regime, $\mathcal{O}(\max(\lambda_2 t, \|[e^{t\mathcal{L}_g}]_{\mathcal{J}-\mathcal{P}}\|)^{1/2} \|\mathcal{L}_g^R\|)$. Thus the cross terms can be neglected when the separation in the spectrum of $\mathcal{L}_{g'}$, $-\lambda_2 \ll -\text{Re} \lambda_3$, is pronounced enough. Moreover, since $\tilde{P}_1 + \tilde{P}_2 = \mathbb{1}_{\mathcal{H}}$, we also have

$$\begin{aligned} -i \text{Tr}(\tilde{P}_1 \mathcal{L}_g^R \tilde{\rho}_1) &= -i \text{Tr}(\mathcal{L}_g^R \tilde{\rho}_1) + \mathcal{O}(\max(\lambda_2 t, \|[e^{t\mathcal{L}_g}]_{\mathcal{J}-\mathcal{P}}\|)^{1/2} \|\mathcal{L}_g^R\|) \\ &= \mu_1 + \mathcal{O}(\max(\lambda_2 t, \|[e^{t\mathcal{L}_g}]_{\mathcal{J}-\mathcal{P}}\|)^{1/2} \|\mathcal{L}_g^R\|), \\ -i \text{Tr}(\tilde{P}_2 \mathcal{L}_g^R \tilde{\rho}_2) &= \mu_2 + \mathcal{O}(\max(\lambda_2 t, \|[e^{t\mathcal{L}_g}]_{\mathcal{J}-\mathcal{P}}\|)^{1/2} \|\mathcal{L}_g^R\|), \end{aligned}$$

leading to the quadratic behaviour of $\Delta^2 G_g(t)$ and hence the QFI in the metastable regime given by the rates of the metastable phases,

$$\Delta^2 G_g(t) = t^2 p_1 p_2 (\mu_1 - \mu_2)^2 + \mathcal{O}(t) + \mathcal{O}(\max(\lambda_2 t, \|[e^{t\mathcal{L}_g}]_{\mathcal{J}-\mathcal{P}}\|)^{1/2} \|\mathcal{L}_g^R\|). \quad (\text{D.3})$$

Proof. Consider the MPS $|\Psi_g^{(1)}(t)\rangle$ and the system state $\rho_g^{(1)}(t)$ corresponding to the initial state $|v^{\text{max}}\rangle$ being the eigenvector of L_2 corresponding to the maximal eigenvalue c_2^{max} , so that during the metastable regime, $\rho_g^{(1)}(t) = \tilde{\rho}_1 + \mathcal{O}(t\lambda_2) + \mathcal{O}(\|[e^{t\mathcal{L}_g}]_{\mathcal{J}-\mathcal{P}}\|)$, cf. (3.8) and (3.11). For time t well within the metastable regime,

so that the leading terms in $\langle \Psi_g^{(1)}(t) | G_g(t)^2 | \Psi_g^{(1)}(t) \rangle$ are quadratic, cf. (B.9), we have

$$\begin{aligned}
 \left| \text{Tr}(\tilde{\mathcal{P}}_2 \mathcal{L}_g^R \rho_g^{(1)}(t)) \right| &= t^{-1} \left| \partial_{g'} \langle \Psi_{g'}^{(1)}(t) | \tilde{\mathcal{P}}_2 \otimes \mathbf{1}_{\text{output}} | \Psi_g^{(1)}(t) \rangle_{g'=g} \right| \\
 &\leq \sqrt{t^{-2} \langle \Psi_g^{(1)}(t) | G_g(t)^2 | \Psi_g^{(1)}(t) \rangle} \sqrt{\text{Tr}(\tilde{\mathcal{P}}_2^2 \rho_g^{(1)}(t))} \\
 &\leq \sqrt{\partial_{g_1} \partial_{g_2} \text{Re Tr}(\mathcal{L}_g^L \mathcal{P} \mathcal{L}_g^R \rho_1) + \mathcal{O}(C(t))} \sqrt{\mathcal{O}(t\lambda_2) + \mathcal{O}(\| [e^{t\mathcal{L}_g}]_{\mathcal{J}-\mathcal{P}} \|)} \\
 &= \mathcal{O}(\|\mathcal{L}_g^R\|) \sqrt{\mathcal{O}(t\lambda_2) + \mathcal{O}(\| [e^{t\mathcal{L}_g}]_{\mathcal{J}-\mathcal{P}} \|)} = \mathcal{O}(\max(\lambda_2 t, \| [e^{t\mathcal{L}_g}]_{\mathcal{J}-\mathcal{P}} \|)^{1/2} \|\mathcal{L}_g^R\|),
 \end{aligned}$$

where the first inequality is the Schwarz inequality and the second inequality simply follows from $0 \leq \tilde{\mathcal{P}}_2 \leq \mathbf{1}_{\mathcal{H}}$ and thus $\tilde{\mathcal{P}}_2^2 \leq \tilde{\mathcal{P}}_2$, cf. (3.12). ■

Furthermore the asymptotic linear scaling of the variance $\Delta G_g^2(t)$ and hence the QFI, cf. Eq. (2.27), is also influenced by the presence of metastability as we have

$$\lim_{t \rightarrow \infty} t^{-1} \Delta G_g^2(t) = \text{Tr}(\mathcal{L}_g^{\text{LR}} \rho_{ss}) - 2 \text{Re Tr} \left(\mathcal{L}_g^L \left[\mathcal{L}_g^{-1} \right]_{\mathcal{J}-\mathcal{P}_{ss}} \mathcal{L}_g^R \rho_{ss} \right),$$

where $\mathcal{J} - \mathcal{P}_{ss}$ is the projection on the complement of the stationary state ρ_{ss} , and $\mathcal{L}_g^{\text{LR}} := \partial_{g_1} \partial_{g_2} \mathcal{L}_{g_1, g_2} |_{g_1=g_2=g}$. Note that the leading contribution is due to the low-lying second mode, so that we have (cf. Eqs. (2.36) and (2.19))

$$\begin{aligned}
 \lim_{t \rightarrow \infty} t^{-1} \Delta G_g^2(t) &\approx -2 \tau \text{Re Tr} \left(\mathcal{L}_g^L \mathbf{R}_2 \right) \text{Tr} \left(\mathbf{L}_2 \mathcal{L}_g^R \rho_{ss} \right) \\
 &\approx -2 \tau p_1^{ss} p_2^{ss} (\mu_1 - \mu_2)^2, \tag{D.4}
 \end{aligned}$$

where $\tau = (-\lambda_2)^{-1}$ is the correlation time/metastable regime length, $p_{1,2}^{ss} = \text{Tr}(\tilde{\mathcal{P}}_{1,2} \rho_{ss})$ and we used $\mathbf{R}_2 = (\tilde{\rho}_1 - \tilde{\rho}_2) / \Delta c_2$, $\mathbf{L}_2 = c_2^{\max} \tilde{\mathcal{P}}_1 + c_2^{\min} \tilde{\mathcal{P}}_2$, $c_2^{\max} / \Delta c_2 = p_2^{ss}$, $c_2^{\min} / \Delta c_2 = -p_1^{ss}$, cf. (3.11), (3.12), and neglected the cross terms $\text{Tr}(\tilde{\mathcal{P}}_1 \mathcal{L}_g^R \tilde{\rho}_2)$, $\text{Tr}(\tilde{\mathcal{P}}_2 \mathcal{L}_g^R \tilde{\rho}_1)$ due to the proof above. For discussion of relation between Eqs. (D.3) and (D.4) see Sec. 2.3.3.

Eqs. (D.1) and (D.3) show that the statistics of $G_g(t)$ is *bimodal* and therefore the QFI in the metastable regime grows quadrati-

cally with time t with constant determined by the rates of two metastable phases. Moreover, from Eq. (D.4) enhancement in the asymptotic linear scaling of the QFI is also determined by the rates of the metastable phases and the length τ of the metastable regime. As the enhancement depends on the rates given by the expected value of the system observable M_g , (2.37), in the two metastable phases, this gives a method to determine whether a given open quantum system dynamics is useful for estimation of a given parameter g .

Finally, note that the quadratic scaling of the QFI in time during the metastable regime is a consequence of a *macroscopic phase* encoded in the system-output MPS during the metastable regime, e.g. for a initial state $|\chi\rangle = \sqrt{p_1} |v^{\max}\rangle + \sqrt{p_2} |v^{\min}\rangle$ evolving into a mixture of metastable phases, $p_1 \tilde{\rho}_1 + p_2 \tilde{\rho}_2$ and the joint MPS given by $|\Psi_g(t)\rangle = \sqrt{p_1} |\Psi_g^{(1)}(t)\rangle + \sqrt{p_2} |\Psi_g^{(2)}(t)\rangle$, as follows. We have that $|\Psi_{g'}(t)\rangle = \mathcal{T} e^{-i \int_{g'}^g dg'' G_{g''}(t)} |\Psi_g(t)\rangle = |\Psi_g(t)\rangle - i(g' - g) G_g(t) |\Psi_g(t)\rangle + \mathcal{O}((g' - g)^2)$ and thus the macroscopic phase for $\langle \Psi_g^{(1,2)}(t) | G_g(t) | \Psi_g^{(1,2)}(t) \rangle \approx t\mu_{1,2}$ and the off-diagonal terms do not contribute, analogously as in the proof of (D.3) above. When measurement is performed only on the system, this relative macroscopic phase is lost and there is no quadratic enhancement in precision, which corresponds to the fact that system state is approximately stationary, $p_1 \tilde{\rho}_1 + p_2 \tilde{\rho}_2$ in the metastable regime, cf. Eq. (D.8).

D.2 METASTABLE PHASES IN BIASED QJMC

When we are interested in the cumulants of an integrated continuous measurement, such as photon counting or an integrated homodyne current, those can be encoded in a cumulant generating function (CGF) or the logarithm of a characteristic function. Interestingly, both of those can be obtained by deformation of a master operator, cf. the superoperator \mathcal{W}_s in Eq. (3.17) for counting CGF and Eqs. (2.21) and (B.25) for the generators leading to respective characteristic functions.

As exploited in the Chapter 2, the characteristic function of a continuous measurement is identical to the fidelity between joint system-output MPSs with different values of a parameter encoded using exactly that continuous measurement as a generator of encoding and the corresponding modified master operator is given by for counting by $\mathcal{L}_{\phi,\phi'}$ in (2.21) and for homodyne current by $\mathcal{L}_{g',g}$ in (B.25), where the difference between parameter values is the argument of the characteristic function. Therefore, we have that $\mathcal{W}_s = \mathcal{L}_{\phi,\phi'}$ for $\Delta\phi = \phi' - \phi = is$, and there is analogous relation for a homodyne current, see CGF in [164]. In particular, for homodyne current in quanta associated with jump J_1 , it follows that

$$\partial_s|_{s=0}\mathcal{W}_s\rho = -i\partial_{\phi'}|_{\phi'=\phi}\mathcal{L}_{\phi,\phi'}\rho = J_1\rho J_1^\dagger. \quad (\text{D.5})$$

Therefore, from the results of the previous Sec. D.1, we obtain that $\text{Tr}(\tilde{\mathcal{P}}_1 J_1 \tilde{\rho}_2 J_1^\dagger)$ and $\text{Tr}(\tilde{\mathcal{P}}_2 J_1 \tilde{\rho}_1 J_1^\dagger)$ are of the order are of the order of a square root of corrections to the stationarity during the metastable regime, $\mathcal{O}(\max(\lambda_2 t, \|[e^{t\mathcal{L}}]_{\mathcal{J}-\mathcal{P}}\|)^{1/2} \times \kappa_1)$, cf. the proof of Eq. (D.3), where $\kappa_1 := \|J_1(\cdot)J_1^\dagger\|$. This leads to one of the metastable phases $\tilde{\rho}_1$ or $\tilde{\rho}_2$ to be approximately (up to $\mathcal{O}(\max(\lambda_2 t, \|[e^{t\mathcal{L}}]_{\mathcal{J}-\mathcal{P}}\|)^{1/2} \times \kappa_1)$) the \mathcal{W}_s eigenmatrix ρ_s corresponding to the maximal eigenvalue $\theta(s)$ for $(-\lambda_2) \ll (1 - e^{-s})\kappa_1 \ll (-\text{Re } \lambda_3)$, with the choice of the metastable phase depends on sign of the parameter s , see Sec. 3.3.3. Analogous results hold for any other integrated continuous measurement, e.g. an integrated homodyne current.

D.3 METASTABILITY IN PERTURBED DEGENERATE SSM AND ENHANCED PARAMETER ESTIMATION

In this appendix we establish connection between the unitary rotation in a perturbed SSM during the metastable regime, cf. the first-order correction $[\mathcal{L}^{(1)}]_{\mathcal{P}_0}$ in Eq. (3.28), and quadratic scaling of the QFI in the parameter estimation using joint system-output MPS.

Consider dynamics \mathcal{L}_g close to \mathcal{L}_0 which features degenerate stationary manifold, as given in Eq. (3.3). Let us assume that \mathcal{L}_0 features a state of full rank, i.e., there is no decay subspace \mathcal{H}_0 , and $\rho_{\text{ss}} = \bigoplus_{l=1}^{m'} p_l \tilde{\rho}_l \otimes \omega_l$. In this case for no rotation in the SSM, it can be shown that the Hamiltonian and jump operators are of the form preserving the block structure of (3.3), i.e., $H = \sum_{l=1}^{m'} H_l \otimes \mathbb{1}_{\mathcal{H}_l}$ and $J_j = \sum_{l=1}^{m'} J_{j,l} \otimes \mathbb{1}_{\mathcal{H}_l}$. This case has been assumed in [206], where for \mathcal{L}_g given by $H_g = H + gH^{(1)} + \mathcal{O}(g^2)$ and $J_{j,g} = J_{j,0} + gJ_j^{(1)} + \mathcal{O}(g^2)$, the Hamiltonian governing the unitary dynamics during the metastable regime, i.e., $g\tilde{\mathcal{L}}^{(1)} = g[\mathcal{L}^{(1)}]_{\mathcal{P}_0} = -ig[\tilde{H}^{(1)}, (\cdot)]$, has been derived as

$$\begin{aligned} \tilde{H}^{(1)} &= \sum_{l=1}^{m'} \mathbb{1}_{\mathcal{H}_l} \otimes \text{Tr}_{\mathcal{H}_l} \left(\left[H^{(1)} + \frac{i}{2} \sum_j \left(J_j J_j^{(1)} - (J_j^{(1)})^\dagger J_j \right) \right] \tilde{\rho}_l \otimes \mathbb{1}_{\mathcal{H}_l} \right) \\ &=: \sum_{l=1}^{m'} \mathbb{1}_{\mathcal{H}_l} \otimes \tilde{H}_l^{(1)}, \end{aligned} \quad (\text{D.6})$$

which preserves the block diagonal structure. Moreover, as $\tilde{H}^{(1)}$ is derived simply as [206]

$$\begin{aligned} &i \mathcal{P}_0 \left(-iH^{(1)}(\cdot) + J_j^{(1)}(\cdot)J_j - \frac{1}{2} \left(J_j J_j^{(1)} + (J_j^{(1)})^\dagger J_j \right) (\cdot) \right) \mathcal{P}_0 \\ &= i \mathcal{P}_0 \partial_{g'} \mathcal{L}_{g',g} \Big|_{g'=g=0} \mathcal{P}_0, \end{aligned}$$

where $\mathcal{L}_{g',g}$ is the deformation master operator yielding fidelity of MPSS corresponding to system-output dynamics at the parameter value g and g' , as $\langle \Psi_g(t) | \Psi_{g'}(t) \rangle = \text{Tr}(e^{t\mathcal{L}_{g',g}} \rho_{\text{in}})$, cf. (2.25), we have the following relation to the observable M_g (2.37), determining quadratic enhancement in the QFI,

$$\tilde{H}^{(1)} = \sum_{l=1}^{m'} \mathbb{1}_{\mathcal{H}_l} \otimes \text{Tr}_{\mathcal{H}_l} (M_g \tilde{\rho}_l \otimes \mathbb{1}_{\mathcal{H}_l}). \quad (\text{D.7})$$

Let us recall here M_g for generic types of parameters, see Sec. 2.4.1. For $g = \Omega$ being a coupling constant in the system Hamiltonian, i.e., $H_\Omega = H_0 + \Omega H_1$, we simply have $M_\Omega = H_1$. On the other hand, for a classical parameter $g = \kappa_j$ with $J_{j,\kappa_j} = \sqrt{\kappa_j} J_j$, there

is no enhancement possible, exactly like in the $m = 2$ phases case, since $M_g = 0$ and thus $\tilde{H}^{(1)} = 0$.

D.3.1 Estimation using system only

For DFSS and NSSs, given by \mathcal{K}_l with $\dim(\mathcal{K}_l) > 1$, $l = 1, \dots, m'$, we have that perturbation of g away from 0 introduces non-trivial unitary dynamics, so that in the metastable regime, cf. Eq. (3.36), we have $\rho_g(t) = \sum_{l=1}^{m'} p_l \tilde{\rho}_l \otimes e^{-igt\tilde{H}_l^{(1)}} \omega_l e^{igt\tilde{H}_l^{(1)}} + \mathcal{O}(g) + \mathcal{O}(\| [e^{t\mathcal{L}_g}]_{\mathcal{J}-\mathcal{P}(g)} \|)$, where $\mathcal{P}(g)$ is the projection of low-lying modes of \mathcal{L}_g corresponding to the lifted degeneracy of the SSM in \mathcal{L}_0 . Consider estimation of a value of the parameter g during the metastable regime by performing measurement on the system. We will have that for $g \approx 0$ the corresponding QFI,

$$F(\rho_g(t)) = t^2 \sum_{l=1}^{m'} p_l F_l(\omega_l) + t \left(\mathcal{O}(1) + \mathcal{O}(g) + \mathcal{O} \left(t \| [e^{t\mathcal{L}_g}]_{\mathcal{J}-\mathcal{P}(g)} \| \right) \right), \quad (\text{D.8})$$

where $F_l(\omega_l)$ is the QFI for phase encoded by $\tilde{H}_l^{(1)}$ on ω_l as $e^{-i\phi\tilde{H}_l^{(1)}} \omega_l e^{i\phi\tilde{H}_l^{(1)}}$, and the leading linear corrections are due to first-order corrections to the metastable manifold, cf. Eq. (3.36). Note that we have *quadratic scaling* of the QFI with time t for a measurement performed solely on the system, cf. the symmetric logarithmic derivative in (2.11), which is due to *coherence preserved* during the metastable regime inside a DFS/NSS represented by ω_l . In particular, when an initial system state evolves into pure ω_l , we further have that the QFI is simply given by the variance $F_l(\omega_l) = 4 \Delta_{\omega_l}^2 \tilde{H}_l^{(1)}$. The quadratic enhancement in the scaling of the QFI is absent for classical phases where $\dim(\mathcal{K}_l) = 1$, since those are not affected by the unitary dynamics during metastable regime as the Hamiltonian introduces only a global phase $t \text{Tr}(M_g \tilde{\rho}_l)$ on $\tilde{\rho}_l$ since $\tilde{H}_l^{(1)} = \mathbb{1}_{\mathcal{K}_l} \times \text{Tr}(M_g \tilde{\rho}_l)$. Similarly, when an initial system state evolves into ω_l being a mixture of $\tilde{H}_l^{(1)}$ eigenstates there is *no quadratic enhancement*. As we show

below, in these two cases it is necessary to consider measuring also the output in order to retrieve the enhancement in precision, cf. the case of two phases in Sec. 2.4.3.

At times $t \geq \tau'(g)$ the effective dissipative dynamics \mathcal{L}_{eff} begins in the MM leading to exponential decay of coherences, so that at $t \geq \tau(g)$ the unique stationary state $\rho_{\text{ss}}(g)$ of \mathcal{L}_g is achieved by the system, see Eqs. (3.36) and (3.39). In particular, the asymptotic QFI is independent of time t , $F(\rho_{\text{ss}}(g))$. Therefore, for total time T for estimation of the parameter g it is optimal to perform $n = T/t$ experiments, where $t \leq \tau'(g)$, which leads to the total QFI

$$\frac{T}{t} F(\rho_g(t)) \approx 4 T \tau'(g) \sum_{l=1}^{m'} p_l \Delta_{\omega_l}^2 \tilde{H}_l^{(1)}, \quad (\text{D.9})$$

where we assumed pure ω_l , $l = 1, \dots, m'$, and we have $\tau(g') \propto g^{-2}$, cf. Sec. C.2.3. See also the discussion in Sec. 2.4.3. When $g = 0$, the optimal choice of time is $t = T$, since the quadratic scaling of the QFI is present for all times.

In the case when dynamics governed by \mathcal{L}_g features a DFS/NSS also at $g \neq 0$, the measurements using solely the system can achieve the quadratic scaling of the estimation precision, for all times t , if and only if, varying of g introduces unitary dynamics within that DFS/NSS in the first-order, cf. (D.6). See also Example II in Sec. 2.4.2.

Let us finally note that the enhanced scaling in (D.8) can be present even if there is no DPT present in the dynamics, e.g when there is only a single DFS present ($m' = 1$) and thus after $t \gg \tau_0$ there are no jumps taking place, or for all NSSs, \mathcal{K}_l , the associated dissipative dynamics in \mathcal{H}_l is identical.

D.3.2 Estimation using both system and output

In contrast, for a pure initial state ρ_{in} of the system and the optimal estimation scheme using the joint system-output MPS, $|\Psi_g(t)\rangle$, we have in the metastable regime (see Appendix B.2.3)

$$\begin{aligned}
 F(|\Psi_g(t)\rangle) &= 4t^2 \left[\text{Re } \partial_{g_1} \partial_{g_2} \text{Tr} (\mathcal{L}_{g_1,g} \mathcal{P}(g) \mathcal{L}_{g,g_2} \mathcal{P}(g) \rho_{\text{in}})_{g_1=g_2=g} + \right. \\
 &\quad \left. - \left| \partial_{g_1} \text{Tr} (\mathcal{L}_{g_1,g} \mathcal{P}(g) \rho_{\text{in}})_{g_1=g} \right|^2 \right] + \mathcal{O}(t) \\
 &= 4t^2 \left[\text{Re } \partial_{g_1} \partial_{g_2} \text{Tr} (\mathcal{L}_{g_1,g} \mathcal{P}_0 \mathcal{L}_{g,g_2} \mathcal{P}_0 \rho_{\text{in}})_{g_1=g_2=0} + \right. \\
 &\quad \left. - \left| \partial_g \text{Tr} (\mathcal{L}_{g,0} \mathcal{P}_0 \rho_{\text{in}})_{g=0} \right|^2 \right] + \\
 &\quad + \mathcal{O}(t) + t^2 \mathcal{O} \left(g \|\partial_g|_{g=0} \mathcal{L}_{g,0}\| \right. \\
 &\quad \left. \times \left(\|\partial_{g_1}|_{g=0} \mathcal{L}_{g,0}\| + \|\partial_{g_1} \partial_{g_2}|_{g_1=g_2=0} \mathcal{L}_{g_1,g_2}\| + \|\partial_g^2|_{g=0} \mathcal{L}_{g,0}\| \right) \right), \quad (\text{D.10})
 \end{aligned}$$

where we used expansion of $\mathcal{P}(g)$ from (3.27). Note that the quadratic scaling of $F(|\Psi_g(t)\rangle)$ at $g = 0$ holds also asymptotically when time $t \rightarrow \infty$. Since $\tilde{H}^{(1)} := i \mathcal{P}_0 \partial_g \mathcal{L}_{g,0}|_{g=0} \mathcal{P}_0$, we further obtain that the leading quadratic terms in the QFI are simply proportional to the variance of $\tilde{H}^{(1)}$ in the metastable state $\mathcal{P}_0 \rho_{\text{in}}$,

$$\begin{aligned}
 F(|\Psi_g(t)\rangle) &\approx 4t^2 \left[\text{Re } \text{Tr} \left(\tilde{H}^{(1)} (\mathcal{P}_0 \rho_{\text{in}}) \tilde{H}^{(1)} \right) - \left| \text{Tr} \left(\tilde{H}^{(1)} \mathcal{P}_0 \rho_{\text{in}} \right) \right|^2 \right] \\
 &= 4t^2 \Delta_{\mathcal{P}_0 \rho_{\text{in}}}^2 \tilde{H}^{(1)} \\
 &= 4t^2 \left[\sum_{l=1}^{m'} p_l \Delta_{\omega_l}^2 \tilde{H}_l^{(1)} + \sum_{l \neq l'=1}^{m'} p_l p_{l'} (\mu_l - \mu_{l'})^2 \right], \quad (\text{D.11})
 \end{aligned}$$

where $\mu_l = \text{Tr}(\tilde{H}_l^{(1)} \omega_l) = \text{Tr}(M_g \tilde{\rho}_l \otimes \omega_l)$, cf. (D.7). We know that due to the system-output MPS being *pure*, the QFI is given by the variance of the stochastic generator $G_g(t)$, see Sec. 2.3.3 in the MPS $|\Psi_g(t)\rangle$. We see that in the case of the perturbed

degenerate dynamics \mathcal{L}_0 we further have that leading terms in the QFI simplify to the variance of the observable $\tilde{H}^{(1)}$ in the metastable state $\mathcal{P}_0\rho_{\text{in}}$.

Firstly, let us note when all phases are classical, $\dim_{\mathcal{H}_l} = 1 \forall l$ so that $m' = m$, we obtain from Eq. (D.11) that the quadratic scaling QFI is a consequence of the $G_g(t)$ distribution being a mixture of m distributions corresponding to the stationary states $\{\tilde{\rho}_l\}_{l=1}^m$ which differ in the rates $\mu_l = \text{Tr}(M_g \tilde{\rho}_l)$. See the bimodal case of $m = 2$ in Sec. 2.3.3. The enhancement is absent when measurements are performed only on the system, cf. (D.8), as the information about the parameter g value is not stored in coherences, but in the joint system-output MPS. This encoding uses resources that can be quantified as the average of $G_g(t)$, which grows linearly with time t , $\langle G_g(t) \rangle = \sum_{l=1}^m p_l \mu_l + \mathcal{O}(1)$. Again, there is a quadratic behaviour of the QFI with time, due to correlations in the MPS that are preserved in the metastable regime ($t \ll \tau''(g)$, cf. Eq.(3.33)). Moreover, note that $t \text{Tr}(M_g \tilde{\rho}_l)$ is the *macroscopic phase* encoded on the MPS for the state initially inside \mathcal{H}_l , and thus the quadratic scaling is again a consequence of a difference in the macroscopic phases, see Sec. 2.3.3.

Secondly, when the state ω_l inside a DFS/NSS is mixed, the output provides additional information about g value, as it purifies the system state and $F_l(\omega_l) \leq 4 \Delta_{\omega_l}^2 \tilde{H}_l^{(1)}$. Moreover, the global phases of ω_l given by $t\mu_l = t\text{Tr}(M_g \omega_l \otimes \tilde{\rho}_l)$ can be resolved as well. This corresponds to the second term in (D.11).

D.3.3 Estimation using output only

When at $g \neq 0$, the degeneracy of stationary state is lifted and the asymptotic scaling of the QFI is necessary linear, cf. (2.27),

$$\lim_{t \rightarrow \infty} t^{-1} F(|\Psi_g(t)\rangle) = 4 \text{Tr} \{ \partial_{g_1} \partial_{g_2} \mathcal{L}_{g_1, g_2} \rho_{\text{ss}}(g) \} - 8 \text{Re} \text{Tr} \left\{ \partial_{g_1} \mathcal{L}_{g_1, g} \left[\mathcal{L}_g^{-1} \right]_{\mathcal{J}-\mathcal{P}_{\text{ss}}(g)} \partial_{g_2} \mathcal{L}_{g, g_2} \rho_{\text{ss}}(g) \right\}_{g_1 = g_2 = g},$$

where $\mathcal{P}_{ss}(g)(\cdot) = \rho_{ss}(g) \text{Tr}(\cdot)$ is the projection on the stationary state $\rho_{ss}(g)$ and we assumed that \mathcal{L}_g features no Jordan blocks. In particular, the leading terms are due to the low-lying eigenmodes of \mathcal{L}_g given by the projection $\mathcal{P}(g)$, and thus we can replace $[\mathcal{L}_g^{-1}]_{\mathcal{J}-\mathcal{P}_{ss}(g)}$ by the resolvent of the effective dynamics operator $\mathcal{L}_{\text{eff}}(g) = [\mathcal{L}_g]_{\mathcal{P}(g)}$. We have that the eigenvalues of $\mathcal{L}_{\text{eff}}(g)$ are given, up to the second order in g , by the eigenvalues of $\tilde{\mathcal{L}}(g) = -i[\tilde{H}^{(1)}, (\cdot)] + \sum_{r=1}^{m''} [\tilde{\mathcal{L}}^{(2)}]_{\mathcal{P}_r}$, where \mathcal{P}_r are the projections on the eigenspaces of $-i[\tilde{H}^{(1)}, (\cdot)]$, see Eq. (3.31). The stationary state ρ_{ss} belongs to \mathcal{P}_1 corresponding to 0 eigenvalue, up to linear corrections in g . Thus, when the degeneracy of the stationary state is lifted in the second-order of perturbation theory, we have

$$\begin{aligned} \lim_{t \rightarrow \infty} t^{-1} F(|\Psi_g(t)\rangle) &\approx -8 \text{Re Tr} \left(\tilde{H}^{(1)} \left[\tilde{\mathcal{L}}(g)^{-1} \right]_{\mathcal{P}_0 - \mathcal{P}_{ss}} \left(\rho_{ss} \tilde{H}^{(1)} \right) \right), \\ &= -g^{-2} 8 \text{Re Tr} \left(\tilde{H}^{(1)} \left[[\tilde{\mathcal{L}}^{(2)}]_{\mathcal{P}_1}^{-1} \right]_{\mathcal{P}_1 - \mathcal{P}_{ss}} \left(\rho_{ss} \tilde{H}^{(1)} \right) \right), \end{aligned} \quad (\text{D.12})$$

where in the second line we used the fact that $\rho_{ss} \tilde{H}^{(1)}$ also belongs to \mathcal{P}_1 . Note that the asymptotic linear scaling can be understood in terms of the decay of the long-lived correlations in the effective dynamics $\tilde{\mathcal{L}}(g)$, i.e., $\text{Re Tr} (\tilde{H}^{(1)} e^{t\tilde{\mathcal{L}}(g)} (\rho_{ss} \tilde{H}^{(1)})) - |\text{Tr} (\tilde{H}^{(1)} \rho_{ss})|^2$, see also Sec. 2.3.3.

Note that as coherences w.r.t. tHf are absent in ρ_{ss} , the enhancement in precision requires measuring the output. Actually, the measurement can be performed *on the output only* [37], as quantum trajectories become uncorrelated at the timescale $\tau(g) \propto g^{-2}$, when the system state reaches the stationary state, see Sec. C.2.5, and the information leaks from DFSS/NSSs to the output. Therefore, this can be viewed as an alternative method of extracting the quadratic scaling of the QFI, instead of exploiting the unitary dynamics induced inside DFSS/NSSs, cf. Sec. D.3.1. Note, however, that such measurements on the output only necessary last at least $t \gg \tau(g) \geq \tau'(g)$, in contrast to the optimal system measurements of the length $t \ll \tau''(g)$.

D.3.4 *Enhanced estimation and metastability in general open quantum system*

Finally, let us note that when the MM of a general open system can be approximated by the structure of a SSM with the same number m of degrees of freedom (cf. Eq. (3.3) and see the second conjecture in Sec. 3.4.1), the quadratic enhancement in the scaling of the QFI in the metastable regime can be explained analogously to the degenerate case above. The presence of coherences during metastable regime will lead to quadratic enhancement in precision also for measurements on the system only, cf. Eq. (D.8), whereas metastability of classical phases differing in rates, cf. (D.10), will lead to the quadratic enhancement requiring a measurement both of the system and the output. This will be analogous to the case of $m = 2$ when the structure of the metastable manifold (see 3.3) is known and simplifies the quadratic behaviour of the QFI, see Appendix D.1.

For general metastable dynamics with a unique stationary state, the asymptotic linear scaling can also be enhanced, see Eq. (2.27). Moreover, this enhancement can be obtained by measuring the output only, since the correlation length τ of the system dynamics is finite [37].

BIBLIOGRAPHY

- ¹V. Giovannetti, S. Lloyd, and L. Maccone, “Quantum Metrology,” *Phys. Rev. Lett.* **96**, 010401 (2006).
- ²V. Giovannetti, S. Lloyd, and L. Maccone, “Advances in quantum metrology,” *Nat. Photon.* **5**, 222–229 (2011).
- ³C. M. Caves, “Quantum-mechanical noise in an interferometer,” *Phys. Rev. D* **23**, 1693–1708 (1981).
- ⁴D. J. Wineland, J. J. Bollinger, W. M. Itano, F. L. Moore, and D. J. Heinzen, “Spin squeezing and reduced quantum noise in spectroscopy,” *Phys. Rev. A* **46(R)**, 6797–6800 (1992).
- ⁵D. Leibfried, M. D. Barrett, T. Schaetz, J. Britton, J. Chiaverini, W. M. Itano, J. D. Jost, C. Langer, and D. J. Wineland, “Toward Heisenberg-Limited Spectroscopy with Multiparticle Entangled States,” *Science* **304**, 1476–1478 (2004).
- ⁶C. F. Roos, M. Chwalla, K. Kim, M. Riebe, and R. Blatt, “‘Designer atoms’ for quantum metrology,” *Nature* **443**, 316–319 (2006).
- ⁷M. A. Nielsen and I. L. Chuang, *Quantum Computation and Quantum Information* (Cambridge University Press, 2000).
- ⁸V. Gorini, A. Kossakowski, and E. C. G. Sudarshan, “Completely positive dynamical semigroups of N-level systems,” *J. Mat. Phys.* **17**, 821–825 (1976).
- ⁹G. Lindblad, “On the generators of quantum dynamical semigroups,” *Commun. Math. Phys* **48**, 119 (1976).
- ¹⁰G. Tóth, “Multipartite entanglement and high-precision metrology,” *Phys. Rev. A* **85**, 022322 (2012).
- ¹¹L. Pezzé and A. Smerzi, “Entanglement, Nonlinear Dynamics, and the Heisenberg Limit,” *Phys. Rev. Lett.* **102**, 100401 (2009).

- ¹²S. F. Huelga, C. Macchiavello, T. Pellizzari, A. K. Ekert, M. B. Plenio, and J. I. Cirac, "Improvement of Frequency Standards with Quantum Entanglement," *Phys. Rev. Lett.* **79**, 3865–3868 (1997).
- ¹³S. Knysh, V. N. Smelyanskiy, and G. A. Durkin, "Scaling laws for precision in quantum interferometry and the bifurcation landscape of the optimal state," *Phys. Rev. A* **83**, 021804 (2011).
- ¹⁴J. Kołodyński and R. Demkowicz-Dobrzański, "Phase estimation without a priori phase knowledge in the presence of loss," *Phys. Rev. A* **82**, 053804 (2010).
- ¹⁵B. Escher, R. de Matos Filho, and L. Davidovich, "General framework for estimating the ultimate precision limit in noisy quantum-enhanced metrology," *Nat. Phys.* **7**, 406–411 (2011).
- ¹⁶R. Demkowicz-Dobrzański, J. Kołodyński, and M. Guță, "The elusive Heisenberg limit in quantum-enhanced metrology," *Nat. Commun.* **3**, 1063 (2012).
- ¹⁷A. Peres, "Zeno paradox in quantum theory," *Am. J. Phys.* **48**, 931–932 (1980).
- ¹⁸G. C. Ghirardi, C. Omero, T. Weber, and A. Rimini, "Small-time behaviour of quantum nondecay probability and Zeno's paradox in quantum mechanics," *Il Nuovo Cimento A (1965-1970)* **52**, 421–442 (1979).
- ¹⁹P. Facchi, H. Nakazato, and S. Pascazio, "From the Quantum Zeno to the Inverse Quantum Zeno Effect," *Phys. Rev. Lett.* **86**, 2699–2703 (2001).
- ²⁰M. C. Fischer, B. Gutiérrez-Medina, and M. G. Raizen, "Observation of the Quantum Zeno and Anti-Zeno Effects in an Unstable System," *Phys. Rev. Lett.* **87**, 040402 (2001).
- ²¹J. A. Jones, S. D. Karlen, J. Fitzsimons, A. Ardavan, S. C. Benjamin, G. A. D. Briggs, and J. J. L. Morton, "Magnetic Field Sensing Beyond the Standard Quantum Limit Using 10-Spin NOON States," *Science* **324**, 1166–1168 (2009).

- ²²Y. Matsuzaki, S. C. Benjamin, and J. Fitzsimons, “Magnetic field sensing beyond the standard quantum limit under the effect of decoherence,” *Phys. Rev. A* **84**, 012103 (2011).
- ²³A. W. Chin, S. F. Huelga, and M. B. Plenio, “Quantum Metrology in Non-Markovian Environments,” *Phys. Rev. Lett.* **109**, 233601 (2012).
- ²⁴K. Macieszczak, “Zeno limit in frequency estimation with non-Markovian environments,” *Phys. Rev. A* **92**, 010102 (2015).
- ²⁵H.-P. Breuer, E.-M. Laine, and J. Piilo, “Measure for the Degree of Non-Markovian Behavior of Quantum Processes in Open Systems,” *Phys. Rev. Lett.* **103**, 210401 (2009).
- ²⁶A. Rivas, S. F. Huelga, and M. B. Plenio, “Entanglement and Non-Markovianity of Quantum Evolutions,” *Phys. Rev. Lett.* **105**, 050403 (2010).
- ²⁷K. Macieszczak, “Upper bounds on the quantum Fisher Information in the presence of general dephasing,” arXiv:1403.0955 (2014).
- ²⁸J. Ma, X. Wang, C. Sun, and F. Nori, “Quantum spin squeezing,” *Phys. Rep.* **509**, 89–165 (2011).
- ²⁹K. Macieszczak, M. Guță, I. Lesanovsky, and J. P. Garrahan, “Dynamical phase transitions as a resource for quantum enhanced metrology,” *Phys. Rev. A* **93**, 022103 (2016).
- ³⁰C. Gardiner and P. Zoller, *Quantum Noise*, 3rd (Springer, Heidelberg, Germany, 2004).
- ³¹J. Bergquist, R. Hulet, W. Itano, and D. Wineland, “Observation of Quantum Jumps in a Single Atom,” *Phys. Rev. Lett.* **57**, 1699–1702 (1986).
- ³²E. Barkai, Y. Jung, and R. Silbey, “Theory of single molecule spectroscopy: Beyond the Ensemble Average,” *Annu. Rev. Phys. Chem.* **55**, 457–507 (2004).
- ³³M. B. Plenio and P. L. Knight, “The quantum-jump approach to dissipative dynamics in quantum optics,” *Rev. Mod. Phys.* **70**, 101–144 (1998).

- ³⁴J. P. Garrahan and I. Lesanovsky, “Thermodynamics of Quantum Jump Trajectories,” *Phys. Rev. Lett.* **104**, 160601 (2010).
- ³⁵I. Lesanovsky, M. van Horsen, M. Guță, and J. P. Garrahan, “Characterization of Dynamical Phase Transitions in Quantum Jump Trajectories Beyond the Properties of the Stationary State,” *Phys. Rev. Lett.* **110**, 150401 (2013).
- ³⁶C. Ates, B. Olmos, J. P. Garrahan, and I. Lesanovsky, “Dynamical phases and intermittency of the dissipative quantum ising model,” *Phys. Rev. A* **85**, 043620 (2012).
- ³⁷M. Guță, “Fisher information and asymptotic normality in system identification for quantum Markov chains,” *Phys. Rev. A* **83**, 062324 (2011).
- ³⁸S. Gammelmark and K. Mølmer, “Fisher Information and the Quantum Cramér-Rao Sensitivity Limit of Continuous Measurements,” *Phys. Rev. Lett.* **112**, 170401 (2014).
- ³⁹C. Catana, L. Bouten, and M. Guță, “Fisher informations and local asymptotic normality for continuous-time quantum Markov processes,” *J. Phys. A* **365301**, 25 (2014).
- ⁴⁰P. Zanardi and M. Rasetti, “Noiseless Quantum Codes,” *Phys. Rev. Lett.* **79**, 3306–3309 (1997).
- ⁴¹P. Zanardi, “Dissipation and decoherence in a quantum register,” *Phys. Rev. A* **57**, 3276–3284 (1998).
- ⁴²D. A. Lidar, I. L. Chuang, and K. B. Whaley, “Decoherence-Free Subspaces for Quantum Computation,” *Phys. Rev. Lett.* **81**, 2594–2597 (1998).
- ⁴³Kielpinski, D. and Meyer, V. and Rowe, M. A. and Sackett, C. A. and Itano, W. M. and Monroe, C. and Wineland, D. J., “A Decoherence-Free Quantum Memory Using Trapped Ions,” *Science* **291**, 1013–1015 (2001).
- ⁴⁴E. Knill, R. Laflamme, and L. Viola, “Theory of Quantum Error Correction for General Noise,” *Phys. Rev. Lett.* **84**, 2525–2528 (2000).
- ⁴⁵P. Zanardi, “Stabilizing quantum information,” *Phys. Rev. A* **63**, 012301 (2000).

- ⁴⁶L. Viola, E. M. Fortunato, M. A. Pravia, E. Knill, R. Laflamme, and D. G. Cory, "Experimental Realization of Noiseless Subsystems for Quantum Information Processing," *Science* **293**, 2059–2063 (2001).
- ⁴⁷B. Gaveau and L. S. Schulman, "Dynamical metastability," *J. Phys. A* **20**, 2865 (1987).
- ⁴⁸B. Gaveau and L. S. Schulman, "Theory of nonequilibrium first-order phase transitions for stochastic dynamics," *J. Math. Phys.* **39**, 1517–1533 (1998).
- ⁴⁹B. Gaveau, A. Lesne, and L. Schulman, "Spectral signatures of hierarchical relaxation," *Phys. Lett. A* **258**, 222–228 (1999).
- ⁵⁰A. Bovier, M. Eckhoff, V. Gayrard, and M. Klein, "Metastability and Low Lying Spectra in Reversible Markov Chains," *Commun. Math. Phys.* **228**, 219–255 (2002).
- ⁵¹B. Gaveau and L. S. Schulman, "Multiple phases in stochastic dynamics: Geometry and probabilities," *Phys. Rev. E* **73**, 036124 (2006).
- ⁵²S. B. Nicholson, L. S. Schulman, and E. jin Kim, "Deciphering interactions of complex systems that do not satisfy detailed balance," *Phys. Lett. A* **377**, 1810–1813 (2013).
- ⁵³J. Kurchan, "Six out of equilibrium lectures," arXiv:0901.1271 (2009).
- ⁵⁴K. Binder and W. Kob, *Glassy Materials and Disordered Solids: An Introduction to Their Statistical Mechanics (Revised Edition)* (World Scientific Publishing Company, 2011).
- ⁵⁵G. Biroli and J. P. Garrahan, "Perspective: The glass transition," *J. Chem. Phys.* **138**, 12A301 (2013) [10.1063/1.4795539](https://doi.org/10.1063/1.4795539).
- ⁵⁶J. P. Garrahan, A. D. Armour, and I. Lesanovsky, "Facets of glass physics," *Phys. Today* **69**, 40 (2016).
- ⁵⁷P. Zanardi and L. Campos Venuti, "Coherent Quantum Dynamics in Steady-State Manifolds of Strongly Dissipative Systems," *Phys. Rev. Lett.* **113**, 240406 (2014).

- ⁵⁸P. Zanardi and L. Campos Venuti, “Geometry, robustness, and emerging unitarity in dissipation-projected dynamics,” *Phys. Rev. A* **91**, 052324 (2015).
- ⁵⁹LIGO Scientific Collaboration, “A gravitational wave observatory operating beyond the quantum shot-noise limit,” *Nat. Phys.* **7**, 962–965 (2011).
- ⁶⁰Abbott, B. P., *et al.* (LIGO Scientific Collaboration and Virgo Collaboration), “Observation of Gravitational Waves from a Binary Black Hole Merger,” *Phys. Rev. Lett.* **116**, 061102 (2016).
- ⁶¹F. Y. Khalili, S. P. Tarabrin, K. Hammerer, and R. Schnabel, “Generalized analysis of quantum noise and dynamic back-action in signal-recycled Michelson-type laser interferometers,” *Phys. Rev. A* **94**, 013844 (2016).
- ⁶²V. Giovannetti, S. Lloyd, and L. Maccone, “Quantum-Enhanced Measurements: Beating the Standard Quantum Limit,” *Science* **306**, 1330–1336 (2004).
- ⁶³G. A. Young and R. L. Smith, *Essentials of Statistical Inference* (Cambridge University Press, 2005).
- ⁶⁴C. Helstrom, “Minimum mean-squared error of estimates in quantum statistics,” *Phys. Lett. A* **25**, 101–102 (1967).
- ⁶⁵C. Helstrom, “The minimum variance of estimates in quantum signal detection,” *IEEE Trans. Inform. Theory* **14**, 234–242 (1968).
- ⁶⁶C. W. Helstrom, *Quantum Detection and Estimation Theory* (Academic Press, New York, 1976).
- ⁶⁷S. L. Braunstein and C. M. Caves, “Statistical Distance and the Geometry of Quantum States,” *Phys. Rev. Lett.* **72**, 3439–3443 (1994).
- ⁶⁸B. Escher, “Quantum Sensitivity,” in *Quantum Information and Measurement* (Optical Society of America, 2013), W6–31.
- ⁶⁹Z. Jiang, “Quantum Fisher information for states in exponential form,” *Phys. Rev. A* **89**, 032128 (2014).

- ⁷⁰F. Y. Edgeworth, "On the Probable Errors of Frequency-Constants," *Journal of the Royal Statistical Society* **71**, 381–97, 499–512, 651–78 (1908).
- ⁷¹R. A. Fisher, "Theory of Statistical Estimation," *Mathematical Proceedings of the Cambridge Philosophical Society* **22**, 700–725 (1925).
- ⁷²L. M. Le Cam, *Locally asymptotically normal families of distributions* (University of California Press, 1960).
- ⁷³B. L. Higgins, D. W. Berry, S. D. Bartlett, H. M. Wiseman, and G. J. Pryde, "Entanglement-free Heisenberg-limited phase estimation," *Nature* **450**, 393–396 (2007).
- ⁷⁴B. L. Higgins, D. W. Berry, S. D. Bartlett, M. W. Mitchell, H. M. Wiseman, and G. J. Pryde, "Demonstrating Heisenberg-limited unambiguous phase estimation without adaptive measurements," *New J. Phys.* **11**, 073023 (2009).
- ⁷⁵D. W. Berry and H. M. Wiseman, "Optimal States and Almost Optimal Adaptive Measurements for Quantum Interferometry," *Phys. Rev. Lett.* **85**, 5098–5101 (2000).
- ⁷⁶R. Demkowicz-Dobrzański, "Optimal phase estimation with arbitrary a priori knowledge," *Phys. Rev. A* **83**, 061802 (2011).
- ⁷⁷K. Macieszczak, M. Fraas, and R. Demkowicz-Dobrzański, "Bayesian quantum frequency estimation in presence of collective dephasing," *New J. Phys.* **16**, 113002 (2014).
- ⁷⁸K. Chabuda, I. D. Leroux, and R. Demkowicz-Dobrzański, "The quantum Allan variance," *New Journal of Physics* **18**, 083035 (2016).
- ⁷⁹H. L. Van Trees, *Detection, Estimation, and Modulation Theory, Part I* (John Wiley and Sons, Inc., 2004).
- ⁸⁰R. D. Gill and B. Y. Levit, "Applications of the van Trees inequality: a Bayesian Cramér-Rao bound," *Bernoulli* **1**, 59–79 (1995).
- ⁸¹M. Tsang, "Ziv-Zakai Error Bounds for Quantum Parameter Estimation," *Phys. Rev. Lett.* **108**, 230401 (2012).

- ⁸²Y. R. Zhang, G. R. Jin, J. P. Cao, W. M. Liu, and H. Fan, “Unbounded quantum Fisher information in two-path interferometry with finite photon number,” *J. Phys. A* **46**, 035302 (2013).
- ⁸³A. Monras, “Optimal phase measurements with pure Gaussian states,” *Phys. Rev. A* **73**, 033821 (2006).
- ⁸⁴B. M. Escher, L. Davidovich, N. Zagury, and R. L. de Matos Filho, “Quantum Metrological Limits via a Variational Approach,” *Phys. Rev. Lett.* **109**, 190404 (2012).
- ⁸⁵R. Demkowicz-Dobrzański, K. Banaszek, and R. Schnabel, “Fundamental quantum interferometry bound for the squeezed-light-enhanced gravitational wave detector GEO 600,” *Phys. Rev. A* **88**, 041802 (2013).
- ⁸⁶P. Hyllus, W. Laskowski, R. Krischek, C. Schwemmer, W. Wieczorek, H. Weinfurter, L. Pezzé, and A. Smerzi, “Fisher information and multiparticle entanglement,” *Phys. Rev. A* **85**, 022321 (2012).
- ⁸⁷H. Strobel, W. Muessel, D. Linnemann, T. Zibold, D. B. Hume, L. Pezzè, A. Smerzi, and M. K. Oberthaler, “Fisher information and entanglement of non-Gaussian spin states,” *Science* **345**, 424–427 (2014).
- ⁸⁸P. Hauke, M. Heyl, L. Tagliacozzo, and P. Zoller, “Measuring multipartite entanglement through dynamic susceptibilities,” *Nat. Phys.* (2016) [10.1038/nphys3700](https://doi.org/10.1038/nphys3700).
- ⁸⁹T. Macrì, A. Smerzi, and L. Pezzè, “Loschmidt echo for quantum metrology,” *Phys. Rev. A* **94**, 010102 (2016).
- ⁹⁰H. Ollivier and W. H. Zurek, “Quantum Discord: A Measure of the Quantumness of Correlations,” *Phys. Rev. Lett.* **88**, 017901 (2001).
- ⁹¹D. Girolami, A. M. Souza, V. Giovannetti, T. Tufarelli, J. G. Filgueiras, R. S. Sarthour, D. O. Soares-Pinto, I. S. Oliveira, and G. Adesso, “Quantum Discord Determines the Interferometric Power of Quantum States,” *Phys. Rev. Lett.* **112**, 210401 (2014).

- ⁹²S. I. Knysh, E. H. Chen, and G. A. Durkin, “True limits to precision via unique quantum probe,” arXiv:1402.0495 (2014).
- ⁹³D. Ulam-Orgikh and M. Kitagawa, “Spin squeezing and decoherence limit in Ramsey spectroscopy,” *Phys. Rev. A* **64**, 052106 (2001).
- ⁹⁴J. Kołodyński and R. Demkowicz-Dobrzański, “Efficient tools for quantum metrology with uncorrelated noise,” *New J. Phys* **15**, 073043 (2013).
- ⁹⁵R. Chaves, J. B. Brask, M. Markiewicz, J. Kołodyński, and A. Acín, “Noisy Metrology beyond the Standard Quantum Limit,” *Phys. Rev. Lett.* **111**, 120401 (2013).
- ⁹⁶J. B. Brask, R. Chaves, and J. Kołodyński, “Improved Quantum Magnetometry beyond the Standard Quantum Limit,” *Phys. Rev. X* **5**, 031010 (2015).
- ⁹⁷E. M. Kessler, I. Lovchinsky, A. O. Sushkov, and M. D. Lukin, “Quantum Error Correction for Metrology,” *Phys. Rev. Lett.* **112**, 150802 (2014).
- ⁹⁸W. Dür, M. Skotiniotis, F. Fröwis, and B. Kraus, “Improved Quantum Metrology Using Quantum Error Correction,” *Phys. Rev. Lett.* **112**, 080801 (2014).
- ⁹⁹G. Arrad, Y. Vinkler, D. Aharonov, and A. Retzker, “Increasing Sensing Resolution with Error Correction,” *Phys. Rev. Lett.* **112**, 150801 (2014).
- ¹⁰⁰J. Jeske, J. H. Cole, and S. F. Huelga, “Quantum metrology subject to spatially correlated Markovian noise: restoring the Heisenberg limit,” *New J. Phys* **16**, 073039 (2014).
- ¹⁰¹S. Simmons, J. A. Jones, S. D. Karlen, A. Ardavan, and J. J. L. Morton, “Magnetic field sensors using 13-spin cat states,” *Phys. Rev. A* **82**, 022330 (2010).
- ¹⁰²A. Smirne, J. Kołodyński, S. F. Huelga, and R. Demkowicz-Dobrzański, “Ultimate Precision Limits for Noisy Frequency Estimation,” *Phys. Rev. Lett.* **116**, 120801 (2016).

- ¹⁰³M. G. Genoni, S. Olivares, and M. G. A. Paris, “Optical Phase Estimation in the Presence of Phase Diffusion,” *Phys. Rev. Lett.* **106**, 153603 (2011).
- ¹⁰⁴A. De Pasquale, D. Rossini, P. Facchi, and V. Giovannetti, “Quantum parameter estimation affected by unitary disturbance,” *Phys. Rev. A* **88**, 052117 (2013).
- ¹⁰⁵S. Pang and T. A. Brun, “Quantum metrology for a general Hamiltonian parameter,” *Phys. Rev. A* **90**, 022117 (2014).
- ¹⁰⁶M. Skotiniotis, P. Sekatski, and W. Dür, “Quantum metrology for the Ising Hamiltonian with transverse magnetic field,” *New J. Phys.* **17**, 073032 (2015).
- ¹⁰⁷L. A. Correa, M. Mehboudi, G. Adesso, and A. Sanpera, “Individual Quantum Probes for Optimal Thermometry,” *Phys. Rev. Lett.* **114**, 220405 (2015).
- ¹⁰⁸W. van Dam, G. M. D’Ariano, A. Ekert, C. Macchiavello, and M. Mosca, “Optimal Quantum Circuits for General Phase Estimation,” *Phys. Rev. Lett.* **98**, 090501 (2007).
- ¹⁰⁹R. Demkowicz-Dobrzański and L. Maccone, “Using Entanglement Against Noise in Quantum Metrology,” *Phys. Rev. Lett.* **113**, 250801 (2014).
- ¹¹⁰L. del Rio, L. Kraemer, and R. Renner, “Resource theories of knowledge,” arXiv:1511.08818 (2015).
- ¹¹¹S. Boixo, S. T. Flammia, C. M. Caves, and J. Geremia, “Generalized Limits for Single-Parameter Quantum Estimation,” *Phys. Rev. Lett.* **98**, 090401 (2007).
- ¹¹²M. Zwiernik, C. A. Pérez-Delgado, and P. Kok, “Ultimate limits to quantum metrology and the meaning of the Heisenberg limit,” *Phys. Rev. A* **85**, 042112 (2012).
- ¹¹³M. J. W. Hall and H. M. Wiseman, “Does Nonlinear Metrology Offer Improved Resolution? Answers from Quantum Information Theory,” *Phys. Rev. X* **2**, 041006 (2012).

- ¹¹⁴H. Häffner, W. Hänsel, C. Roos, J. Benhelm, M. Chwalla, T. Körber, U. Rapol, M. Riebe, P. Schmidt, C. Becher, et al., “Scalable multiparticle entanglement of trapped ions,” *Nature* **438**, 643–646 (2005).
- ¹¹⁵D. Burgarth and K. Yuasa, “Quantum System Identification,” *Phys. Rev. Lett.* **108**, 080502 (2012).
- ¹¹⁶A. S. Holevo, *Probabilistic and Statistical Aspects of Quantum Theory* (North Holland, Amsterdam, 1982).
- ¹¹⁷R. D. Gill and M. Guță, “On asymptotic quantum statistical inference,” in *From Probability to Statistics and Back: High-Dimensional Models and Processes – A Festschrift in Honor of Jon A. Wellner*, Vol. 9, Collections (Institute of Mathematical Statistics, Beachwood, Ohio, USA, 2013), pp. 105–127.
- ¹¹⁸K. Matsumoto, “A new approach to the Cramér-Rao-type bound of the pure-state model,” *J. Phys. A* **35**, 3111 (2002).
- ¹¹⁹P. C. Humphreys, M. Barbieri, A. Datta, and I. A. Walmsley, “Quantum Enhanced Multiple Phase Estimation,” *Phys. Rev. Lett.* **111**, 070403 (2013).
- ¹²⁰M. G. Genoni, M. G. A. Paris, G. Adesso, H. Nha, P. L. Knight, and M. S. Kim, “Optimal estimation of joint parameters in phase space,” *Phys. Rev. A* **87**, 012107 (2013).
- ¹²¹M. D. Vidrighin, G. Donati, M. G. Genoni, X.-M. Jin, W. S. Kolthammer, M. Kim, A. Datta, M. Barbieri, and I. A. Walmsley, “Joint estimation of phase and phase diffusion for quantum metrology,” *Nat. Commun.* **5** (2014) 10.1038/ncomms4532.
- ¹²²P. J. D. Crowley, A. Datta, M. Barbieri, and I. A. Walmsley, “Tradeoff in simultaneous quantum-limited phase and loss estimation in interferometry,” *Phys. Rev. A* **89**, 023845 (2014).
- ¹²³M. Tsang, H. M. Wiseman, and C. M. Caves, “Fundamental Quantum Limit to Waveform Estimation,” *Phys. Rev. Lett.* **106**, 090401 (2011).
- ¹²⁴M. Szczykulska, T. Baumgratz, and A. Datta, “Multi-parameter quantum metrology,” *Advances in Physics: X* **1**, 621–639 (2016).

- ¹²⁵S. Amari and H. Nagaoka, *Methods of Information Geometry (Translations of Mathematical Monographs)* (American Mathematical Society and Oxford University Press, 2000).
- ¹²⁶D. Petz and C. Sudár, “Geometries of quantum states,” *J. Math. Phys.* **37**, 2662–2673 (1996).
- ¹²⁷D. Petz, “Covariance and Fisher information in quantum mechanics,” *J. Phys. A* **35**, 929 (2002).
- ¹²⁸M. Wolf, G. Ortiz, F. Verstraete, and J. Cirac, “Quantum Phase Transitions in Matrix Product Systems,” *Phys. Rev. Lett.* **97**, 110403 (2006).
- ¹²⁹P. Zanardi and N. Paunković, “Ground state overlap and quantum phase transitions,” *Phys. Rev. E* **74**, 031123 (2006).
- ¹³⁰P. Zanardi, P. Giorda, and M. Cozzini, “Information-Theoretic Differential Geometry of Quantum Phase Transitions,” *Phys. Rev. Lett.* **99**, 100603 (2007).
- ¹³¹P. Zanardi, M. G. A. Paris, and L. Campos Venuti, “Quantum criticality as a resource for quantum estimation,” *Phys. Rev. A* **78**, 1–7 (2008).
- ¹³²L. Mandelstam and I. Tamm, “The uncertainty relation between energy and time in nonrelativistic quantum mechanics,” *J. Phys. USSR* **9**, 249 (1945).
- ¹³³M. M. Taddei, B. M. Escher, L. Davidovich, and R. L. de Matos Filho, “Quantum Speed Limit for Physical Processes,” *Phys. Rev. Lett.* **110**, 050402 (2013).
- ¹³⁴I. Marvian, R. W. Spekkens, and P. Zanardi, “Quantum speed limits, coherence, and asymmetry,” *Phys. Rev. A* **93**, 052331 (2016).
- ¹³⁵D. P. Pires, M. Cianciaruso, L. C. Céleri, G. Adesso, and D. O. Soares-Pinto, “Generalized Geometric Quantum Speed Limits,” *Phys. Rev. X* **6**, 021031 (2016).
- ¹³⁶S. L. Braunstein, C. M. Caves, and G. Milburn, “Generalized Uncertainty Relations: Theory, Examples, and Lorentz Invariance,” *Annals Phys.* **247**, 135–173 (1996).

- ¹³⁷P. Busch, "The Time–Energy Uncertainty relation," in *Time in Quantum Mechanics*, edited by J. Muga, R. S. Mayato, and Í. Egusquiza (Springer, Berlin, Heidelberg, 2008), pp. 73–105.
- ¹³⁸N. Margolus and L. B. Levitin, "The maximum speed of dynamical evolution," *Phys. D* **120**, 188–195 (1998).
- ¹³⁹A. del Campo, I. L. Egusquiza, M. B. Plenio, and S. F. Huelga, "Quantum Speed Limits in Open System Dynamics," *Phys. Rev. Lett.* **110**, 050403 (2013).
- ¹⁴⁰S. Deffner and E. Lutz, "Quantum Speed Limit for Non-Markovian Dynamics," *Phys. Rev. Lett.* **111**, 010402 (2013).
- ¹⁴¹A. Smerzi, "Zeno Dynamics, Indistinguishability of State, and Entanglement," *Phys. Rev. Lett.* **109**, 150410 (2012).
- ¹⁴²K. Macieszczak, "Quantum Fisher Information: Variational principle and simple iterative algorithm for its efficient computation," arXiv:1312.1356 (2013).
- ¹⁴³F. Hansen and G. K. Pedersen, "Jensen's Operator Inequality," *Bull. London Math. Soc.* **35**, 553–564 (2003).
- ¹⁴⁴D. Burgarth, V. Giovannetti, A. N. Kato, and K. Yuasa, "Quantum estimation via sequential measurements," *New J. Phys.* **17**, 113055 (2015).
- ¹⁴⁵A. P. Dempster, N. M. Laird, and D. B. Rubin, "Maximum likelihood from incomplete data via the EM algorithm," *J. of the Royal Statistical Society, Ser B* **39**, 1–38 (1977).
- ¹⁴⁶R. M. Neal and G. E. Hinton, "A View of the EM Algorithm that Justifies Incremental, Sparse, and other Variants," in *Learning in Graphical Models*, edited by M. I. Jordan (Springer Netherlands, Dordrecht, 1998), pp. 355–368.
- ¹⁴⁷N. F. Ramsey, *Molecular Beams* (Oxford University Press, New York, 1956).
- ¹⁴⁸G. M. Palma, K.-A. Suominen, and A. K. Ekert, "Quantum Computers and Dissipation," *Proc. R. Soc. London, Ser. A* **452**, 567–584 (1996).
- ¹⁴⁹C. Gardiner, *Stochastic Methods, A Handbook for the Natural and Social Sciences* (Springer, Berlin, 2009).

- ¹⁵⁰S. Daffer, K. Wódkiewicz, J. D. Cresser, and J. K. McIver, “Depolarizing channel as a completely positive map with memory,” *Phys. Rev. A* **70**, 010304 (2004).
- ¹⁵¹M. Ringbauer, C. J. Wood, K. Modi, A. Gilchrist, A. G. White, and A. Fedrizzi, “Characterizing Quantum Dynamics with Initial System-Environment Correlations,” *Phys. Rev. Lett.* **114**, 090402 (2015).
- ¹⁵²F. A. Pollock, C. Rodríguez-Rosario, T. Frauenheim, M. Paterostro, and K. Modi, “Complete framework for efficient characterisation of non-Markovian processes,” arXiv:1512.00589 (2015).
- ¹⁵³M. Tukiainen, H. Lyyra, G. Sarbicki, and S. Maniscalco, “Fidelity of dynamical maps,” arXiv:1609.00482 (2016).
- ¹⁵⁴J. Iles-Smith, N. Lambert, and A. Nazir, “Environmental dynamics, correlations, and the emergence of noncanonical equilibrium states in open quantum systems,” *Phys. Rev. A* **90**, 032114 (2014).
- ¹⁵⁵R. Blatt, G. J. Milburn, and A. Lvovsky, “The 20th anniversary of quantum state engineering,” *J. Phys. B* **46**, 100201 (2013).
- ¹⁵⁶S. Diehl, A. Micheli, A. Kantian, B. Kraus, H. P. Büchler, and P. Zoller, “Quantum states and phases in driven open quantum systems with cold atoms,” *Nat. Phys.* **4**, 878–883 (2008).
- ¹⁵⁷B. Kraus, H. P. Büchler, S. Diehl, A. Kantian, A. Micheli, and P. Zoller, “Preparation of entangled states by quantum Markov processes,” *Phys. Rev. A* **78**, 042307 (2008).
- ¹⁵⁸M. M. Wolf, *Quantum channels and operations: Guided tour* (2012).
- ¹⁵⁹F. Verstraete and J. I. Cirac, “Continuous Matrix Product States for Quantum Fields,” *Phys. Rev. Lett.* **104**, 190405 (2010).
- ¹⁶⁰J. Haegeman, J. I. Cirac, T. J. Osborne, and F. Verstraete, “Calculus of continuous matrix product states,” *Phys. Rev. B* **88**, 085118 (2013).

- ¹⁶¹M. Jarzyna and R. Demkowicz-Dobrzański, “Matrix Product States for Quantum Metrology,” *Phys. Rev. Lett.* **110**, 240405 (2013).
- ¹⁶²S. Sachdev, *Quantum Phase Transitions, Second Edition* (Cambridge University Press, 2011).
- ¹⁶³M. van Horssen and M. Guță, “Large Deviations, Central Limit and dynamical phase transitions in the atom maser,” arXiv:1206.4956 (2012).
- ¹⁶⁴J. M. Hickey, S. Genway, I. Lesanovsky, and J. P. Garrahan, “Thermodynamics of quadrature trajectories in open quantum systems,” *Phys. Rev. A* **86**, 063824 (2012).
- ¹⁶⁵F. den Hollander, *Large Deviations*, 1st (American Mathematical Society, Providence, Rhode Island, USA, 2000).
- ¹⁶⁶H. Touchette, “The large deviation approach to statistical mechanics,” *Phys. Rep.* **478**, 1–69 (2009).
- ¹⁶⁷T. Kato, *Perturbation Theory for Linear Operators* (Springer, 1995).
- ¹⁶⁸V. M. Bastidas, C. Emary, G. Schaller, and T. Brandes, “Nonequilibrium quantum phase transitions in the Ising model,” *Phys. Rev. A* **86**, 063627 (2012).
- ¹⁶⁹M. Heyl, A. Polkovnikov, and S. Kehrein, “Dynamical Quantum Phase Transitions in the Transverse-Field Ising Model,” *Phys. Rev. Lett.* **110**, 135704 (2013).
- ¹⁷⁰E. Canovi, P. Werner, and M. Eckstein, “First-Order Dynamical Phase Transitions,” *Phys. Rev. Lett.* **113**, 265702 (2014).
- ¹⁷¹M. Guță and J. Kiukas, “Equivalence Classes and Local Asymptotic Normality in System Identification for Quantum Markov Chains,” *Commun. Math. Phys.* **335**, 1397–1428 (2015).
- ¹⁷²D. C. Rose, K. Macieszczak, I. Lesanovsky, and J. P. Garrahan, “Metastability in an open quantum Ising model,” *Phys. Rev. E* **94**, 052132 (2016).
- ¹⁷³H. Preston-Thomas, “The new international temperature scale of 1990 (ITS-90),” *Metrologia* **27**, 3–10 (1990).
- ¹⁷⁴T. C. Ralph, “Coherent Superposition States as Quantum Rulers,” *Phys. Rev. A* **65**, 042313 (2002).

- ¹⁷⁵J. Joo, W. J. Munro, and T. P. Spiller, “Quantum Metrology with Entangled Coherent States,” *Phys. Rev. Lett.* **107**, 083601 (2011).
- ¹⁷⁶C. C. Gerry and J. Mimih, “Heisenberg-limited interferometry with pair coherent states and parity measurements,” *Phys. Rev. A* **82**, 013831 (2010).
- ¹⁷⁷M. Cozzini, R. Ionicioiu, and P. Zanardi, “Quantum fidelity and quantum phase transitions in matrix product states,” *Phys. Rev. B* **76**, 104420 (2007).
- ¹⁷⁸M. Guta and J. Kiukas, “Information geometry and local asymptotic normality for multi-parameter estimation of quantum Markov dynamics,” arXiv:1601.04355 (2016).
- ¹⁷⁹J. M. Hickey, S. Genway, and J. P. Garrahan, “Dynamical phase transitions, time-integrated observables, and geometry of states,” *Phys. Rev. B* **89**, 054301 (2014).
- ¹⁸⁰Y. V. Nazarov and M. Kindermann, “Full counting statistics of a general quantum mechanical variable,” *Eur. Phys. J. B* **35**, 413–420 (2003).
- ¹⁸¹M. R. Hush, I. Lesanovsky, and J. P. Garrahan, “Generic map from non-Lindblad to Lindblad master equations,” *Phys. Rev. A* **91**, 032113 (2015).
- ¹⁸²K. Mølmer, “Hypothesis Testing with Open Quantum Systems,” *Phys. Rev. Lett.* **114**, 040401 (2015).
- ¹⁸³B. Sciolla, D. Poletti, and C. Kollath, “Two-Time Correlations Probing the Dynamics of Dissipative Many-Body Quantum Systems: Aging and Fast Relaxation,” *Phys. Rev. Lett.* **114**, 170401 (2015).
- ¹⁸⁴A. Polkovnikov, K. Sengupta, A. Silva, and M. Vengalattore, “*Colloquium* : nonequilibrium dynamics of closed interacting quantum systems,” *Rev. Mod. Phys.* **83**, 863–883 (2011).
- ¹⁸⁵J. Eisert, M Friesdorf, and C Gogolin, “Quantum many-body systems out of equilibrium,” *Nat. Phys.* **11**, 7 (2014).

- ¹⁸⁶L. D'Alessio, Y. Kafri, A. Polkovnikov, and M. Rigol, "From quantum chaos and eigenstate thermalization to statistical mechanics and thermodynamics," *Adv. Phys.* **65**, 239–362 (2016).
- ¹⁸⁷J. Eisert, M. Friesdorf, and C. Gogolin, "Quantum many-body systems out of equilibrium," *Nat. Phys.* **11**, 124–130 (2015).
- ¹⁸⁸R. Nandkishore and D. A. Huse, "Many-Body Localization and Thermalization in Quantum Statistical Mechanics," *Annu. Rev. Condens. Matter Phys.* **6**, 15–38 (2015).
- ¹⁸⁹N. Yao, C. Laumann, J. I. Cirac, M. Lukin, and J. Moore, "Quasi many-body localization in translation invariant systems," arXiv:1410.7407 (2014).
- ¹⁹⁰W. De Roeck and F. Huveneers, "Scenario for delocalization in translation-invariant systems," *Phys. Rev. B* **90**, 165137 (2014).
- ¹⁹¹T. Prosen, "Open XXZ Spin Chain: Nonequilibrium Steady State and a Strict Bound on Ballistic Transport," *Phys. Rev. Lett.* **106**, 217206 (2011).
- ¹⁹²T. E. Markland, J. A. Morrone, B. J. Berne, K. Miyazaki, E. Rabani, and D. R. Reichman, "Quantum fluctuations can promote or inhibit glass formation," *Nat. Phys.* **7**, 134–137 (2011).
- ¹⁹³B. Olmos, I. Lesanovsky, and J. P. Garrahan, "Facilitated Spin Models of Dissipative Quantum Glasses," *Phys. Rev. Lett.* **109**, 020403 (2012).
- ¹⁹⁴van Horssen, Merlijn and Levi, Emanuele and Garrahan, Juan P., "Dynamics of many-body localization in a translation-invariant quantum glass model," *Phys. Rev. B* **92**, 100305 (2015).
- ¹⁹⁵M. Žnidarič, "Relaxation times of dissipative many-body quantum systems," *Phys. Rev. E* **92**, 042143 (2015).
- ¹⁹⁶K. Macieszczak, M. Guță, I. Lesanovsky, and J. P. Garrahan, "Towards a Theory of Metastability in Open Quantum Dynamics," *Phys. Rev. Lett.* **116**, 240404 (2016).

- ¹⁹⁷P. M. Chaikin and T. C. Lubensky, *Principles of Condensed Matter Physics, Vol. 1* (Cambridge University Press, 2000).
- ¹⁹⁸B. Gaveau and L. Schulman, “Dynamical distance: coarse grains, pattern recognition, and network analysis,” *Bull. Sci. math* **129**, 631–642 (2005).
- ¹⁹⁹B. Baumgartner and H. Narnhofer, “Analysis of quantum semigroups with GKS–Lindblad generators: II. General,” *J. Phys. A* **41**, 395303 (2008).
- ²⁰⁰V. V. Albert, B. Bradlyn, M. Fraas, and L. Jiang, “Geometry and Response of Lindbladians,” *Phys. Rev. X* **6**, 041031 (2016).
- ²⁰¹B. Gaveau and M. Moreau, “Metastable relaxation times and absorption probabilities for multidimensional stochastic systems,” *J. Phys. A* **33**, 4837 (2000).
- ²⁰²L. O. Hedges, R. L. Jack, J. P. Garrahan, and D. Chandler, “Dynamic Order-Disorder in Atomistic Models of Structural Glass Formers,” *Science* **323**, 1309–1313 (2009).
- ²⁰³C. Giardinà, J. Kurchan, V. Lecomte, and J. Tailleur, “Simulating Rare Events in Dynamical Processes,” *J. Stat. Phys.* **145**, 787–811 (2011).
- ²⁰⁴Andrew J. Daley, “Quantum trajectories and open many-body quantum systems,” *Adv. Phys.* **63**, 77–149 (2014).
- ²⁰⁵V. V. Albert and L. Jiang, “Symmetries and conserved quantities in Lindblad master equations,” *Phys. Rev. A* **89**, 022118 (2014).
- ²⁰⁶P. Zanardi, J. Marshall, and L. Campos Venuti, “Dissipative universal Lindbladian simulation,” *Phys. Rev. A* **93**, 022312 (2016).
- ²⁰⁷L. M. Sieberer, M. Buchhold, and S. Diehl, “Keldysh field theory for driven open quantum systems,” *Rep. Prog. Phys.* **79**, 096001 (2016).
- ²⁰⁸M. F. Maghrebi and A. V. Gorshkov, “Nonequilibrium many-body steady states via Keldysh formalism,” *Phys. Rev. B* **93**, 014307 (2016).

- ²⁰⁹E. G. D. Torre, S. Diehl, M. D. Lukin, S. Sachdev, and P. Strack, “Keldysh approach for nonequilibrium phase transitions in quantum optics: Beyond the Dicke model in optical cavities,” *Phys. Rev. A* **87**, 023831 (2013).
- ²¹⁰M. Idel, *On the structure of positive maps* (MSc Thesis at TU München, 2013).
- ²¹¹A. Rosmanis, “Fixed space of positive trace-preserving super-operators,” *Linear Algebra Appl.* **437**, 1704–1721 (2012).
- ²¹²A. Y. Kitaev, “Fault-tolerant quantum computation by anyons,” *Annals Phys.* **303**, 2–30 (2003).
- ²¹³G. Biroli and J. Kurchan, “Metastable states in glassy systems,” *Phys. Rev. E* **64**, 016101 (2001).
- ²¹⁴B. Olmos, I. Lesanovsky, and J. P. Garrahan, “Out-of-equilibrium evolution of kinetically constrained many-body quantum systems under purely dissipative dynamics,” *Phys. Rev. E* **90**, 042147 (2014).
- ²¹⁵M. Merkli, H. Song, and G. P. Berman, “Multiscale dynamics of open three-level quantum systems with two quasi-degenerate levels,” *J. Phys. A* **48**, 275304 (2015).
- ²¹⁶R. W. Yeung, *A First Course in Information Theory (Information Technology: Transmission, Processing and Storage)* (Springer-Verlag New York, 2006).
- ²¹⁷C. Eichler, J. Mlynek, J. Butscher, P. Kurpiers, K. Hammerer, T. J. Osborne, and A. Wallraff, “Exploring Interacting Quantum Many-Body Systems by Experimentally Creating Continuous Matrix Product States in Superconducting Circuits,” *Phys. Rev. X* **5**, 041044 (2015).
- ²¹⁸E. B. Davies, *One-parameter semigroups* (Academic Press, 1980).
- ²¹⁹J. Watrous, “Notes on Super-operator Norms Induced by Schatten Norms,” *Quantum Info. Comput.* **5**, 58–68 (2005).

COLOPHON

This thesis was typeset using style based on the `classicthesis` developed by André Miede, which is available at <https://bitbucket.org/amiede/classicthesis/>.